Synthesis of Enantiomerically Pure Helical Aromatics Such As NHC Ligands and Their Use in Asymmetric Catalysis

Dissertation

zur Erlangung des akademischen Grades

doctor rerum naturalium (Dr. rer. nat.)

in der Wissenschaftsdisziplin „Organische Chemie“

der Mathematisch-Naturwissenschaftlichen Fakultät

der Universität Potsdam

und

der Faculty of Science

der Charles University

von

Manfred Karras

Potsdam/Prag

2018

First reviewer Prof. Bernd Schmidt
Second reviewer Dr. Ivo Starý
Third reviewer Prof. Jan Veselý

Date of defence 20.11.2018

Published online at the
Institutional Repository of the University of Potsdam:
URN urn:nbn:de:kobv:517-opus4-421497
https://nbn-resolving.org/urn:nbn:de:kobv:517-opus4-421497

Die Ruhe sei dir heilig, nur Verrückte haben's eilig.

Edith Schultz

Declaration

I confirm that I composed the present thesis discretely, without the use of more resources than stated.

_____

place, date, signature

Acknowledgement

I would like to thank my Supervisors Bernd Schmidt, Ivo Starý and Irena G. Stará for providing me with this challenging project, for giving me freedom of expression and creation and for always being helpful in any regards. Many thanks also go to Karol Grela and Michał Dąbrowski for providing an excellent work environment during my stay in Warsaw. Special thanks go to Jiří Rybáček for always providing help and constructive advice. I would also like to thank Radek Pohl for solving all NMR riddles, Lucie Bednárová for optical measurements, Jaroslav Vacek for DFT calculations and all members of the groups of Bernd Schmidt (University Potsdam), Ivo Starý (IOCB Prague) and Karol Grela (University of Warsaw) for being amazing colleagues and friends. Gratitude also goes to Sofiane Merakeb and Simon Culdaut for helping with the Figure of the two human hands. Thanks to the following institutions for funding:

Universität Potsdam

ÚOCHB AV ČR IOCB PRAGUE

DAAD Deutscher Akademischer Austausch Dienst German Academic Exchange Service

University of Warsaw Biological and Chemical Research Centre

CHARLES UNIVERSITY Faculty of science

Thanks to all my family and friends for providing me with the necessary amount of energy to go through this challenging venture and help me to grow in all aspects.

Publications related to this work

Articles in Journals

- M. Karras, M. Dąbrowski, R. Pohl, J. Rybáček, J. Vacek, L. Bednárová, K. Grela, I. Starý, I. G. Stará, B. Schmidt, *Chem. Eur. J.* **2018**, *24*, 10994-10998.
- M. Karras, J. Holec, L. Bednárová, R. Pohl, B. Schmidt, I. G. Stará, I. Starý, *J. Org. Chem.* **2018**, *83*, 5523-5538.
- I. Gay Sánchez, M. Šámal, J. Nejedlý, M. Karras, J. Klívar, J. Rybáček, M. Buděšínský, L. Bednárová, B. Seidlerová, I. G. Stará, I. Starý, *Chem. Commun.* **2017**, *53*, 4370-4373.

Poster Presentations

- Barrande-Vltava (French-Czech chemistry meeting), Prague **2017**
- EuCheMS, Seville **2016**
- Liblice ("Advances in Organic, Bioorganic and Pharmaceutical Chemistry"), Olomouc **2015**
- Chirality, Prague **2014**

Oral Presentations

- Interdisciplinary Meeting of Young Life Scientists, Milovy **2018**
- Liblice ("Advances in Organic, Bioorganic and Pharmaceutical Chemistry"), Lázne Bělohrad **2017**

Abstract

Various ways of preparing enantiomerically pure 2-amino[6]helicene derivatives were explored. Ni(0) mediated cyclotrimerization of enantiopure triynes provided (*M*)- and (*P*)-7,8-bis(*p*-tolyl)hexahelicene-2-amine in >99% *ee* as well as its benzoderivative in >99% *ee*. The stereocontrol was found to be inefficient for a 2-aminobenzo[6]helicene congener with an embedded five-membered ring. Helically chiral imidazolium salts bearing one or two helicene moieties have been synthesized and applied in enantioselective [2+2+2] cyclotrimerization catalyzed by an *in situ* formed Ni(0)-NHC complex. The synthesis of the first helically chiral Pd- and Ru-NHC complexes and their application in enantioselective catalysis was demonstrated. The latter shows promising results in enantioselective olefin metathesis reactions. A mechanistic proposal for asymmetric ring closing metathesis is provided.

Table of Contents

1. Introduction 1
   1.1 Chirality 1
      History and Significance 1
      Types of Molecular Chirality 2
   1.2 Helicenes 4
      History and Significance 4
      Stereoselective Synthesis of Helicenes 6
      Application of Helicenes 10
   1.3 N-Heterocyclic Carbenes 13
      Structural Features 13
      Synthesis 14
      NHC-Metal Complexes 16
   1.4 Asymmetric Catalysis 17
      History, Principles and Significance 17
      Selected Examples 19
2. Objectives 24
3. Results and Discussion 26
   3.1 Synthesis of Helicenes 26
      Enantiopure Amino[6]helicene 26
      Enantiopure Monobenzo Amino[6]helicene (-)-(*M*)-118 34
      Simplified Access to 2-Amino[6]helicene-Like Structure 38
   3.2 Synthesis of Imidazolium Salts 43
      Imidazolium Salts with Two Helicene Moieties 43
      Imidazolium Salt with One Helicene Moiety 44
   3.3 Synthesis of Helically Chiral NHC-Metal Complexes 45
      Ag-Complexes 45
      Ru-Complexes 47
      Pd-Complexes 49
   3.4 Enantioselective Cyclotrimerization with *In Situ* Generated Ni-Complexes 51
   3.5 Investigations with Ru-Complex (-)-(*M*)-147 52
      Catalytic Activity 52
      Application in Asymmetric Olefin Metathesis 54
      Structural and Mechanistic Investigations of the Ru Complex (-)-(*M*)-147 56
      Ru-Catalyzed Formation of Helicene 63
   3.6 Investigations with Pd-Complexes 63

4. Conclusion and Outlook 66
5. Experimental 68
6. Literature 118

List of Schemes

Scheme 1: Intramolecular cyclization of optically pure biaryl (-)-**6** to [7]helicene (-)-(*M*)-**7**. 6
Scheme 2: Photochemical synthesis of [6]helicene with CPL..... 7
Scheme 3: Enantioselective [2+2+2] cycloisomerization of triynes..... 8
Scheme 4: Au-catalyzed enantioselective synthesis of substituted [6]helicenes. 8
Scheme 5: Diastereoselective synthesis of oxahelicenes. 9
Scheme 6: Diastereoselective synthesis of carbohelicenes. 10
Scheme 7: Synthesis of symmetrical imidazolium salts.....15
Scheme 8: Synthesis of unsymmetrical imidazolium salts.....15
Scheme 9: Principles of asymmetric catalysis.....18
Scheme 10: Asymmetric metathesis reactions.....20
Scheme 11: Synthesis of atropisomers *via* Suzuki-Miyaura coupling. 22
Scheme 12: Objectives of the Thesis. 24
Scheme 13: Retrosynthetic scheme for helically chiral NHC-metal complexes. 25
Scheme 14: Retrosynthesis of building block *rac*-**71**. 26
Scheme 15: Synthesis of aldehyde **77**. 26
Scheme 16: Synthesis of racemic diyne building block *rac*-**81**. 27
Scheme 17: Retrosynthesis of enantiopure building block (*S*)-**85**.....28
Scheme 18: Synthesis of terminal alkyne **88**.....29
Scheme 19: Synthesis of *rac*-**86**. 30
Scheme 20: Synthesis of chiral building block **85**.....31
Scheme 21: Synthesis of triyne (*RS*,*S*)-**97**. 32
Scheme 22: Synthesis of enantiopure amino[6]helicene (-)-(*M*)-**69**. 34
Scheme 23: Retrosynthesis of monobenzo amino[6]helicene (*M*)-**100**. 35
Scheme 24: Synthesis of alkyne building block **111**. 36
Scheme 25: Synthesis of triyne **116**. 37
Scheme 26: Synthesis of monobenzo amino[6]helicene (-)-(*M*)-**118**. 38
Scheme 27: Simplification and structural modification of amino[6]helicene synthesis. 39
Scheme 28: The four possible stereoisomers of aminobenzo[6]helicene **121**. 40
Scheme 29: Synthesis of building blocks *rac*-**127** and **129**. 41
Scheme 30: Synthesis of building block *rac*-**130**. 42
Scheme 31: Synthesis of 2-amino[6]helicene-like compound **134**. 43
Scheme 32: Synthesis of imidazolium salts (+)-(*P*,*P*)-**135** and (-)-(*M*,*M*)-**136** with two helicene moieties.....44
Scheme 33: Synthesis of imidazolium salt (-)-(*M*)-**14** with one helicene moiety.....45
Scheme 34: Synthesis of Ag-NHC complex (*P*,*P*,*P*,*P*)-**141**. 46
Scheme 35: Synthesis of Ag-NHC (*M*,*M*)-**143**. 47
Scheme 36: An attempt at the synthesis of Hoveyda-Grubbs type catalyst (*P*,*P*)-**145**.....48
Scheme 37: An attempt at the synthesis of Grubbs type catalyst (*P*,*P*)-**146**. 48
Scheme 38: Synthesis of helically chiral Ru-NHC complex (-)-(*M*)-**147**. 49
Scheme 39: Synthesis of Pd complex (+)-(*P*,*P*)-**148** with two helicene moieties. 50
Scheme 40: Synthesis of Pd complex (-)-(*M*)-**149** with one helicene moiety. 50
Scheme 41: Enantioselective cyclotrimerization with (-)-(*M*,*M*)-**135** and (-)-(*M*,*M*)-**136**.....51
Scheme 42: Activity tests of Ru-complex (-)-(*M*)-**147**. 52
Scheme 43: Activity test in cross metathesis. 54
Scheme 44: AROCM with (-)-(*M*)-**147**. 56
Scheme 45: Mechanism of ARCM mediated by chiral Ru-catalyst (-)-(*M*)-**147**. 59
Scheme 46: Ligand orientation within the catalyst-substrate complex **IV**.....60

Scheme 47: Formation of (*R*)-**161**. 62
Scheme 48: Ru-catalyzed synthesis of dibenzo[6]helicene **14**. 63
Scheme 49: Suzuki-Miyaura coupling catalyzed by (+)-(*P*,*P*)-**148** and (-)-(*M*)-**149**. 64

List of Figures

Figure 1: The human hands as chiral objects. 1
Figure 2: Different types of molecular chirality. 3
Figure 3: Early milestones of helicene chemistry. 4
Figure 4: Historical overview of all publications about helicenes till 2017. 5
Figure 5: Two record holders in helicene chemistry. 6
Figure 6: Selected helically chiral ligands and catalysts. 12
Figure 7: The first isolated N-heterocyclic carbene. 13
Figure 8: Different N-heterocyclic carbenes. 14
Figure 9: Comparison of phosphine and NHC ligands. 16
Figure 10: Different biological activities of enantiomeric compounds. 19
Figure 11: Selected chiral Ru-NHC metathesis catalysts. 21
Figure 12: Selected Pd-PEPPSI catalysts. 23
Figure 13: Activity tests of Ru-complex (-)-(*M*)-**147** compared to **156**. 53
Figure 14: NOE interactions of in complex (-)-(*M*)-**147**. 57
Figure 15: DFT calculated model (left) and topographic steric map[a] of (-)-(*M*)-**147** (right). 57
Figure 16: Folding of the catalyst-substrate complex **V**. 61
Figure 17: Selected Pd-PEPPSI complexes. 65
Figure 18: Overview of successfully synthesized compounds. 66

List of Tables

Table 1: ARCM catalyzed by (-)-(*M*)-**147**.....55
Table 2: $\%V_{bur}$ values for selected Pd-PEPPSI complexes.....65

List of Abbreviations

Ad	adamantyl
ACM	asymmetric cross metathesis
APCI	atmospheric-pressure chemical ionization
aq.	aqueous
ARCM	asymmetric ring-closing metathesis
AROCM	asymmetric ring-opening cross metathesis
BINAP	(2,2'-bis(diphenylphosphino)-1,1'-binaphthyl)
Boc	*tert*-butyloxycarbonyl
Boc_2O	di-*tert*-butyl dicarbonate
conc.	concentrated
conv.	conversion
Cosmo	implicit salvation model
Cp	cyclopentadienyl
CPL	circularly polarized light
de	diastereomeric excess
DFT	density functional theory
DIPA	diisopropylamine
DMAP	4-(dimethylamino)pyridine
DMF	*N*,*N*-dimethylformamide
DMPU	1,3-dimethyl-3,4,5,6-tetrahydro-2(1H)-pyrimidinone
DMSO	dimethyl sulfoxide
DNA	deoxyribonucleic acid
ee	enantiomeric excess
ESI	electrospray ionization
GD3	Grimme dispersion type-3
HPLC	high-performance liquid chromatography
HR	high resolution
IPr	isopropyl
IPent	isopentyl

l-CPL	left circularly polarized light
IR	infrared
LiHMDS	lithium bis(trimethylsilyl)amide
MALDI	matrix-assisted laser desorption/ionization
Mes	mesityl
MOM	methoxymethyl
M.p.	melting point
MS	mass spectrometry
MW	microwave
NBS	*N*-bromosuccinimide
NHC	N-heterocyclic carbene
NMO	4-methylmorpholine *N*-oxide
NMR	nuclear magnetic resonance
org.	organic
^{i}Pr	isopropyl
quant.	quantitative
RCM	ring-closing metathesis
r-CPL	right circularly polarized light
RI-DFT	resolution of identity density functional theory
RNA	ribonucleic acid
rt	room temperatur
sat.	saturated
sol.	solution
TADDOL	α,α,α',α'-tetraaryl-2,2-disubstituted 1,3-dioxolane-4,5-dimethanol
TAPA	2-(2,4,5,7-tetranitro-9-fluorenylideneaminooxy)propionic acid
THF	tetrahydrofuran
TIPS	triisopropylsilyl
UV/Vis	ultraviolet-visible spectroscopy

1. Introduction

1.1 Chirality

History and Significance

“I call any geometrical figure, or any group of points, chiral, and say that it has chirality, if its image in a plane mirror, ideally realized, cannot be brought to coincide with itself” (W. H. Thompson Lord Kelvin).[1] With that quote Sir William H. Thompson in 1894 first introduced the word chirality into science. The word chirality is derived from the Greek word *kheir* which means hand. The first known serious examinations towards the property of handedness were carried out by Immanuel Kant.[2] While debating about the nature of space he was referring to the two hands of one being and stated that they are not congruent (**Figure 1**). He called objects of these kind incongruent counterparts. The first discovery of these counterparts on a molecular level was made by Louis Pasteur. In 1848 Pasteur found that the crystals of optically inactive, racemic (derives from Latin *racemus*, cluster of grapes) sodium ammonium tartrate are not identical. He separated the two non-superimposable, mirror-image crystals and found that their values of optical rotation (J. B. Biot, 1815)[3] are identical in absolute magnitude but differ in their sign.[4] The two enantiomers (derives from Greek *enántios méros*, opposite shape) of the racemic tartrate resolved spontaneously during crystallization. His findings led him to the realization that the molecules he was investigating had to be chiral, although he used the term dissymmetric at that time.

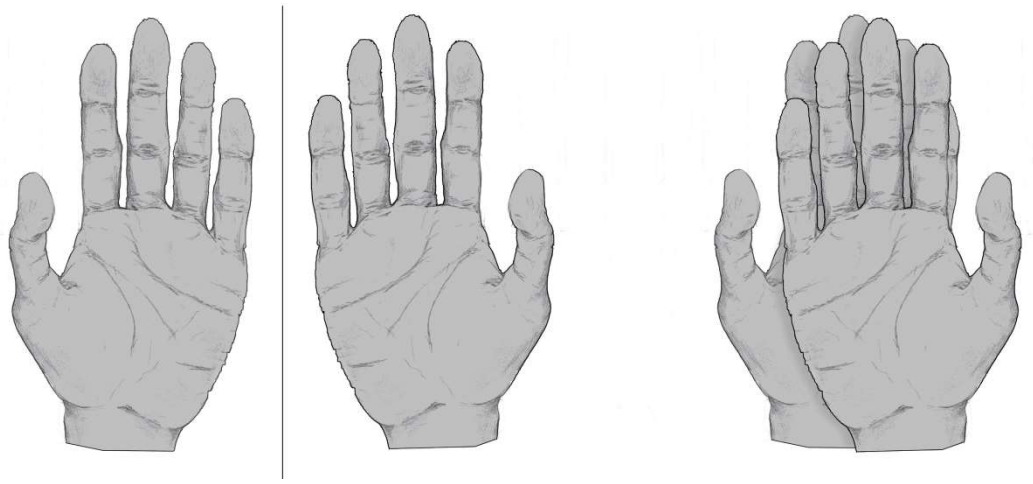

Figure 1: The human hands as chiral objects.

“An economic and efficient turnover requires a homochiral biochemistry, just as efficient engineering depends upon the use of right-handed homochiral screws” (S. Mason).[5] Chirality is ubiquitous on earth and a prerequisite for the existence of life as we know it. Nucleic acids, the building blocks of DNA and RNA, contain exclusively right handed (*D*) sugars and natural proteins are all composed out of a pool of 20 left handed (*L*) amino acids. Homochirality is believed to be indispensable for life-sustaining processes. For example, regular secondary structures of proteins such as β-pleated sheets, which play a key role in the catalytic activity, cannot be formed with equal amounts of amino acid enantiomers.[6]

Enantiomers have the same reactivity towards achiral molecules, the same physical properties (possibly varying in sign) and were believed to be energetically exactly equivalent. Recent calculations contradict this theory and a symmetry violation was found to be the cause of energy discrepancies between enantiomers.[7]

Due to the overabundance of possible explanations for the origin of biomolecular homochirality as well as other asymmetries observed in nature, such as the dominance of matter over antimatter in the observable universe or irreversibility of processes providing a preferred arrow of time, scientists throughout the whole world are still struggling with questions of this kind and only few mechanisms have been experimentally investigated in detail.[7, 8, 9, 10, 11]

Types of Molecular Chirality

There are different types of molecular chirality (**Figure 2**). The most common one is central chirality. If an atom is connected to four different binding partners ($R^{1\text{-}4}$) in a tetrahedral arrangement, it is considered to be a stereogenic center. As soon as any two of the four neighboring substituents are identical, *e.g.* $R^1 = R^2$, there is a plane of symmetry and the chirality is lost. In organic chemistry, not only carbon but also silicon, phosphorus, sulfur or nitrogen atoms can become a source of central chirality.[12]

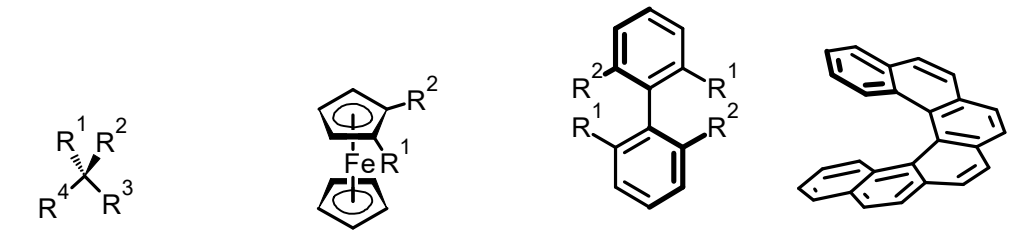

Figure 2: Different types of molecular chirality.

Planarly chiral molecules exhibit a chiral plane in which substituents are arranged differently for the two enantiomers. In case of the ferrocene complex shown in **Figure 2**, the top Cp ligand has two different substituents (R^1 and R^2). The chiral plane can be oriented through the iron atom, parallel to the Cp units. The two substituents destroy a plane of symmetry, perpendicular to the chiral plane, which would be present in a symmetrically substituted ($R^1 = R^2$) ferrocene. Other molecular classes featuring this mode of chirality are cyclophanes, chiral *trans*-cycloalkanes and ansa compounds.[13]

The axial chirality of the biaryl shown in **Figure 2** is caused by its substituents (R^1 and R^2) which hinder free rotation around the biaryl bond, the chiral axis. In this case the enantiomers can be seen as conformers (atropisomers) whose interconversion holds a sufficiently high energy barrier. The steric congestion around the chiral axis must be due to different R^1 and R^2 substituents, otherwise the molecule has a plane of symmetry which makes it achiral. Allenes, alkylidene cycloalkanes, spiranes and cumulenes can possess chiral axis as well.[13]

Helical chirality is a special case of axial chirality. The most prominent example of helical chirality is DNA. Well known exemplars of man-made helically chiral molecules are helicenes. **Figure 2** shows hexahelicene in which the chirality is inherent in its molecular framework. This C_2 symmetric compound (substitution may break this symmetry) winds, due to steric repulsion between the terminal rings, screw-like along the chiral axis. Starting from top ring downwards, the two enantiomers, can either wind clockwise (*P*-helicity) or counterclockwise (*M*-helicity).

1.2 Helicenes

This chapter is mostly focused on fully aromatic carbohelicenes.

History and Significance

The history of helicenes dates back to 1903 when Meisenheimer and Witte were investigating the reduction of 2-nitronaphthalene and identified heterohelicene **1** (**Figure 3**) in a mixture of products.[14] In 1956 Newman and Lednicer synthesized intentionally the carbohelicene hexahelicene ([6]helicene) and introduced "the systematic name helicene for nuclei of the continuously coiled type".[15] The newly found type of structure, with its inherently chiral chromophore, spirals up into a helical shape to decrease van der Waals interactions. The resolution of [6]helicene into its enantiomers was done by using the chiral π-complexing agent TAPA ((-)-(*S*)- or (+)-(*R*)-**3**), providing (+)-(*P*)-**2** or (-)-(*M*)-**2** with exceptionally high specific rotation ($[\alpha]_D$) values.[16] As a general trend in the series of carbohelicenes, dextrorotatory (+) isomers possess (*P*)-helicity and levorotatory (-) isomers (*M*)-helicity.[17] [6]Helicene is the smallest non-substituted helicene which is stable towards racemization at ambient and even elevated temperatures. The numbering was adopted from Newman's suggestion as shown in (+)-(*P*)-**2**.

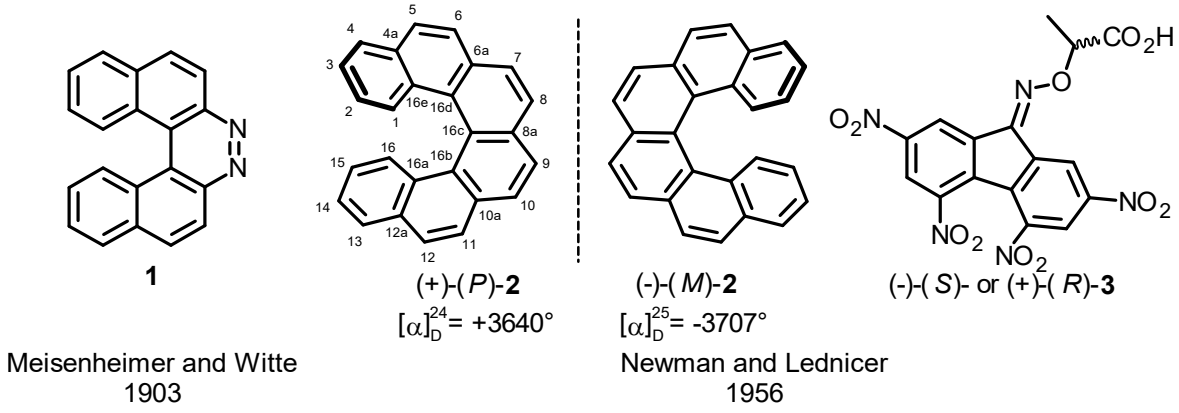

Figure 3: Early milestones of helicene chemistry.

From the early 1990's, the helicene chemistry has been receiving continuously increasing attention, in particular since 2010. **Figure 4**[18] illustrates all published records obtained from *SciFinder* using "helicene" as a search term. Among them there are several comprehensive review articles and book chapters.[19]

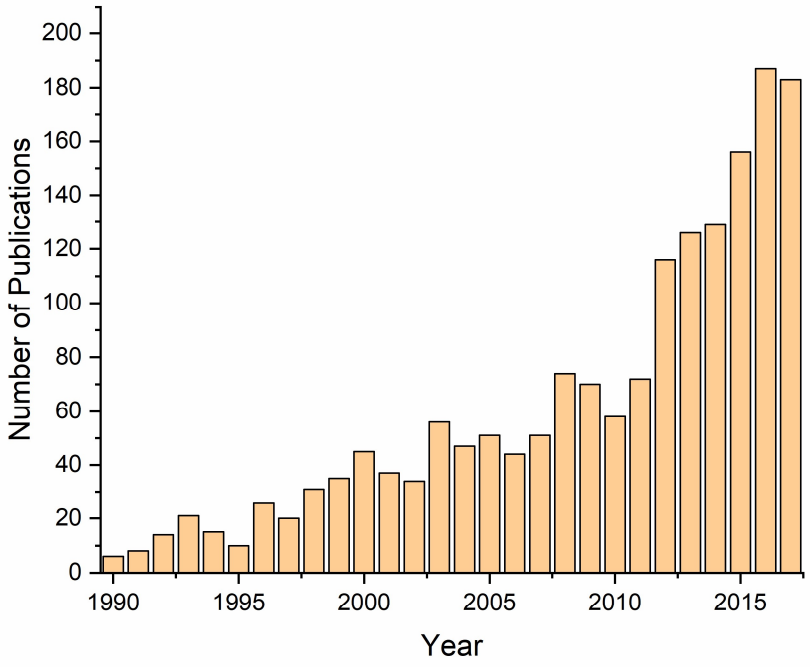

Figure 4: Historical overview of all publications about helicenes till 2017.

Figure 5 shows two record holders in helicene chemistry. The structural complexity of compounds *rac*-**4** and (-)-(*M*,*R*,*R*)-**5** is representative of the dramatic progress the field has experienced during the last decades. Compound *rac*-**4** is the longest known fully aromatic carbohelicene. Mori, Murase and Fujita employed a sextuple photodehydrocyclization constructing six benzene rings in one step, with 7% yield of the key step in the formation of the helical scaffold.[20] Although *rac*-**4** is almost insoluble in any common organic solvent, they could prove the structure by MALDI-TOF mass spectrometry and ^{1}H NMR spectroscopy. The synthesis of diastereomerically and enantiomerically pure oxa[19]helicene (-)-(*M*,*R*,*R*)-**5** was published by Starý and Stará *et al*. In the key step, a diastereoselective quadruple [2+2+2] cycloisomerization, 12 new rings were formed in the flow reactor.[21] Molecule (-)-(*M*,*R*,*R*)-**5** with the longest known helical backbone was found to be soluble in common organic solvents and fully characterized.

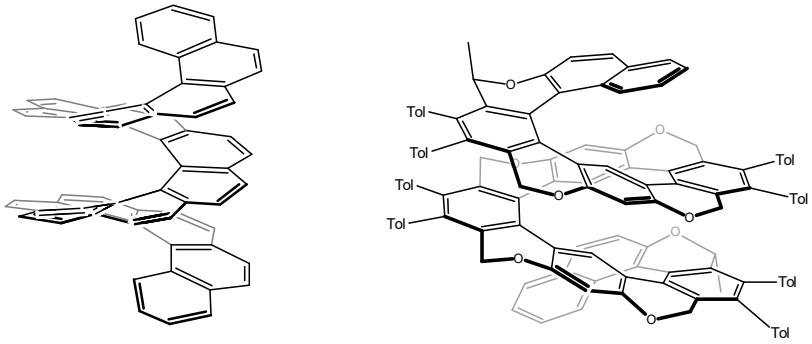

rac-**4** (-)-(*M*,*R*,*R*)-**5**

Figure 5: Two record holders in helicene chemistry.

Stereoselective Synthesis of Helicenes

Due to the demanding synthesis of tetranitro compound **3** (**Figure 3**), which is commercially available but expensive, alternative routes towards enantiomerically pure helicenes were established during the years. Although HPLC separations on chiral stationary phases have become common practice for resolution of racemic mixtures of helical compounds, there is still an interest in their asymmetric synthesis. The availability of general synthetic routes towards enantiomerically pure helicenes is desirable for future applications requiring large amounts of material.

The approach shown in **Scheme 1** is based on cyclization of an optically pure precursor. Gingras *et al.* reported the intramolecular benzylic coupling of axially chiral biaryl (-)-**6**.[22] Compound (-)-**6** was available on a gram scale after resolution of its diol precursor. [23] A mechanistic study proposed an electrocyclic rearrangement of intermediate **8** after elimination of HBr, followed by an additional elimination of HBr to aromatize the system and yield [7]helicene (-)-(*M*)-**7**. The helicity of (-)-(*M*)-**7** could be predicted from the chirality of the precursor (-)-**6**.

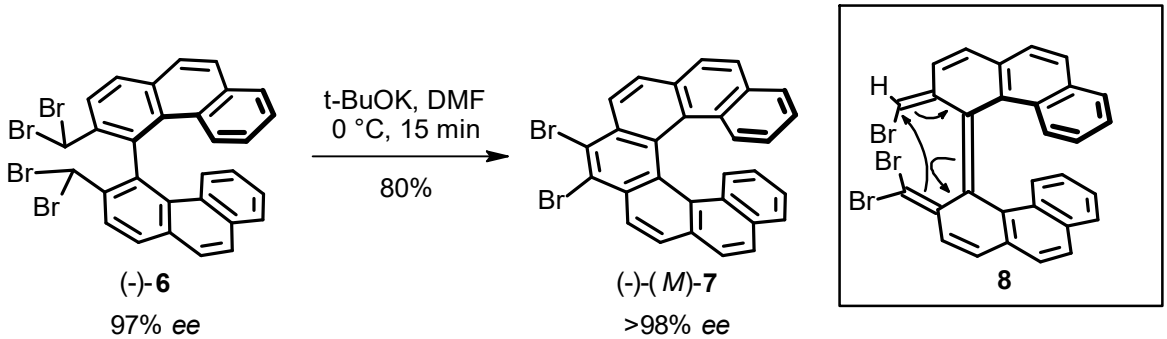

(-)-**6**
97% *ee*

(-)-(*M*)-**7**
>98% *ee*

8

Scheme 1: Intramolecular cyclization of optically pure biaryl (-)-**6** to [7]helicene (-)-(*M*)-**7**.

A photochemical approach towards optically active helicenes was demonstrated by Kagan *et al.* in 1971 (**Scheme 2**).[24] Right or left circularly polarized light (r-CLP or l-CLP) from the UV region was employed in the photodehydrocyclization[25] of *Z*- alkene **9** into dihydro[6]helicene **10**, which was then aromatized by oxygen in the presence of catalytic amount of iodine to [6]helicene **2**. Although their optical yields (quotient of $[\alpha]_D^{20}$ of the synthesized product and $[\alpha]_D^{20}$ of the optically pure product x 100) were just around 0.2%, the observed optical rotations were nevertheless experimentally significant. This small amount of enantiomeric excess could only be observed due to the exceptionally high optical rotation of [6]helicene **2**.

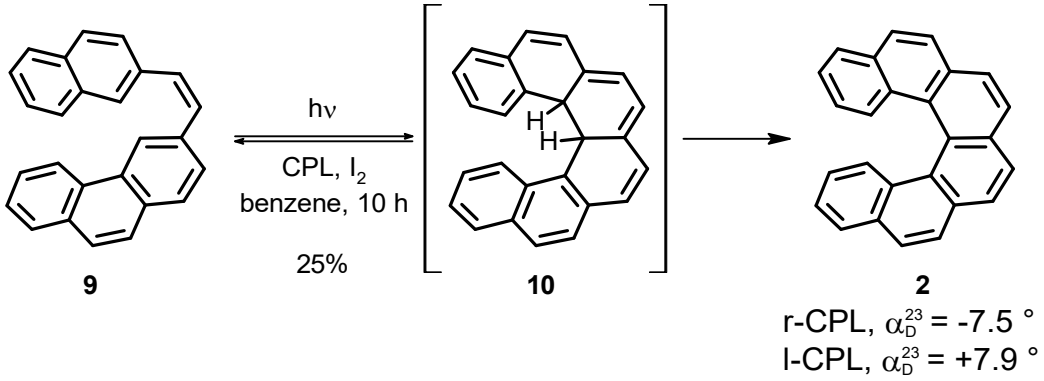

Scheme 2: Photochemical synthesis of [6]helicene with CPL.

A catalytic methodology was developed by Starý and Stará (**Scheme 3**). Employing axially chiral phosphine (*R*)-QUINAP ((*R*)-**13**), they reported the enantioselective [2+2+2] cycloisomerization of triyne **11** to dibenzo[6]helicene (+)-(*P*)-**14** in 80% *ee*.[26] After single crystallization the enantiopurity was increased to 95% *ee*. Later they extended their synthetic scope, obtaining amino-substituted dibenzo[6]helicene (+)-(*P*)-**15** in 67% *ee*.[27] Recently, *in situ* generated helically chiral N-heterocyclic carbenes as ligands for Ni(0) catalyst were investigated as well.[28]

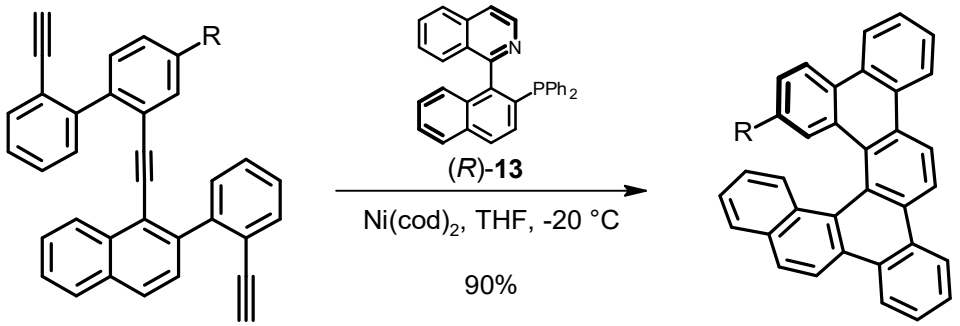

11, R = H
12, R = $N(Boc)_2$

(+)-(*P*)-**14**, R = H, 80% *ee*
(+)-(*P*)-**15**, R = $N(Boc)_2$, 67% *ee*

Scheme 3: Enantioselective [2+2+2] cycloisomerization of triynes.

Alcarazo *et al.* reported on asymmetric synthesis of substituted [6]helicenes with high enantioselectivities (**Scheme 4**).[29] Au catalysts with TADDOL based phosphonite ligands (*e.g.* (*R*,*R*)-**17**) bearing a cationic imidazolium unit were found to promote sequential intramolecular hydroarylation of diynes such as compound **16**. Due to the cationic nature of the catalysts, they exhibit strong π-acceptor properties which enhance the activity towards π-acid catalysis. The aromatic substituents of the TADDOL and the imidazolium moiety create a chiral cavity around the ligating phosphonite. Complex (*R*,*R*)-**17** was the most potent example from a series giving 11 examples of [6]helicene derivatives ((+)-(*P*)-**18**) in good to quantitative yields reaching up to 99% *ee*.

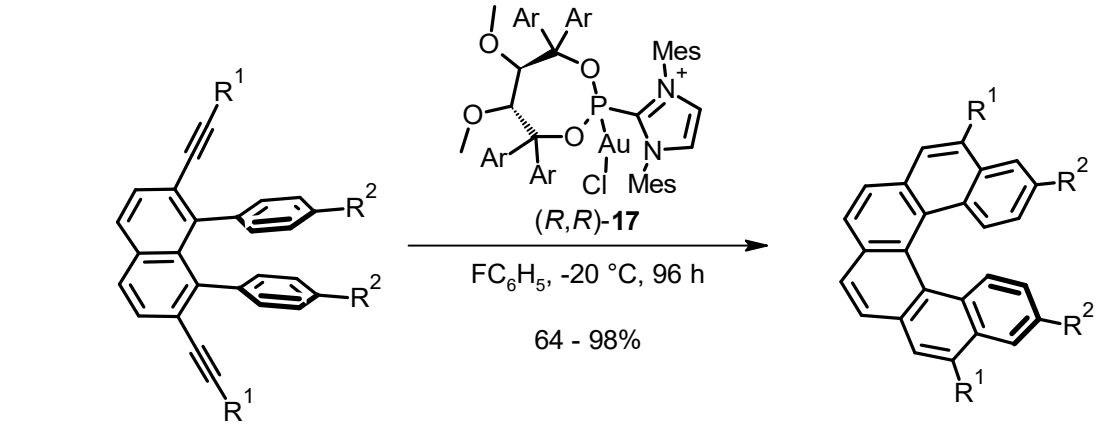

16

Ar = 4-$CF_3(C_6H_5)$

(+)-(*P*)-**18**
11 examples
up to 99% *ee*

Scheme 4: Au-catalyzed enantioselective synthesis of substituted [6]helicenes.

A diastereoselective approach towards homochiral helical compounds was developed by Starý and Stará (**Scheme 5**).[30] Triyne (*R*,*R*)-**19** underwent Co-catalyzed [2+2+2] cycloisomerization to form oxa[5]helicene (-)-(*M*,*R*,*R*)-**20** with uniform helicity. The syntheses of the corresponding oxa[6] and oxa[7]helicenes were also feasible. The stereochemistry of this reaction is controlled by a 1,3-allylic type strain (depicted in red) between the methyl and the tolyl groups. The methyl groups can either be oriented pseudoequatorially in a molecule having (*P*) helicity ((+)-(*P*,*R*,*R*)-**20**, isomer with higher energy) or pseudoaxially in a molecule with (*M*) helicity ((-)-(*M*,*R*,*R*)-**20**, isomer with lower energy). If the energy difference between two stereolabile diastereomers is significant (>2.7 kcal·mol^{-1}), in thermodynamic equilibrium the ratio between the two possible isomers will be >99 : <1. In this scenario, any stereochemical outcome of the actual cyclization reaction presented in **Scheme 5** is overwritten by the post-cyclization equilibration process provided that the temperature and time are sufficient to overcome the interconversion barrier of the transition state (TS, *i.e.* 11.9 kcal·mol^{-1} from (+)-(*P*,*R*,*R*)-**20** to (-)-(*M*,*R*,*R*)-**20**). Oxahelicene (-)-(*M*,*R*,*R*)-**20** was obtained diastereomerically pure after 20 min at 180 °C using a microwave reactor.

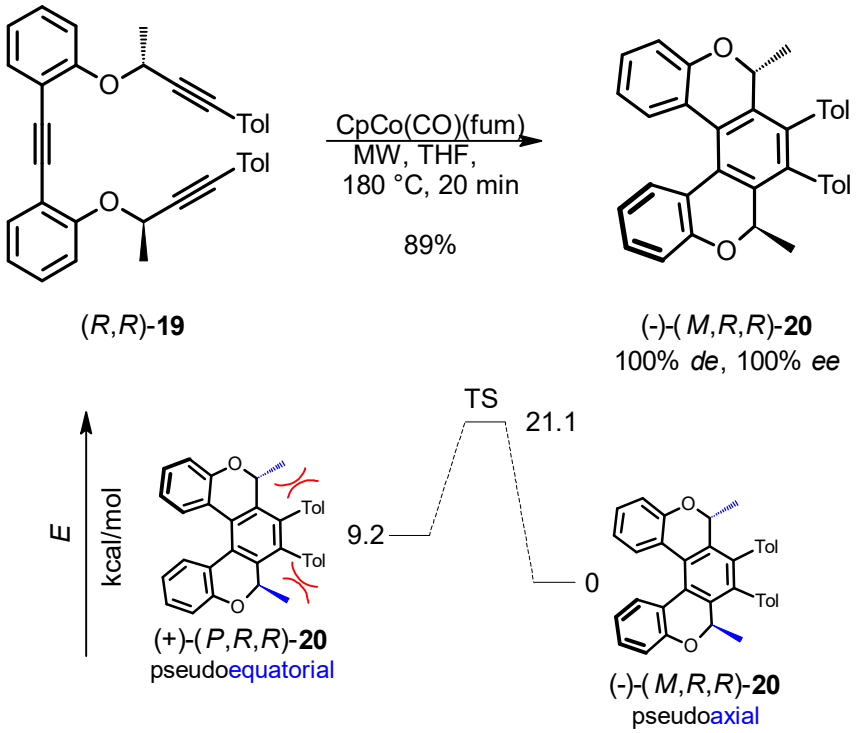

Scheme 5: Diastereoselective synthesis of oxahelicenes.

Later, Starý and Stará published an extension of this concept towards fully aromatic carbohelicenes using traceless chiral auxiliary.[31] **Scheme 6** illustrates the key steps of the synthesis of enantiomerically pure [6]helicene (+)-(*P*)-**23**. The central chirality of triyne (*RS*,*R*)-**21** induces helical chirality into tetrahydrohelicene (+)-(*P*,*RS*,*R*)-**22**. Relative energies of the four isomers of tetrahydrohelicene **24**, a simplified model of **22**, demonstrate that one chiral center is enough to fully control its helicity. Again, the important stereocenter is the one providing the 1,3-allylic type strain with the tolyl group (position C^9, red), while the effect of the other stereocenter (positions C^5, blue) is negligible due to the small 1,3-allylic type strain between the H and the OH group (blue), so this can be racemic. After the acid-catalyzed removal of the OMOM groups, fully aromatic (+)-(*P*)-**23** can be obtained with uniform helicity.

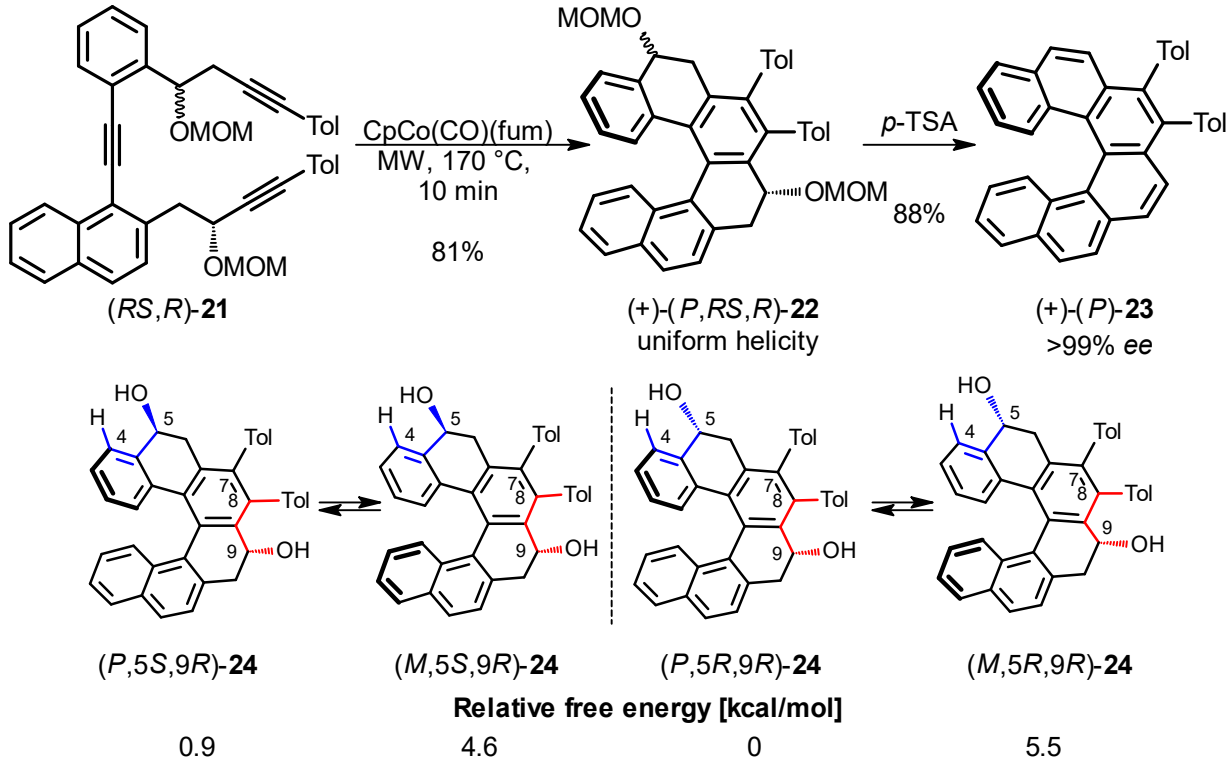

Scheme 6: Diastereoselective synthesis of carbohelicenes.

Application of Helicenes

Due to their outstanding physicochemical and optical properties helicenes are applied in many different fields[32] such as polymers,[33, 34] molecular machines,[35] dye

materials, [36] molecular recognition, [37, 38] Langmuir Blodgett films, [39, 40] organic electronics[41],[42] and liquid crystals[43].

After the development of scalable synthetic protocols, helicene chemistry has found increasing application in a field predestined for inherently chiral molecules, asymmetric catalysis. **Figure 6** shows selected examples of fully aromatic, helically chiral ligands or complexes. The most common way how to introduce the helicene scaffold into a catalyst is *via* a phosphine ligating group. The first example of a helicene based asymmetric catalytic system was reported only in 1997. Reetz *et al.* published helically chiral diphosphine (+)-(*P*)-**25**, which was obtained enantiomerically pure by resolution of its bromo precursor *via* chiral HPLC.[44] After the *in situ* formation of its Rh(I) complex, enantioselective hydrogenation of itaconic acid ester was performed with moderate enantioselectivity. Later this reaction was reexamined by Yamaguchi *et al.* employing bis(helicenol) based chiral ligand (+)-(*M*,*M*,*S*,*I*)-**26**, obtaining the hydrogenation product with an excellent *ee*.[45] Phosphite (+)-(*M*,*M*,*S*,*I*)-**26** possesses four stereogenic elements, two helicenes, one chiral biaryl axis and the central chirality of the menthyl unit. Several possible isomers were investigated and the (+)-(*M*,*M*,*S,I*) isomer turned out to be the most successful. Complex (+)-(*P*,S_p,*I*)-**27** represents one example of several helically chiral phosphine-Au catalysts reported by Voituriez and Marinetti *et al.* in 2014.[46] A menthyl chiral auxiliary was embedded into the phosphines in order to diastereoselectively obtain ligands with uniform helicity. The efficiency of the novel complexes was demonstrated in Au-catalyzed 1,6-enyne cycloisomerization, providing high enantioselectivities. In 2016 Suemune and Usui published two [5]helicenes with PPh_2 as a ligating moiety, (+)-(*P*)-**28** and its 7,8-dihydro derivative (+)-(*P*)-**29**.[47] Both ligands were found to be conformationally stable due to the steric hindrance provided by the phosphine substituent at the C^1 position. Furthermore, the π-donating character of the helical scaffold was envisaged to have chelating effects on metal centers. Compound (+)-(*P*)-**28** was found to be efficient in promoting Pd-catalyzed asymmetric Suzuki-Miyaura couplings of biaryls, whereas (+)-(*P*)-**29** was applied in asymmetric allylation reactions of indoles and etherifications of alcohols achieving high *ee*'s in both cases.

Besides phosphines, helically chiral compounds with other ligating groups were published. [5]HELOL (+)-(*P*,*P*,*S*)-**30** was prepared by Katz and co-workers as an analogy to the widely used BINOL[48] ligand.[49] Unlike BINOL, the [5]HELOL has two

independent chiral domains, the helicity and the biaryl axis. The diastereomerically pure form of (+)-(*P*,*P*,*S*)-**30** was obtained *via* diastereoselective resolution of the corresponding camphanate esters. The free diol was applied in the enantioselective addition of diethylzinc to aldehydes, surpassing commercially available BINOL in both stereoselectivity and yield. An NHC-Ir complex was published in 2016 by Crassous *et al.*[50] Cycloiridiated complex (P,S_{Ir})/(M,R_{Ir})-**31**, exhibiting the helicene moiety and the Ir-center as stereogenic elements, was synthesized by employing a racemic [6]helicene containing imidazolium salt precursor. Nevertheless, compound (P,S_{Ir})/(M,R_{Ir})-**31** was obtained diastereomerically pure. The racemic (P,S_{Ir})/(M,R_{Ir})-**31** spontaneously resolved into homochiral crystals of (P,S_{Ir})-**31** and the structure was confirmed *via* x-ray analysis. Although the novel NHC-metal complex was not applied to enantioselective catalysis, interesting electronic and chiroptical properties were observed. So far, only a few examples of helically chiral NHC-metal complexes are known.[51, 52, 53, 54, 55, 28]

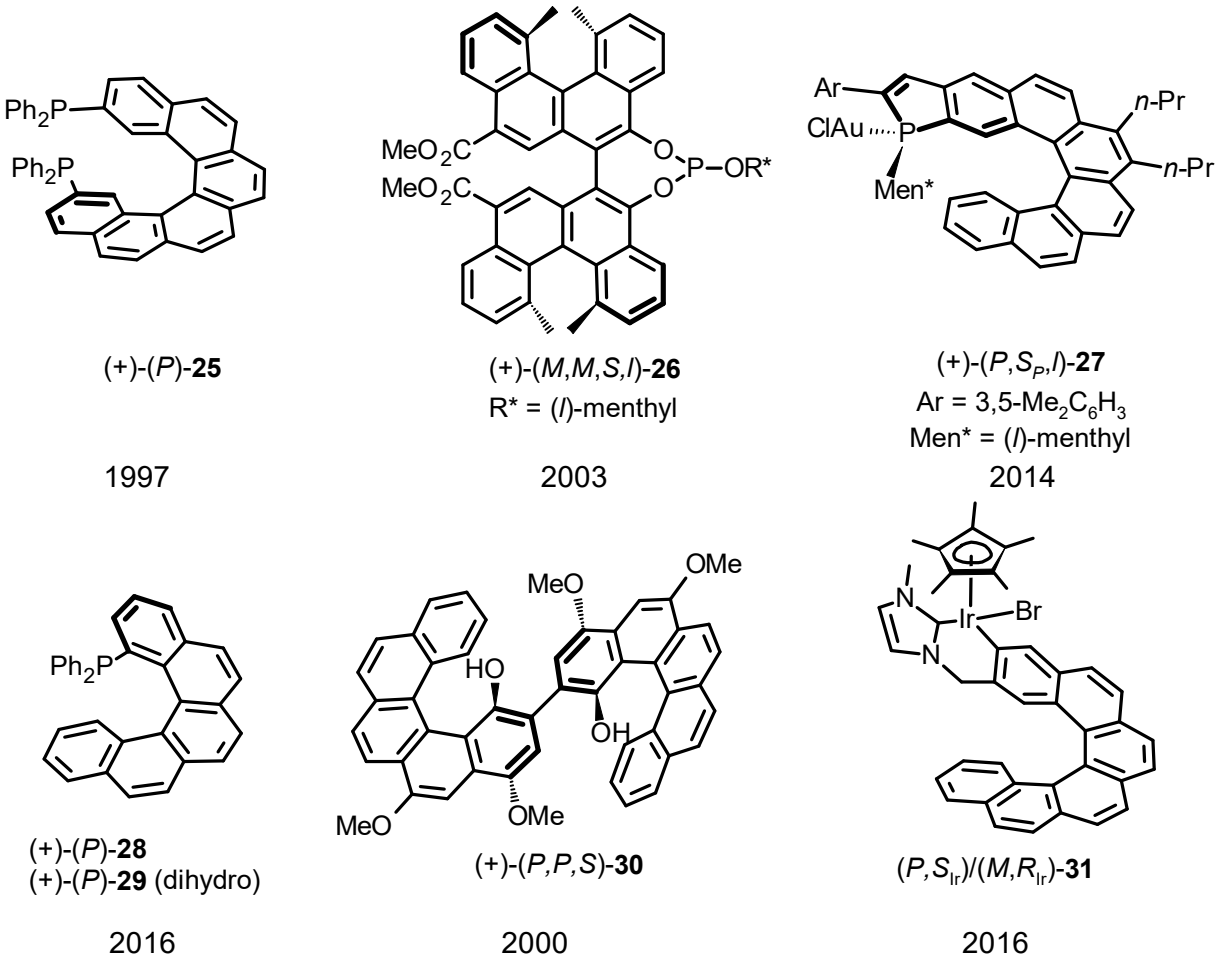

Figure 6: Selected helically chiral ligands and catalysts.

1.3 N-Heterocyclic Carbenes

Structural Features

Before the first isolation of a free carbene, neutral compounds featuring a divalent carbon atom with six-electron valence shell were only considered as highly reactive transient intermediates and laboratory curiosities. However, in 1988 Bertrand *et al.* published the first isolation of a carbene stabilized by adjacent silicon and phosphorus substituents.[56] Inspired by earlier work on metal carbene complexes[57, 58] Arduengo *et al.* reported the first 'bottleable', crystalline carbene.[59] **Figure 7** shows carbene **32** which is incorporated in a nitrogen heterocycle and, therefore, called an N-heterocyclic carbene (NHC). The remarkable stability of this compound class is the result of a steric and electronic stabilization of the C^2 carbene caused by its environment.[60]

The two adamantyl substituents at the nitrogen atoms provide bulkiness around the carbene (orange lines) and thus disfavor kinetic dimerization to the corresponding olefin (Wanzlick equilibrium)[61]. Therefore, most NHCs feature spacious substituents adjacent to the carbene. An even stronger beneficial interaction for the C^2 carbene is the electronic stabilization by the neighboring nitrogen atoms. NHCs such as **32** exhibit a singlet ground state configuration since the cyclic nature forces them into a bent sp^2-like arrangement with angles around 100 – 110°, whereas triplet carbenes exhibit angles around 130 – 150° or an *sp*-like structure.[62, 63] The HOMO is best described as a formally sp^2 lone pair and the LUMO as an empty *p*-orbital. N^1 and N^3 stabilize C^2 with their positive mesomeric effect on the empty *p*-orbital (blue arrows) and electron withdrawing effect on the σ-bond (red arrows). With this "push pull" interaction they donate electron density into the empty *p*-orbital and lower the energy of the occupied σ-orbital (a larger energy gap between HOMO and LUMO is beneficial for the singlet state). Due to the lone pair situated in the plane of the heterocyclic ring and the mesomerically decreased electrophilicity of the empty *p*-orbital NHCs are nucleophilic, which is in contrast to most transient carbenes, which

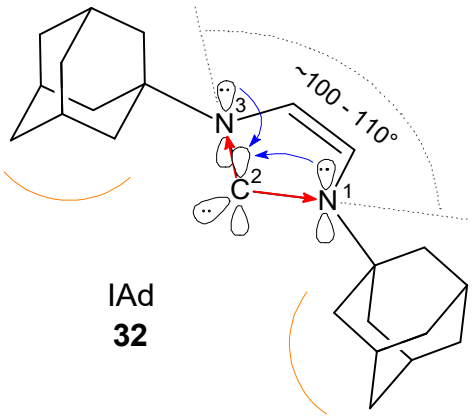

IAd
32

Figure 7: The first isolated N-heterocyclic carbene.

are typically electrophilic. As a consequence, the compound class of **32** is prone to act as σ-donors, which enables the formation of an NHC-metal bond with a high dissociation energy compared to many common ligands including the well-known phosphines. [64] The empty *p*-orbital of the carbene allows π-backbonding to compensate excess charge from the metal atom. This effect was found to be negligible,[65, 66] although views on that topic differ.[67]

The "I" in IAd (**32**) is an abbreviation for imidazolylidene (**Figure 8**, compound **34**) followed by the abbreviation (Ad in IAd) of the substituent on the nitrogen atoms. The partially aromatic nature of **34** (see ylide **33**) is beneficial for its stability in comparison to the saturated version **35** where the corresponding ylide structure is non-aromatic. Due to this effect, which is calculated to be around 25 kcal·mol^{-1}, imidazolylidenes (**34**) allow less steric demand of the R groups than their saturated analogues (**35**). The simple methyl-substituted NHC, IMe was found to be persistent in solution.[68] In addition to imidazole and imidazoline, rings with other heteroatoms[69] incorporated such as sulfur (**36**) or oxygen (**37**) are also accessible and rings with only one nitrogen atom (cyclic (alkyl)(amino)carbenes, CAACs, **38**)[70] are receiving rising attention (**Figure 8**).

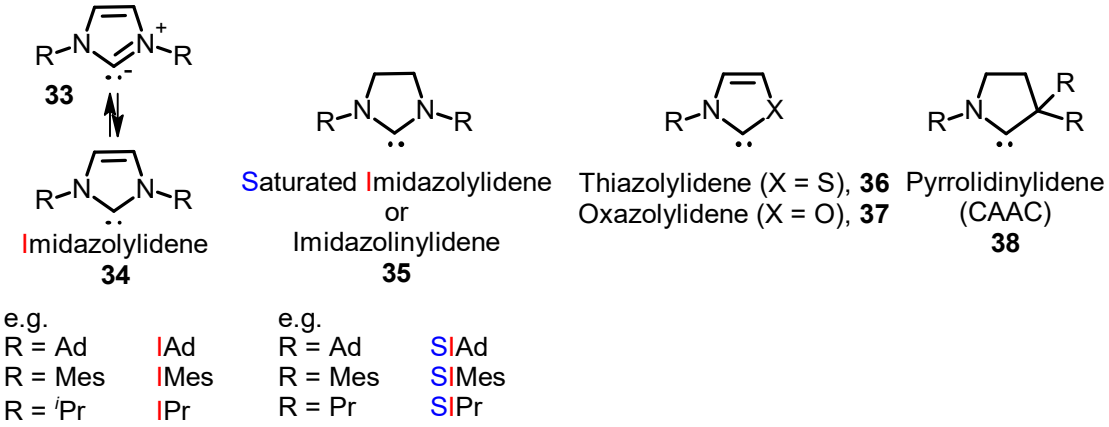

Figure 8: Different N-heterocyclic carbenes.

Synthesis

The most straightforward ways to obtain NHCs is by deprotonation of the corresponding azolium salt. The synthesis of these precursors benefits from a long history of research on heterocyclic compounds. For most NHCs the facile access to a variety of steric and electronic modifications is enabled by simply changing the

starting material. Various modular synthetic strategies have been developed.[71] **Scheme 7** shows the synthesis of imidazolium salts with identical substituents on the two nitrogen atoms (**39**). The acid-catalyzed condensation of primary amine, glyoxal and formaldehyde can either be done in a multicomponent one-pot fashion, or through isolation of the diimine **40**. Hintermann proposed a mechanism involving a 1,5-dipolar electrocyclization for this type of reactions.[72]

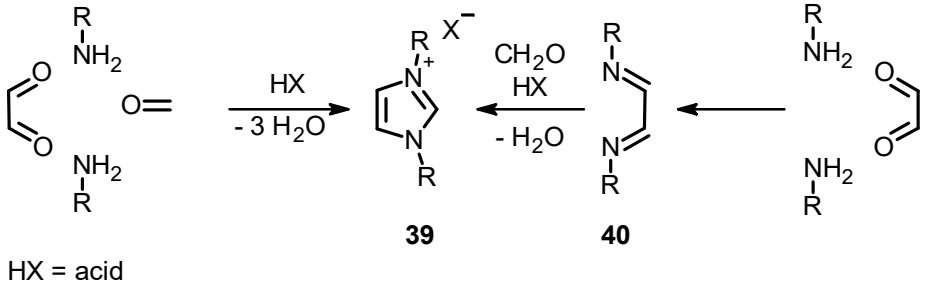

Scheme 7: Synthesis of symmetrical imidazolium salts.

Imidazolium salts with different substituents on the two nitrogen atoms are available as well. A modular approach developed by Fürstner *et al.* provides access to a variety of substitution patterns on the nitrogen and the $C^{4,5}$ atoms of **43** (**Scheme 8**).[73] Oxazolium salt **41** bearing substituent R^1 on the nitrogen atom is reacted with a primary amine with R^2 substituent. In the next step of the one-pot procedure dihydroimidazolium salt **42** undergoes acid catalyzed elimination to form the desired unsymmetrical imidazolium salt **43**.

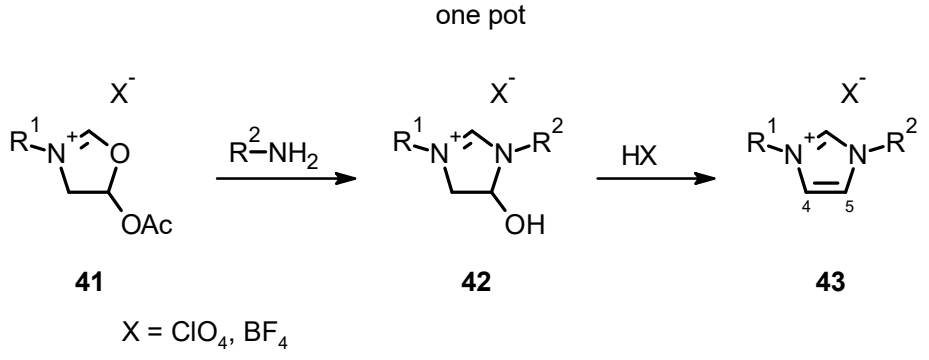

Scheme 8: Synthesis of unsymmetrical imidazolium salts.

NHC-Metal Complexes

Since Arduengo's discovery[59] the research in this field has exploded and an enormous amount of NHC-metal complexes have been reported.[74, 75, 76] Most of the complexes involve the coordination of the carbene to a σ-accepting orbital of a transition metal. The nature of this bonding has been described in comprehensive studies on the topic.[77, 78] N-heterocyclic carbenes also brought a lot of innovation into the design and tunability of ligands. For example, in olefin metathesis the NHC ligand in the second generation Grubbs catalysts (**45**) dissociates much less rapidly from the metal center than the phosphine ligand in the first generation catalyst (**44**) and, therefore, exhibits improved thermal and oxidative stability. Furthermore, the mesityl (Mes) groups of the NHC in **45** are projected towards the coordination sphere of the metal in contrast to the cyclohexyl (Cy) groups of phosphine in **44** and, therefore, induce different steric effects.[79] The second generation Grubbs catalyst shows two orders of magnitude higher activity in olefin metathesis than its first generation antecessor. For this type of catalyst the efficiency depends on initiation (dissociation of one PCy_3), PCy_3 rebinding, reaction of a 14-electron ruthenium species with an olefin and the rate of catalyst decomposition.[80] There are several studies which provide explanations for the difference in reactivity.[81, 82, 83, 84, 85]

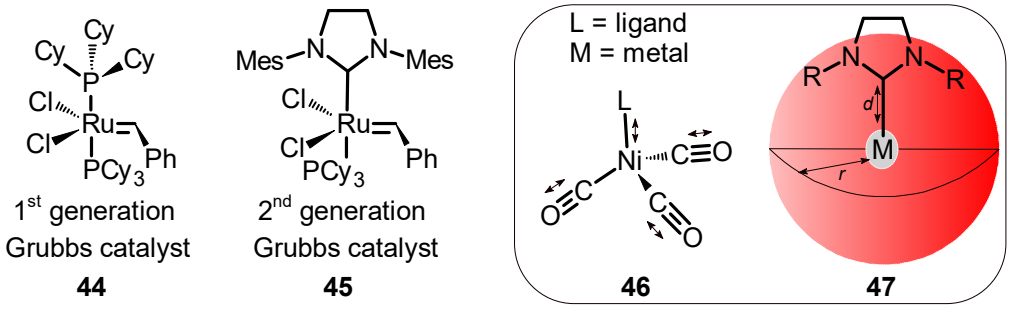

Figure 9: Comparison of phosphine and NHC ligands.

Molecular descriptors for a quantitative evaluation of ligands can be split in two categories. Either they influence the catalytic behavior by altering the electronic status of the metal or by constraining the space around the metal. The two most commonly used parameters are the Tolman electronic parameter (TEP)[86] and the buried volume ($\%V_{bur}$)[87] for sterics introduced by Nolan, Cavallo and co-workers. The TEP describes the electron-donating ability of a ligand. It derives from the carbonyl stretching frequency in model transition metal carbonyl complexes (**44**). The more

electron-donating the ligand of interest, the more electron density is transferred onto the metal which then increases π-backbonding towards the carbonyl ligands. As a result, their bond order and infrared stretching frequency are decreased. Instead of the initially used [LNi(CO)$_3$] model **46**, less toxic complexes, *e.g. cis*-[LIrCl(CO)$_2$] and *cis*-[LRhCl(CO)$_2$], are more frequently used nowadays. To quantify the steric properties of a ligand such as the NHC in complex **47** (**Figure 9**), a sphere of an arbitrarily defined radius (*r*, typically 3.0 or 3.5 Å) with the metal atom at its center and the carbene-metal bond distance *d* of 2 Å (this parameter can also be derived from calculations or crystallographic data) is drawn. The percentage of the sphere's volume occupied by the NHC-ligand is called the buried volume, %V_{bur}.

1.4 Asymmetric Catalysis

History, Principles and Significance

"I shall, therefore…call it that body's catalytic force, the decomposition of other bodies by this force catalysis, just as we signify by the word analysis the separation of the constituents of bodies by the usual chemical affinities." (Jöns Jacob Berzelius, 1835) The word catalysis (derives from Greek *katálȳsis*, dissolution) in 1835 was introduced into science inspired by the work of Döbereiner, who found platinum to catalyze the reaction of H_2 with O_2 to H_2O. Berzelius at that time viewed catalysis as a special force and a catalyst as an agent which causes change without being changed itself.[88]

Decades of extensive research[89] brought light into the mystic nature of catalysis and it became an essential part of science. Several chemistry Nobel Prizes were related to catalysis with the most recent ones in 2010 (R. F. Heck, A. Suzuki and E. Negishi "for palladium-catalyzed cross couplings in organic synthesis"), 2005 (R. R. Schrock, R. Grubbs and Y. Chauvin "for the development of the metathesis method in organic chemistry") and 2001 (B. Sharpless, W. S. Knowles and R. Noyori "for their work on chirally catalysed hydrogenation reactions").[90] "Asymmetric catalysis is a type of catalysis in which a chiral catalyst directs the formation of a chiral compound such that formation of one particular stereoisomer is favored. Since the catalyst is not consumed in this process it may be used in a substoichiometric quantity – potentially improving efficiency and avoiding waste."[91]

Scheme 9 illustrates the principle of asymmetric catalysis. First, a chiral catalyst (the different colors symbolize the asymmetric environment, in which the chiral information is stored) coordinates the substrates (can also be just one molecule), which arrange in the energetically preferred areas of the catalyst. These molecules then react in the asymmetric sphere where the chiral information is transferred from the catalyst to the substrates. After elimination, the product, which carries the chiral information, is released. Different terms can be used for stereoselectively catalyzed processes. The exact definitions of the terms asymmetric, enantioselective and diastereoselective depends on the point of view. In this work, asymmetric and enantioselective catalysis are considered as synonyms whereas diastereoselective catalysis is a special case which describes the formation of one thermodynamically preferred diastereomer over the other(s). In asymmetric (or enantioselective) catalysis the preference of one enantiomer, which is thermodynamically equal to the other, is based on the formation of diastereomeric intermediates or transient species with the chiral catalyst during the catalytic cycle.

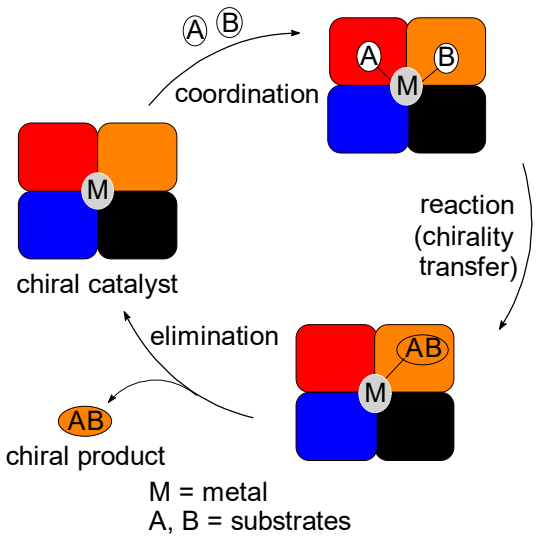

Scheme 9: Principles of asymmetric catalysis.

As discussed in Chapter 1.1, life on our planet depends on inherently dissymmetric biological processes, where chiral host molecules interact with enantiomeric guest molecules in different ways. For example, the chiral receptor sites of the olfactory system can tell us the difference between two enantiomers. Therefore, our brain recognizes the smell of (*R*)-carvone ((*R*)-**48**) as a sweetish mint flavor like spearmint leaves and (*S*)-carvone ((*S*)-**48**) as a spicy aroma like caraway seeds.[92] The same thing happens with pharmaceuticals in our body where the wrong enantiomer can have undesirable effects on our system. A very tragic and prominent example is Thalidomide. The drug was administrated *i.a.* to alleviate morning sickness of pregnant women in the 1960's. (*R*)-Thalidomide ((*R*)-**49**) has sedative effects on the patient, whereas the (*S*)-**49** enantiomer is teratogenic. As a result, thousands of infants were born with phocomelia.[93] The US Food and Drug Administration (FDA)

today recommends the elaboration of biological activity profiles of each enantiomer for racemic drugs and promotes the development of new chiral pharmaceuticals as single enantiomers.[94] Therefore, the chemical industry highly depends on the development of synthetic methods to obtain enantiomerically pure compounds.[95]

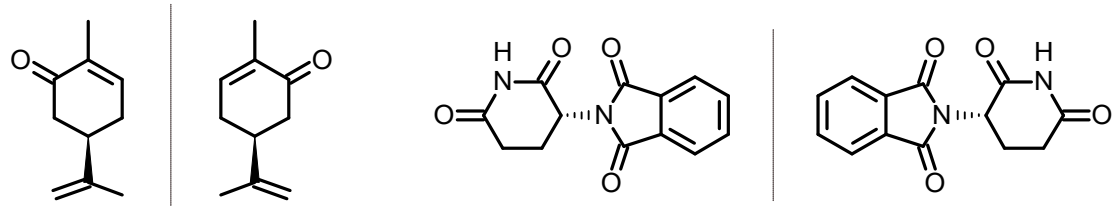

(*R*)-carvone mint odor | (*S*)-carvone caraway odor | (*R*)-thalidomide sedative | (*S*)-thalidomide teratogenic

(*R*)-**48** | (*S*)-**48** | (*R*)-**49** | (*S*)-**49**

Figure 10: Different biological activities of enantiomeric compounds.

Selected Examples

Fundamental research plays a key role in providing a broad pool of tools for any potential application on asymmetric catalysis. First, simple model systems are chosen to investigate the basic principles of an asymmetric process in order to develop suitable catalysts and optimize their design. Comprehensive review articles and book chapters on the topic are available[96, 97] and some examples related to this work are mentioned below.

Olefin metathesis is a widely applied tool in construction of complex structures *via* C-C-bond formation.[98, 99, 100] A general mechanism of the process was introduced by Chauvin and Hérisson.[101] Asymmetric metathesis does not involve the formation of an sp^3-hybridized stereogenic center. Instead, the chiral information is induced indirectly *via* desymmetrization of an achiral compound (**Scheme 10**). The chiral catalyst discriminates between enantiotopic groups of prochiral meso compounds (**50**, **52**, **54**) to release enantiomerically enriched chiral products (**51**, **53**, **55**) after the catalytic cycle. The most common reactions of this type are asymmetric ring-closing metathesis (ARCM) and asymmetric ring-opening cross metathesis (AROCM). Examples of asymmetric cross metathesis (ACM) are also described.[102]

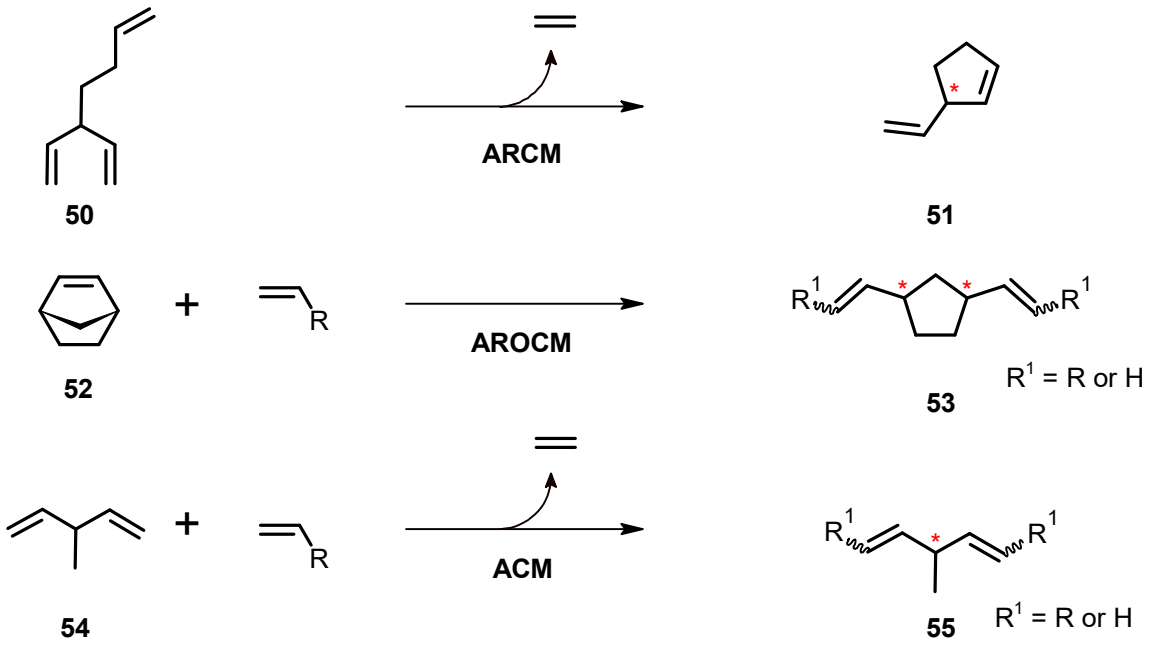

Scheme 10: Asymmetric metathesis reactions.

Selected prominent examples of chiral Ru-NHC metathesis catalysts are illustrated in **Figure 11**. The first chiral Ru catalyst for asymmetric olefin metathesis was reported by Grubbs *et al.* in 2001.[103] C_2-symmetric chloride **56** showed low enantioselectivities in ARCM. The *in situ* substitution of the chlorides with iodides led to a dramatic increase in selectivity. With the bulkier iodides in complex **57**, high *ee* values up to 90% were achieved. Collins and co-workers published C_1-symmetric complex **58** with a sterically less demanding methyl group on one nitrogen atom and more bulky *tert*-butyl groups in the NCH backbone.[104] With **58** high *ee* values of 82% were obtained for the same transformation compared to **57** without the *in situ* generation of an iodo species. The asymmetric periphery of the Ru center in **56**, **57** and **58** is created due to a so called "gearing effect".[105] The chirality installed in the stereogenic centers (C^4 and C^5) of the NHC backbone is transferred to the substituents of the nitrogen atoms. The unsymmetrically substituted aryl groups (*ortho* ^{i}Pr) reside on the face opposite to the bulky substituents in C^4 and C^5 positions. As a result, one of the enantiotopic coordination hemispheres of the Ru becomes sterically more congested compared to the other, which leads to an asymmetric environment. This principle has been adopted in the design of catalyst **59**, reported by Blechert *et al.*[106] By tethering the N-aryl ring to the chiral center in the NHC backbone it is twisted "out of plane" (the plane perpendicular to the NHC ring). Catalyst **59** provides high *ee*'s up to 98% in

AROCM. In 2002 Hoveyda and co-workers reported an alternative concept of installing chirality in a metathesis catalyst.[107] C_1 symmetric complex **60** lacks any backbone substitution but incorporates an axially chiral bidentate NHC. The alkoxy group of the chiral binaphthyl substituent at the nitrogen diastereoselectively chelates the Ru which creates a stereocenter at the metal (stereogenic-at-Ru catalyst). Catalyst **60** shows diminished reactivity due to the decreased Lewis acidity of the metal and high steric congestion around the Ru. Nevertheless, high enantioselectivities up to >98% were obtained and the catalyst could be recycled. Sterically and electronically modified versions with enhanced activity were published later.[108]

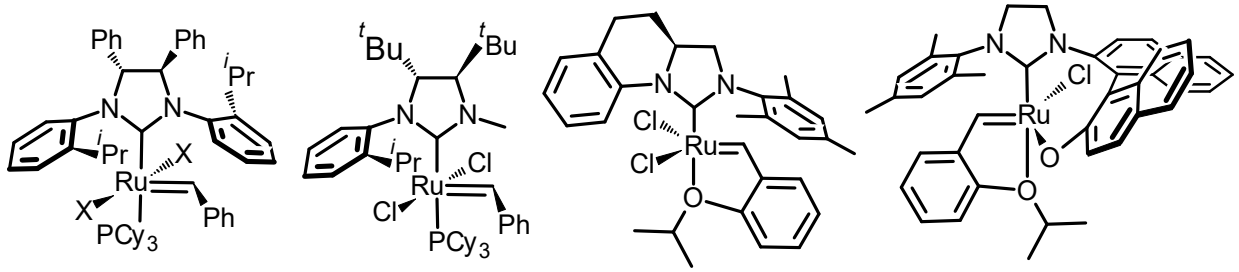

Grubbs 2001 | Collins 2007 | Blechert 2011 | Hoveyda 2002

X = Cl, **56**
X = I, **57**

58 | **59** | **60**

Figure 11: Selected chiral Ru-NHC metathesis catalysts.

The Suzuki-Miyaura coupling is by far the cross-coupling reaction with the highest number of publications per year.[109] The reaction employs organoboron reagents and sp^2-electrophiles as coupling partners. Boronic acids, which possess several advantages over other organometallic species, are the most prevalent. An enormous library of boronic acids is commercially available and most of the compounds exhibit stability towards air, moisture and heat. The mechanism of this reaction with a tremendous potential in C-C-bond formation follows the general principle of cross coupling reactions.[110] An enantioselective variant of the Suzuki-Miyaura coupling involves the formation of axially chiral biaryls which are valuable organic compounds due to their abundance in natural products and application in asymmetric catalysis.[111, 112] However, atropisomeric biaryls are distinguished from ordinary rotamers by virtue of a minimum rotational barrier of 23 kcal·mol^{-1} for the interconversion of enantiomers.[113] Therefore, the chirality of these compounds depends on a high degree of steric hindrance in the *ortho* positions which makes the

coupling between two aryl units challenging. **Scheme 11** illustrates the general synthesis of atropisomerically stable biaryls *via* Suzuki-Miyaura coupling. A Boronic acid **61** is coupled with an electrophile **62** where a variety of leaving groups X are possible. The most common metals employed in this transformation are Pd and Ni. In order to be chiral, **63** must possess two different *ortho* substituents R^1 and R^2.

Potent catalysts for this type of transformation are *e.g.* the Pd-PEPPSI (Pyridine Enhanced Precatalyst Preparation, Stabilization (and) Initiation) complexes reported in 2006 by Organ and co-workers.[114] Complex **64** (IPr PEPPSI) with the IPr ligand is commercially available. Only a few chiral versions are available up to date. The first were published by Shi and co-workers, although they did not test their catalysts in asymmetric transformations. [115] Kündig *et al.* published in 2014 the first application of chiral Pd-PEPPSI complexes in enantioselective catalysis. [116] Catalyst **65**, which was reported among four other complexes, showed good activities and moderate to good selectivities in asymmetric Suzuki-Miyaura coupling. The selectivities highly depended on the substrates used. The best example was the coupling of 1-bromo-2-methylnaphthalene with 1-naphthylboronic acid, where the atropisomeric product was obtained in 80% *ee*. Recently, Fukuzawa *et al.* reported a chiral triazolylidene-Pd-PEPPSI complex.[117] The ferrocene-based planarly chiral **66** gave moderate to good yields and *ee* values up to 75%. Sakar *et al.* also reported chiral triazolidene-Pd-PEPPSI complexes but did not study their enantioinduction.[118]

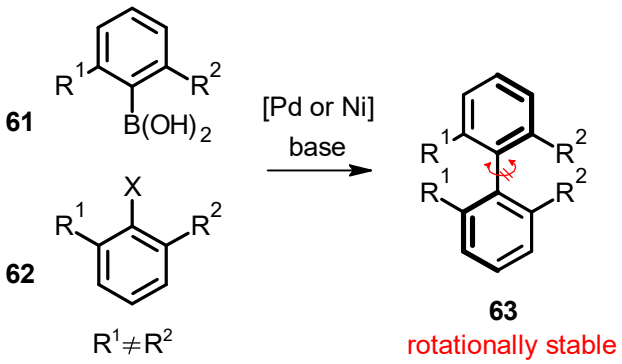

Scheme 11: Synthesis of atropisomers *via* Suzuki-Miyaura coupling.

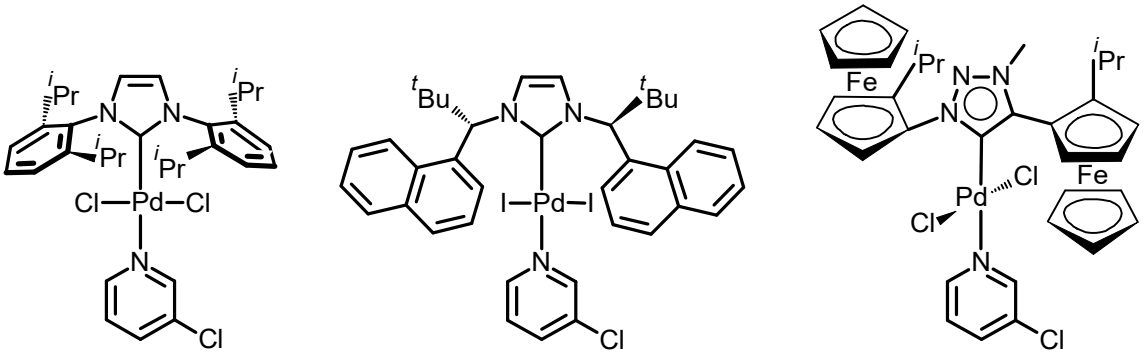

Organ 2006 **64** | Kündig 2014 **65** | Fukuzawa 2017 **66**

Figure 12: Selected Pd-PEPPSI catalysts.

2. Objectives

As shown in Chapter 1.2, helicenes have proved their potential as chiral ligands in enantioselective catalysis. The NHC's discussed in Chapter 1.3 are nowadays a well-established class of compounds and became indispensable in the ligand portfolio of enantioselective catalysis (Chapter 1.4). The aim of this work is to combine the three topics. Therefore, enantiomerically pure helicene-bearing NHC's are first synthesized and then ligated within transition metal complexes. Such complexes are further applied in enantioselective catalysis in order to explore the power of stereoinduction caused by the helically chiral NHC ligands in the asymmetric process (**Scheme 12**).

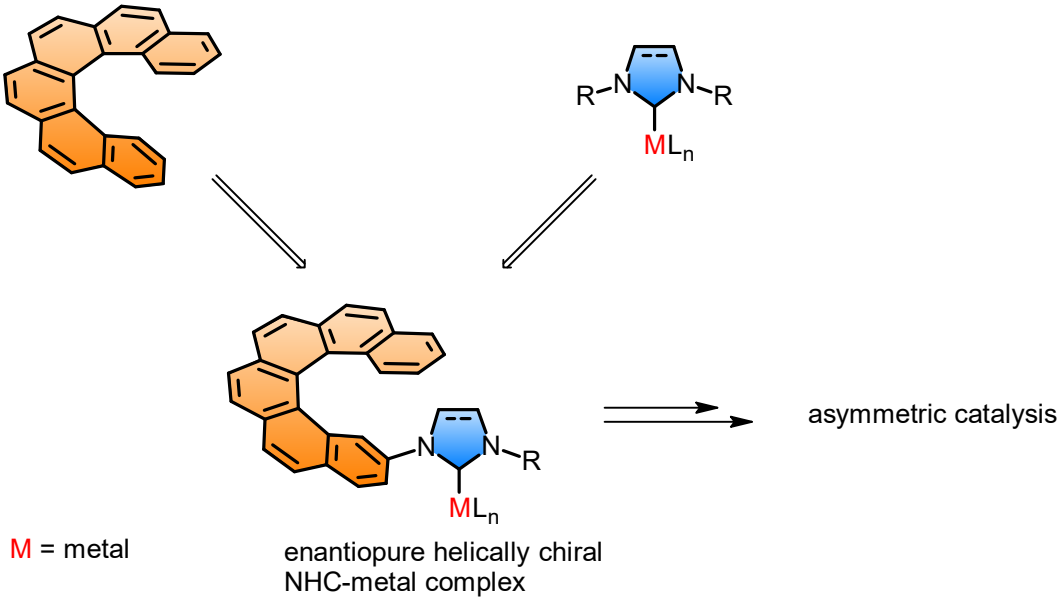

Scheme 12: Objectives of the Thesis.

Scheme 13 illustrates the retrosynthesis of helically chiral NHC-metal complexes such as (*M*)-**67**, which can be derived from its imidazolium salt precursors (*M*)-**68**. Unsaturated imidazolium salts were chosen for the simplicity of their preparation compared to their saturated imidazolinium analogs. In order to have a conformationally stable helical scaffold with uniform helicity, amino[6]helicene (*M*)-**69** was designed after a recently published protocol of Starý and Stará.[31] This helicene can be constructed *via* [2+2+2] cycloisomerization from the centrally chiral triyne (*RS*,*S*)-**70**. This triyne is accessible by Sonogashira cross-coupling of enantiopure halide (*S*)-**72** and racemic alkyne *rac*-**71**. For the efficient application of (*M*)-**67** in asymmetric catalysis sufficient amount of the amino[6]helicene (*M*)-**69** is required.

Therefore, a gram-scale synthesis of (*M*)-**69** needs to be developed and optimized. Importantly, the optically pure amino[6]helicene building block can be prepared easily in either of its stereochemical configurations (*P* or *M*) depending on the chirality of the starting alkyne **72** (*R* or *S*).

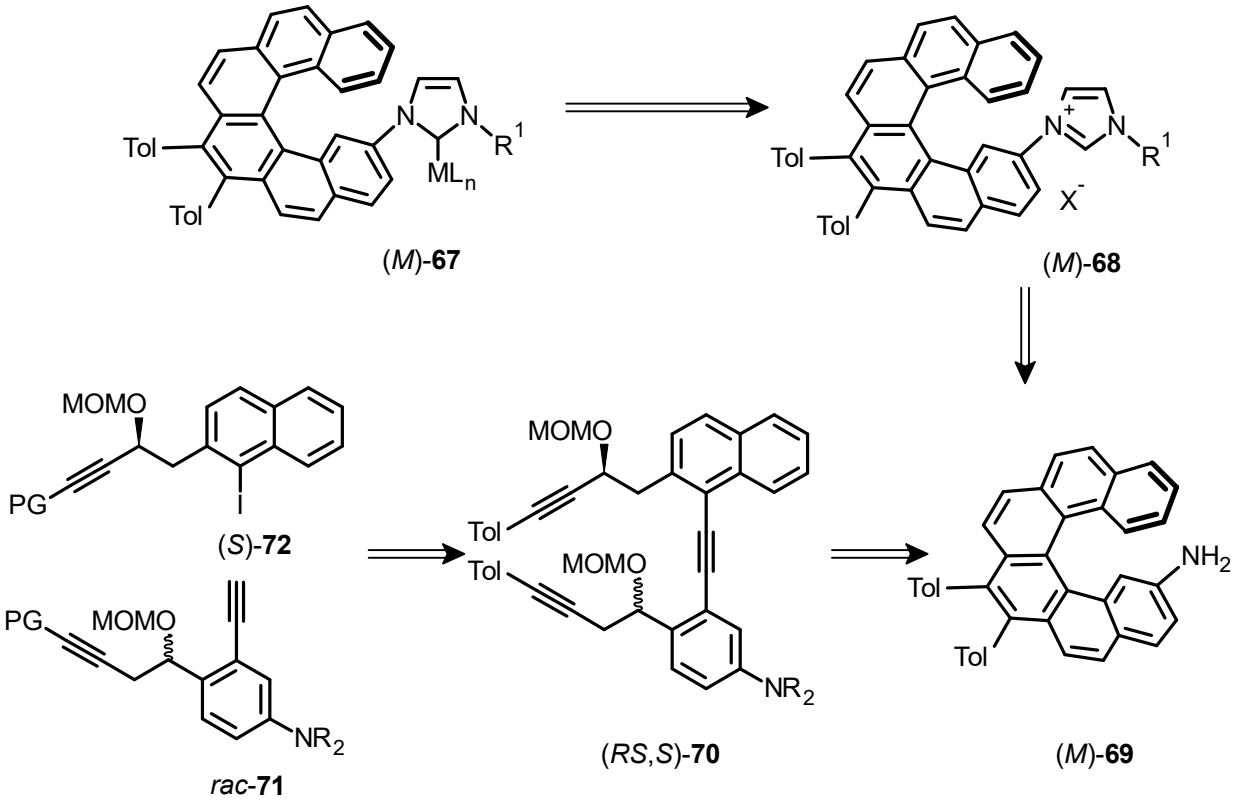

Scheme 13: Retrosynthetic scheme for helically chiral NHC-metal complexes.

3. Results and Discussion

3.1 Synthesis of Helicenes

Enantiopure Amino[6]helicene

Synthesis of Racemic Diyne Building Block *rac*-81

The first goal was to obtain the building block *rac*-**71** which can be synthesized from commercially available aniline **75**. After a retrosynthetic analysis, the strategy to formylate **75** to **74**, add the propargyl moiety to the aldehyde to generate *rac*-**73** which then undergoes MOM-protection and Sonogashira coupling to the desired *rac*-**71** was developed (**Scheme 14**).

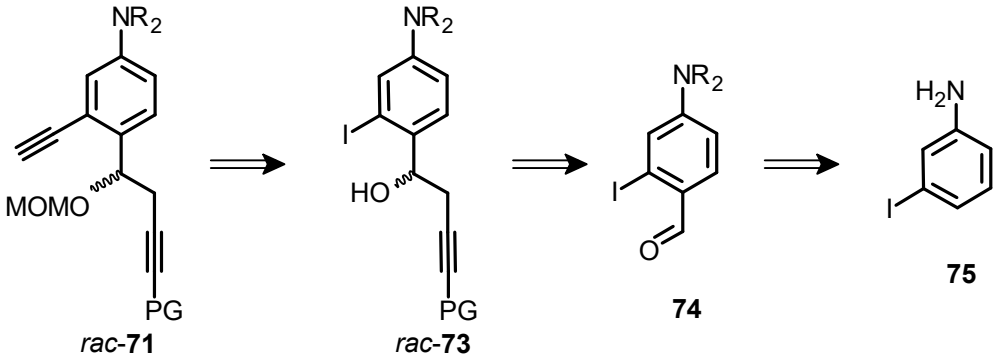

Scheme 14: Retrosynthesis of building block *rac*-**71**.

Direct formylation of unprotected aniline **75** was not possible due to side reactions of the free amino group with formylating agents. Therefore, **75** was first doubly benzyl-protected and then formylated under Vilsmeier-Haack conditions to obtain **77** in high yields for both steps. Upscaling proceeded without any problems.

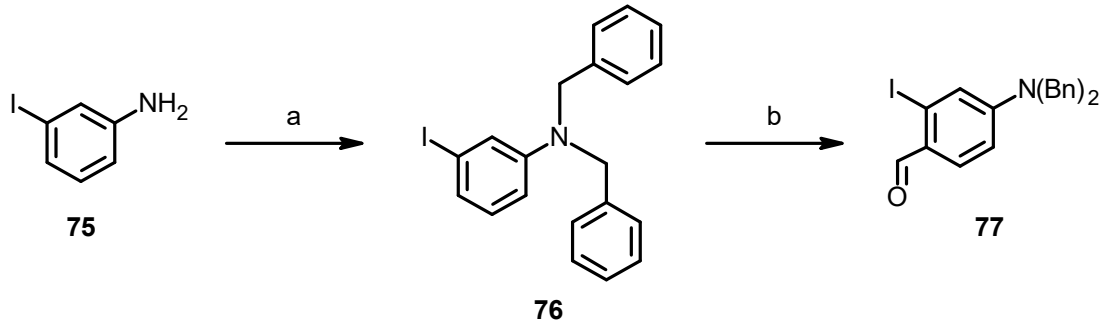

a) BnBr (4.0 equiv.), K_2CO_3 (5.0 equiv.), EtOH/H_2O 1:1, reflux, 10 h, 97%; b) $POCl_3$ (6.5 equiv.), DMF (5.0 equiv.), 0 °C, 1 h, then 50 °C, 5 h, 95%.

Scheme 15: Synthesis of aldehyde **77**.

The installation of the first alkyne unit was conveniently done by the addition of TIPS-propargyllithium to the aldehyde group of **77** so that *rac*-**78** could be obtained in high yield (**Scheme 16**). The MOM protection of secondary alcohol *rac*-**78** with MOMBr always gave poor yields and mixtures of products. When MOMCl was employed instead, the reaction was cleaner and the desired MOM ether *rac*-**79** could be isolated in high yield. The following Sonogashira coupling (to *rac*-**80**) was performed with quantitative yield employing diisopropylamine as both a solvent and a base. When a mixture of THF/Et_3N was used, the yields were much lower. The selective cleavage of the more labile trimethylsilyl group to *rac*-**81** was feasible by employing K_2CO_3 in methanol. Steps c) and d) could be combined in a two-step sequence without the isolation of *rac*-**80** to give *rac*-**81** in an almost quantitative yield. All steps from aniline **77** to diyne building block *rac*-**81** were easily upscaled and their high yields were preserved.

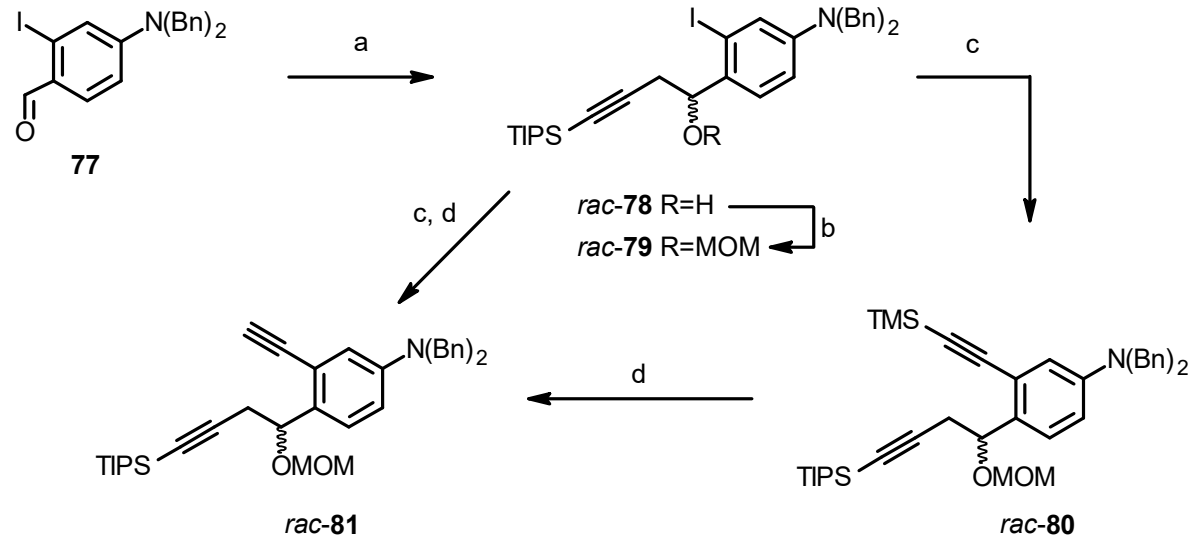

a) TIPS-C≡C-CH_3 (1.05 equiv.), *n*-BuLi (1.05 equiv.), THF, -78 °C, 20 min, 96%; b) MOMCl (1.5 equiv.), DMAP (10 mol%), *i*-Pr_2NEt (1.4 equiv.), CH_2Cl_2, 35 °C, 16 h, 93%; c) TMS-C≡CH (1.2 equiv.), $Pd(PPh_3)_2Cl_2$ (2 mol%), CuI (4 mol%), *i*-Pr_2NH, rt, 18 h, 99%; d) K_2CO_3 (1.5 equiv.), CH_3OH, rt, 3 h, 95%; c, d) without isolation of *rac*-**80**, 97% after two steps.

Scheme 16: Synthesis of racemic diyne building block *rac*-**81**.

Synthesis of Chiral Building Block (*S*)-85

The retrosynthesis of the desired enantiopure amino[6]helicene (*M*)-**69** discussed in Chapter 2 involves the introduction of a chiral building block (*S*)-**83**. The synthesis of (*R*)- and (*S*)-**83** was feasible starting from commercially available **82** by following the literature procedure, which involves biocatalytic kinetic resolution of *rac*-**84** as the key step.[31] Due to the high price of the starting compound **82** and with regard to the large-scale synthesis of the desired amino[6]helicene (*M*)-**69**, a chiral building block obtainable from a cheaper starting material was desirable. Therefore, the triflate building block (*S*)-**85** was designed as a viable alternative to (*S*)-**83**. The retrosynthesis of (*S*)-**85** is shown in **Scheme 17**. In analogy to (*S*)-**83**, the homochirality of (*S*)-**85** would result from biocatalytic kinetic resolution of *rac*-**86**, which can be obtained *via* addition of alkynyl organometallic reagent to aldehyde **87**. Compound **87** is accessible by ozonolysis or dihydroxylation of the terminal double bond of alkene **88** followed by oxidative cleavage. Allylnaphthol **88** can be synthesized by allylation of 1-naphthol (**90**) followed by Claisen rearrangement of ether **89**. The use of inexpensive 1-naphthol (**90**, 500 g = 56 €) guarantees a more economic synthesis of enantiopure amino[6]helicene (*M*)-**69** compared to the functionalized naphthalene **82** (25 g = 340 €).[119] This aspect is important, especially in terms of providing a good catalyst for possible practical applications.

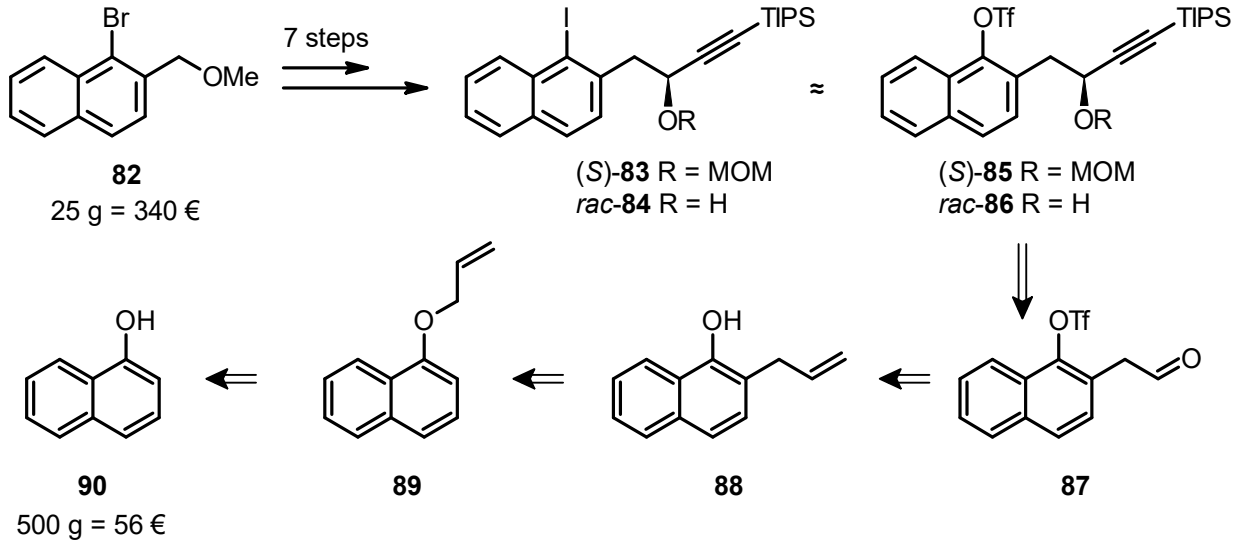

82
25 g = 340 €

(*S*)-**83** R = MOM
rac-**84** R = H

(*S*)-**85** R = MOM
rac-**86** R = H

90
500 g = 56 €

89

88

87

Scheme 17: Retrosynthesis of enantiopure building block (*S*)-**85**.

The allylation of the hydroxy group of commercially available 1-naphthol (**90**) was accomplished in quantitative yield employing the literature procedure.[120] In the same publication, the Claisen rearrangement from **89** to **88** was reported. By conducting the experiment in DMF in an oil bath at 180 °C for 12 h the authors were able to obtain product **88** in 72% yield. A more convenient approach was found following a protocol developed by Schmidt *et al*.[121] When this rearrangement was done in a microwave reactor at 250 °C using *N*,*N*-dimethylaniline as a solvent, the yield could be increased to 93% after 1 h reaction time.

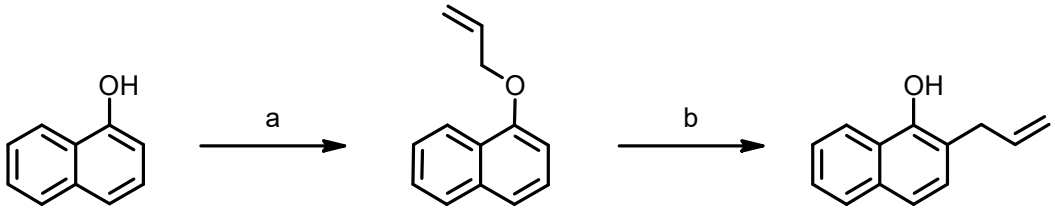

90 **89** **88**

a) K_2CO_3 (2.0 equiv.), allyl bromide (1.2 equiv.), acetone, reflux, 2.5 h, 96%; b) $PhNMe_2$, microwave reactor, 250 °C, 1 h, 93%.

Scheme 18: Synthesis of terminal alkyne **88**.

Unfortunately, neither ozonolysis nor a dihydroxylation-oxidative cleavage of the free naphthol **88** employing OsO_4-$NaIO_4$ led to the desired product **93** and only decomposition was observed. In order to avoid possible problems caused by the free hydroxy group, **88** was directly converted into triflate **91**. The dihydroxylation of the terminal alkene **91** was feasible by employing the OsO_4/NMO catalyst/reoxidant system, providing diol **92** in high yield. The subsequent oxidative cleavage with $NaIO_4$ worked also well, but the obtained homobenzylic aldehyde **87** was found to be unstable. Possible aldol reactions might be a reason for decomposition. Therefore, diol **92** was converted to secondary alcohol *rac*-**86** in a two-step sequence without the isolation of **87**. The addition of the alkyne moiety to the aldehyde **92** was first carried out with the *in situ* generated triisopropylsilylethynyllithium which gave poor yields. By generating an organomagnesium species instead, the yield could be improved and *rac*-**86** was obtained in good overall yields.

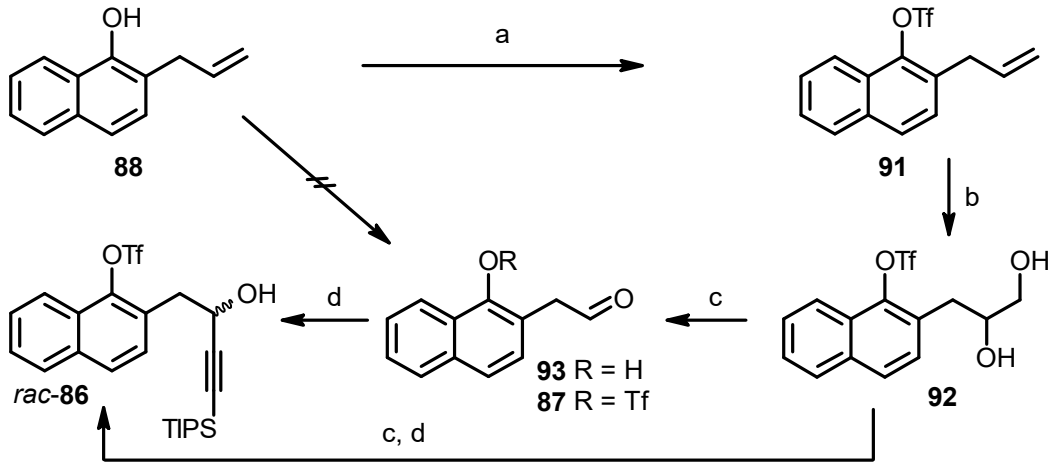

a) Tf_2O (1.2 equiv.), pyridine (2.0 equiv.), CH_2Cl_2, 0 °C to rt, 20 h, 79%; b) NMO (1.0 equiv.), OsO_4 (10 mol%), THF/H_2O 1:1, rt, 18 h, 91%; c) $NaIO_4$ (2.0 equiv.), CH_2Cl_2, rt, 4 h, 88%; d) TIPS-C≡CH (2.0 equiv.), EtMgBr (2.0 equiv.), THF, 0 °C, 1 h, 74% after 2 steps.

Scheme 19: Synthesis of *rac*-**86**.

The kinetic resolution of *rac*-**86** was indeed feasible by Novozyme 435 catalyzed acetylation. The conversion and *ee* values of (*R*)-**94** and (*S*)-**86** were followed *via* chiral HPLC; 24 h at 40 °C were found to be the optimum reaction conditions. (*R*)-**94** and (*S*)-**86** were obtained in high yields and *ee* values of >99% (determined after saponification of (*R*)-**94** to alcohol (*R*)-**85**) and >99%, respectively. The acetate (*R*)-**94** then had to be saponified. The use of strong bases such as KOH/MeOH led to fast decomposition of the product (*R*)-**86**. Slowing down the reaction by employing a weakly basic system of K_2CO_3/MeOH in catalytic amount gave access to the desired free alcohol (*R*)-**86**, which was not isolated but directly protected as a MOM-ether to (*R*)-**85** in the same manner as (*S*)-**85** in high yields.

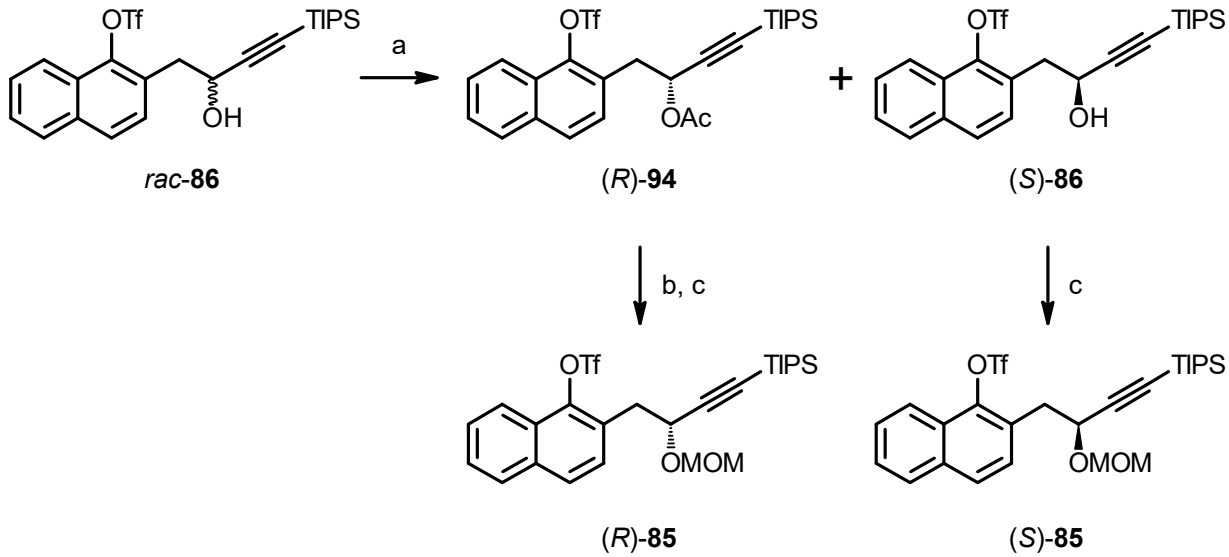

rac-**86** (*R*)-**94** (*S*)-**86** (*R*)-**85** (*S*)-**85**

a) Novozyme 435, isopropenyl acetate (5.0 equiv.), 4 Å molecular sieves, toluene, 40 °C, 24 h, 46% of (*R*)-**94** (>99% *ee*[a]) and 48% of (*S*)-**86** (>99% *ee*[a]); b) K_2CO_3 (5 mol%), MeOH, rt, 3 h, used further without purification; c) $CH_2(OCH_3)_2$ (3.0 equiv.), $BF_3{\cdot}Et_2O$ (1.1 equiv.), 4 Å molecular sieves, CH_2Cl_2, rt, 2 h, 77% (*S*)-**85**, (*R*)-**85** 88% (after 2 steps). [a]Determined by HPLC on chiral stationary phase.

Scheme 20: Synthesis of chiral building block **85**.

Construction of Enantiopure Amino[6]helicene (-)-(*M*)-69

The cyclotrimerization precursor (*RS*,*S*)-**97** was synthesized from both the triflate building block (*S*)-**85** and the iodo building block (*S*)-**83** to compare which route is superior (**Scheme 21**). Any attempt at coupling of triflate (*S*)-**85** with the terminal alkyne *rac*-**81** under Sonogashira conditions failed. Moreover, triflate (*S*)-**85** could not even be coupled with the highly reactive trimethylsilylacetylene. Fortunately, Kumada-Corriu conditions could be successfully employed. After *in situ* formation of the organomagnesium intermediate *rac*-**95** *via* reaction of ethylmagnesium bromide and *rac*-**81**, it was coupled with the building block (*S*)-**85** and successively desilylated to afford the triyne (*RS*,*S*)-**96** in moderate yields. Starting from the iodo building block (*S*)-**83**, the coupling with *rac*-**81** was conveniently feasible under Sonogashira conditions, affording (*RS*,*S*)-**96** after desilylation in high yields. A two-fold Sonogashira coupling of (*RS*,*S*)-**96** with 4-iodotoluene led to the desired triyne (*RS*,*S*)-**97**. Comparing the two building blocks (*S*)-**85** and (*S*)-**83**, one can say that triflate (*S*)-**85** is a good and more economic alternative to iodo compound (*S*)-**83** concerning the synthesis of the building block itself. But regarding its reactivity, with the optimizations done so far, (*S*)-**83** provides the more convenient coupling partner in further synthesis and upscaling. Nevertheless, the Kumada-Corriu conditions

found represent a good alternative for this kind of couplings where Sonogashira conditions fail. This can become important with respect to future modifications on the molecule skeleton, which might be necessary in order to modify the catalyst design.

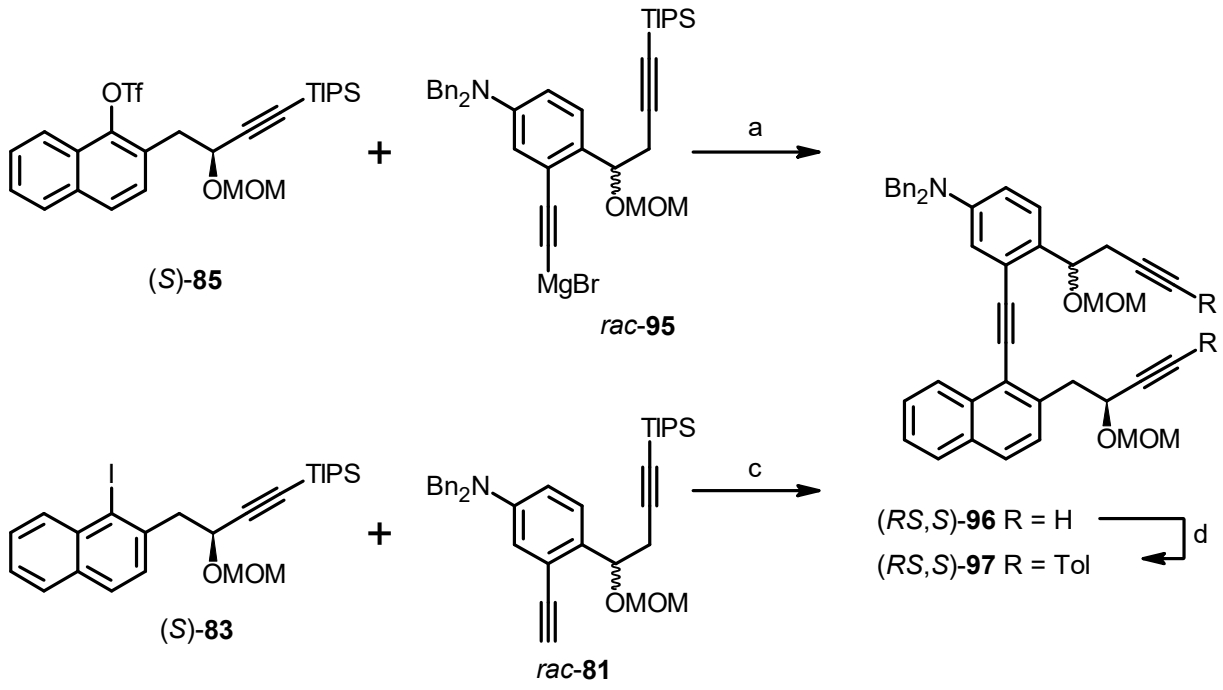

a) i) *rac*-**81** (1.4 equiv.), $PdCl_2$(dppp) (20 mol%), THF/toluene 2:1, 70 °C, 16 h, used further without isolation ii) *n*-Bu_4NF (3.0 equiv.), THF, rt, 16 h, 64% after 2 steps; c) i) *rac*-**81** (1.2 equiv.), $Pd(PPh_3)_2Cl_2$ (2 mol%), CuI (4 mol%), *i*-Pr_2NH, rt, 16 h, used further without isolation ii) *n*-Bu_4NF (3.0 equiv.), THF, rt, 16 h, 93% after 2 steps; d) 4-iodotoluene (3.0 equiv.), $Pd(PPh_3)_2Cl_2$ (5 mol%), CuI (10 mol%), *i*-Pr_2NH, rt, 16 h, 94%.

Scheme 21: Synthesis of triyne (*RS*,*S*)-**97**.

The assembly of tetrahydrohelicene (-)-(*M*,*RS*,*S*)-**98** *via* [2+2+2] cycloisomerization was feasible in moderate yield by employing $CpCo(CO)_2$, which was commonly used in the published protocols by Starý and Stará (**Scheme 22**, a).[31] In order to improve the yield $Ni(cod)_2$ was tested (b). The cyclotrimerization with $Ni(cod)_2$ is usually done at ambient temperature due to high reactivity of the catalyst, which also requires a glovebox and makes the procedure more cumbersome. With this system, the tetrahydrohelicene (-)-(*M*,*RS*,*S*)-**98** was obtained quantitatively but as a 1 : 1 mixture of two pairs of diastereomers ((+)-(*P*,*RS*,*S*)-**98** and (-)-(*M*,*RS*,*S*)-**98**) due to the low temperatures which disable the thermodynamic equilibration of the helical units. The two pairs of diastereomers (+)-(*P*,*RS*,*S*)-**98** and (-)-(*M*,*RS*,*S*)-**98** can be separated conveniently *via* column chromatography, which enabled the determination of their 1 : 1 ratio. Unfortunately, attempts to carry out a sequential reaction (first b) and then apply elevated temperature for post cyclization thermodynamic equilibration) worked

in some cases but were not reproducible. Occasionally, it led to the partial aromatization to fully aromatic product **99** with low *ee* values. These problems were overcome by employing a different Ni(0) catalyst at elevated temperatures (c). $Ni(CO)_2(PPh_3)_2$ at 150 °C afforded the desired product (-)-(*M*,*RS*,*S*)-**98** in good yields and with high stereoselectivity. Substoichiometric amounts of $Ni(CO)_2(PPh_3)_2$ resulted in lower conversions to the desired helicene (-)-(*M*,*RS*,*S*)-**95**. Upscaling of this procedure above 0.2 mmol was difficult due to the requirement of a pressure reactor, in which the reaction can be heated above the boiling point of toluene. The use of a high-temperature high-pressure flow reactor was found to be beneficial (180 °C, 8 min residential time, 90% yield of (-)-(*M*,*RS*,*S*)-**95**) but attempts at upscaling resulted in precipitation and eventually clogging of the flow system, most likely due to the decomposition of $Ni(CO)_2(PPh_3)_2$. The acid-catalyzed aromatization to the fully aromatic helicene (-)-(*M*)-**96** was feasible in good yields. In order to remove both benzyl groups to generate a free amine moiety, harsh reductive conditions were necessary. The *in situ* formation of H_2 from NH_4HCO_2 in the presence of Pd/C at elevated temperature was found to provide the desired aminohelicene (-)-(*M*)-**69** in high yield. The optical purity of (-)-(*M*)-**69** corresponds to the chiral building blocks (*S*)-**84** or (*S*)-**82**. Due to the heterogeneous reaction caused by low solubility of precursor (-)-(*M*)-**96** in the required (in order to dissolve the NH_4HCO_2) polar solvent and the heterogeneous catalyst, a fine dispersion had to be formed *via* long sonication prior to reaction. Otherwise, the time to reach full conversion to (-)-(*M*)-**69** takes too long and the helicene scaffold is partially hydrogenated ($[M+H_2+H]^+$ ion was observed in ESI-MS and additional aliphatic protons were observed in NMR of crude (-)-(*M*)-**69**). The upscaling of this heterogeneous process was also not quite straightforward and a 1 mmol-scale in refluxing ethanol for 2 h was found to be the optimum.

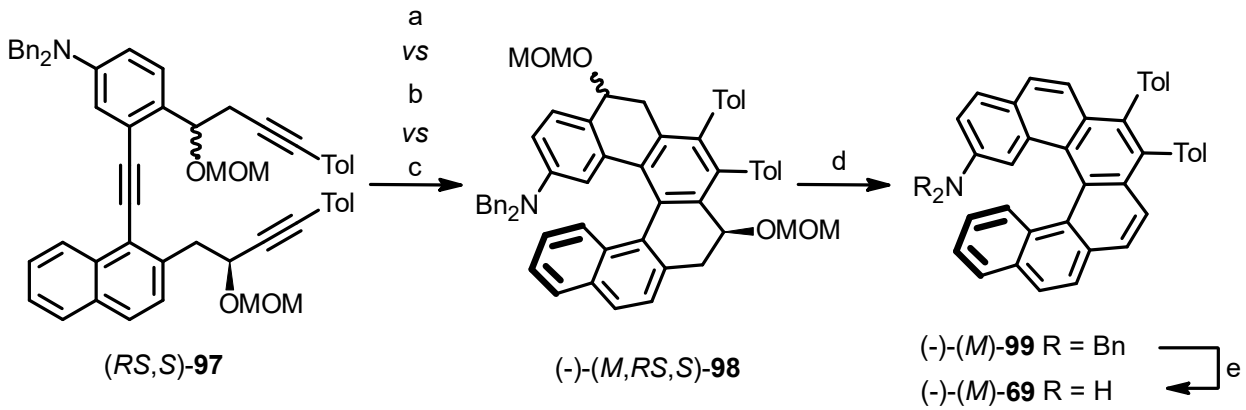

(*RS*,*S*)-**97**

(-)-(*M*,*RS*,*S*)-**98**

(-)-(*M*)-**99** R = Bn

(-)-(*M*)-**69** R = H

a) $CpCo(CO)_2$ (0.5 equiv.), THF, $[bdmim]BF_4$, microwave reactor, 170 °C, 20 min, 70%; b) $Ni(cod)_2$ (0.5 equiv.), PPh_3 (1.0 equiv.), THF, rt, 1 h, 99%; c) $Ni(CO)_2(PPh_3)_2$ (1.1 equiv.), toluene, 150 °C, 15 min, 82%; d) *p*-TsOH (10.0 equiv.), toluene, 40 °C, 16 h, 94%; e) NH_4HCO_2 (20.0 equiv.), Pd/C (12 mol%), EtOH, reflux, 2 h, 97% (>99% *ee*[a]). [a]Determined by HPLC on chiral stationary phase.

Scheme 22: Synthesis of enantiopure amino[6]helicene (-)-(*M*)-**69**.

Enantiopure Monobenzo Amino[6]helicene (-)-(*M*)-118

A structural modification of amino[6]helicene **69** was proposed in which one extra benzene ring is fused to the outer rim of the [6]helicene scaffold. Thus the aminobenzo[6]helicene (*M*)-**100** was designed and, as seen from the retrosynthetic analysis in **Scheme 23**, the key chiral building block (*S*)-**72** can be advantageously used for its construction. The desired enantiopure helicene (*M*)-**100** can be obtained from dihydrohelicene (*M*)-**101** *via* acid-catalyzed elimination of the chiral auxiliary. Triyne (*S*)-**102** was designed as a cyclotrimerization precursor, which can be synthesized from the three building blocks **103**, **104** and (*S*)-**72**.

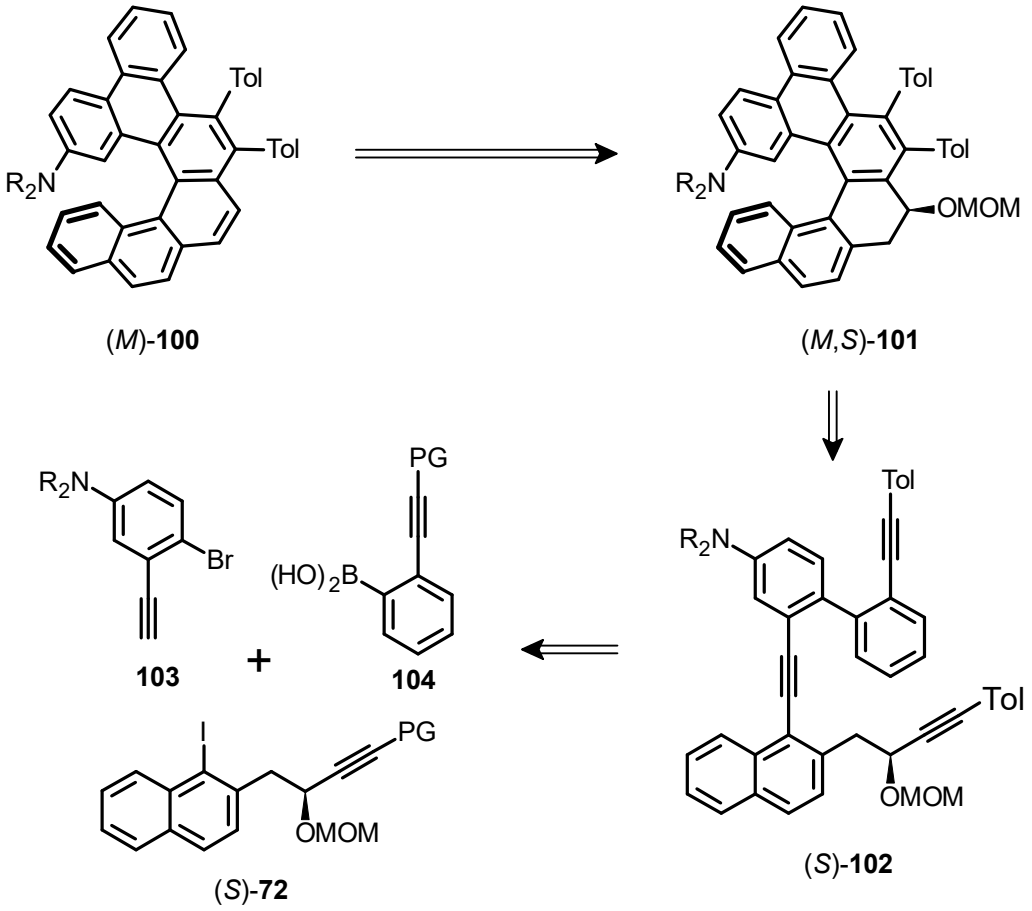

Scheme 23: Retrosynthesis of monobenzo amino[6]helicene (*M*)-**100**.

Since both alkynes **104**[26] and (*S*)-**72**[31] are known compounds, the challenge here was to synthesize the terminal alkyne **103**. First, aniline **75** was brominated in the preferred *para* position[122] to **105** (**Scheme 24**). In order to prevent interactions of the free amino functional group with *e.g.* transitions metals, the protection of the amino group was assumed to be beneficial. Carbamate (Boc) was chosen as a protecting group because of its stability under basic conditions, which need to be applied in the following synthetic steps. Bis-carbamate **106** was prepared in a reaction of **105** with 4 equivalents of Boc-anhydride because with lower excess of the reagent the mono-Boc-protected product was always accompanied by the bis-carbamate **106** and the starting material (a 1:1:1 ratio, according to TLC). Unfortunately, the Sonogashira coupling of **106** with trimethylsilylacetylene or triisopropylsilylacetylene gave the desired alkynes **107** and **108** in poor yields, even though full conversion of **106** was observed in both cases (according to TLC). This was most likely due to the partial cleavage of the Boc groups (according to NMR of the side products). Surprisingly,

when the free aniline **115** was directly coupled with trimethylsilylacetylene, the desired product **109** could be obtained quantitatively. The following Boc-protection to carbamate **110** and its desilylation to terminal alkyne **111** worked smoothly and could also be conveniently carried out without the isolation of intermediate **110**.

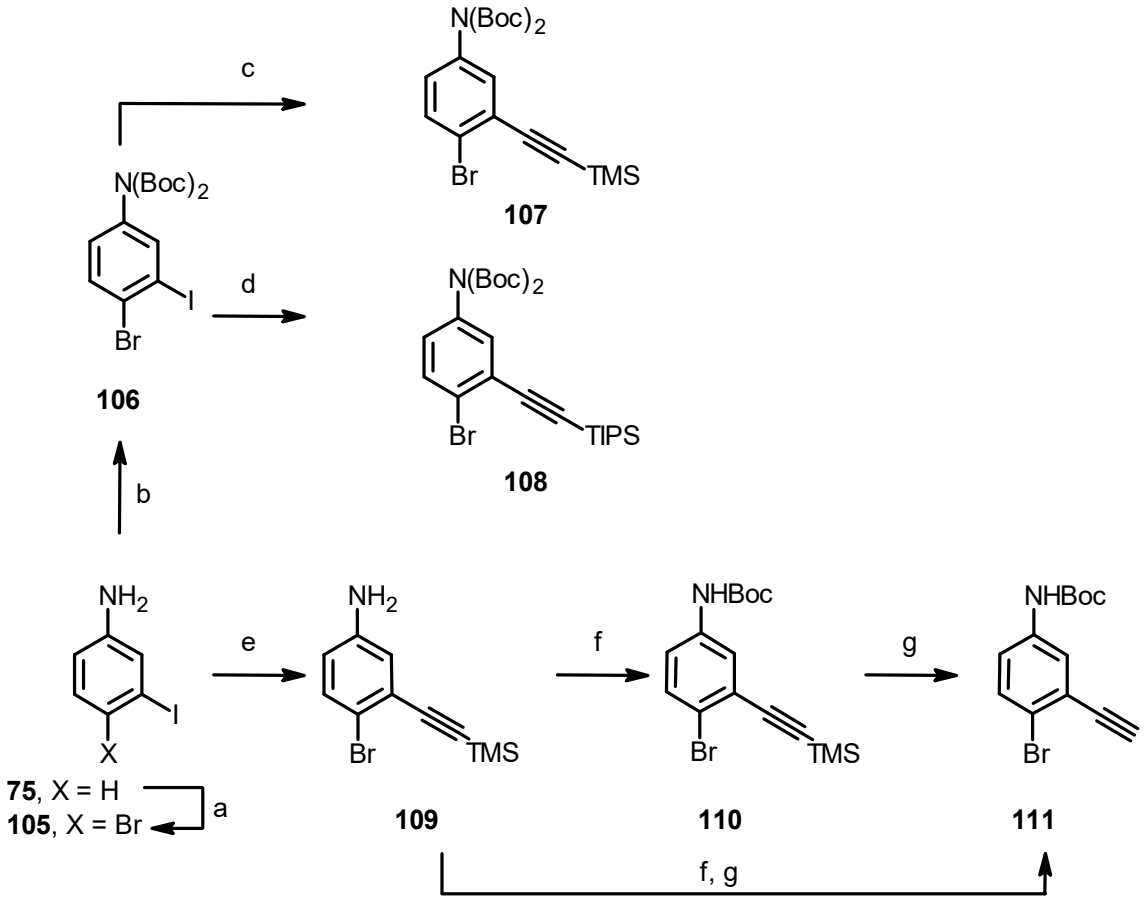

a) NBS (1.0 equiv.), DMF, rt, 20 h, 74%; b) Boc_2O (4.0 equiv.), DMAP (10 mol%), THF, reflux, 2 h, 95%; c) TMS-C≡CH (1.05 equiv.), $Pd(PPh_3)_2Cl_2$ (2 mol%), CuI (4 mol%), *i*-Pr_2NH, 0 °C to rt, 2 h, 38%; d) TIPS-C≡CH (1.1 equiv.), $Pd(PPh_3)_2Cl_2$ (2 mol%), CuI (4 mol%), *i*-Pr_2NH, rt, 1 h, 38%; e) TMS-C≡CH (1.05 equiv.), $Pd(PPh_3)_2Cl_2$ (2 mol%), CuI (4 mol%), *i*-Pr_2NH, 0 °C to rt, 16 h; 99%; f) Boc_2O (1.5 equiv.), EtOH, rt, 16 h, 99%; g) K_2CO_3 (1.5 equiv.), CH_3OH, rt, 3 h, 99%; f, g) without isolation of **110**, 89% over 2 steps.

Scheme 24: Synthesis of alkyne building block **111**.

The construction of the cyclotrimerization precursor (*S*)-**116** is shown in **Scheme 25**. First, the chiral building block (*S*)-**83** was coupled with the terminal alkyne **111** under Sonogashira conditions in high yield. In the next step, an additional benzene unit was connected to the molecule *via* Suzuki-Miyaura coupling with the building block **113** to afford the silylated triyne (*S*)-**114** in quantitative yield. Afterward, the TIPS groups were exchanged for tolyl groups *via* desilylation to (*S*)-**115** and two-fold Sonogashira coupling with 4-iodotoluene led to the desired triyne (*S*)-**116**.

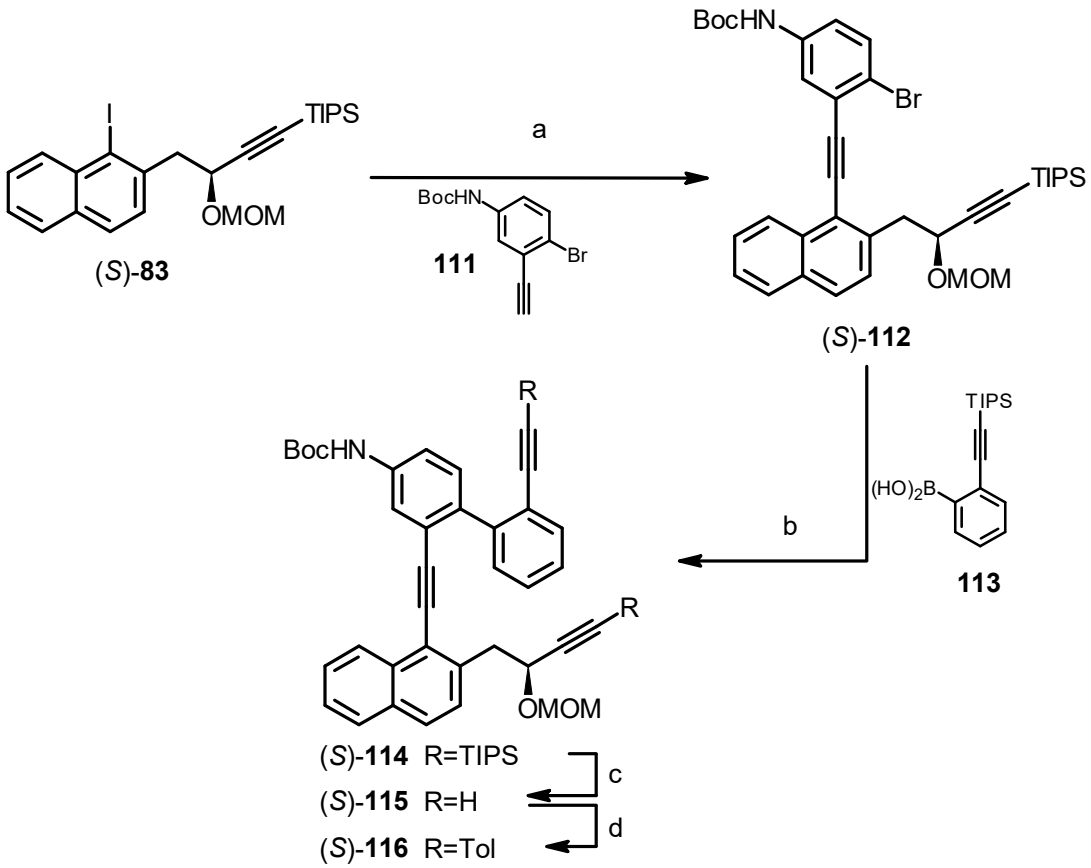

a) **111** (1.3 equiv.), $Pd(PPh_3)_2Cl_2$ (2 mol%), CuI (4 mol%), *i*-Pr_2NH, rt, 16 h, 91%; b) **113** (1.3 equiv.), $Pd(PPh_3)_2Cl_2$ (10 mol%), K_2CO_3 (1.05 equiv.), propanol/toluene/water 4:4:1, reflux, 5 h, 98%; c) *n*-Bu_4NF (3.0 equiv.), THF, rt, 6 h, 93%; f) 4-iodotoluene (3.0 equiv.), $Pd(PPh_3)_2Cl_2$ (4 mol%), CuI (8 mol%), *i*-Pr_2NH, rt, 16 h, 93%.

Scheme 25: Synthesis of triyne **116**.

The next step was the cyclotrimerization of triyne (*S*)-**116** (**Scheme 26**). In order to analyze properly the diastereomeric purity of the formed dihydrohelicene (-)-(*M*,*S*)-**117**, a sample with 75% *de* in favor of (-)-(*M*,*S*)-**117** was prepared by conducting the cyclotrimerization at 120 °C for 15 min. HPLC separation of the two diastereomers was possible. Afterward, the conditions of the cyclotrimerization of (*S*)-**116** to diastereomerically pure (-)-(*M*,*S*)-**117** needed to be optimized because too high temperature and prolonged reaction time led to the formation of by-products. This was probably due to partial aromatization and cleavage of the Boc group, which is undesirable before full equilibration of the system to the thermodynamically preferred (-)-(*M*,*S*)-**117**. A balance between complete thermodynamic equilibration and the onset of side reactions was found by heating to 150 °C for 10 min providing the dihydrohelicene (-)-(*M*,*S*)-**117** in >99% *de*. Since the OMOM and the Boc protecting groups are both acid-labile, they could be advantageously cleaved in one step by

treatment with a solution of HCl in dioxane. The desired fully aromatic (-)-(*M*)-**118** with a primary amine moiety could be obtained in good yields.

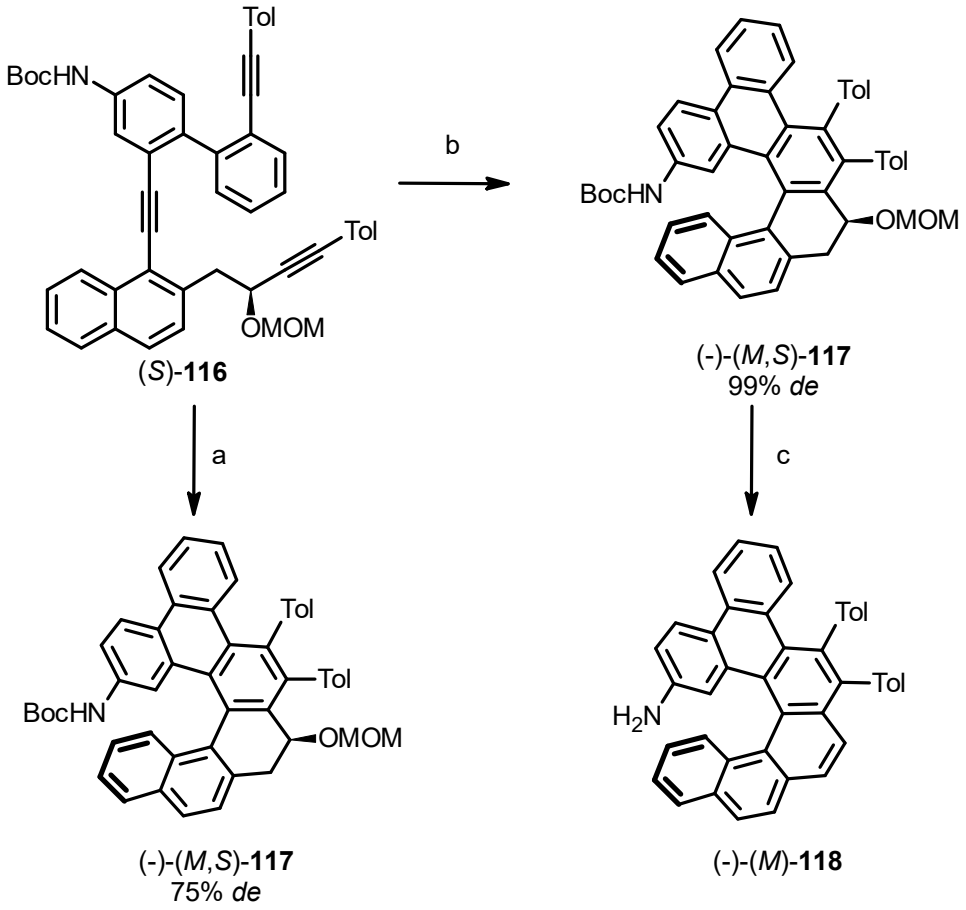

a) $Ni(CO)_2(PPh_3)_2$ (50 mol%), THF, microwave reactor, 120 °C, 15 min, 80% (75% *ee*[a]); b) $Ni(CO)_2(PPh_3)_2$ (30 mol%), toluene, 150 °C, 10 min, 84% (99% *ee*[a]); c) HCl (60.0 equiv.), dioxane, rt, 19 h, 83%. [a]Determined by HPLC on chiral stationary phase.

Scheme 26: Synthesis of monobenzo amino[6]helicene (-)-(*M*)-**118**.

Simplified Access to 2-Amino[6]helicene-Like Structure

In order to simplify the access to optically pure amino[6]helicenes, the design of structure **119** was modified according to **Scheme 27**. Due to the lengthy synthesis and high price of the starting material for the chiral naphthalene building block (*S*)-**83** (*cf.* **Scheme 17**), the installation of the helicity-defining stereocenter in the amino building block would be beneficial. It would also present a more modular approach, in which the structure of the helicene scaffold can easily be modified by employing different naphthalene building blocks (**Scheme 27**, blue). Due to the widely explored enantioselective addition of terminal alkynes to benzaldehydes,[123,124] alkyne **123** with the chiral center (red star) in the benzylic position was designed as an alternative to

the alkyne *rac*-**71**. This modification results in an amino[6]helicene **120** with one five-membered ring embedded.

Such a structurally novel system has so far not been investigated in the diastereoselective synthesis of helicenes and the stereoinduction of helicity by the chiral center in the five-membered ring needed to be investigated experimentally. Therefore, model aminobenzo[6]helicene **121** was designed. The additional fused benzene unit was introduced to further simplify the synthesis. Helicene **121** can be synthesized from triyne **122** which is derived from the building blocks *rac*-**71**, **123**, **124** and acetylene.

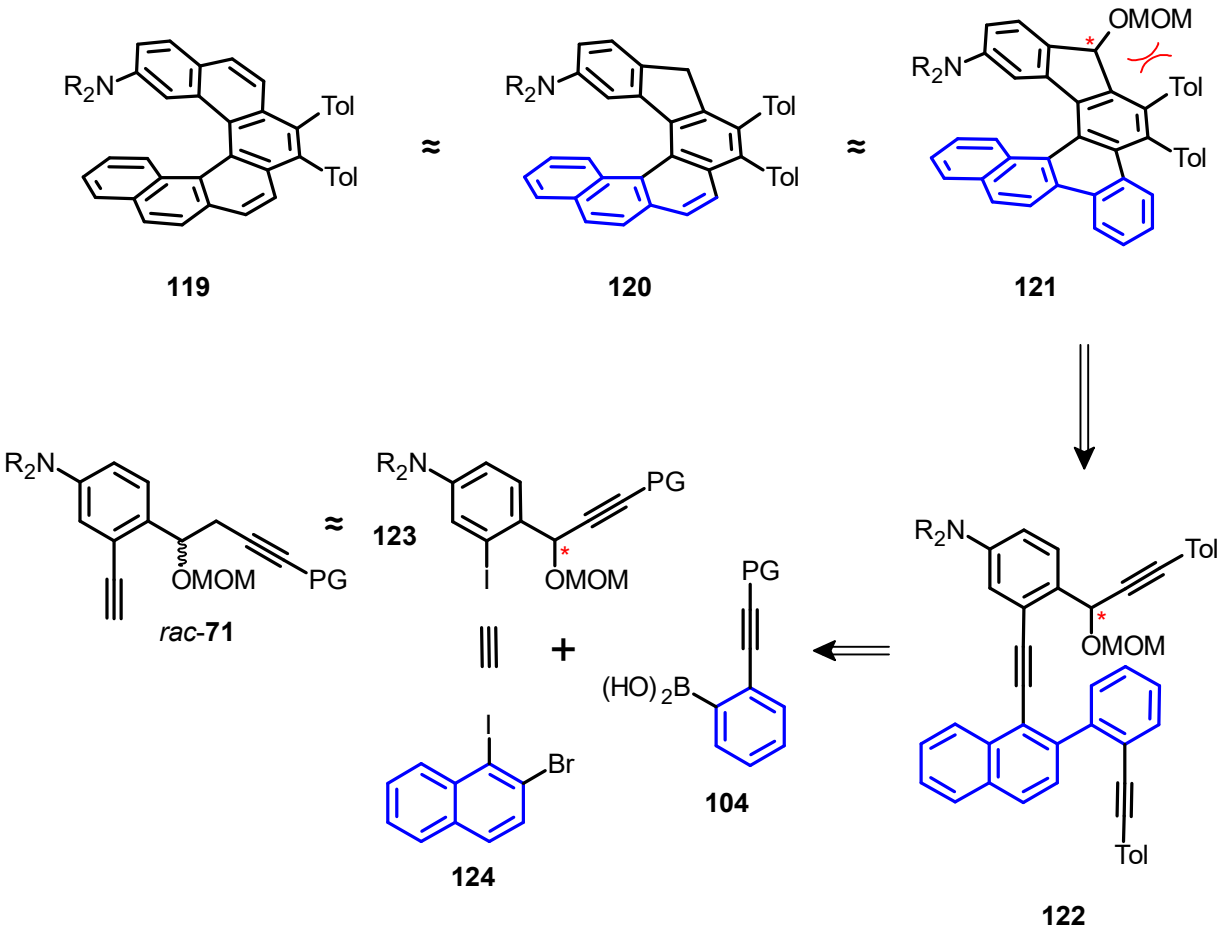

Scheme 27: Simplification and structural modification of amino[6]helicene synthesis.

Conveniently, racemic triyne **131** can be used in the cyclotrimerization to assess the degree of stereocontrol. **Scheme 28** shows the four possible isomers which can be formed during the cyclization. If the stereoinduction is complete, only one diastereomer would be obtained (either (*P*,*S*)/(*M*,*R*)-**121** or (*M*,*S*)/(*P*,*R*)-**121**). An

incomplete stereoinduction would lead to the formation of diastereomers (each one being a racemic mixture) that could be identified in the NMR spectrum featuring two sets of signals of the resulting aminobenzo[6]helicene **121**.

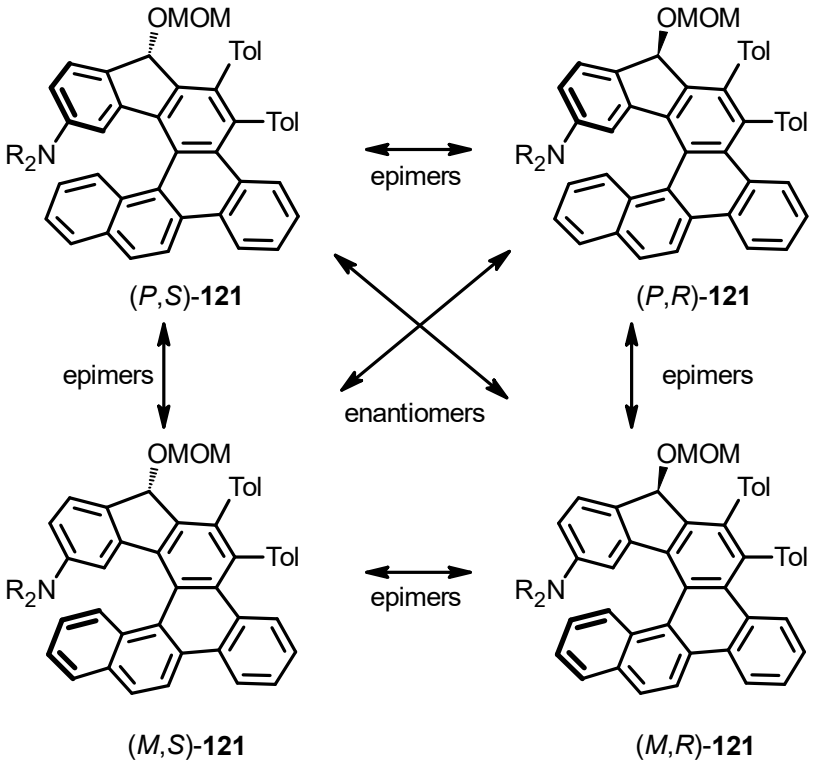

Scheme 28: The four possible stereoisomers of aminobenzo[6]helicene **121**.

In order to find the most efficient route to aminobenzo[6]helicene **121**, the scope and accessibility of the building blocks *rac*-**127** and **129** were explored (**Scheme 29**). An alkyne moiety was added to aldehyde **77** to form the secondary alcohol *rac*-**125**, which was subsequently protected as MOM ether *rac*-**126**. After Sonogashira coupling and desilylation, the terminal alkyne *rac*-**127** was obtained.

Starting from naphthalene **124**, the chemoselective Sonogashira reaction in the position 1 with TIPS protected acetylene followed by desilylation, led to terminal alkyne **128** in good yield after two steps. Suzuki-Miyaura coupling with boronic acid **113** gave diyne **129** in moderate yield.

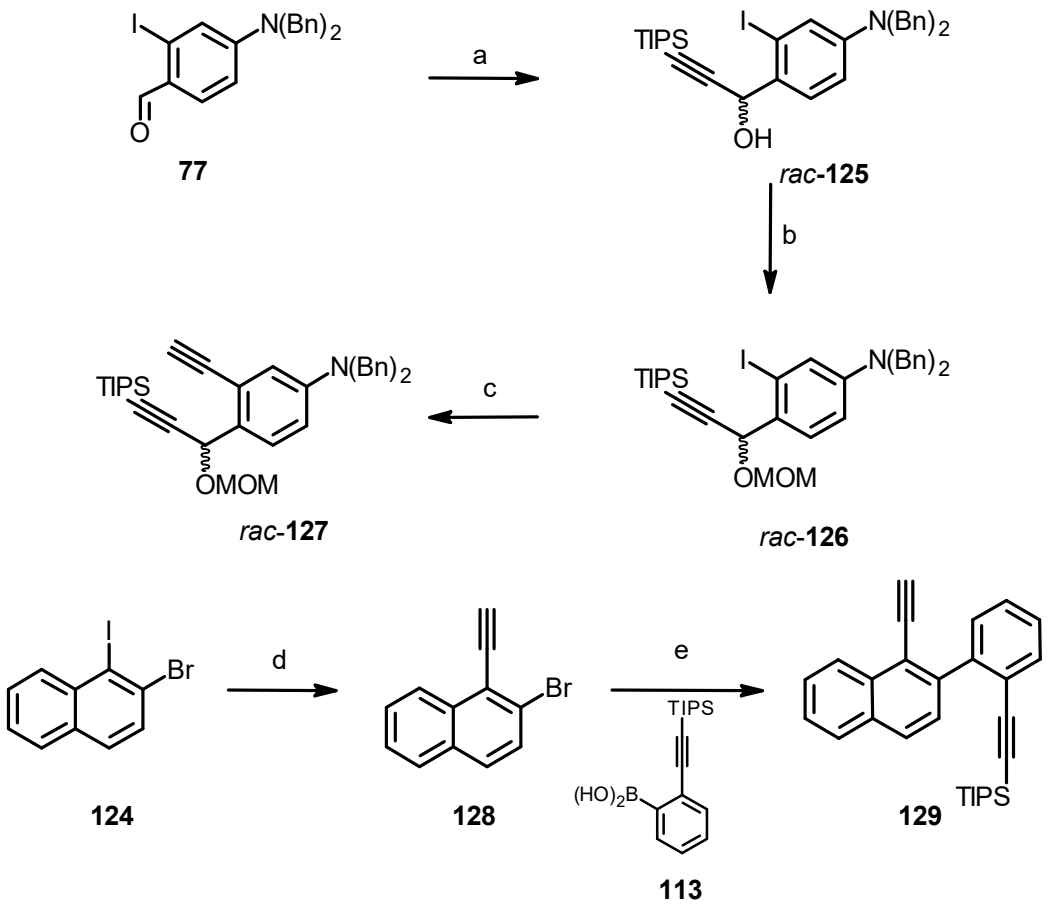

a) TIPS-C≡CH (1.05 equiv.), *n*-BuLi (1.05 equiv.), THF, -78 °C, 30 min, 95%; b) MOMCl (1.5 equiv.), *i*-Pr_2NEt (1.4 equiv.), DMAP (10 mol%), CH_2Cl_2, 35 °C, 16 h, 78%; c) i) TMS-C≡CH (1.2 equiv.), $Pd(PPh_3)_2Cl_2$ (2 mol%), CuI (4 mol%), *i*-Pr_2NH, rt, 2 h, used further without purification, ii) K_2CO_3 (1.5 equiv.), CH_3OH, rt, 2 h, 92% after 2 steps; d) i) TIPS-C≡CH (1.05 equiv.), $Pd(PPh_3)_2Cl_2$ (5 mol%), CuI (10 mol%), *i*-Pr_2NH, rt, 18 h, used further without purification, ii) *n*-Bu_4NF (2.0 equiv.), CH_3OH-THF (1:12), rt, 4 h, 74% after 2 steps; e) **113** (1.3 equiv.), $Pd(PPh_3)_2Cl_2$ (10 mol%), K_2CO_3 (1.05 equiv.), propanol/toluene/water 4:4:1, reflux, 3 h, 53%.

Scheme 29: Synthesis of building blocks *rac*-**127** and **129**.

The central triple bond in triyne **122** (**Scheme 27**) can originate either from the terminal alkyne unit of compound *rac*-**127** by Sonogashira coupling with iodide **124**, or similarly from the reaction of alkyne **128** with iodide *rac*-**126** (**Scheme 30**). Both routes were tested to see which of the two combinations is more advantageous. When terminal alkyne *rac*-**127** was coupled with building block **124** chemoselectively with respect to the iodo substituent, the desired diyne *rac*-**130** was obtained in low yield. Alkyne *rac*-**127** was fully consumed during the reaction and around 15% of the homocoupled tetrayne (according to ESI-MS of the isolated side product) was observed, which partially explains the low conversion of **124**. The complementary combination of reactants *rac*-**126** and **128** gave a better result; the desired diyne *rac*-**130** was obtained in good yield.

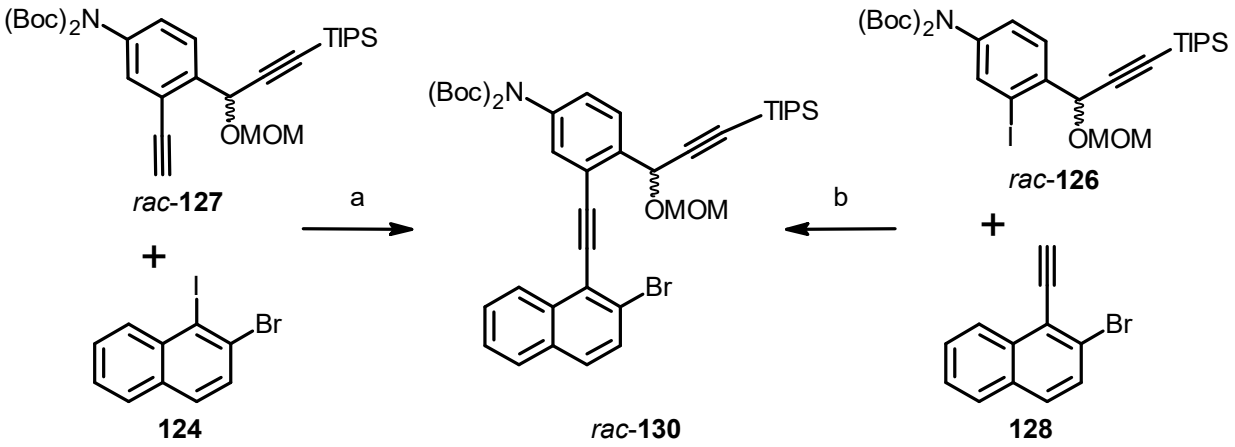

a) *rac*-**127** (1.05 equiv.), $Pd(PPh_3)_2Cl_2$ (2 mol%), CuI (4 mol%), *i*-Pr_2NH, rt, 16 h, 40%; b) **128** (1.2 equiv.), $Pd(PPh_3)_2Cl_2$ (2 mol%), CuI (4 mol%), *i*-Pr_2NH, rt, 16 h, 80%.

Scheme 30: Synthesis of building block *rac*-**130**.

The next step was the construction of helicene **134** to study the efficiency of stereoinduction. First, diyne *rac*-**130** was transformed into triyne *rac*-**131** *via* Suzuki-Miyaura coupling in high yield. Then, the two TIPS groups were exchanged to tolyl groups by desilylation of *rac*-**131** to *rac*-**132** and its subsequent Sonogashira coupling with iodotoluene to provide the cyclization precursor *rac*-**133**. In order to give the system enough energy for a complete thermodynamic equilibration, the Co-mediated cyclotrimerization of *rac*-**133** was performed in a microwave reactor at 180 °C for 15 min. An NMR analysis of the obtained material revealed that there were two different diastereomers in a ratio of 1.7 to 1. Unfortunately, the helicene **134** readily decomposes during chromatography and thus the individual diastereoisomers could not be separated and characterized. Nevertheless, the contraction of the six-membered ring containing the essential stereogenic center as in (-)-(*M*,*RS*,*S*)-**98** (**Scheme 22**) or (-)-(*M*,*S*)-**117** (**Scheme 26**) to a five-membered ring as in **134** (**Scheme 31**) destroys the effective stereocontrol by the 1,3-allylic type strain. Accordingly, the latter approach to enantiopure helicenes cannot be used.

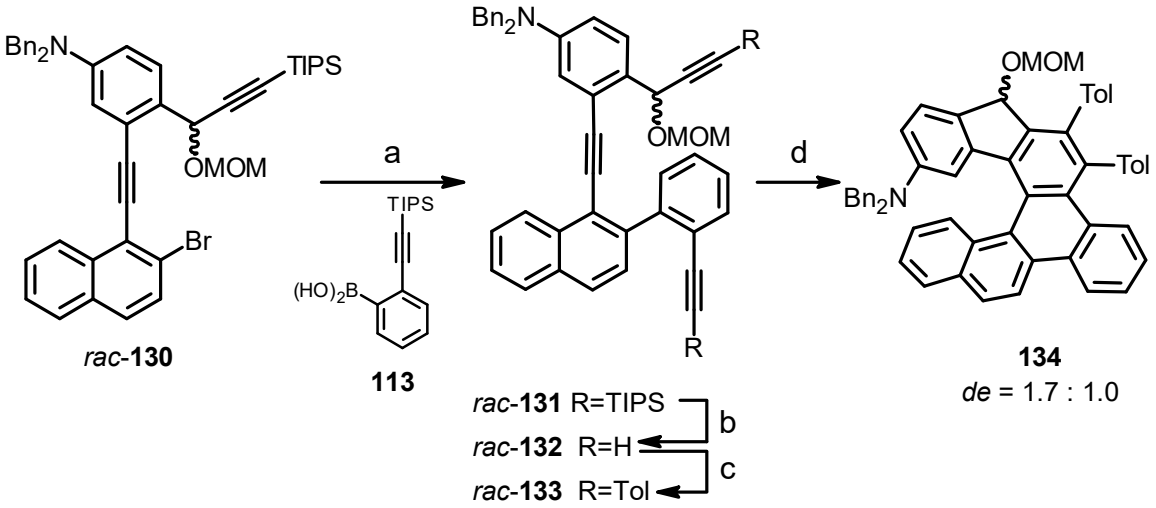

a) **113** (1.3 equiv.), $Pd(PPh_3)_2Cl_2$ (10 mol%), K_2CO_3 (1.05 equiv.), propanol/toluene/water 4:4:1, reflux, 5 h, 88%; b) *n*-Bu_4NF (3.0 equiv.), THF, rt, 2h, 74%; c) 4-iodotoluene (3.0 equiv.), $Pd(PPh_3)_2Cl_2$ (5 mol%), CuI (10 mol%), *i*-Pr_2NH, rt, 16 h, 72%; d) $CpCo(CO)_2$ (1.0 equiv.), $[bdmim]BF_4$, microwave reactor, THF, 180 °C, 15 min, 73%.

Scheme 31: Synthesis of 2-amino[6]helicene-like compound **134**.

3.2 Synthesis of Imidazolium Salts

Imidazolium Salts with Two Helicene Moieties

In order to minimize the number of steps of the imidazolium salt synthesis, one pot procedures (**Scheme 7**) were investigated. Following a protocol by Herrmann *et al.*,[125] the reaction of amino[6]helicenes (+)-(*P*)-**69** and (-)-(*M*)-**118** with glyoxal and paraformaldehyde in toluene for 24 h provided the imidazolium salts (+)-(*P*,*P*)-**135** and (-)-(*M*,*M*)-**136** in moderate yields (**Scheme 32**, a). When aqueous conditions[126] (b) were applied, yields were found to be lower, probably due to the poor solubility of (+)-(*P*,*P*)-**135** and (-)-(*M*,*M*)-**136** in aqueous media. An attempt to increase the yield by faster reaction at elevated temperature in a microwave reactor led to numerous side products (according to TLC) but did not lead to the improved yield of (+)-(*P*,*P*)-**135** (c). When the same conditions (a) were applied and the reaction time was extended to 45 h, imidazolium salt (+)-(*P*,*P*)-**135** was obtained in good yield (d).

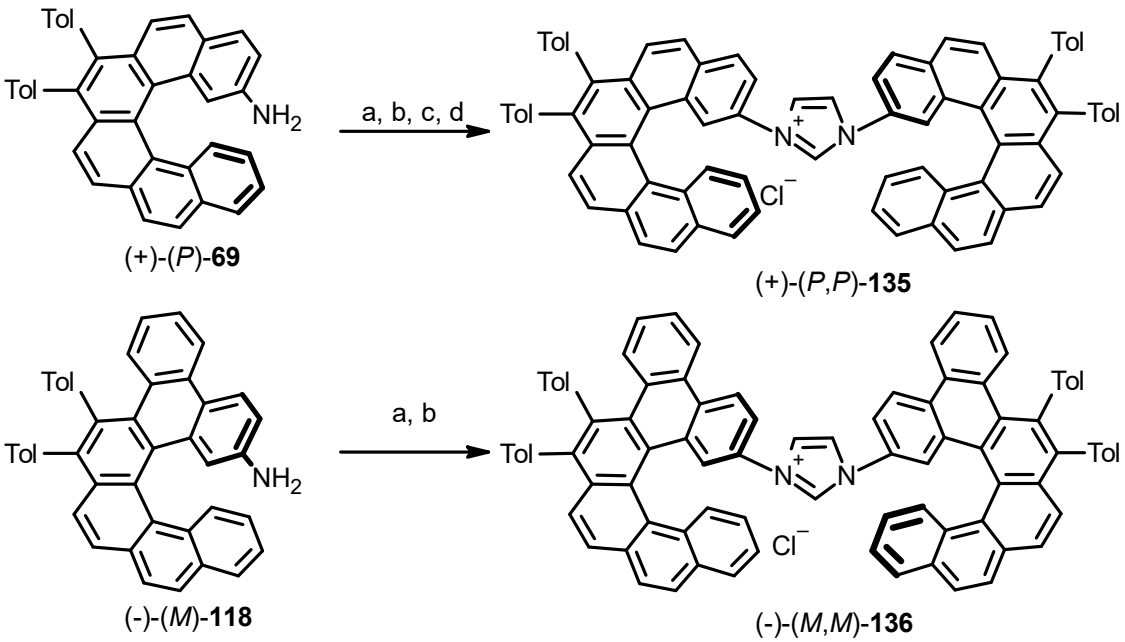

a) glyoxal (0.5 equiv.), paraformaldehyde (0.5 equiv.), HCl (0.6 equiv.), toluene, 40 °C, 17 h, 39% ((*M*,*M*)-**135**) and 39% ((*M*,*M*)-**136**); b) glyoxal (0.5 equiv.), formaldehyde (0.5 equiv.), acetic acid, 60 °C, 1 h, 30% ((*P*,*P*)-**135**) and 26% ((*M*,*M*)-**136**); c) glyoxal (0.5 equiv.), paraformaldehyde (0.5 equiv.), HCl (0.6 equiv.), toluene, microwave reactor, 100 °C, 1.5 h, 36%; d) glyoxal (0.5 equiv.), paraformaldehyde (0.5 equiv.), HCl (0.6 equiv.), toluene, 40 °C, 45 h, 72%.

Scheme 32: Synthesis of imidazolium salts (+)-(*P*,*P*)-**135** and (-)-(*M*,*M*)-**136** with two helicene moieties.

Imidazolium Salt with One Helicene Moiety

A protocol by Fürstner *et al.* (**Scheme 8**)[73] was employed to synthesize an unsymmetrical imidazolium salt bearing a [6]helicenyl chiral substituent on one nitrogen atom and a mesityl group on the other (**Scheme 33**). First, formamide **137** was transformed into oxazolium salt **138** which was subsequently reacted with amino[6]helicene (-)-(*M*)-**69**. The hydroxy-dihydroimidazolium intermediate (*M*)-**139** was subsequently aromatized to the desired imidazolium salt (-)-(*M*)-**140** in moderate overall yield.

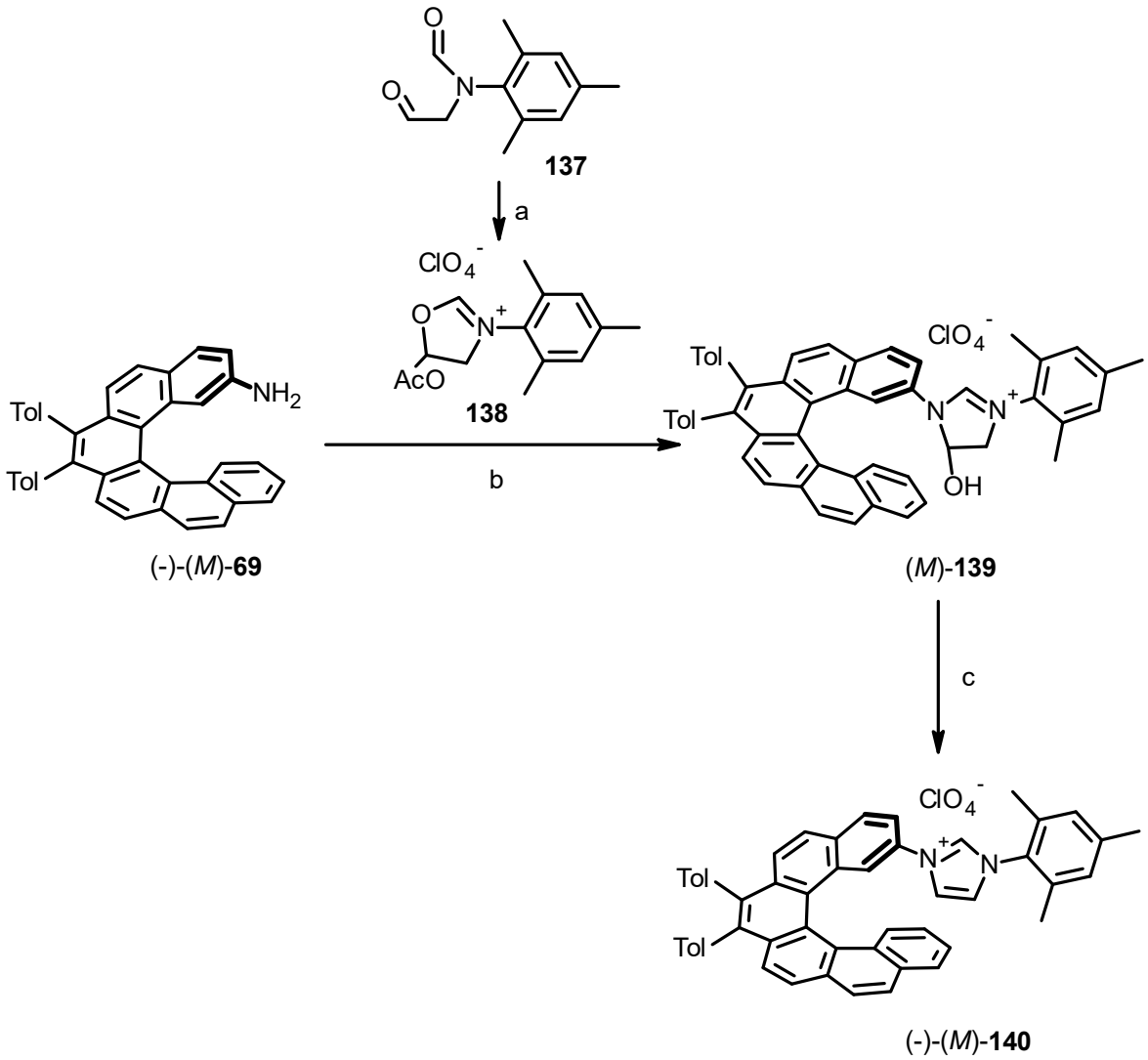

a) **137** (1.7 equiv.), $HClO_4$ (1.96 equiv.), Ac_2O (38.0 equiv.), rt, 8 h, used further without isolation; b) toluene, rt, 21 h, used further without isolation; c) $HClO_4$ (1.0 equiv.), 52% after 3 steps.

Scheme 33: Synthesis of imidazolium salt (-)-(*M*)-**140** with one helicene moiety.

3.3 Synthesis of Helically Chiral NHC-Metal Complexes

Ag-Complexes

The Ag-NHC complexes serve as useful intermediates for the transmetallation to other desired transition metal complexes.[127] Their synthesis is very convenient because Ag_2O can be used as a silver containing base.[128] By mixing this reagent with an imidazolium halide of choice, the latter is deprotonated and the free carbene is coordinated to form the Ag-NHC complex.[129] **Scheme 34** shows the synthesis of $AgCl(NHC)_2$ (*P*,*P*,*P*,*P*)-**141** (structure was confirmed by ESI-MS) from the symmetrical imidazolium chloride (+)-(*P*,*P*)-**135**. The crude complex (*P*,*P*,*P*,*P*)-**141**

was analyzed by NMR spectroscopy which showed no signal of the C^2 proton of (+)-(*P*,*P*)-**135** anymore, so full conversion was assumed and the material was used in further steps without purification.

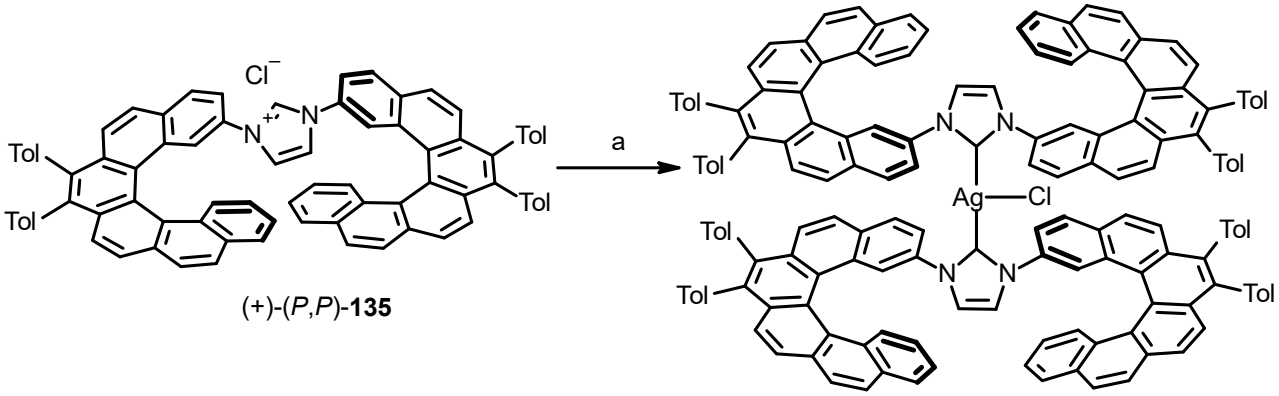

(+)-(*P*,*P*)-**135**

(*P*,*P*,*P*,*P*)-**141**

a) Ag_2O (0.75 equiv.), dichloromethane, rt, 24 h, quant. (crude).

Scheme 34: Synthesis of Ag-NHC complex (*P*,*P*,*P*,*P*)-**141**.

Imidazolium perchlorate (-)-(*M*)-**140** had to be first transformed into the imidazolium halide species (-)-(*M*)-**142**. Counter ions other than halides might complicate the procedure and require the use of additives such as additional halide sources.[130] Inspired by the work of Robinson *et al.*[131] who used an ion exchange resin to replace the counterion of a saturated imidazolium salt from BF_4^- to HCO_3^-, the imidazolium perchlorate (-)-(*M*)-**140** was converted into chloride (-)-(*M*)-**142**. The change of the counterion could be observed by TLC and NMR spectroscopy (the proton in the C^2 position shifts from 8.12 ppm in (-)-(*M*)-**140** to 10.31 ppm in (-)-(*M*)-**142**). After the reaction of halide (-)-(*M*)-**142** with Ag_2O, the desired Ag-NHC complex (*M*,*M*)-**143** was obtained and an NMR analysis of the crude mixture revealed complete conversion (the signal of the proton in the C^2 position was not observed).

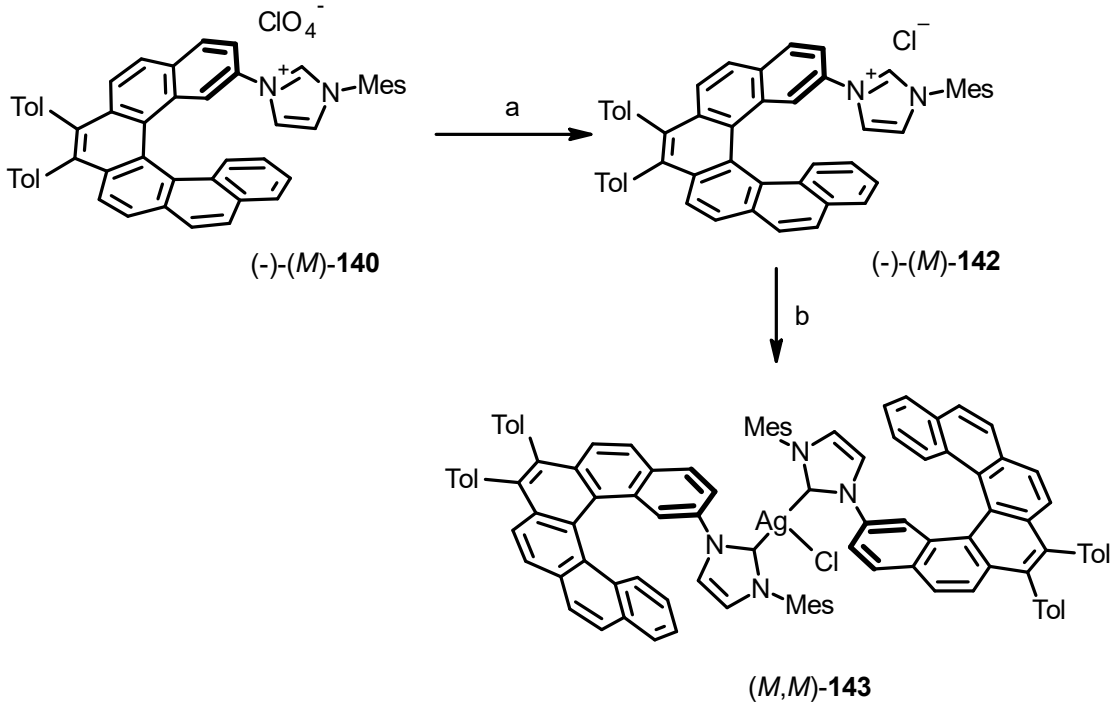

a) Amberlite IRA-400 chloride, MeOH, 97%; b) Ag_2O (0.75 equiv.), CH_2Cl_2, rt, 72 h, quant. (crude).

Scheme 35: Synthesis of Ag-NHC (*M*,*M*)-**143**.

Ru-Complexes

Scheme 36 shows attempts at the synthesis of Hoveyda-Grubbs type catalyst of the second generation ((*P*,*P*)-**145**). Initially, the symmetric imidazolium salt (+)-(*P,P*)-**135** bearing two helicene moieties was chosen as the NHC source in order to introduce maximal chiral environment around the metal coordination sphere. Unfortunately, substitution of the PCy_3 ligand in the starting material **144** by the deprotonated salt (+)-(*P,P*)-**135** was unsuccessful. Any newly formed Ru-benzylidene species would be easily identified by NMR analysis of the crude reaction mixture (observing a new peak around 16 ppm in ^{1}H NMR). Hoveyda *et al.* reported that transmetallation from a Ag-NHC complex can be beneficial for installing bulky carbene ligands at the second generation Ru catalyst.[132] Thus, transmetallation at Ag-NHC complex (*P*,*P*,*P*,*P*)-**141** to Ru complex **144** was attempted in an NMR tube in C_7D_8. Again, no new signal around 16 ppm was observed.

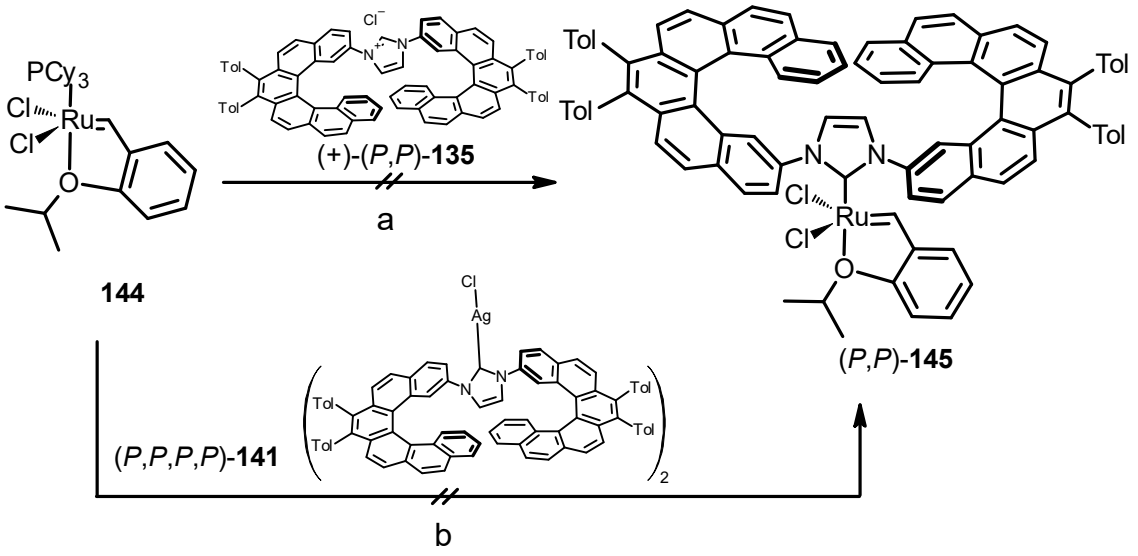

a) (+)-(*P*,*P*)-**135** (1.1 equiv.), $(CH_3)_3COK$ (1.05 equiv.), CuCl (2.0 equiv.), toluene, 80 °C, 30 min, no product observed; b) (*P*,*P*,*P*,*P*)-**141** (0.52 equiv.), C_7D_8, 80 °C, 24 h, no product observed.

Scheme 36: An attempt at the synthesis of Hoveyda-Grubbs type catalyst (*P*,*P*)-**145**.

Even though the Grubbs type catalyst of the second generation (**Scheme 37**, compound (*P*,*P*)-**146**) should provide sufficient space for accommodation of a bulky NHC-ligand due to the benzylidene proton being in plane with the two chloro ligands rather than pointing towards the NHC-ligand, the carbene with two helicenes probably causes too much steric congestion, which prevents the formation of the catalyst.

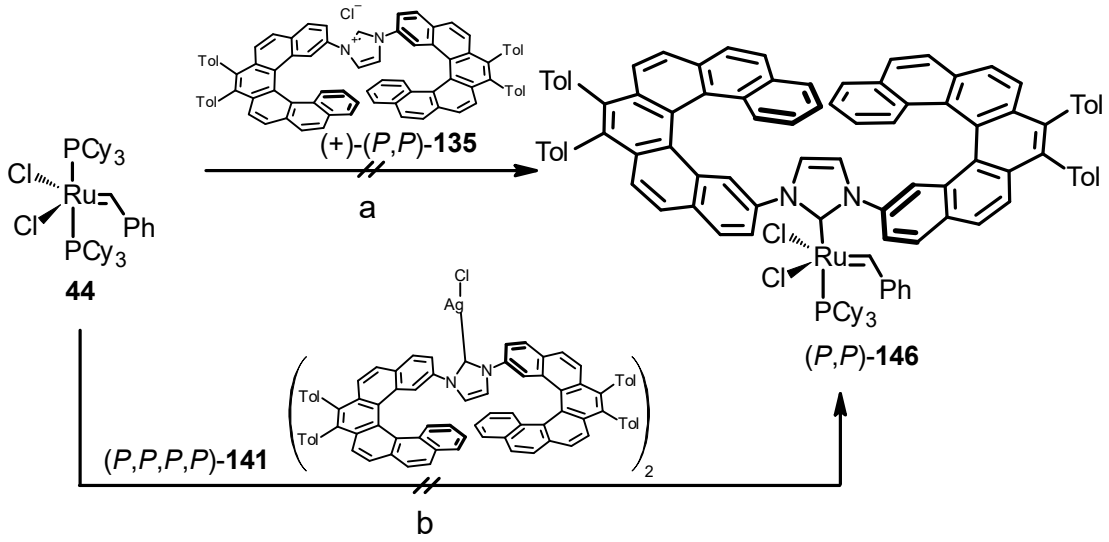

a) (+)-(*P*,*P*)-**135** (1.1 equiv.), $(CH_3)_3COK$ (1.05 equiv.), toluene, 60 °C, 30 min, no product observed; b) (*P*,*P*,*P*,*P*)-**141** (0.52 equiv.), C_7D_8, 80 °C, 24 h, no product observed.

Scheme 37: An attempt at the synthesis of Grubbs type catalyst (*P*,*P*)-**146**.

On the other hand, the sterically less demanding imidazolium salt (-)-(*M*)-**140** bearing only one helicene moiety was found suitable for the synthesis of a Hoveyda-Grubbs type catalyst of the second generation. The first generation catalyst **144** was reacted with the deprotonated salt (-)-(*M*)-**140** to form the helically chiral Ru-NHC complex (-)-(*M*)-**147** in moderate yield (**Scheme 38**, a). Although the conversion of **144** was not complete (according to TLC), the reaction was stopped after 25 min in order to balance conversion of the starting material **144** and decomposition of the product (-)-(*M*)-**147**. Changing the base to LiHMDS led to a lower yield in spite of the fact that no starting material could be observed after 30 min (b). Surprisingly, the transmetallation from silver salt (*M*,*M*)-**143** did not result in the formation of the desired complex (-)-(*M*)-**147** (c), checked by TLC).

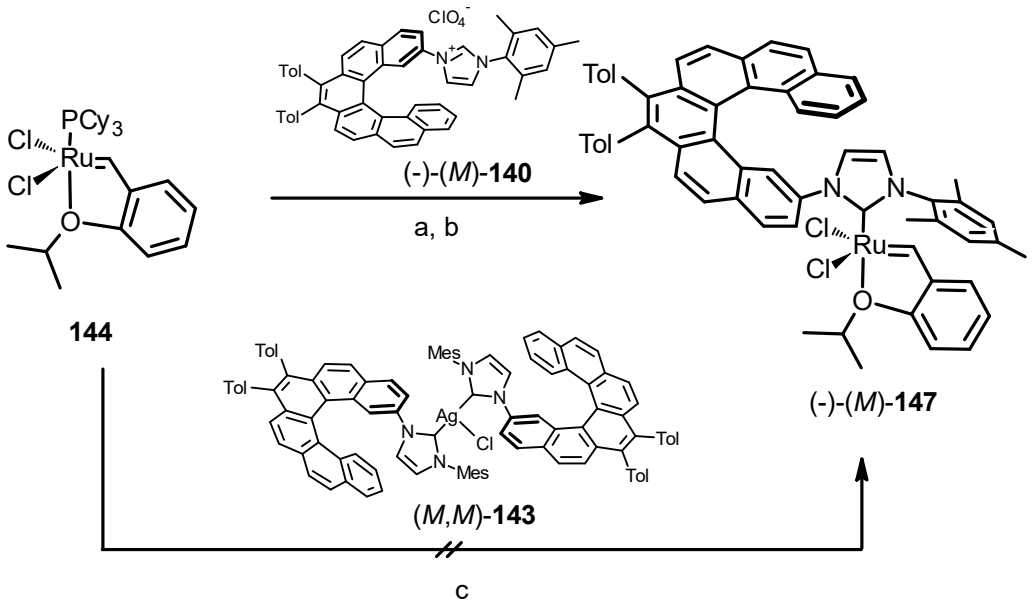

a) (-)-(*M*)-**140** (1.1 equiv.), $(CH_3)_3COK$ (1.05 equiv.), toluene, 80 °C, 25 min, 36%; b) (-)-(*M*)-**140** (1.1 equiv.), LiHMDS (1.1 equiv.), toluene, 80 °C, 30 min, 19%; c) (*M*,*M*)-**143** (0.55 equiv.), toluene, 80 °C, 24 h, no product observed.

Scheme 38: Synthesis of helically chiral Ru-NHC complex (-)-(*M*)-**147**.

Pd-Complexes

Pd-PEPPSI type complexes are less sterically crowded around the metal center than the Ru complexes shown in **Scheme 36** and **37**. Therefore they provide more space for the coordination of bulky carbene ligands. The synthesis of Pd-complex (+)-(*P*,*P*)-**148** with two helicene moieties was accomplished starting from the Ag-NHC complex (*P*,*P*,*P*,*P*)-**141** by transmetallation onto Pd, followed by the reaction with 3-chloropyridine to afford (+)-(*P*,*P*)-**148** in good yield (**Scheme 39**). The purification of

the crude mixture of (-)-(*P*,*P*)-**148** was difficult due to its decomposition during filtration through silica gel, which is typically applied for PEPPSI type complexes.[114] Fortunately, clean material of (+)-(*P*,*P*)-**148** could be obtained by precipitation with Et_2O/heptane out of the reaction mixture followed by filtration and recrystallization from DCM/MeOH.

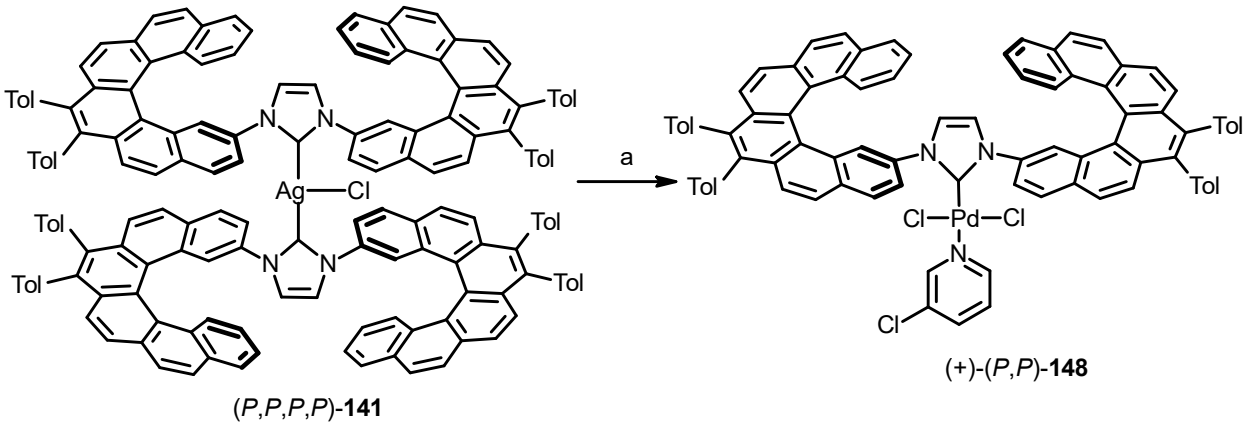

a) i) $PdCl_2(MeCN)_2$ (1.0 equiv.), (*P*,*P*,*P*,*P*)-**141** (0.52 equiv.), CH_2Cl_2, rt, 48 h ii) 3-chloropyridine (3.0 equiv.), CH_2Cl_2, rt, 5 h, 67%.

Scheme 39: Synthesis of Pd complex (+)-(*P*,*P*)-**148** with two helicene moieties.

The synthesis of Pd-complex (-)-(*M*)-**149** was feasible by applying the same protocol (**Scheme 40**). Ag-NHC complex (*M*,*M*)-**143** (**Scheme 35**) was subjected to transmetallation onto Pd followed by the reaction with 3-chloropyridine. After precipitation of crude product and recrystallization, clean material of the desired Pd-PEPPSI complex (-)-(*M*)-**149** was obtained in good yield.

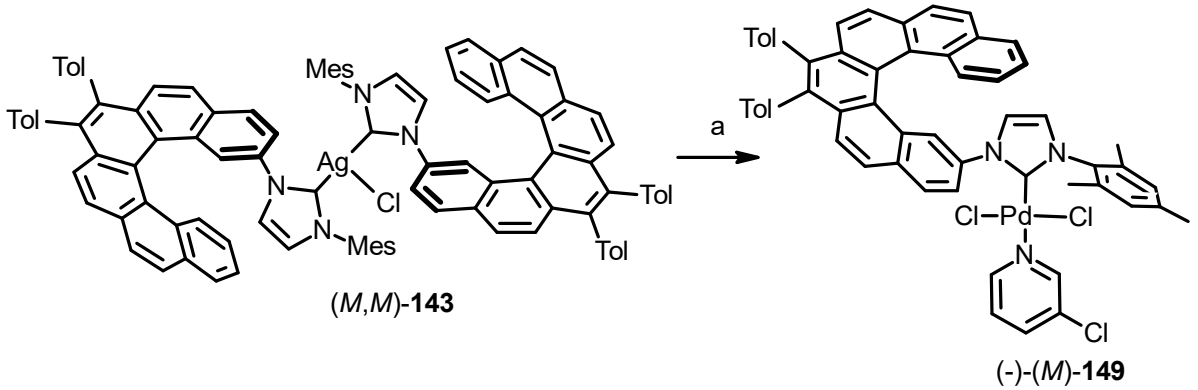

a) i) $PdCl_2(MeCN)_2$ (1.0 equiv.), (*M*,*M*)-**143** (0.55 equiv.), CH_2Cl_2, rt, 48 h ii) 3-chloropyridine (2.0 equiv.), CH_2Cl_2, rt, 4 h, 80%.

Scheme 40: Synthesis of Pd complex (-)-(*M*)-**149** with one helicene moiety.

3.4 Enantioselective Cyclotrimerization with *In Situ* Generated Ni-Complexes

Following a recently published procedure by Starý and Stará *et al.*, the asymmetric induction by the novel imidazolium salts (-)-(*M*,*M*)-**135** and (-)-(*M*,*M*)-**136** in enantioselective [2+2+2] cyclotrimerization was investigated (**Scheme 41**).[28] Thus, triyne **11** was reacted with an *in situ* generated Ni(0)-NHC complex which catalyzed the conversion to dibenzo[6]helicene (+)-(*P*)-**14** with an enantiomeric excess. By employing the imidazolium salts (-)-(*M*,*M*)-**135** and (-)-(*M*,*M*)-**136**, (+)-(*P*)-**14** was obtained in 35% *ee* (70% yield) and 10% *ee* (50% yield), respectively. The conversion was complete in both cases (according to TLC). The lower yield obtained with (-)-(*M*,*M*)-**135** probably resulted from two column chromatography separations needed to purify (+)-(*P*)-**14**, whereas one column chromatography was sufficient to obtain pure material of (+)-(*P*)-**14** in the case of utilizing (-)-(*M*,*M*)-**136**. The lower *ee* value observed for (-)-(*M*,*M*)-**136** gives information that steric bulk in the $C^{5,6}$ positions of the helicene scaffold in the *in situ* formed Ni(0)-NHC complex is probably disadvantageous for this transformation. Non-symmetric imidazolium salts gave lower *ee* values in all reported[28] cases, so (-)-(*M*)-**140** or (-)-(*M*)-**142** were not employed.

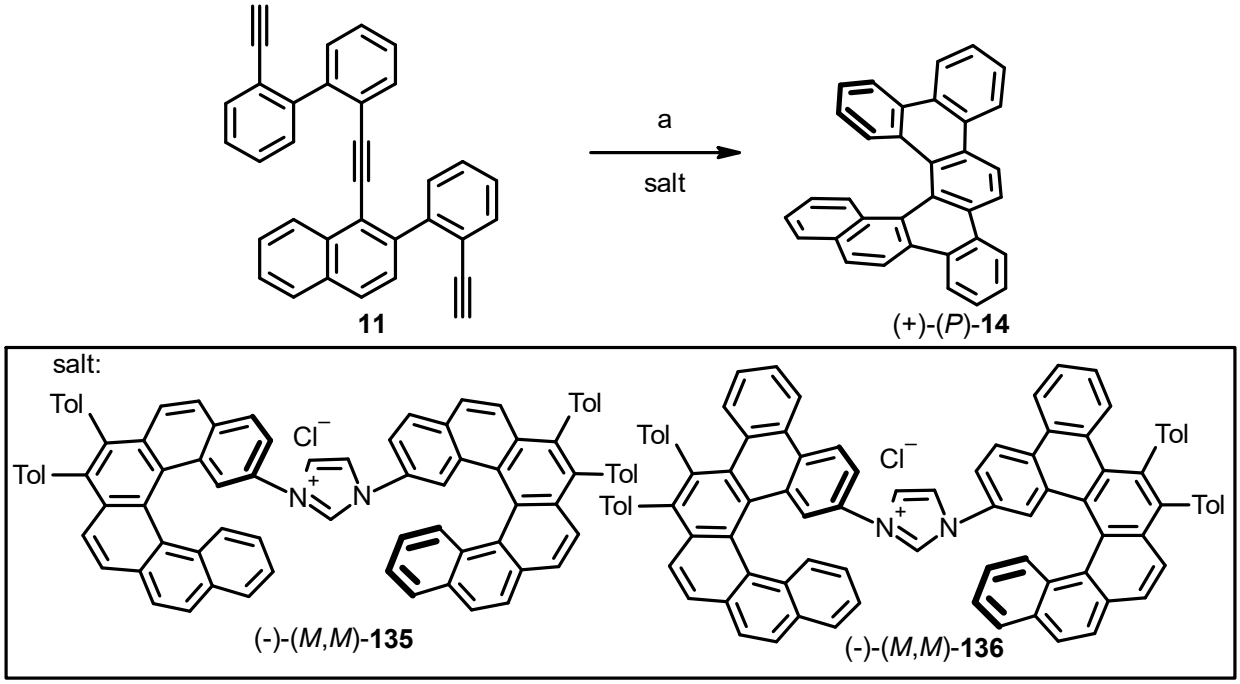

a) (-)-(*M*)-**135** or (-)-(*M*)-**136** (0.44 equiv.), EtMgCl (0.92 equiv.), $Ni(acac)_2$ (0.2 equiv.), THF, rt, 2 h, 70% with (-)-(*M*,*M*)-**135** (35% *ee*) and 50% with (-)-(*M*,*M*)-**136** (10% *ee*).

Scheme 41: Enantioselective cyclotrimerization with (-)-(*M*,*M*)-**135** and (-)-(*M*,*M*)-**136**.

3.5 Investigations with Ru-Complex (-)-(*M*)-147

Catalytic Activity

In order to evaluate the catalytic activity of the novel catalyst (-)-(*M*)-**147** in metathesis reactions, it was compared to a structurally similar and commercially available Hoveyda-Grubbs catalyst of the second generation (**156**). The substrates were chosen from those ones commonly used to evaluate the efficiency of olefin metathesis catalysts published by Grubbs and co-workers.[133]

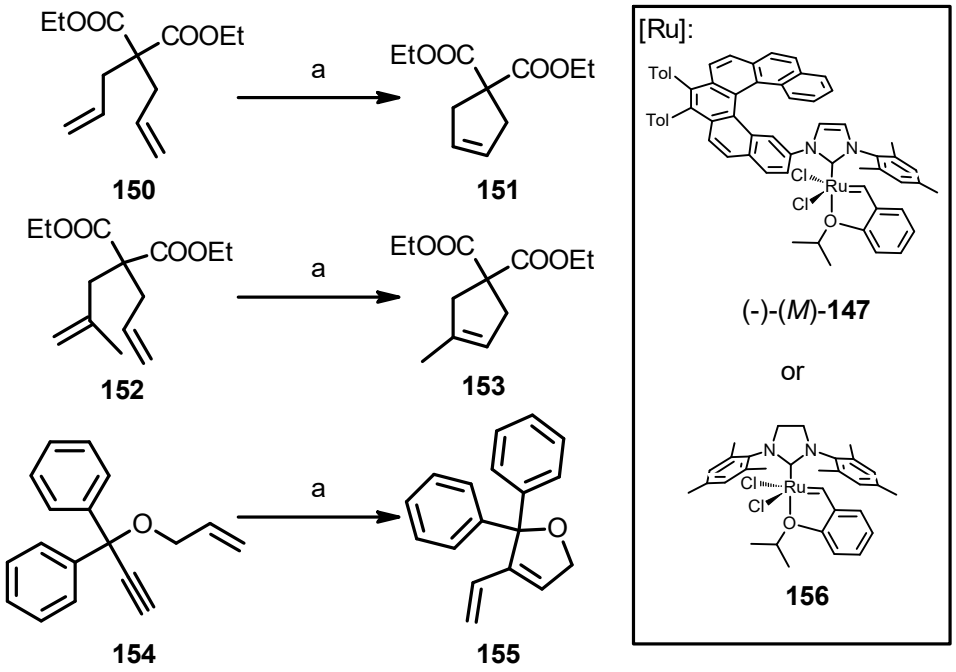

a) (-)-(M)-**147** or **156** (1 mol%), C_7D_8, 0.1 M, 40 °C.

Scheme 42: Activity tests of Ru-complex (-)-(*M*)-**147**.

All reactions were conducted in deuterated toluene in an NMR-tube and the conversion was monitored by NMR-spectroscopy. **Scheme 42** shows the test reactions which were performed to see the activity of catalyst (-)-(*M*)-**147** in ring closing metathesis. In all cases the novel catalyst (-)-(*M*)-**147** was much less active than the commercially available catalyst **156**. The formation of disubstituted double bonds in ring systems was tested by RCM of **150** to **151** (**Figure 13**, (-)-(*M*)-**147** (**150**) and **156** (**150**)). Full conversion was achieved after 20 min with catalyst (-)-(*M*)-**147**. The conversion of **152** to **153** shows the activity towards the formation of trisubstituted double bonds, which is slower due to the steric hindrance of the

additional methyl group ((-)-(M)-**147** (**152**) and **156** (**152**)). Conversion over 95% was achieved after 30 min with catalyst (-)-(*M*)-**147**. Activity in enyne metathesis was tested by converting dienyne **154** to cyclic diene **155** ((-)-(*M*)-**147** (**154**) and **156** (**154**)). Conversion over 95% was achieved after 24 min with catalyst (-)-(*M*)-**147**. The reduced activity of catalyst (-)-(*M*)-**147** compared to catalyst **156** does not necessarily present a disadvantage. Slower reaction rates might be beneficial with regard to higher selectivities in asymmetric transformations.

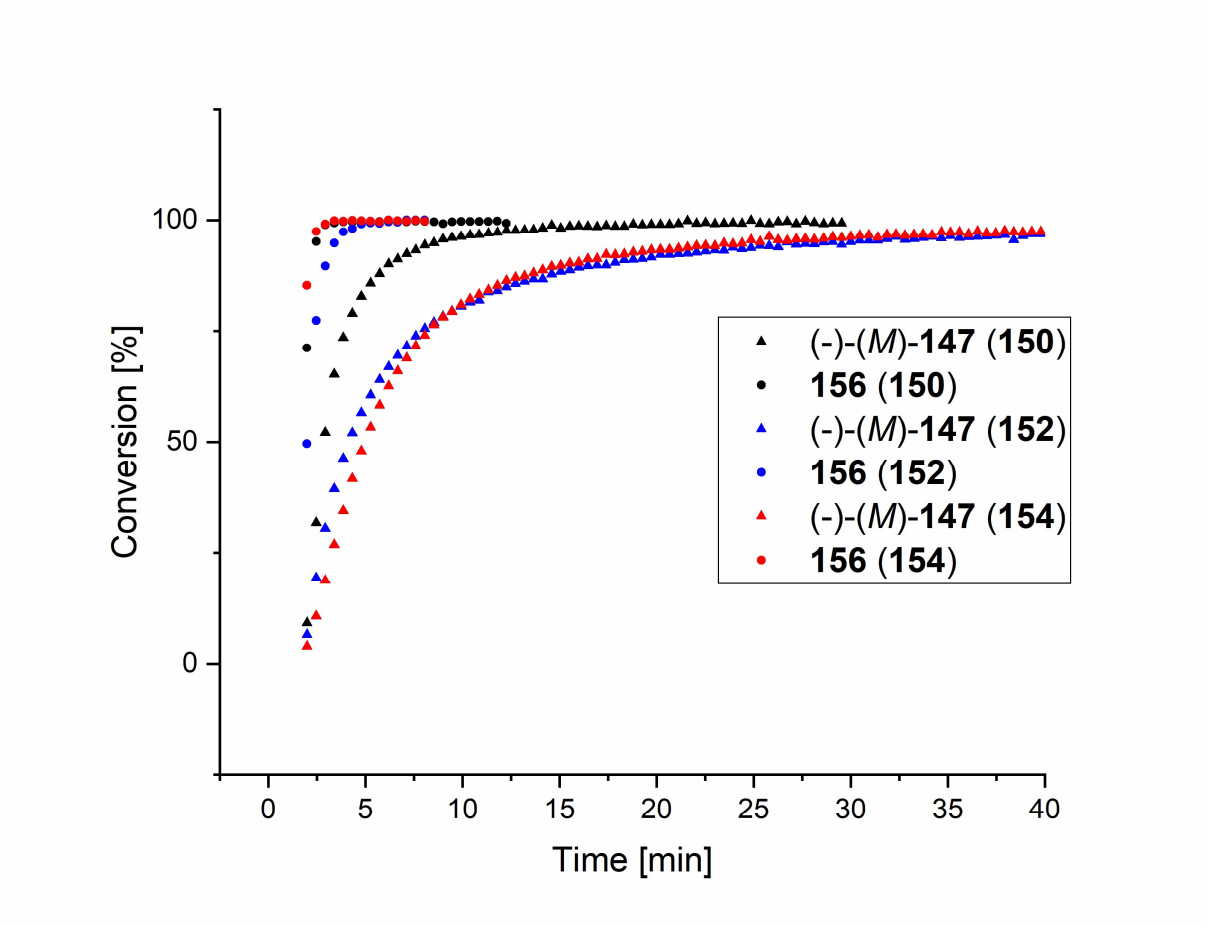

Legend of the curves: catalyst (substrate).

Figure 13: Activity tests of Ru-complex (-)-(*M*)-**147** compared to **156**.

The activity of catalyst (-)-(*M*)-**147** in cross metathesis (CM) was tested in the reaction of allylbenzene (**157**) with olefin **158** (**Scheme 43**). The reactivity of complex (-)-(*M*)-**147** was again compared with the reactivity of complex **156**. Both catalysts gave good yields and selectivities towards the thermodynamically preferred *E* isomer.

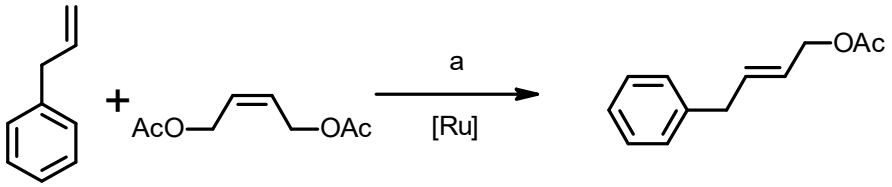

157 **158** **159**

a) **158** (16.7 equiv.), (-)-(*M*)-**147** or **156** (1 mol%), toluene, 0.2 M, 40 °C, 20 h, 75% with (-)-(*M*)-**147** (*E*/*Z* = 9 : 1) and 77% with **156** (*E*/*Z* = 10 : 1).

Scheme 43: Activity test in cross metathesis.

Application in Asymmetric Olefin Metathesis

As explained in **Scheme 10**, an asymmetric olefin metathesis usually includes a desymmetrization operation. A typical substrate to test the stereoinduction of a new chiral metathesis catalyst in ARCM is the prochiral triene **160** (**Table 1**).[103] A solvent screening (entries 1-6) identified THF as the best solvent regarding both conversion and enantioselectivity. Under optimized conditions, the novel helically chiral catalyst (-)-(*M*)-**147** transformed allyl ether **160** to (*R*)-**161** with 83% conversion and 60% *ee* (entry 5). The absolute configuration of the major enantiomer obtained was determined to be (*R*) (see Chapter 5). An increase in the catalyst loading did not improve the enantiomeric excess (entry 7), while lower catalyst loadings (entry 8-10) resulted in incomplete conversions. Notably, the use of 0.5 mol% of (-)-(*M*)-**147** still catalyzed the reaction resulting in more than 50% conversion of **160** (entry 9). The *in situ* formation of other halides of the catalytically active complex proved to be beneficial for some reported systems, especially the exchange of Cl^- with I^- (*e.g.* **57**, **Figure 11**).[103] In case of (-)-(*M*)-**147**, no positive effect could be observed after the addition of halide salts (entries 11-13). In all cases, a dramatic decrease in conversion was observed and even a loss of enantioselectivity with NaI (entry 11) was noticed.

Table 1: ARCM catalyzed by (-)-(*M*)-**147**.

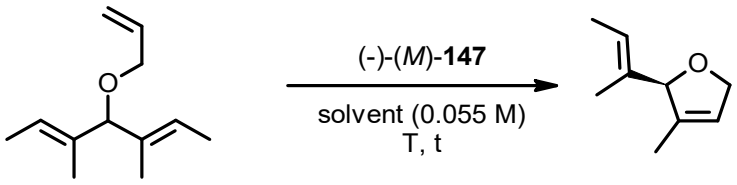

160 (*R*)-**161**

entry	(-)-(*M*)-**147** [mol%]	solvent	T [°C]	t [h]	Conv.[a] [%]	*ee*[b] [%]
1	4.0	CH_2Cl_2	20	24	75	54
2	4.0	CH_2Cl_2	40	4	85	44
3	4.0	toluene	20	24	>95	40
4	4.0	toluene	60	24	>95	28
5	4.0	THF	20	24	83	60
6	4.0	THF	40	4	>95	56
7	10.0	THF	40	4	>95	56
8	0.1	THF	40	4	12	56
9	0.5	THF	40	4	52	56
10	1.0	THF	40	4	61	56
11[c]	4.0	THF	40	4	30	40
12[d]	4.0	THF	40	4	42	60
13[e]	4.0	THF	40	4	23	60

[a]Determined by ^{1}H-NMR spectroscopy. [b]Determined by HPLC on chiral stationary phase. [c]With addition of NaI (1.0 equiv.). [d]With addition of NaBr (1.0 equiv.). [e]With addition of CsF (1.0 equiv.).

As an example of an AROCM, the prochiral *endo*-carboxylic anhydride **162** was reacted with styrene (**163**).[134] By employing 1 mol% of (-)-(*M*)-**147** the chiral all-*cis*-configured cyclopentane **164** was obtained with 40% *ee*, 86% conversion and high *E* selectivity. The absolute stereochemistry of **164** was not determined (see Chapter 5).

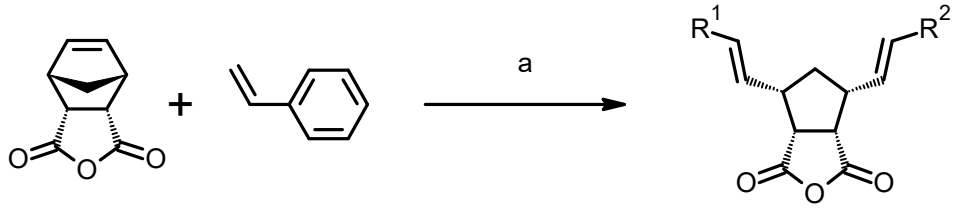

162 **163** **164** (R^1,R^2 = H,Ph)

a) **163** (4.0 equiv.), (-)-(*M*)-**147** (1 mol%), CH_2Cl_2 (0.05 M), 86% conv.[a], *ee*[b] = 40%, *E*/*Z*[c] = 95 : 5. [a]Determined by ^{1}H NMR spectroscopy. [b]Determined by HPLC on chiral stationary phase. [c]Determined by GC-MS.

Scheme 44: AROCM with (-)-(*M*)-**147**.

Structural and Mechanistic Investigations of the Ru Complex (-)-(*M*)-147

To gain further insight into the structural behavior of the novel catalyst (-)-(*M*)-**147**, a ROESY NMR experiment and DFT structure optimization were performed. The NOE interactions in the complex (-)-(*M*)-**147** are displayed in **Figure 14**. Since the benzylidene proton interacts through space only with a methyl group of the mesityl substituent (NOE 1), it can be concluded that the carbene-Ru bond is not freely rotating. The helicene substituent bound to the other nitrogen atom shows NOEs between the hydrogen atoms at the $C^{3,\ 4}$ positions and a methyl group of the isopropoxy unit (NOE 2, 3). Furthermore, the hydrogen atoms at the $C^{1,\ 13}$ positions of the helicene interact with the hydrogen atoms at the C^4 position of the NHC backbone (NOE 4, 5). These interactions reveal that the benzene ring of the helicene connected to the nitrogen atom is twisted around the C-N-bond out of the plane perpendicular to the NHC-ring. The suggested preferred conformation of (-)-(*M*)-**147** was confirmed by DFT calculations (**Figure 15**, left). Several conformers were explored and the global minimum of the complex was found to be in good agreement with the solution based NMR study, giving support for all NOE interactions.

To calculate the buried volume, *i.e.* the space occupied by the new carbene ligand in (-)-(*M*)-**147**, a topographic steric map (**Figure 15**, right) was generated using SambVca 2.0 web tool.[135] Topographic steric maps present a useful way of displaying the steric demands of a ligand bound to a metal center, thereby giving

information about the steric hindrance in the regions relevant for the catalytic process. The coordination sphere is visualized as a projection along the z-axis through the Ru metal center coming from the oxygen atom of the isopropoxy unit. The steric extension along this axis is illustrated by iso-contour curves, with red color indicating high and blue color low steric demand of the ligand. The overall $\%V_{bur}$ value of the helically chiral NHC ligand of (-)-(*M*)-**147** was calculated to be 33.6. For the structurally similar complex **156** and a derivative of its unsaturated IMes-analogue $\%V_{bur}$ values of 33.7 and 31.9, respectively, were reported.[79] For the complexes, where unsymmetrical NHC ligands do not freely rotate around the metal-carbene bond, the overall $\%V_{bur}$ is only of limited relevance. Therefore, the $\%V_{bur}$ values were also calculated for the individual quadrants of the topographic steric map. Northeast (NE), northwest (NW) and southwest (SW) quadrants provide similar $\%V_{bur}$ values (from 30.4 to 32.0). The southeast (SE) quadrant is of importance as it is significantly more congested ($\%V_{bur}$ = 40.5) than the other three. According to the NOE interactions and DFT based model, this is a result of the proton in the C^1 position of the helicene pointing toward the coordination sphere of the metal center.

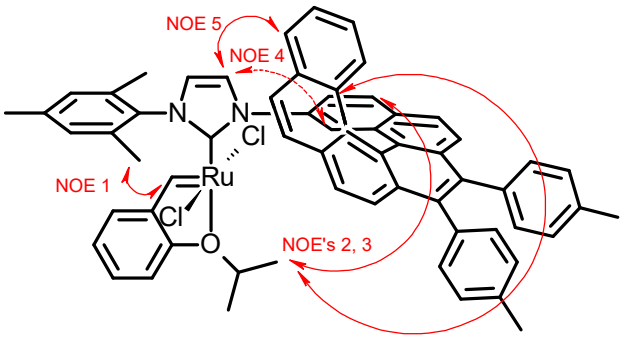

(-)-(*M*)-**147**

Figure 14: NOE interactions of in complex (-)-(*M*)-**147**.

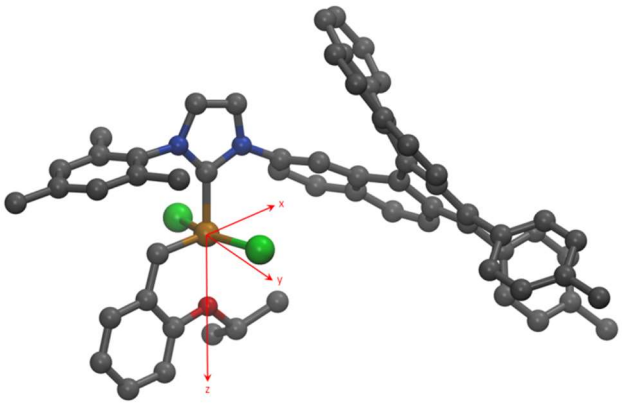

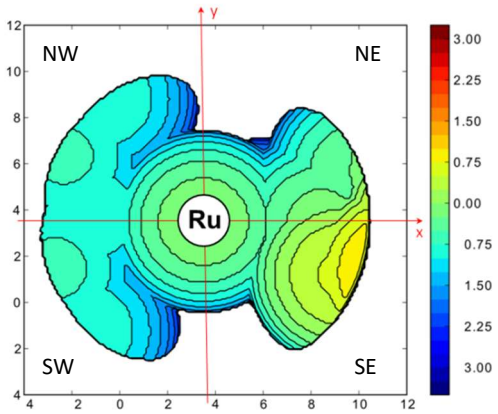

[a]View from the z-axis onto the x-y-plane. All scales are in Å.

Figure 15: DFT calculated model (left) and topographic steric map[a] of (-)-(*M*)-**147** (right).

The stereoinduction in ARCM was discussed at length by Costabile and Cavallo[136] and later reviewed by Blechert *et al*.[137] Although, the mechanism is described for C_2 symmetric complexes such as **56** and **57** (**Figure 11**), an analogy for the catalyst (-)-(*M*)-**147** can be drawn. The same out-of-plane twist of the aryl substituents on the nitrogen atoms in **56** or **57**, which results in a steric congestion of the Ru-coordination sphere caused by the *ortho* proton, was also observed in complex (-)-(*M*)-**147**, *vide infra*.

Scheme 45 shows the mechanism of the ARCM of prochiral triene **160** catalyzed by (-)-(*M*)-**147**. Initially, a 14 valence electron species (**I**) is formed after dissociation of the ether chelating moiety of (-)-(*M*)-**147**. Then the least substituted olefin of triene **160** is coordinated regioselectively and intermediate **II** is formed. **II** undergoes [2+2] cycloaddition (**III**) and cycloreversion (**IV**). The chirality installed within the formed complex **IV** leads to a selective reaction with one of the prochiral enantiofaces of the triene, setting up the desired stereocenter in **V**. Subsequent cycloreversion releases the enantiomerically enriched product **161** with a preferred (*R*)-configuration and the active 14 valence electron complex **I**.

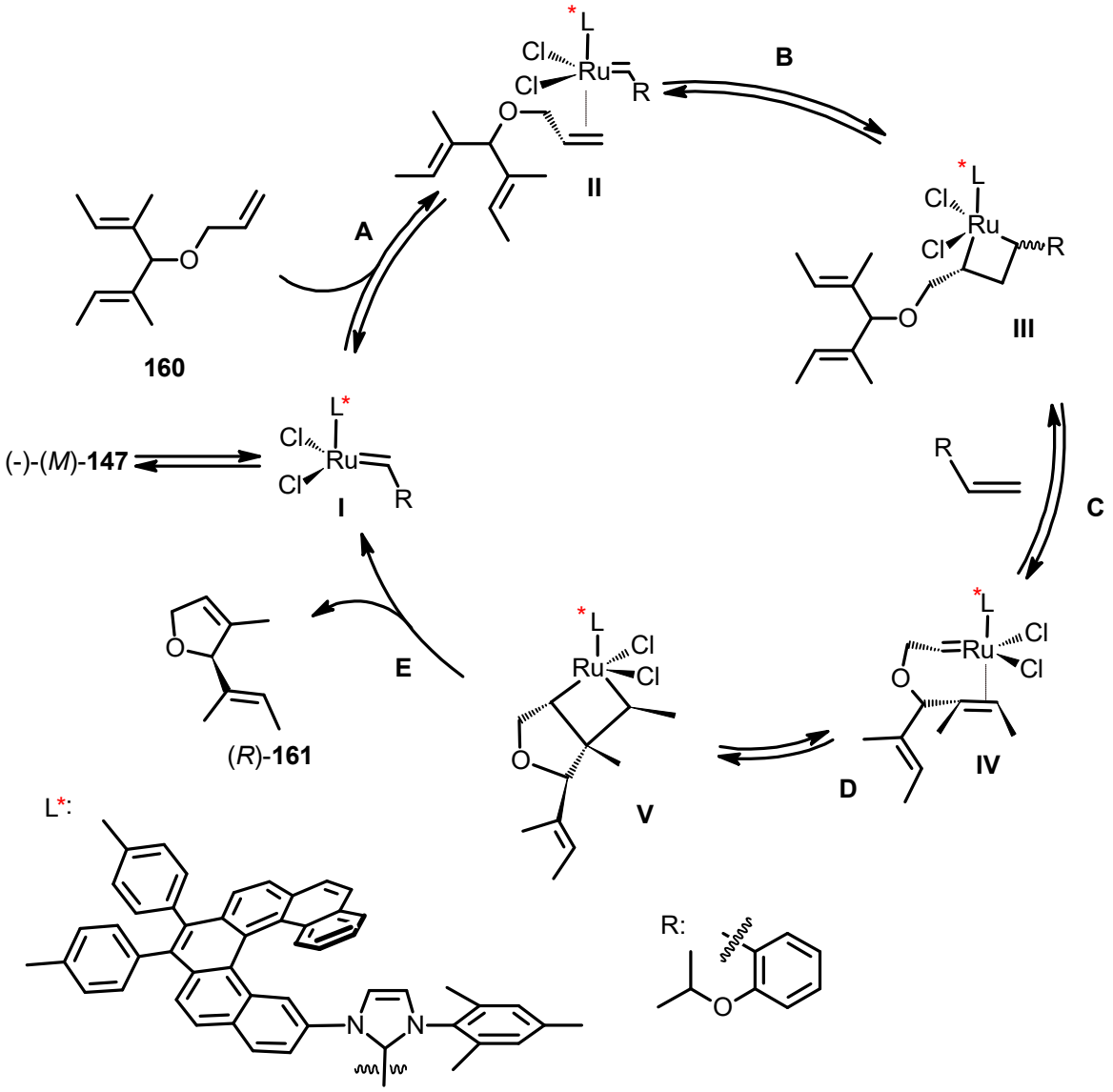

Scheme 45: Mechanism of ARCM mediated by chiral Ru-catalyst (-)-(*M*)-**147**.

Potentially any step can be involved in the enantiodetermination of (*R*)-**161**. Following the model proposed by Costabile and Cavallo, the focus is centered on intermediates **IV** and **V**. The Newman projection in **Scheme 46** shows the influence of the out-of-plane rotated protons (red and blue) which are forced in this conformation due to the helicene moiety (for explanation see **Figure 14** and **Figure 15**). The red proton is bent down to the equatorial plane margining one of the enantiofaces of the alkylidene double bond within the coordination sphere of the complex. Thus, two energetically different stereoisomers of intermediate **IV** can be formed. **IV**-a and **IV**-b differ in their orientation of the bound olefin substrate. The substrate can either orient in proximity to the proton pointing down (red, see also

Figure 15 SE quadrant), resulting in isomer **IV**-a, or in proximity to the proton pointing up (blue, see also **Figure 15** NE quadrant), resulting in **IV**-b. Due to minimized steric interaction of the methylene moiety of the olefin (orange arrow) with the nearby proton (blue) the formation of structure **IV**-b is kinetically favored.

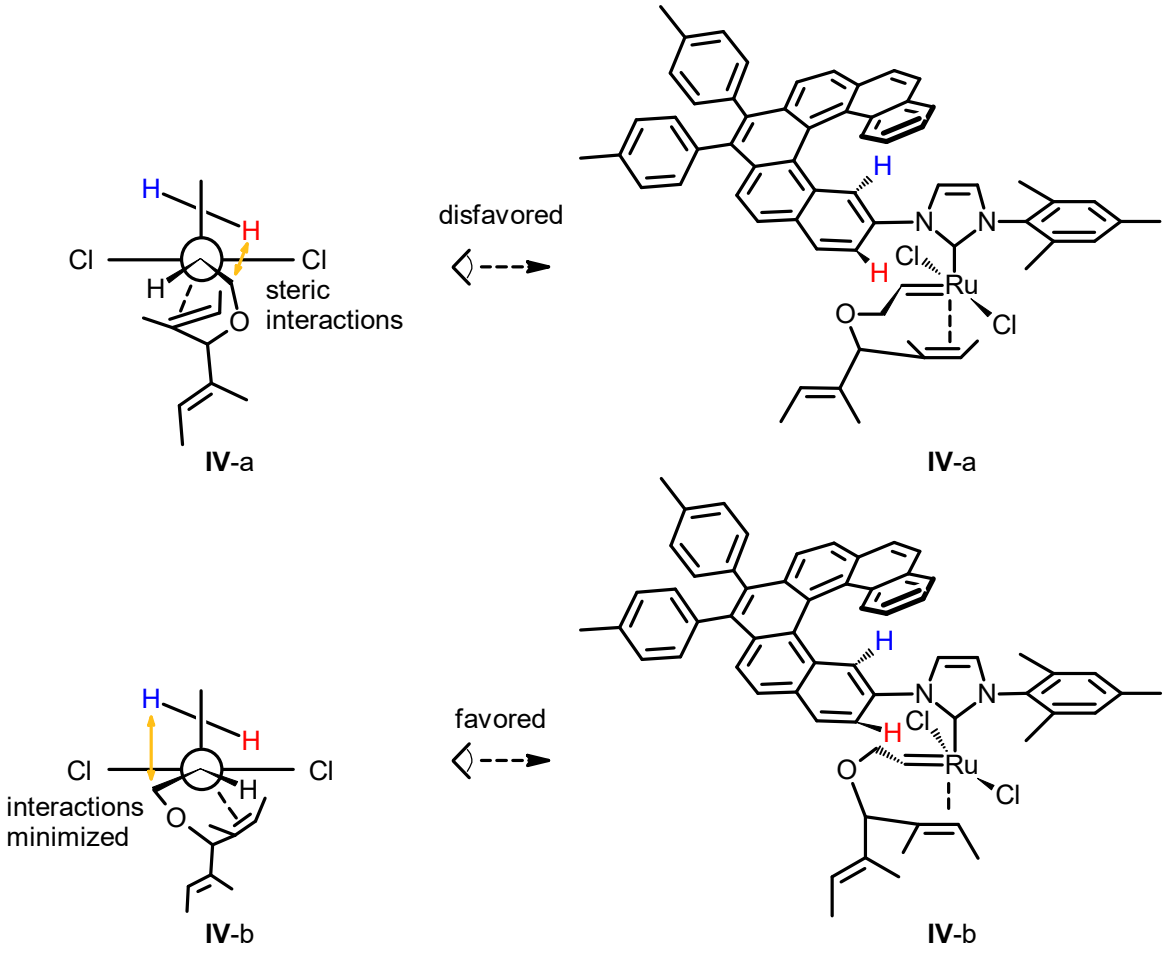

Scheme 46: Ligand orientation within the catalyst-substrate complex **IV**.

In the study by Costabile and Cavallo it was also suggested that the chiral orientation, resulting from the interaction described in **Scheme 46**, selects one of the prochiral enantiofaces of the olefin through a well defined folding of the complex. Initiated by the preferred formation of **IV**-b (**Scheme 46**), the five-membered ring in **V** can be closed by reversible cycloaddition with either of the two pedant double bonds, leading to two possible, energetically different olefin structures (**Figure 16**). The unbound olefin moiety in **V** can either be located in the axial (**V**-axial) or equatorial (**V**-equatorial) position of the five-membered ring. The equatorial position is oriented into an empty area, which is substantially away from all the other groups of the system. The axial position is at short distance from the proton (green) of the CH

group of the reacting C=C double bond and the chlorine atom.[136] Due to reduced steric interactions, **V**-equatorial, where the uncoordinated olefin is located in the equatorial position, is favored over **V**-axial.

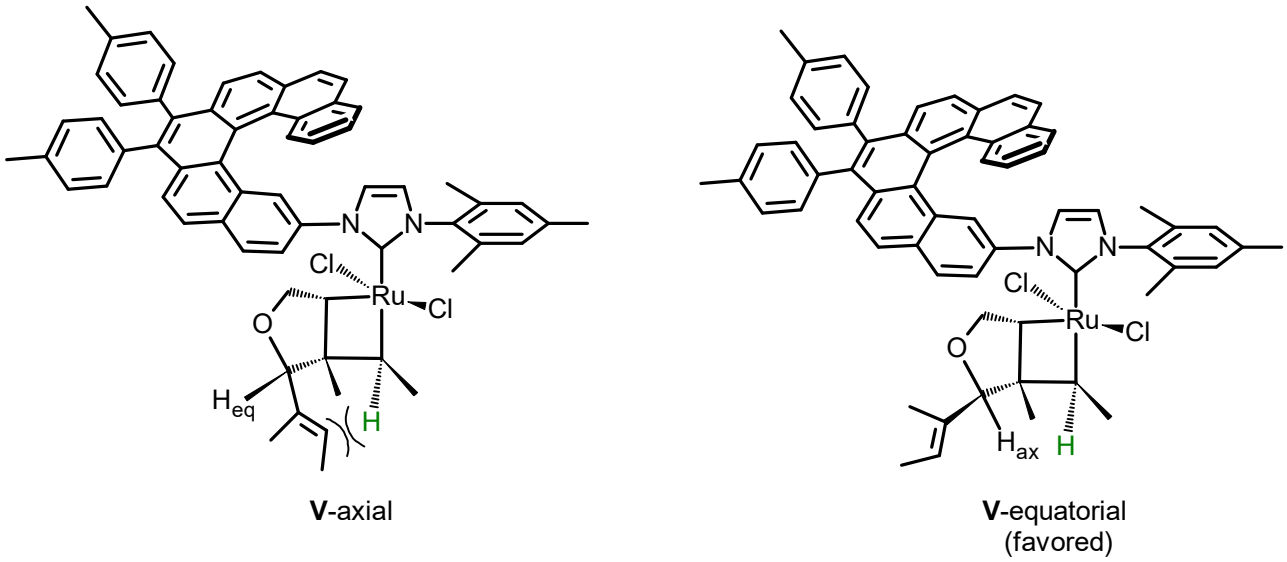

V-axial

V-equatorial
(favored)

Figure 16: Folding of the catalyst-substrate complex **V**.

With the energetically preferred structures **IV**-b and **V**-equatorial in the catalytic cycle, formation of an excess of the (*R*) enantiomer of chiral olefin **161** can be expected in the reaction mediated by (-)-(*M*)-**147** (**Scheme 47**), which is in agreement with the experiment. On the other hand, exchange of the chloro ligands by larger iodo ligands should further increase the strain in **V**-axial due to steric interactions between the halide and the proton (green) mentioned above and, therefore, lead to higher enantioselectivity, which was not observed in the case of (-)-(*M*)-**147**. Collins *et al.* also reported drop in enantioselectivity by employing NaI as an additive together with their C_1-symmetric catalyst in the RCM of triene **160**.[138] They proposed a rotation around the NHC-Ru bond, observed at ambient temperature for their catalyst, to be the cause of the decreased *ee* values of product **161**.

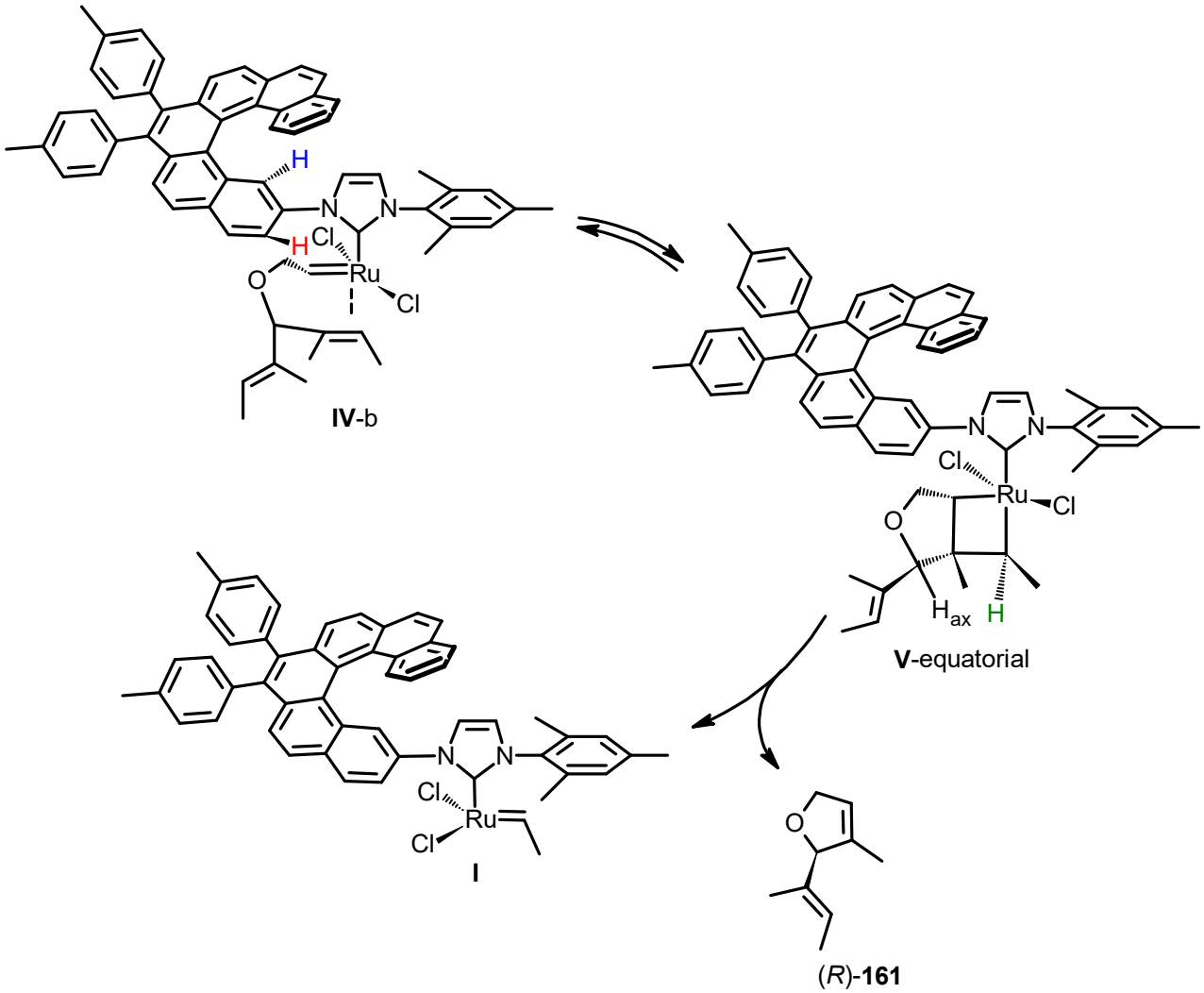

Scheme 47: Formation of (*R*)-**161**.

Ru-Catalyzed Formation of Helicene

Inspired by a study by Blechert and Peters, who reported the Ru-catalyzed isomerization of triynes to benzene derivatives,[139] catalyst (-)-(*M*)-**147** was applied in the synthesis of dibenzo[6]helicene **14**. Blechert proposed a cascade of four metathesis reactions as a mechanistic explanation. First, the more reactive catalyst **156** was tested to see if the procedure is also suitable for the formation of helicenes. The desired dibenzo[6]helicene was obtained in low yield after 24 h at ambient temperature (**Scheme 48**). When (-)-(*M*)-**147** was employed as a catalyst, the reaction conditions had to be changed and, after 19 h at 60 °C, the desired compound **14** was also obtained with only low conversion. Moreover, an HPLC analysis of the mixture revealed that helicene **14** was obtained in a racemic form.

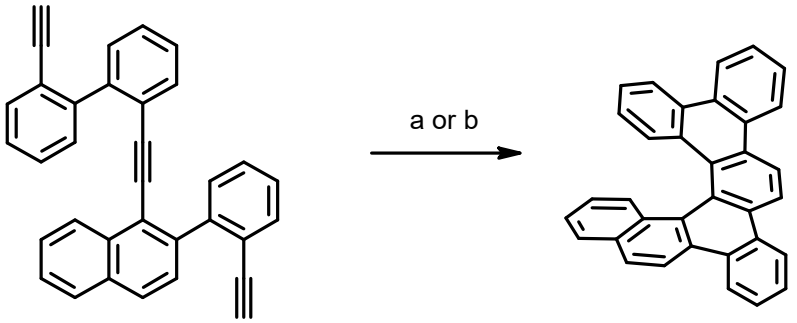

11 **14**

a) **156** (10 mol%), CH_2Cl_2, rt, 24 h, 10%; b) (-)-(*M*)-**147** (10 mol%), toluene, 60 °C, 19 h, 10% conversion[a] (0% ee[b]). [a]According to TLC analysis. [b]Determined by HPLC on chiral stationary phase.

Scheme 48: Ru-catalyzed synthesis of dibenzo[6]helicene **14**.

3.6 Investigations with Pd-Complexes

In order to investigate the stereoinduction of the novel Pd-PEPPSI complexes (+)-(*P*,*P*)-**148** and (-)-(*M*)-**149**, the asymmetric Suzuki-Miyaura coupling was chosen as a test reaction (**Scheme 49**). Common substrates for such a study are naphthylhalides (**165** or **166**) and naphthylboronic acid **167**, which react to rotationally stable biaryl **168**.[116, 117] First, the reaction conditions reported by Kündig *et al.*[116] were found to give incomplete conversion of **165** (checked by TLC) and were then slightly changed (a 1:1 ratio of dioxane/water was changed to 9:1) in order to increase the solubility of the reactants. That resulted in a full conversion of **165** and the desired biaryl **168** was obtained in 86% yield employing commercially available Pd-PEPPSI complex **60** (**Figure 17**).

When the helically chiral catalysts (+)-(*P*,*P*)-**148** and (-)-(*M*)-**149** were used, the bromo compound **165** was found to be unreactive and was thus replaced by the iodo derivative **166**. When complex (-)-(*M*)-**149** was applied in the process, biaryl **168** was obtained with 27% conversion of **166**. Disappointingly, no asymmetric induction was observed and binaphthyl **168** was obtained as a racemate. In addition to that, formation of homocoupling by-product **169** was also observed by GC-MS. As the optimization of the reaction conditions for a catalyst with no initial stereoinduction at all is a desperate venture, complex (-)-(*M*)-**149** was dismissed from further investigations. Complex (+)-(*P*,*P*)-**148** seemed to be more promising with regard to stereoinduction due to the larger chiral NHC with two helicene moieties. When (+)-(*P*,*P*)-**148** was tested under the same conditions (b), no conversion of **166** was observed. Only homocoupling by-product **169** was obtained according to GC-MS. After optimization of the solvent system and base, complex (+)-(*P*,*P*)-**148** was found to mediate the reaction of iodide **166** to biaryl **168** in 91% conversion (c). Unfortunately, **168** was obtained again as a racemate, which leads to the conclusion that complex (+)-(*P*,*P*)-**148** also shows no stereoinduction at all in the studied reaction.

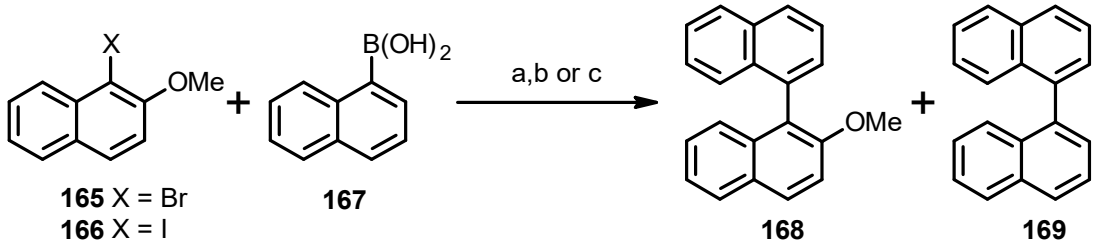

165 X = Br
166 X = I

167

168

169

a) **165**, **167** (1.5 equiv.), **60** (5 mol%), KOH (3.0 equiv.) dioxane/water 9 : 1, rt, 24 h, 86%; b) **166**, **167** (1.5 equiv.), (+)-(*P*,*P*)-**148** or (-)-(*M*)-**149** (5 mol%), KOH (3.0 equiv.) dioxane-water 9 : 1, rt, 24 h, 0% conversion[a] with (+)-(*P*,*P*)-**148** and 27% conversion[a] (0% *ee*[b]) with (-)-(*M*)-**149**; c) **166**, **167** (2.0 equiv.), (+)-(*P*,*P*)-**148** (5 mol%), *n*-Bu_4NF (3.0 equiv.), DMPU/water 10 : 1, 60 °C, 18 h, 91% conversion[a] (0% ee[b]). [a]Determined by GC-MS. [b]Determined by HPLC on chiral stationary phase.

Scheme 49: Suzuki-Miyaura coupling catalyzed by (+)-(*P*,*P*)-**148** and (-)-(*M*)-**149**.

Since there are only two successful catalysts of this type published so far,[116, 117] it seems too early to compare catalyst designs and draw conclusions in order to explain the failure of the novel complexes (+)-(*P*,*P*)-**148** and (-)-(*M*)-**149** (**Figure 17**). What can easily be compared is the $\%V_{bur}$ value. The two successfully stereoinducing catalysts **65** and **66** exhibit $\%V_{bur}$ values of 35.9 and 42.2 (**Table 2**, entries 3 and 4). The $\%V_{bur}$ values for complexes (+)-(*P*,*P*)-**148** and (-)-(*M*)-**149** were

obtained in the same way as described for the Ru complex (-)-(*M*)-**147** (**Figure 15**), both equal 32.7 and are much lower in comparison with entries 1 and 2. This reduced asymmetric congestion around the coordination sphere of the Pd center might provide an explanation for the missing stereoinduction. Moreover, Organ and co-workers reported that more bulky substituents on the nitrogen atoms (*e.g.* entry 6 compared to entry 5) can be beneficial for the activity of the catalyst.[140] The relatively low $\%V_{bur}$ values of complexes (+)-(*P*,*P*)-**148** and (-)-(*M*)-**149**, therefore, might give an explanation for their reduced activity in Suzuki-Miyaura cross coupling.

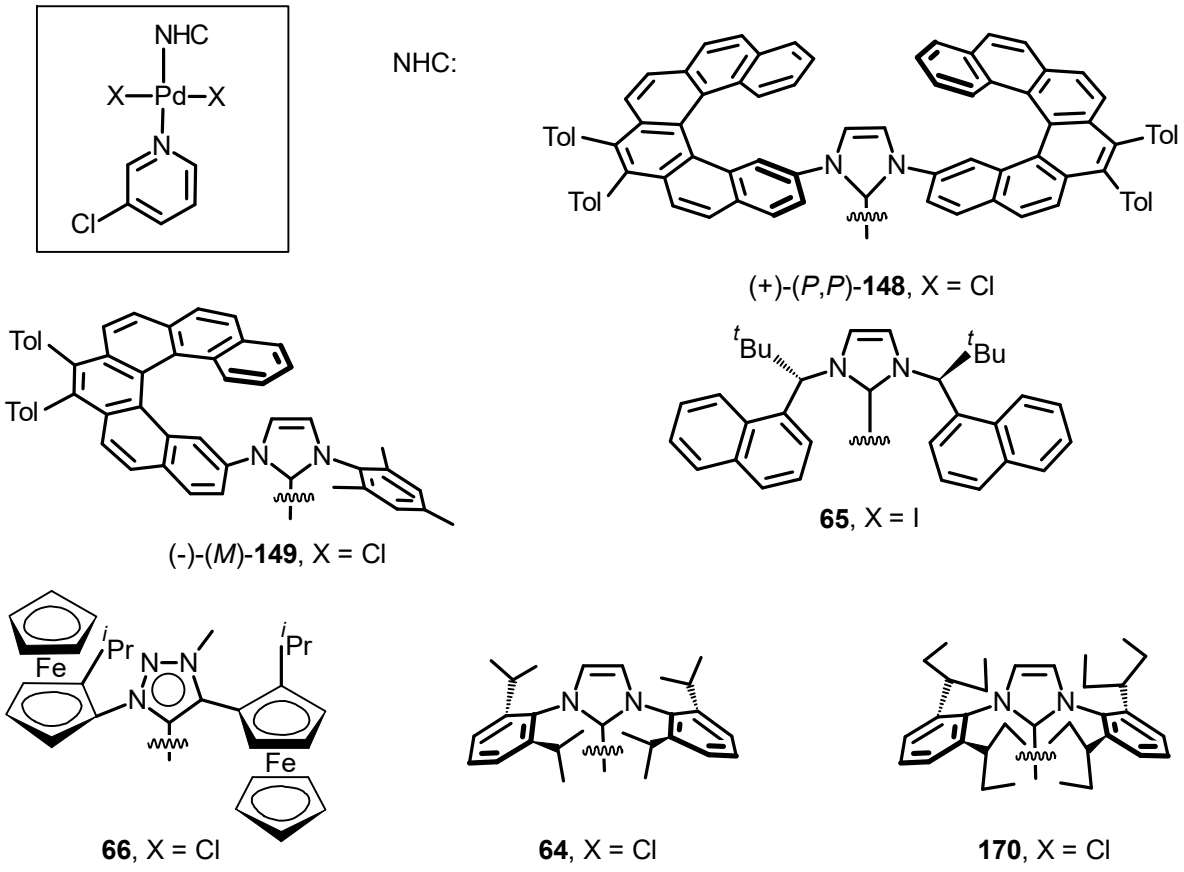

Figure 17: Selected Pd-PEPPSI complexes.

Table 2: $\%V_{bur}$ values for selected Pd-PEPPSI complexes.

entry	complex	Pd-NHC [Å]	$\%Vol_{bur}$
1	(+)-(*P*,*P*)-**148**	1.980	32.7
2	(-)-(*M*)-**149**	1.990	32.7
3	**65**[116]	2.000	35.9
4	**66**[117]	1.971	42.2
5	**60** [116]	2.000	34.3
6	**170**[116]	2.000	37.9

4. Conclusion and Outlook

A versatile approach to fully aromatic 2-amino[6]helicenes (-)-(*M*)-**69** and (-)-(*M*)-**118** was developed (**Figure 18**). Helicene **69** was obtained in both enantiomeric forms ((-)-(*M*) and (+)-(*P*)) on a multigram scale. Full stereocontrol could not be obtained in the case of amino[6]helicene derivative **143**. Employing **69**, the first helically chiral Ru ((-)-(*M*)-**147**) and Pd ((+)-(*P*,*P*)-**148** and (-)-(*M*)-**149**) NHC complexes have been synthesized and characterized. (-)-(*M*)-**147** has shown a promising stereoinduction in asymmetric olefin metathesis reactions. An NMR study and DFT-calculations suggest that complex (-)-(*M*)-**147** is conformationally rigid and forced in a preferred conformation, which creates an asymmetric steric congestion in the coordination sphere of the Ru atom. Pd-PEPPSI type complexes (-)-(*M*)-**149** and (+)-(*P*,*P*)-**148** were found to give no stereoinduction in asymmetric Suzuki-Miyaura coupling.

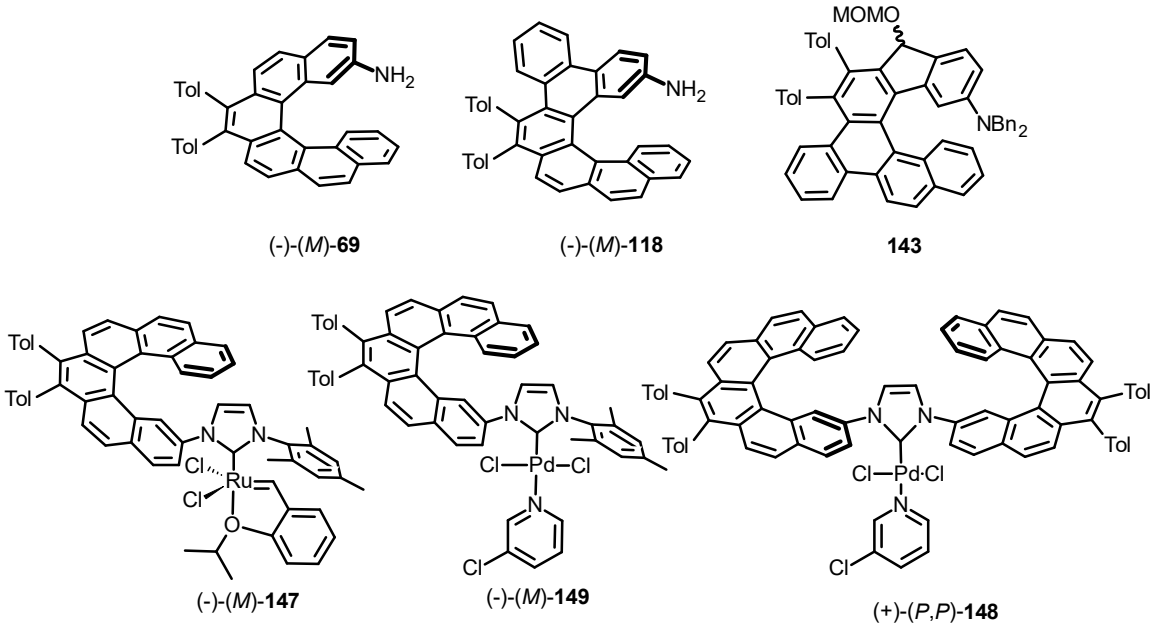

Figure 18: Overview of successfully synthesized compounds.

With the synthesis of these new helically chiral amines and respective NHC complexes, a new field of research has been opened. Due to the promising results with (-)-(*M*)-**147** in asymmetric olefin metathesis, different helically chiral Ru-NHC complexes should be prepared in the future and compared to study the influence of certain structural features of the helicene skeleton on enantioinduction. First ideas about the enantiocontrol were discussed and the respective mechanism was

proposed. (-)-(*M*)-**149** and (+)-(*P*,*P*)-**148** should be tested in different coupling reactions to find a suitable application.

5. Experimental

General: Melting points were determined on Mikro-Heiztisch Polytherm A (Hund, Wetzlar) apparatus and are uncorrected. The ^{1}H NMR spectra were measured at 300 MHz, 400 MHz, 500 MHz, and 600 MHz, the ^{13}C NMR spectra at 75 MHz, 101 MHz, 126 MHz, and 151 MHz in $CDCl_3$, CD_2Cl_2 or toluene-d_8 as indicated in 5 mm PFG probe. For standardization of ^{1}H NMR spectra, the internal signal of TMS (δ 0.0, $CDCl_3$) or residual signals of solvents (δ 5.32 for $CHDCl_2$, δ 7.26 for $CHCl_3$ or δ 7.00 or 2.09 for toluene-d_8) were used. In the case of ^{13}C spectra, the residual signals of solvents (δ 77.16 for $CDCl_3$, δ 54.00 for CD_2Cl_2) were used. The chemical shifts are given in δ-scale, the coupling constants *J* are given in Hz. For the complete assignment of both the ^{1}H and ^{13}C NMR spectra of key compounds, COSY, HSQC and HMBC experiments were performed. The IR spectra were measured in $CHCl_3$ on FT-IR spectrometer Bruker Equinox 55 or neat on FT-IR spectrometer Nicolet 6700 with the ATR unit Smart Performer from Thermo Electron Corporation. The EI mass spectra were determined at an ionizing voltage of 70 eV, recorded in the positive ion mode, and the *m/z* values are given along with their relative intensities (%). The sample was dissolved in chloroform, loaded into a quartz cup of the direct probe and inserted into the ion source. The source temperature was 220 °C. For exact mass measurement, the spectrum was internally calibrated using perfluorotri-*n*-butylamine (Heptacosa). The ESI mass spectra were recorded using ZQ micromass mass spectrometer (Waters) equipped with an ESCi multi-mode ion source and controlled by MassLynx software. Alternatively, the low resolution ESI mass spectra were recorded using a quadrupole orthogonal acceleration time-of-flight tandem mass spectrometer (Q-Tof micro, Waters) and high resolution ESI mass spectra using a hybrid FT mass spectrometer combining a linear ion trap MS and the Orbitrap mass analyzer (LTQ Orbitrap XL, Thermo Fisher Scientific). The conditions were optimized for suitable ionization in the ESI Orbitrap source (sheath gas flow rate 35 a.u., aux gas flow rate 10 a.u. of nitrogen, source voltage 4.3 kV, capillary voltage 40 V, capillary temperature 275 °C, tube lens voltage 155 V). The samples were dissolved in methanol and applied by direct injection. As a mobile phase was used 80% methanol (flow rate 100 µl/min. MALDI spectra were recorded using UltrafleXtreme™MALDI-TOF/TOF mass spectrometer (Bruker Daltonik, Bremen, Germany) operated in reflectron mode. Samples were prepared using dried droplet method with 2,5-dihydroxybenzoic acid matrix. Desorption and ionization was

accomplished by a Smartbeam laser (Nd:YAG 355 nm) operated at 1 kHz with optimized delayed extraction time. Positive ions were accelerated by voltage of 25 kV. Data were collected by means of FlexControl software. The APCI mass spectra were recorded using an LTQ Orbitrap XL (Thermo Fisher Scientific) hybrid mass spectrometer equipped with an APCI ion source. The APCI vaporizer and heated capillary temperatures were set to 400 °C and 200 °C, respectively; the corona discharge current was 3.5 μA. Nitrogen served both as the sheath and auxiliary gas at flow rate 55 and 5 arbitrary units, respectively. The ionization conditions were the same for low-resolution as well as high-resolution experiment. The HR spectra were acquired at a resolution of 100 000. The CI mass spectra in the positive ion mode were recorded using an orthogonal acceleration time-of-flight mass spectrometer GCT Premier (Waters) coupled to a 7890A gas chromatograph (Agilent). The ion source temperature 140 °C, the electron energy 70 eV and methane as the reagent gas were used. The spectra were internally calibrated using tris(trifluoromethyl)triazine. UV/Vis spectra were recorded on SPECORD 250 PLUS (Analytik Jena AG) with pure solvent ($CHCl_3$ for HPLC) as a baseline. Optical rotations were measured in $CHCl_3$ using an Autopol IV instrument (Rudolph Research Analytical). The CD spectra were acquired on a J-815 CD spectrometer (Jasco Analytical Instruments, Inc.) in THF (10^{-4} M solutions) using 10 mm quartz sample cell. HPLC analyses were performed using an instrument consisting of an isocratic HPLC pump (Knauer Smartline 1000), a variable wavelength UV detector (Knauer Smartline 2500), a polarimetric detector (Chiralyser LED 426 nm, IBZ Messtechnik) and a PC workstation with Clarity software (Dataapex). Chiral GC-MS analysis was performed on a 5975C/7890A apparatus (Agilent Technologies) with a CP-Chirasil-Dex CB column (25 m, 0.25 mm, 0.25 μm, 7 inch cage).TLC was performed on Silica gel 60 F_{254}-coated aluminium sheets (Merck) and spots were detected by an aqueous solution of $Ce(SO_4)_2 \cdot 4\ H_2O$ (1%) and $H_3P(Mo_3O_{10})_4$ (2%) in sulphuric acid (10%). The flash chromatography was performed on Silica gel 60 (0.040-0.063 mm, Merck) or on Biotage® KP- C18-HS SNAP cartridges using Isolera One HPFC system (Biotage, Inc.). Biotage Initiator EXP EU (300 W power) was used for a reaction carried out in microwave reactor. *N*,*N*-Diisopropylamine was distilled from calcium hydride under nitrogen, THF was distilled from sodium/benzophenone under nitrogen, toluene was distilled from sodium under nitrogen, and dichloromethane was distilled from phosphorous pentoxide under nitrogen. *N*,*N*-

Dimethylformamide was taken from Sure/Seal™ bottles with molecular sieves (purchased from Sigma Aldrich). All other commercially available catalysts and reagent grade materials were used as received. The following test substrates and starting materials were synthesized following previously published procedures: iodonaphthalene **166**, [141] iodonaphtalene (*S*)-**82**,[31] boronic acid **113**,[26] iodonaphthalene **124**,[26] formamide **137**,[73] triyne **11**,[26] dienes **152** [142] and **150**,[142] enyne **154**,[143] triene **160**.[105]

N,*N*-Dibenzyl-3-iodoaniline 76[144]

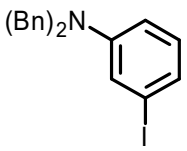

A flask was charged with aniline **75** (3.286 g, 15.0 mmol), K_2CO_3 (10.365 g, 75.0 mmol, 5.0 equiv.) in a mixture of ethanol-water (30 mL, 1:1) and benzyl bromide (10.262 g, 60.0 mmol, 4.0 equiv.) was added. The reaction mixture was stirred under reflux for 3 h and at 60 °C overnight. The white precipitate was filtered off on a frit and washed with water (10 mL) and ethanol (10 mL). The precipitate and the filtrate were worked up separately. The precipitate was dissolved in dichloromethane (15 mL), dried over anhydrous $MgSO_4$, and solvent was removed *in vacuo* to give a portion of the benzylated aniline **76** (5.989 g, 89%) as a white solid. The aqueous layer was extracted with ethyl acetate (3 × 15 mL) and dichloromethane (3 × 15 mL). The combined organic portions were dried over anhydrous $MgSO_4$ and concentrated under reduced pressure to provide a brownish oil, to which ethanol (100 mL) was added. After 2 d in a fridge, the formed precipitate was filtered off on a frit and washed with ethanol (10 mL) to provide a second portion of the benzylated aniline **76** (498 mg, 8%) as a white solid. **M.p.**: 117 – 118 °C (ethanol).**^{1}H NMR** (300 MHz, $CDCl_3$): δ 7.28 – 7.13 (m, 6H), 7.13 – 7.06 (m, 4H), 6.99 (dd, *J* = 2.5, 1.5 Hz, 1H), 6.94 – 6.87 (m, 1H), 6.77 – 6.69 (m, 1H), 6.59 – 6.51 (m, 1H), 4.48 (s, 4H).**^{13}C NMR** (75 MHz, $CDCl_3$): δ 150.49, 137.88, 130.73, 128.86, 127.22, 126.71, 125.86, 121.12, 111.86, 95.75, 54.03. **IR** (neat): 3081 vw, 3062 vw, 3022 w, 3000 vw, 2918 w, 2859 w, 1580 s, 1488 s, 1352 m, 979 m, 944 m, 760 s, 731 s, 693 s cm^{-1}. **EI MS**: 399 ($M^{\bullet+}$, 18), 308 (7), 180 (11), 91 (100), 65 (20). **HR EI MS**: calcd for $C_{20}H_{18}NI$ 399.0484, found 399.0475.

4-(Dibenzylamino)-2-iodobenzaldehyde 77

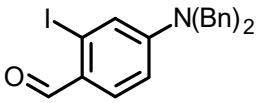

An oven-dried Schlenk flask was charged with *N*,*N*-dimethylformamide (5 mL, 65.0 mmol, 5.0 equiv.), cooled to 0 °C, and phosphoryl chloride (7.876 mL, 84.5 mmol, 6.5 equiv.) was slowly added. The reaction was warmed to room temperature, stirred at this temperature for 1 h, and then cooled again to 0 °C. To this mixture, *N*,*N*-dibenzyl-3-iodoaniline **76** (5.190 g, 13.0 mmol) was slowly added as a suspension in dimethylformamide (10 mL). After stirring at 0 °C for 1 h, the reaction was stirred at 50 °C for additional 5 h. The cooled solution was poured into ice water, basified with a NaOH solution (3 N), extracted with ethyl acetate (3 × 20 mL), dichloromethane (3 × 20 mL), the organic phases were combined, and dried over anhydrous $MgSO_4$. The crude product was purified by column chromatography on silica gel (hexane-methyl *tert*-butyl ether 10:1 to 2:1 to 0:1) to afford benzaldehyde **77** (5.278 g, 95%) as a white solid. **M.p.**: 106 – 108 °C (hexane-methyl *tert*-butyl ether).**^{1}H NMR** (300 MHz, $CDCl_3$): δ 9.79 (s, 1H), 7.71 (d, *J* = 8.9 Hz, 1H), 7.42 – 7.28 (m, 6H), 7.27 – 7.24 (m, 1H), 7.20 (d, *J* = 7.0 Hz, 4H), 6.77 (dd, *J* = 8.9, 2.5 Hz, 1H), 4.70 (s, 4H). **^{13}C NMR** (75 MHz, $CDCl_3$): δ 194.14, 154.19, 136.33, 131.60, 129.13, 127.72, 126.51, 124.69, 122.52, 112.12, 104.36, 53.97. **IR** (neat): 3084 vw, 3050 vw, 3017 vw, 2942 w, 2830 w, 2733 vw, 1660 m, 1575 s, 1503 m, 1449 s, 1401 w, 1359 w, 1230 s, 1013 m, 728 s, 694 m cm^{-1}. **EI MS**: 427 ($M^{\bullet+}$, 15), 336 (7), 180 (4), 91 (100), 65 (15). **HR EI MS**: calcd for $C_{21}H_{18}ONI$ 427.0433, found 427.0441.

***rac*-1-[4-(Dibenzylamino)-2-iodophenyl]-4-[tris(1-methylethyl)silyl]but-3-yn-1-ol 78**

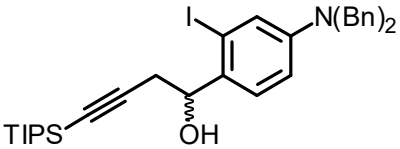

A solution of *n*-butyllithium (2.5 M in hexanes, 6.3 mL, 15.75 mmol, 1.05 equiv.) was added dropwise at -78 °C under argon to a solution of (triisopropylsilyl)propyne (3.77 mL, 15.75 mmol, 1.05 equiv.) in tetrahydrofuran (18 mL). After stirring at -78 °C for 10 min, the cooling bath was removed and the reaction mixture was stirred for additional 40 min reaching room temperature. Then the mixture was cooled again to -78 °C and a solution of benzaldehyde **77** (6.41 g, 15.0 mmol) in tetrahydrofuran (15 mL) was added. The reaction was stirred at -78 °C for 20 min. After completion (checked by TLC), it was quenched with an HCl solution (1 M). The layers were

separated and the aqueous one was extracted with ethyl acetate (3 × 50 mL). The combined organic layers were washed with a saturated $NaHCO_3$ solution (50 mL), dried over anhydrous $MgSO_4$, and evaporated to dryness. The crude product was purified by column chromatography on silica gel (hexane-ethyl acetate 10:1) to afford the alkynol *rac*-**78** (8.997 g, 96%) as a colorless oil. **^{1}H NMR** (400 MHz, $CDCl_3$): δ 7.37 – 7.31 (m, 4H), 7.30 – 7.24 (m, 3H), 7.24 – 7.18 (m, 5H), 6.73 (dd, *J* = 8.8, 2.7 Hz, 1H), 4.96 (ddd, *J* = 7.2, 5.0, 3.7 Hz, 1H), 4.60 (s, 4H), 2.82 (dd, *J* = 16.8, 5.0 Hz, 1H), 2.60 (dd, *J* = 16.9, 7.2 Hz, 1H), 2.42 (d, *J* = 3.8 Hz, 1H), 1.10 – 0.98 (m, 21H). **^{13}C NMR** (101 MHz, $CDCl_3$): δ 149.79, 137.90, 131.97, 128.88, 127.36, 127.25, 126.75, 122.34, 112.78, 104.39, 99.39, 84.09, 75.23, 54.03, 29.63, 18.78, 11.36. **IR** (neat): 3089 vw, 3064 vw, 3030 w, 2922 m, 2863 m, 1598 s, 1502 m, 1453 m, 1228 w, 1015 w, 731 w, 677 w cm^{-1}. **EI MS**: 623 ($M^{+\bullet}$, 22), 428 (44), 181 (9), 91 (100), 75 (11), 43 (11). **HR EI MS**: calcd for $C_{33}H_{42}ONISi$ 623.2080, found 623.2096.

rac-*N*,*N*-Dibenzyl-3-iodo-4-{1-(methoxymethoxy)-4-[tris(1-methylethyl)silyl]but-3-yn-1-yl}-aniline 79

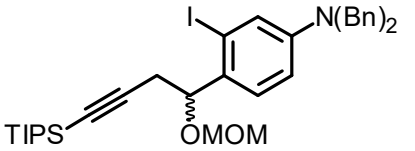

A Schlenk flask was charged with a solution of alkynol *rac*-**78** (5.831 g, 9.35 mmol) in dichloromethane (65 mL) and 4-(dimethylamino)pyridine (114 mg, 0.940 mmol, 10 mol%), *i*-Pr_2NEt (2.28 mL, 13.09 mmol, 1.4 equiv.), and chloromethyl methyl ether (1.0 mL, 14.0 mmol, 1.5 equiv.) were subsequently added, the flask was closed with a glass stopper and a solution was stirred at 35 °C for 16 h. Afterward, the reaction was quenched with a saturated $NaHCO_3$ solution (30 mL), the layers were separated, and the aqueous one was extracted with dichloromethane (3 × 30 mL). The combined organic layers were dried over anhydrous $MgSO_4$ and the solvent was removed *in vacuo*. The crude product was purified by column chromatography on silica gel (hexane-ethyl acetate 10:1) to give MOM-ether *rac*-**79** (5.682 g, 93%) as a white solid. **M.p.**: 89–91 °C (hexane-ethyl acetate). **^{1}H NMR** (400 MHz, $CDCl_3$): δ 7.36 – 7.30 (m, 4H), 7.26 (s, 2H), 7.23 – 7.16 (m, 6H), 6.71 (dd, *J* = 8.7, 2.7 Hz, 1H), 4.94 (t, *J* = 6.3 Hz, 1H), 4.60 – 4.57 (m, 6H), 3.39 (s, 3H), 2.80 – 2.63 (m, 2H), 1.03 – 0.98 (m, 21H). **^{13}C NMR** (75 MHz, $CDCl_3$): δ 149.65, 137.80, 130.79, 128.89, 128.22, 127.31, 126.87, 122.39, 113.06, 104.75, 100.51, 94.76, 82.32, 79.40, 55.89, 54.14, 28.18, 18.79, 11.43. **IR** (neat): 3087 vw, 3063 vw, 3027 vw, 2940 m, 2864 m, 1462 w, 1149 m, 1097 m, 1026 s, 919 w, 882 m, 809 m, 753 w, 677 m cm^{-1}. **EI MS**: 667 ($M^{+\bullet}$,

1), 472 (9), 412 (7), 145 (7), 117 (7), 91 (100), 71 (11), 57 (11), 45 (2). **HR EI MS**: calcd for $C_{35}H_{46}O_2NISi$ 667.2337, found 667.2387.

rac-*N*,*N*-Dibenzyl-4-(1-(methoxymethoxy)-4-(triisopropylsilyl)but-3-yn-1-yl)-3-((trimethylsilyl)ethynyl)aniline 80

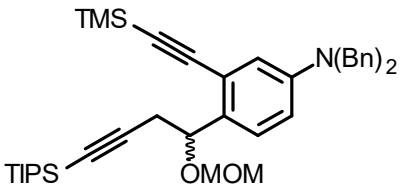

A Schlenk flask was charged with iodo compound *rac*-**79** (134 mg, 0.2 mmol), $Pd(PPh_3)_2Cl_2$(3 mg, 0.004 mmol, 2 mol%), CuI (1.5 mg, 0.008 mmol, 4 mol%) and flushed with nitrogen. Then diisopropylamine (2 mL) was added and the mixture was degassed by three freeze pump thaw cycles. (Trimethylsilyl)acetylene (0.034 mL, 0.24 mmol, 1.2 equiv.) was added *via* syringe and the reaction mixture was stirred for 18 h at room temperature. The solvent was removed in *vacou* and the crude product purified by column chromatography (hexane-methyl *tert*-butyl ether 10:1) to give diyne *rac*-**80** (127 mg, 99%) as an orange oil. **^{1}H NMR** (300 MHz, $CDCl_3$) δ 7.36 – 7.27 (m, 6H), 7.25 – 7.19 (m, 5H), 6.85 (d, *J* = 2.6 Hz, 1H), 6.71 (dd, *J* = 8.7, 2.6 Hz, 1H), 5.19 (dd, *J* = 7.6, 5.2 Hz, 1H), 4.63 (d, *J* = 0.7 Hz, 2H), 4.60 (s, 4H), 3.39 (s, 3H), 2.87 – 2.59 (m, 2H), 1.10 – 0.92 (m, 21H), 0.23 (s, 9H).**^{13}C NMR** (75 MHz, $CDCl_3$) δ 148.88, 138.09, 130.67, 128.82, 127.21, 127.16, 126.97, 122.68, 115.31, 113.73, 111.23, 110.36, 105.70, 95.09, 81.54, 74.44, 55.78, 54.01, 28.23, 18.78, 11.43, 0.09. **IR**: 3058 vw, 3017 vw, 2941 m, 2860 m, 2170 w, 1601 m, 1249 m, 1150 m, 1030 m, 842 s, 730 w, 696 m, 660 m cm^{-1}. **EI MS**: 637 ($M^{+\bullet}$, 18), 442 (32), 382 (2), 338 (2), 310 (2), 246 (1), 219 (1), 149 (2), 145 (9), 117 (9), 91 (100), 73 (45), 59 (16), 45 (23). **HR EI MS**: calcd for $C_{40}H_{55}O_2N^{28}Si_2$ 637.3766, found 637.3753.

rac-*N*,*N*-Dibenzyl-3-ethynyl-4-{1-(methoxymethoxy)-4-[tris(1-methylethyl)silyl] but-3-yn-1-yl}-aniline 81

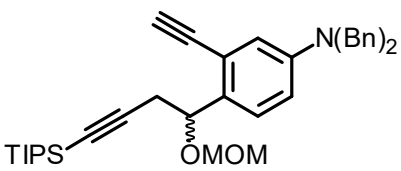

A Schlenk flask was charged with iodide *rac*-**79** (668 mg, 1.00 mmol), $Pd(PPh_3)_2Cl_2$ (14.0 mg, 0.020 mmol, 2 mol%), CuI (8.0 mg, 0.040 mmol, 4 mol%), and flushed with nitrogen. Then diisopropylamine (10 mL) was added and the mixture was degassed by three freeze-pump-thaw cycles. (Trimethylsilyl)acetylene (170 µL, 1.20 mmol, 1.2 equiv.) was added *via* a syringe

and the reaction mixture was stirred at room temperature for 5 h. The solvent was removed *in vacuo*, the crude trimethylsilyl alkyne was filtered through a small pad of silica gel (ethyl acetate), and evaporated to dryness. Then the protected alkyne was dissolved in methanol (6 mL) and K_2CO_3 (207 mg, 1.50 mmol, 1.5 equiv.) was added. The reaction mixture was stirred at room temperature for 3 h. After completion (checked by TLC), the reaction was quenched with a saturated NH_4Cl solution (10 mL), the layers were separated, and the aqueous one extracted with dichloromethane (3 × 10 mL). The combined organic layers were dried over anhydrous $MgSO_4$, the solvent was removed *in vacuo*, and the crude product purified by column chromatography on silica gel (hexane-methyl *tert*-butyl ether 10:1) to furnish alkyne *rac*-**81** (549 mg, 97%, after 2 steps) as a yellow solid. **M.p.**: 103 – 105 °C (hexane-methyl *tert*-butyl ether). **^{1}H NMR** (300 MHz, $CDCl_3$): δ 7.37 – 7.27 (m, 6H), 7.25 – 7.19 (m, 5H), 6.86 (d, *J* = 2.7 Hz, 1H), 6.74 (dd, *J* = 8.7, 2.6 Hz, 1H), 5.19 (t, *J* = 6.4 Hz, 1H), 4.64 – 4.58 (m, 6H), 3.38 (s, 3H), 3.18 (s, 1H), 2.88 – 2.69 (m, 2H), 1.03 – 0.97 (m, 21H). **^{13}C NMR** (75 MHz, $CDCl_3$): δ 148.49, 138.20, 131.21, 128.84, 127.69, 127.17, 126.78, 121.82, 115.82, 113.64, 105.23, 94.91, 82.22, 82.03, 81.06, 74.20, 55.81, 54.01, 28.18, 18.74, 11.41. **IR** (neat): 3284 w, 2936 m, 2860 m, 2174 w, 1602 s, 1452 m, 1357 m, 1234 m, 1149 m, 1096 m, 1030 vs, 962 m, 882 m, 732 s, 696 s, 660 vs cm^{-1}. **EI MS**: 565 ($M^{+\bullet}$, 44), 370 (100), 310 (9), 280 (2), 248 (2), 155 (3), 91 (44), 71 (9), 57 (15). **HR EI MS**: calcd for $C_{37}H_{47}O_2NSi$ 565.3371, found 565.3370.

1-(Allyloxy)naphthalene 89[120]

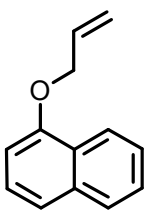

To a stirred solution of 1-naphthol **90** (1.441 g, 10.0 mmol, 1.0 equiv.) in acetone (50 mL), K_2CO_3 (2.764 g, 20.0 mmol, 2.0 equiv.) and allyl bromide (1.038 mL, 12 mmol, 1.2 equiv.) were added at room temperature and the mixture was heated under reflux for 2.5 h. After filtration through a small pad of silica gel (hexane), allyl ether **89** (1.767 g, 96%) was obtained as a colorless oil. **^{1}H NMR** (300 MHz, $CDCl_3$) δ 8.37 – 8.30 (m, 1H), 7.85 – 7.78 (m, 1H), 7.55 – 7.33 (m, 4H), 6.83 (d, *J* = 7.4 Hz, 1H), 6.20 (ddt, *J* = 17.2, 10.4, 5.1 Hz, 1H), 5.54 (ddd, *J* = 17.3, 3.2, 1.6 Hz, 1H), 5.36 (dd, *J* = 10.5, 1.5 Hz, 1H), 4.79 – 4.64 (m, 2H). **^{13}C NMR** (75 MHz, $CDCl_3$) δ 154.48, 134.70, 133.50, 127.58, 126.52, 125.92, 125.74. 125.32, 122.24, 120.53, 117.49, 105.22, 69.09.

2-(Prop-2-en-1-yl)naphthalen-1-ol 88[120]

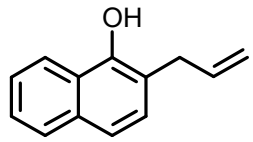

Allyl ether **89** (1.336 g, 0.5 mmol) was dissolved in *N*,*N*-diethylaniline (18 mL) and heated in a microwave reactor at 250 °C for 1 h. The reaction mixture was treated with HCl (1 M, 300 mL) and extracted with methyl *tert*-butyl ether (3 × 100 mL). The combined org. layers were dried over anhydrous $MgSO_4$, the solvent was removed *in vacuo* and the crude product purified by flash chromatography (hexane-methyl *tert*-butyl ether 20:1) to afford naphthol **88** (1.190 g, 89%) as a brownish oil. **^{1}H NMR** (300 MHz, $CDCl_3$) δ 8.37 – 8.30 (m, 1H), 7.85 – 7.78 (m, 1H), 7.55 – 7.33 (m, 4H), 6.83 (d, *J* = 7.4 Hz, 1H), 6.20 (ddt, *J* = 17.2, 10.4, 5.1 Hz, 1H), 5.54 (dd, *J* = 17.3, 1.6 Hz, 1H), 5.36 (dd, *J* = 10.5, 1.5 Hz, 1H), 4.74 (d, *J* = 5.1 Hz, 2H). **^{13}C NMR** (75 MHz, $CDCl_3$) δ 149.67, 136.25, 133.89, 128.54, 127.66, 125.88, 125.41, 124.99, 121.44, 120.51, 118.00, 117.03, 35.79.

2-Allylnaphthalen-1-yl trifluoromethanesulfonate 91 [145]

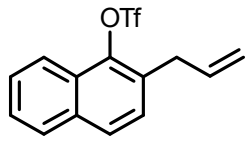

Naphthol **88** (3.684 g, 20.0 mmol), pyridine (3.23 mL, 40.0 mmol, 2.0 equiv.) and dichloromethane (54 mL) were placed in an oven-dried Schlenk flask. The mixture was cooled to 0 °C and trifluoroacetic anhydride (4.031 mL, 24 mmol, 1.2 equiv.) was added slowly. The reaction mixture was allowed to warm up to ambient temperature and stirred for 20 h. The mixture was evaporated to dryness, the residue dissolved in dichloromethane and all insoluble solids filtered off with a frit. The filtrate was dry-loaded on silica gel and purified by flash chromatography (hexane-methyl *tert*-butyl ether 20:1) affording triflate **91** (4.958 g, 79%) as a white solid.

^{1}H NMR (300 MHz, $CDCl_3$) δ 8.10 (d, *J* = 8.4 Hz, 1H), 7.87 (d, *J* = 8.0 Hz, 1H), 7.82 (d, *J* = 8.5 Hz, 1H), 7.68 – 7.51 (m, 2H), 7.42 (d, *J* = 8.5 Hz, 1H), 6.08 – 5.87 (m, 1H), 5.24 – 5.13 (m, 2H), 3.69 (d, *J* = 6.6 Hz, 2H). **^{13}C NMR** (75 MHz, $CDCl_3$) δ 142.28, 134.98, 133.94, 130.57, 128.67, 127.99, 127.97, 127.88, 127.29, 126.85, 121.47, 118.91 (q, J_{CF} = 320 Hz), 117.73, 34.68.

2-(2,3-Dihydroxypropyl)naphthalen-1-yl trifluoromethanesulfonate 92

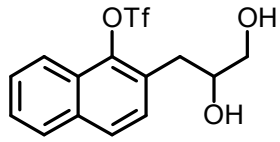

To a solution of olefin **91** (155 mg, 0.49 mmol) and NMO (66 mg, 0.49 mmol, 1.0 equiv.) in THF (0.5 mL) and H_2O (0.25 mL) a solution of OsO_4 (0.2 M in H_2O, 0.245 mL, 0.05 mmol, 10 mol%) was added. The reaction mixture was stirred at ambient temperature for 18 h. Then Na_2SO_3 (690 mg, 4.36 mmol, 8.9 equiv.) was added and the mixture stirred for another 30 min. Afterward, the reaction mixture was diluted with ethyl acetate (3 mL) and H_2O (3 mL). The phases were separated, the aqueous layer extracted with EtOAc (3 x 5 mL) and the combined organic layers dried over anhydrous $MgSO_4$. After removal of solvent, the crude product was purified by column chromatography (hexane-ethyl acetate 1:1) to afford diol **92** (156 mg, 91%) as a beige solid. **M.p.**: 81 – 82 °C. **^{1}H NMR** (300 MHz, $CDCl_3$) δ 8.07 (d, *J* = 8.4 Hz, 1H), 7.86 (d, *J* = 8.1 Hz, 1H), 7.81 (d, *J* = 8.5 Hz, 1H), 7.67 – 7.46 (m, 3H), 4.15 – 4.03 (m, 1H), 3.71 (dd, *J* = 11.2, 3.1 Hz, 1H), 3.53 (dd, *J* = 11.2, 6.9 Hz, 1H), 3.15 – 2.98 (m, 2H), 2.39 (s, 2H). **^{13}C NMR** (75 MHz, $CDCl_3$) δ 142.88, 134.08, 129.09, 128.74, 128.56, 127.99, 127.96, 127.18, 127.01, 121.37, 118.84 (q, *J* = 320 Hz), 71.96, 66.25, 34.37. **^{19}F NMR** (282 MHz, $CDCl_3$) δ -73.05. **IR**: 3356 w, 2928 w, 1402 m, 1207 s, 1134 s, 1020 m, 891 m, 813 s, 765 w, 637 w, 593 w, 502 m cm^{-1}. **EI MS**: 350 ($M^{+\bullet}$, 7), 290 (20), 239 (7), 200 (7), 191 (9), 186 (20), 169 (7), 157 (100), 141 (7), 128 (20), 99 (2), 85 (4), 69 (7), 57 (7), 43 (7). **HR EI MS**: calcd for $C_{14}H_{13}O_5F_3{}^{32}S$ 350.0430, found 350.0423.

2-(2-Oxoethyl)naphthalen-1-yl trifluoromethanesulfonate 87 [146]

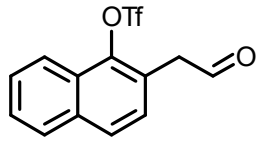

Diol **92** (175 mg, 0.5 mmol) was dissolved in dichloromethane (3 mL) and a solution of $NaIO_4$ (214 mg, 1.0 mmol, 2.0 equiv.) in H_2O (2.5 mL) was added. The emulsion was stirred at room temperature for 4 h. The phases were separated and the aqueous layer was extracted with dichloromethane (3 × 10 mL). The combined organic layers were dried over anhydrous $MgSO_4$, the solvent was removed in *vacuo* and the crude product purified by column chromatography (hexane-methyl *tert*-butyl ether 5:1) to give aldehyde **87** (130 mg, 88%) an orange oil. **^{1}H NMR** (300 MHz, $CDCl_3$) δ 9.83 (s, 1H), 8.11 (d, *J* = 8.4 Hz, 1H), 7.94 – 7.86 (m, 2H), 7.71 – 7.55 (m, 2H), 7.36 (d, *J* = 8.5 Hz, 1H), 4.05 (s, 2H). **^{13}C NMR** (75 MHz, $CDCl_3$) δ 197.04, 142.77, 134.56, 129.18,

128.26 (2C), 128.11, 127.55, 127.31, 123.50, 121.60, 118.79 (q, *J* = 320.0 Hz), 45.39.

rac-2-(2-Hydroxy-4-(triisopropylsilyl)but-3-yn-1-yl)naphthalen-1-yl trifluoromethanesulfonate 86

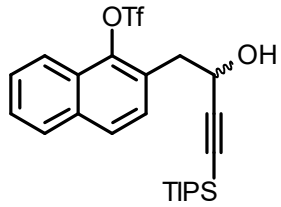

To a solution of diol **92** (1.121 g, 3.2 mmol) in dichloromethane (19 mL) $NaIO_4$ (1.369 g, 6.4 mmol, 2.0 equiv.) in H_2O (16 mL) was added. The reaction mixture was stirred for 6 h at room temperature. The phases were separated and the aqueous layer was extracted with dichloromethane (3 × 50 mL). The combined organic extracts were dried over anhydrous $MgSO_4$ and solvent was removed *in vacuo* to give crude aldehyde **87**.

(triisopropylsilyl)acetylene (1.436 mL, 6.4 mmol, 2.0 equiv.) and THF (14.5 mL) were added to an oven-dried Schlenk flask and the stirred mixture cooled to 0 °C. Then ethylmagnesium bromide (1 M in THF, 6.4 mL, 6.4 mmol, 2.0 equiv.) was added and the mixture was allowed to warm up to room temperature and stirred for 1 h. Afterward, a solution of crude aldehyde **87** in THF (5 mL) was added over a period of 10 min. After stirring the reaction mixture for an additional hour, the reaction was poured into ice water, the mixture was acidified with 1 M HCl sol., the layers were separated and the aqueous layer extracted with methyl *tert*-butyl ether (3 × 50 mL), the combined org. layers were washed with sat. $NaHCO_3$ sol., dried over anhydrous $MgSO_4$ and solvent was removed *in vacuo*. The crude product was purified by column chromatography (hexane-methyl *tert*-butyl ether 5:1) to obtain alcohol *rac*-**86** (1.120 g, 70% after 2 steps) as an orange oil. **^{1}H NMR** (300 MHz, $CDCl_3$) δ 8.10 (d, *J* = 8.3 Hz, 1H), 7.87 (d, *J* = 7.9 Hz, 1H), 7.82 (d, *J* = 8.5 Hz, 1H), 7.67 – 7.52 (m, 3H), 4.78 (t, *J* = 6.6 Hz, 1H), 3.44 – 3.28 (m, 2H), 1.85 (s, 1H), 0.99 – 0.96 (m, 21H). **^{13}C NMR** (126 MHz, $CDCl_3$) δ 142.98, 134.25, 128.69, 128.48, 128.02, 127.93, 127.83, 127.28, 127.02, 121.65, 118.85 (q, *J* = 320 Hz), 107.20, 87.39, 62.66, 38.77, 18.54, 11.15. **^{19}F NMR** (282 MHz, $CDCl_3$) δ -73.12 (s). **IR**: 3050 vw, 2921 m, 2869 m, 1729 w, 1458 w, 1406 m, 1382 w, 1214 s, 1137 m, 1028 m, 975 w, 884 m, 814 m, 758 s, 665 m, 585 w, 503 w cm^{-1}. **HR ESI MS**: calcd for $C_{24}H_{31}F_3NaO_4SSi$ 523.1557, found 523.1569.

(*R*)-1-(1-(((trifluoromethyl)sulfonyl)oxy)naphthalen-2-yl)-4-(triisopropylsilyl)but-3-yn-2-yl acetate 94, (*S*)-2-(2-Hydroxy-4-(triisopropylsilyl)but-3-yn-1-yl)naphthalen-1-yl trifluoromethanesulfonate 86 and (*R*)-2-(2-Hydroxy-4-(triisopropylsilyl)but-3-yn-1-yl)naphthalen-1-yl trifluoromethanesulfonate 86

Alcohol *rac*-**86** (12.740 g, 25.447 mmol), Novozyme 435 (3.65 g) and molecular sieves (4 Å, 25 g) were added to an oven-dried Schlenk flask, which was then flushed with argon. Toluene (100 mL) and isopropenyl acetate (13.8 mL, 127.235 mmol, 5.0 equiv.) were added subsequently, the flask was sealed with a glass stopper and the reaction mixture stirred at 40 °C for 24 h. The reaction mixture was filtered through a short pad of celite, the solvent removed *in vacuo* and the crude product purified by column chromatography (hexane-methyl *tert*-butyl ether 20:1 to 10:1) to obtain acetate (*R*)-**94** (6.390 g, 46%) colorless oil and alcohol (*S*)-**86** (6.05 g, 48%, >99% ee) as yellow oil. The absolute configurations of products were established by analogy.[31]

(*R*)-1-(1-(((Trifluoromethyl)sulfonyl)oxy)naphthalen-2-yl)-4-(triisopropylsilyl)but-3-yn-2-yl acetate **94**

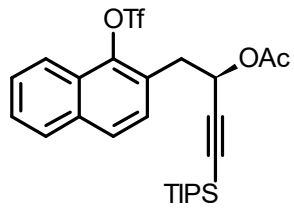

Optical rotation: $[\alpha]^{20}_D$ = +36° (c 0.298, $CHCl_3$). **^{1}H NMR** (300 MHz, $CDCl_3$) δ 8.10 (d, *J* = 8.4 Hz, 1H), 7.87 (d, *J* = 8.2 Hz, 1H), 7.82 (d, *J* = 8.5 Hz, 1H), 7.68 – 7.48 (m, 3H), 5.74 (t, *J* = 6.8 Hz, 1H), 3.42 (d, *J* = 6.9 Hz, 2H), 2.05 (s, 3H), 1.00 – 0.88 (m, 21H). **^{13}C NMR** (75 MHz, $CDCl_3$) δ 169.64, 143.03, 134.33, 128.60, 128.31, 127.95, 127.92, 127.30, 127.17, 127.16, 121.72, 118.86 (d, *J* = 320.0 Hz), 103.26, 88.35, 63.64, 35.87, 21.00, 18.49, 11.10. **^{19}F NMR** (377 MHz, $CDCl_3$) δ -73.14 (s).

(*S*)-2-(2-Hydroxy-4-(triisopropylsilyl)but-3-yn-1-yl)naphthalen-1-yl trifluoromethanesulfonate **86**

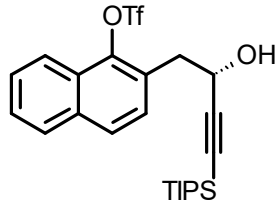

Optical rotation: $[\alpha]^{20}_D$ = +21° (c 0.315, $CHCl_3$). **Chiral HPLC**: Chiral Art Amylose-SA column (250 × 4.6 mm, 5 µm, YMC), mobile phase: hexane-isopropanol (95:5), flow rate: 1 mL/min, retention time: 6.8 min.

(*R*)-2-(2-Hydroxy-4-(triisopropylsilyl)but-3-yn-1-yl)naphthalen-1-yl trifluoromethanesulfonate **86**

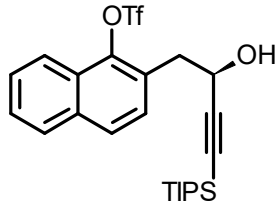

An oven-dried Schlenk flask was charged with acetate (*R*)-**94** (103 mg, 0.19 mmol) and K_2CO_3 (1.3 mg, 0.01 mmol, 5 mol%). The solids were suspended in MeOH (1 mL) and stirred for 3 h at ambient temperature. Hexane (5 mL) was added, the solvents removed *in vacuo* and the crude product purified by flash chromatography (haxane-ethyl acetate 20 :1 to 10 : 1) to afford alcohol (*R*)-**86** (77 mg, 81%, >99% ee) as a colorless oil. **Optical rotation**: $[\alpha]^{20}_D$ = -22° (c 0.240, $CHCl_3$). **Chiral HPLC**: Chiral Art Amylose-SA column (250 × 4.6 mm, 5 µm, YMC), mobile phase: hexane-isopropanol (95:5), flow rate: 1 mL/min, retention time: 6.3 min.

(*S*)-2-(2-(Methoxymethoxy)-4-(triisopropylsilyl)but-3-yn-1-yl)naphthalen-1-yl trifluoromethanesulfonate 85

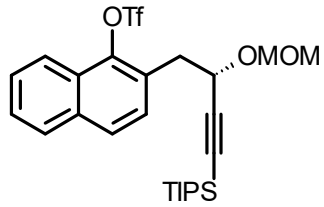

Alcohol (S)-**86** (6.048 g, 12.08 mmol) and activated molecular sieves (4 Å, 7.250 g) were placed in an oven-dried Schlenk flask and flushed with nitrogen. Then dichloromethane (24 mL) and dimethoxymethane (2.14 mL, 13.29 mmol, 2.0 equiv.) were added. Afterward, $BF_3{\cdot}Et_2O$ (1.68 mL, 13.29 mmol, 1.1 equiv.) was added dropwise over 5 min at room temperature and the resulting mixture was stirred for additional 2 h. After completion (checked by TLC), sat. $NaHCO_3$ sol. (60 mL) was added, the phases were separated and the aqueous layer extracted with dichloromethane (3 × 50 mL). The combined organic layers were dried over anhydrous $MgSO_4$, the solvent was removed *in vacuo* and the crude product purified by column chromatography (hexane-methyl *tert*-butyl ether, 10:1) to afford ether (*S*)-**85** (5.060 g, 77%) as a yellow amorphous solid. **Optical rotation**: $[\alpha]^{20}_D$ = -52° (c 0.303, $CHCl_3$). **^{1}H NMR** (300 MHz, $CDCl_3$) δ 8.10 (d, *J* = 8.3 Hz, 1H), 7.86 (d, *J* = 7.7 Hz, 1H), 7.80 (d, *J* = 8.5 Hz, 1H), 7.66 – 7.51 (m, 3H), 4.97 (d, *J* = 6.8 Hz, 1H), 4.73 (t, *J* = 6.8 Hz, 1H), 4.57 (d, *J* = 6.8 Hz, 1H), 3.48 – 3.29 (m, 2H), 3.19 (s, 3H), 1.00 – 0.93 (m, 21H). **^{13}C NMR** (75 MHz, $CDCl_3$) δ 142.99, 134.21, 129.06, 128.32, 128.24, 127.89, 127.77, 127.26, 126.96, 121.67, 118.89 (d, *J* = 320.0 Hz), 104.81, 94.07, 88.14, 65.54, 55.72, 36.83, 18.56, 11.18. **^{19}F NMR** (282 MHz, $CDCl_3$) δ -73.14 (s). **IR** ($CHCl_3$): 3062 vw, 2957 m, 2945 s, 2867 s, 2827 w, 2171vw, 1629 vw, 1604

w, 1571 vw, 1506 w, 1463 m, 1442 vw, 1420 m, 1406 s, 1385 w, 1366 w, 1245 m, 1152 m, 1137 vs, 1098 m, 1045 s, 1023 s, 924 w, 885 s, 865 w, 816 s, 680 m, 662 m, 619 vw, 592 w, 575 w, 504 m cm^{-1}. **HR ESI MS:** calcd for $C_{26}H_{35}O_5F_3NaSSi$ 567.1819, found 567.1819.

(-)-*N*,*N*-Dibenzyl-4-[(1*RS*)-(methoxymethoxy)but-3-yn-1-yl]-3-({2-[(2*S*)-2-(methoxy-methoxy)-but-3-yn-1-yl]naphthalen-1-yl}ethynyl)aniline 96

Synthesis with iodo building block (*S*)-**83**:

A Schlenk flask was charged with iodide (*S*)-**83** (1.229 g, 2.352 mmol), $Pd(PPh_3)_2Cl_2$ (33.0 mg, 0.047 mmol, 2 mol%), CuI (18 mg, 0.094 mmol, 4 mol%), and flushed with argon. Then diisopropylamine (25 mL, degassed by the three freeze-pump-thaw cycles) was added *via* cannula. Another Schlenk flask was charged with diyne *rac*-**81** (1.597 g, 2.822 mmol, 1.2 equiv.), flushed with argon, and diisopropylamine (25 mL, degassed by the three freeze-pump-thaw cycles) was added *via* cannula. Then a diyne solution was added dropwise *via* cannula to the iodide solution over 10 min and the resulted mixture was stirred at room temperature for 16 h. After completion (checked by TLC), the solvent was removed *in vacuo*, the crude intermediate was filtered through a small pad of silica gel (ethyl acetate), and the solvent was removed under reduced pressure. The residue was dissolved in tetrahydrofuran (30 mL) and a solution of tetrabutylammonium fluoride trihydrate (1 M in tetrahydrofuran, 7 mL, 7.056 mmol, 3.0 equiv.) was added. The mixture was stirred at room temperature for 5 h and then quenched with methanol (10 mL). The solvents were removed *in vacuo*, the crude product was purified by flash chromatography on silica gel (hexane-ethyl acetate 10:1) to afford triyne (*RS*,*S*)-**96** (1.412 g, 93%, after 2 steps) as a yellow oil. The product was obtained as a diastereomeric mixture.

Synthesis with triflate building block (*S*)-**85**:

Rac-**81** (1.839 g, 2.8 mmol, 1.4 equiv.) was placed in an oven-dried Schlenk flask, flushed with argon and dissolved in toluene (6 mL). Ethylmagnesium bromide (1 M in THF, 3.05 mL, 3.05 mmol, 1.53 equiv.) was added slowly at ambient temperature and the mixture stirred for 1 h. In a second oven-dried pressure reactor triflate (*S*)-**85** (1.089 g, 2.0 mmol) was placed, flushed with argon and dissolved in THF (10 mL). The solution of Grignard reagent was then added to the pressure reactor and the resulting mixture was stirred at 70 °C for 17 h. Then the reaction was quenched with

sat. NH_4Cl sol. (30 mL), the phases were separated, the aqueous layer extracted with methyl *tert*-butyl ether (3 × 30 mL), the combined org. layers dried over $MaSO_4$ and the solvents removed *in vacuo*. The residue was dissolved in tetrahydrofuran (26 mL) and a solution of tetrabutylammonium fluoride trihydrate (1 M in tetrahydrofuran, 6 mL, 6.0 mmol, 3.0 equiv.) was added. The mixture was stirred at room temperature for 16 h and then quenched with methanol (20 mL). The solvents were removed *in vacuo*, the crude product was purified by flash chromatography on silica gel (hexane-ethyl acetate 10:1) to afford triyne (*RS*,*S*)-**96** (830 mg, 64%, after 2 steps) as a yellow oil. The product was obtained as a diastereomeric mixture.

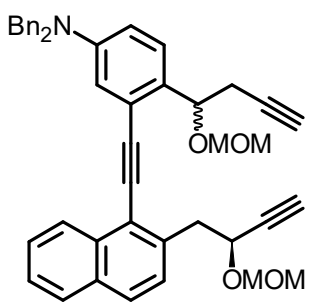

Optical rotation: $[\alpha]^{20}_D$ = -43° (c 0.168, $CHCl_3$). **^{1}H NMR** (300 MHz, $CDCl_3$) (a mixture of diastereoisomers): δ 8.44 (d, *J* = 8.2 Hz, 1H), 7.86 – 7.80 (m, 1H), 7.76 (d, *J* = 8.5 Hz, 1H), 7.61 – 7.45 (m, 3H), 7.41 – 7.22 (m, 11H), 7.10 (s, 1H), 6.80 (dd, *J* = 8.7, 2.4 Hz, 1H), 5.53 – 5.44 (m, 1H), 4.84 – 4.73 (m, 2H), 4.73 – 4.61 (m, 6H), 4.47 (d, *J* = 6.8 Hz, 1H), 3.60 – 3.36 (m, 5H), 2.97 (s, 3H), 2.90 – 2.69 (m, 2H), 2.26 (dd, *J* = 8.9, 1.9 Hz, 1H), 2.09 – 2.00 (m, 1H). **^{13}C NMR** (75 MHz, $CDCl_3$) (a mixture of diastereoisomers): δ 148.65, 138.30, 138.25, 133.67, 132.26, 130.29, 128.87, 128.68, 128.15, 127.49, 127.25, 127.00, 126.63, 126.11, 123.02, 122.99, 120.43, 115.85, 113.75, 97.41, 94.58, 94.53, 94.28, 94.25, 90.00, 89.95, 82.51, 81.70, 81.65, 74.18, 73.92, 73.78, 69.98, 69.93, 65.82, 55.81, 55.41, 55.39, 54.27, 54.23, 41.72, 27.57. **IR** (neat): 3288 w, 3059 vw, 2928 w, 1599 m, 1504 m, 1449 w, 1360 w, 1204 w, 1148 m, 1097 m, 1019 s, 963 m, 913 m, 810 m, 731 s, 696 m, 646 m, 564 w, 450 w cm^{-1}. **EI MS**: 647 ($M^{+\bullet}$, 13), 608 (44), 575 (4), 532 (18), 502 (11), 441 (13), 364 (7), 308 (9), 289 (38), 276 (27), 267 (20), 239 (40), 211 (16), 199 (44), 191 (24), 155 (16), 141 (16), 127 (15), 99 (20), 91 (100), 84 (31), 71 (16), 57 (18), 45 (47). **HR EI MS**: calcd for $C_{44}H_{41}O_4N$ 647.3036, found 647.3038.

(+)-*N*,*N*-Dibenzyl-4-[(1*RS*)-(methoxymethoxy)-4-(4-methylphenyl)but-3-yn-1-yl]-3-({2-[(2*S*)-2-(methoxymethoxy)-4-(4-methylphenyl)but-3-yn-1-yl]naphthalen-1-yl}ethynyl)aniline 97

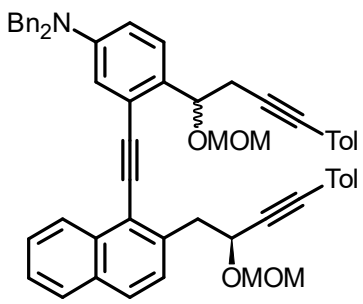

4-Iodotoluene (1.413 g, 6.483 mmol, 3.0 equiv.), $Pd(PPh_3)_2Cl_2$ (76.0 mg, 0.108 mmol, 5 mol%), and CuI (41.0 mg, 0.216 mmol, 10 mol%) were placed in a Schlenk flask and flushed with argon. Diisopropylamine (25 mL, degassed by three freeze-pump-thaw cycles) was added *via* cannula and a mixture was stirred at room temperature for 5 min. Another Schlenk flask was charged with triyne (*RS*,*S*)-**96** (1.4 g, 2.16 mmol), flushed with argon, and diisopropylamine (25 mL, degassed by three freeze-pump-thaw cycles) was added *via* cannula. Then the triyne solution was added dropwise to the mixture of 4-iodotoluene and catalyst *via* cannula over 10 min. The resulting mixture was stirred at room temperature for 16 h. After completion (checked by TLC), the solvent was removed *in vacuo*, the crude product was purified by flash chromatography on silica gel (hexane-ethyl acetate 5:1). The desired triyne (*RS*,*S*)-**97** (1.675 g, 94%) was obtained as a white solid. The product was obtained as a diastereomeric mixture. **M.p.**: 75 – 77 °C (hexane-methyl *tert*-butyl ether). **Optical rotation**: $[\alpha]^{20}_D$ = +18° (c 0.264, $CHCl_3$). ^{1}H NMR (500 MHz, $CDCl_3$) (a mixture of diastereoisomers): δ 8.48 (d, *J* = 8.3 Hz, 1H), 7.82 (d, *J* = 7.9 Hz, 1H), 7.78 (d, *J* = 8.3 Hz, 1H), 7.56 (d, *J* = 8.4 Hz, 1H), 7.54 – 7.49 (m, 1H), 7.49 – 7.44 (m, 1H), 7.40 (d, *J* = 8.6 Hz, 1H), 7.37 – 7.32 (m, 4H), 7.31 – 7.22 (m, 10H), 7.13 (d, *J* = 2.2 Hz, 1H), 7.07 – 7.01 (m, 4H), 6.80 (dd, *J* = 8.8, 2.8 Hz, 1H), 5.57 (dd, *J* = 7.8, 4.8 Hz, 1H), 5.03 – 4.97 (m, 1H), 4.89 – 4.86 (m, 1H), 4.75 – 4.60 (m, 6H), 4.55 – 4.50 (m, 1H), 3.66 – 3.53 (m, 2H), 3.47 (s, 3H), 3.09 – 2.94 (m, 5H), 2.33 – 2.31 (m, 6H). **^{13}C NMR** (126 MHz, $CDCl_3$) (a mixture of diastereoisomers): δ 148.52, 148.45, 138.48, 138.32, 137.52, 133.67, 132.22, 131.80, 131.60, 129.06, 128.96, 128.81, 128.07, 128.04, 127.48, 127.18, 127.17, 126.99, 126.98, 126.63, 126.01, 123.02, 121.02, 120.49, 119.73, 115.85, 113.66, 97.33, 94.52, 94.30, 90.04, 87.24, 86.72, 86.36, 82.13, 74.29, 74.23, 66.63, 55.77, 55.38, 54.27, 41.84, 28.63, 21.59, 21.53. **IR** ($CHCl_3$): 3061 w, 3031 w, 2825 w, 2226 w, 1601 m, 1568 w, 1557 w, 1510 s, 1495 m, 1471 w, 1466 w, 1453 m, 1298 w, 1180 w, 1150 m, 1118 w, 1099 m, 1060 m, 1028 s, 1022 m, 954 w, 866 w, 819 m, 697 m, 543 w, 459 w cm^{-1}. **ESI MS**: 829 ($[M+H]^+$). **HR ESI MS**: calcd for $C_{58}H_{54}NO_4$ 828.4047, found 828.4048.

(-)-(*M*,5*RS*,9*S*)-*N*,*N*-Dibenzyl-5,9-bis(methoxymethoxy)-7,8-bis(4-methylphenyl)-5,6,9,10-tetrahydrohexahelicen-2-amine 98

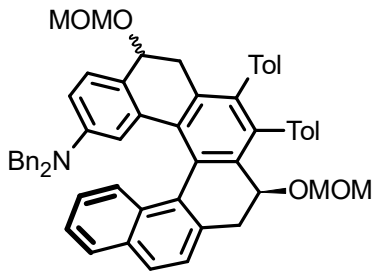

A microwave vial was charged with triyne (*RS*,*S*)-**97** (166 mg, 0.200 mmol), $Ni(CO)_2(PPh_3)_2$ (140 mg, 0.220 mmol, 1.1 equiv.), closed with a crimp seal, and flushed with argon. Toluene (20 mL) was added and argon was kept to bubble through the stirring mixture for 10 min. Then it was immersed in an oil bath and stirred at 150 °C for 15 min. The reaction mixture was cooled down, the solvent removed *in vacuo*, and the crude product purified by flash chromatography on silica gel (hexane-ethyl acetate 10:1) to give the tetrahydrohelicene (-)-(*M*,*RS*,*S*)-**98** (136 mg, 82%) as a yellow solid. The product was obtained as a diastereomeric mixture. **M.p.**: 98 – 101 °C (hexane-ethyl acetate). **Optical rotation**: $[\alpha]^{20}_D$ = -183° (c 0.360, $CHCl_3$). **^{1}H NMR** (500 MHz, $CDCl_3$): δ 2.26, 2.27, 2.28 (3 × s, 12H), 2.47 (dd, *J* = 15.0, 12.7 Hz, 1H), 2.73 (dd, *J* = 16.9, 3.5 Hz, 1H), 2.89 – 2.95 (m, 2H), 2.90 (dd, *J* = 15.0, 4.7 Hz, 1H), 2.90, 2.92 (2 × s, 9H), 2.98 (dd, *J* = 16.9, 2.6 Hz, 1H), 3.34 (dd, *J* = 15.8, 2.8 Hz, 2H), 3.35, 3.36 (2 × s, 6H), 3.81, 3.83, 3.98, 3.99 (4 × d, *J* = 17.3 Hz, 8H), 4.221, 4.224 (2 × d, *J* = 7.2 Hz, 2H), 4.31 – 4.36 (m, 4H), 4.58 (d, *J* = 6.5 Hz, 1H), 4.67 (dd, *J* = 3.5, 2.6 Hz, 1H), 4.80, 4.83 (2 × d, *J* = 6.7 Hz, 2H), 4.90 (ddd, *J* = 12.7, 4.7, 0.9 Hz, 1H), 4.93 (d, *J* = 6.5 Hz, 1H), 5.88 (d, *J* = 2.7 Hz, 1H), 5.98 (d, *J* = 2.7 Hz, 1H), 6.15 (dd, *J* = 8.3, 2.7 Hz, 1H), 6.23 (dd, *J* = 8.5, 2.7 Hz, 1H), 6.73 – 6.80, 6.84 – 7.07 (m, 25H), 7.15 – 7.27 (m, 15H), 7.33, 7.34 (2 × ddd, *J* = 8.1, 6.8, 1.2 Hz, 2H), 7.544, 7.546 (2 × d, *J* = 8.1 Hz, 2H), 7.68 (dd, *J* = 8.6, 1.2 Hz, 1H), 7.75 – 7.80 (m, 4H), 7.89 (d, *J* = 8.6 Hz, 1H). **^{13}C NMR** (126 MHz, $CDCl_3$): δ 21.19, 21.20, 21.23, 34.81, 35.33, 36.90, 53.76, 53.83, 55.18, 55.43, 55.50, 69.43, 73.05, 73.13, 73.98, 92.65, 95.66, 96.61, 96.73, 109.46, 110.56, 113.48, 113.60, 121.80, 122.93, 124.20, 124.21, 124.98, 125.08, 126.17, 126.25, 126.40, 126.47, 126.84, 126.85, 127.34, 127.47, 127.55, 127.62, 127.63, 127.65, 127.87, 127.91, 127.95, 127.99, 128.26, 128.31, 128.35, 128.45, 129.48, 129.83, 129.92, 129.94, 130.03, 130.10, 130.12, 130.15, 130.17, 130.22, 130.90, 130.95, 132.41, 132.75, 133.00, 133.04, 133.19, 133.82, 133.96, 134.08, 134.17, 134.59, 135.46, 135.52, 135.67, 135.79, 135.96, 136.06, 136.41, 136.53, 136.68, 136.96, 137.30, 138.41, 138.71, 139.98, 140.07, 140.22, 140.54, 146.10, 147.24. **IR** ($CHCl_3$): 3080 vw, 3063 w, 3051 w, 3031 w, 2948 w, 2927 w, 2890 w, 2845 vw, 2825 w, 1611 m, 1605 m, 1559 w, 1542 vw, 1517 w, 1511 m, 1494 m, 1465

w, 1451 m, 1442 w, 1390 w, 1361 m, 1184 vw, 1147 m, 1120 w, 1095 m, 1076 w, 1035 vs, 1002 vw, 911 w, 864 vw, 819 w, 696 w cm^{-1}. **MALDI MS**: 827 ($[M]^+$). **HR MALDI MS**: calcd for $C_{58}H_{53}NO_4$ 827.3974, found 827.3974.

(-)-(*M*)-*N*,*N*-Dibenzyl-7,8-bis(4-methylphenyl)hexahelicen-2-amine 99

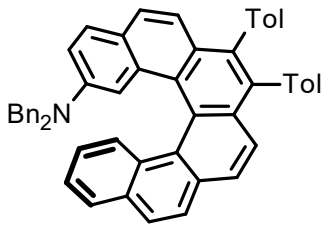

A flask was charged with tetrahydrohelicene (-)-(*M*,*RS*,*S*)-**98** (2.328 g, 2.811 mmol), *p*-toluenesulfonic acid monohydrate (5.347 g, 28.11 mmol, 10.0 equiv.), and flushed with argon. Toluene (75 mL) was added, the flask sealed with a stopcock, and the reaction mixture was stirred at 40 °C for 16 h. After completion (checked by TLC), the reaction was quenched with a saturated solution of $NaHCO_3$ (100 mL), the layers were separated, and the aqueous layer extracted with ethyl acetate (3 × 50 mL). The combined organic layers were dried over anhydrous $MgSO_4$, the solvents were removed *in vacuo*, and the crude product was purified by column chromatography on silica gel (hexane-ethyl acetate 40:1) to furnish helicene (-)-(*M*)-**99** (1.863 g, 94%, >99% *ee*) as a yellow solid. Chiral HPLC: Chiralpak IA column (250 × 4.6 mm, 5 µm, Chiral Technologies), mobile phase: hexane-dichloromethane (90:10 with 0.1% diethylamine), flow rate: 1 mL/min, retention time: 10.28 min. **M.p.**: 145 – 146 °C (hexane-ethyl acetate). **Optical rotation**: $[\alpha]^{20}_D$ = -1409° (c 0.260, $CHCl_3$). **^{1}H NMR** (400 MHz, $CDCl_3$): δ 7.92 – 7.85 (m, 3H), 7.83 (d, *J* = 8.5 Hz, 1H), 7.73 (d, *J* = 8.5 Hz, 1H), 7.62 (d, *J* = 8.8 Hz, 1H), 7.61 (d, *J* = 8.5 Hz, 1H), 7.57 (d, *J* = 8.8 Hz, 1H), 7.42 (ddd, *J* = 8.0, 6.9, 1.1 Hz, 1H), 7.34 (d, *J* = 8.8 Hz, 1H), 7.23 – 7.05 (m, 14H), 7.03 (d, *J* = 2.5 Hz, 1H), 6.86 (ddd, *J* = 8.4, 6.9, 1.4 Hz, 1H), 6.83 – 6.76 (m, 4H), 6.73 (dd, *J* = 8.8, 2.6 Hz, 1H), 4.12 – 3.98 (m, 4H), 2.36 (s, 3H), 2.35 (s, 3H). **^{13}C NMR** (101 MHz, $CDCl_3$): δ 146.25, 138.42, 137.95, 137.29, 137.02, 136.80, 135.94, 135.87, 132.35, 132.02, 131.75, 131.72, 131.50, 131.03, 130.80, 130.73, 130.70, 128.54, 128.46, 128.45, 128.44, 128.40, 128.36, 128.32, 127.74, 127.64, 127.51, 127.50, 127.20, 126.82, 126.71, 126.60, 126.27, 125.82, 125.56, 124.83, 124.33, 124.10, 120.86, 113.89, 109.25, 53.93, 21.44. **IR** ($CHCl_3$): 3086 w, 3063 w, 3052 w, 3033 w, 2958 m, 2871 m, 1615 s, 1605 m, 1586 vw, 1564 w, 1521 vs, 1494 m, 1466 m, 1452 m, 1444 w, 1413 vw, 1388 m, 1360 m, 1298 w, 1189 m, 1167 w, 1080 w, 1028 w, 1110 w, 1022 m, 835 m, 830 m, 822 m, 700 w cm^{-1}. **MALDI MS**: 703 ($[M]^+$). **HR MALDI MS**: calcd for $C_{54}H_{41}N$

703.3239, found 703.2334. **UV/Vis** (tetrahydrofuran): λ_{max} (log ε) = 253 (4.83), 275 (4.74), 315 nm (4.58). **Fluorescence** (tetrahydrofuran, λ_{exc} = 345 nm): λ_{max} = 480 nm.

(-)-(*M*)-7,8-Bis(4-methylphenyl)hexahelicen-2-amine 69

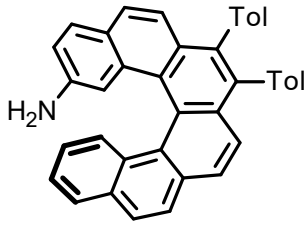

A flask was charged with the protected helicene (-)-(*M*)-**99** (739 mg, 1.05 mmol), ammonium formate (1.324 g, 21.0 mmol, 20.0 equiv.), and palladium (10% on activated charcoal, 134 mg, 0.126 mmol, 12 mol%). Then ethanol (105 mL) was added and the mixture was sonicated at room temperature for 1 h. Afterward, the reaction mixture was refluxed for 2 h. After completion (checked by TLC), the solvent was removed *in vacuo* and the crude product was filtered through a short pad of celite (ethyl acetate) to provide aminohelicene (-)-(*M*)-**69** (533 mg, 97%, >99% *ee*) as a yellow solid. **Chiral HPLC**: Chiralpak IA column (250 × 4.6 mm, 5 µm, Chiral Technologies), mobile phase: hexane-dichloromethane (3:1 with 0.1% diethylamine), flow rate: 1 mL/min, retention time: 16.69 min. **M.p.**: 299 – 302 °C (heptane). **Optical rotation**: $[\alpha]^{20}_{D}$ = -2074° (c 0.114, $CHCl_3$). **^{1}H NMR** (400 MHz, CD_2Cl_2): δ 7.96 – 7.90 (m, 2H), 7.86 – 7.84 (m, 1H), 7.82 (d, *J* = 8.6 Hz, 1H), 7.76 – 7.72 (m, 1H), 7.66 (d, *J* = 8.7 Hz, 1H), 7.60 (d, *J* = 8.5 Hz, 1H), 7.59 (d, *J* = 8.4 Hz, 1H), 7.34 – 7.27 (m, 2H), 7.22 – 7.09 (m, 8H), 6.81 – 6.74 (m, 2H), 6.66 (dd, *J* = 8.4, 2.3 Hz, 1H), 3.22 (s, 2H), 2.37 (s, 3H), 2.37 (s, 3H). **^{13}C NMR** (101 MHz, CD_2Cl_2): δ 144.87, 138.32, 137.74, 137.48, 137.26, 136.71, 136.63, 132.75, 132.48, 132.17, 132.14, 131.82, 131.50, 131.43, 131.10, 131.07, 130.94, 129.14, 128.92, 128.85, 128.83, 128.75, 128.27, 127.95, 127.90, 127.87, 127.52, 126.94, 126.80, 126.68, 126.17, 126.13, 125.77, 125.12, 124.54, 121.55, 116.76, 111.55, 21.54. **IR** ($CHCl_3$): 3480 vw, 3449 vw, 3379 w, 3052 w, 2957 m, 1625 s, 1605 m, 1519 s, 1463 m, 1426 w, 1382 m, 1363 w, 1339 w, 1306 w, 1282 w, 1272 w, 1253 m, 1237 m, 1183 m, 1146 w, 1109 m, 1079 w, 1052 w, 1040 w, 1022 m, 959 w, 875 w, 834 vs, 818 m cm^{-1}. **ESI MS**: 524 ($[M+H]^+$). **MALDI MS**: 523 ($[M]^+$). **HR MALDI MS**: calcd for $C_{40}H_{29}N$ 523.2300, found 523.2295. **UV/Vis** (tetrahydrofuran): λ_{max} (log ε) = 207 (4.95), 210 (4.94), 248 (4.93), 270 (4.93), 314 (4.65), 335 nm (4.54). **Fluorescence** (tetrahydrofuran, λ_{exc} = 430 nm): λ_{max} = 487 nm.

(+)-(*P*)-7,8-Bis(4-methylphenyl)hexahelicen-2-amine 69

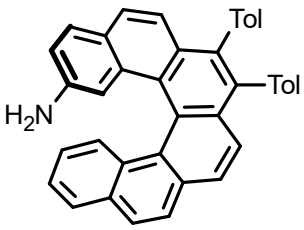

Chiral HPLC: Chiralpak IA column (250 × 4.6 mm, 5 µm, Chiral Technologies), mobile phase: hexane-dichloromethane (3:1 with 0.1% diethylamine), flow rate: 1 mL/min, retention time: 8.14 min (>99% *ee*). **M.p.**: 300 – 303 °C (heptane). **Optical rotation**: $[\alpha]^{20}_D$ = +2179° (c 0.118, $CHCl_3$).

4-Bromo-3-iodoaniline 105[147]

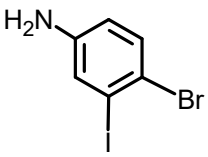

To a solution of 3-iodoaniline **75** (5.476 g, 25.0 mmol) in DMF (25 mL) a solution of NBS (4.450 g, 25.0 mmol, 1.00 equiv.) in DMF (25 mL) was added dropwise. The mixture was stirred at room temperature for 20 h. Afterward, it was poured into water (25 mL) and extracted with dichloromethane (3 x 30 mL). The solvents were removed under reduced pressure and the crude product was purified by flash chromatography on silica gel (hexane-ethyl acetate 4:1) affording bromo aniline **105** (5.529 g, 74%) as a brown solid. **^{1}H NMR** (401 MHz, $CDCl_3$) δ 7.28 (d, *J* = 8.6 Hz, 1H), 7.15 (d, *J* = 2.7 Hz, 1H), 6.48 (dd, *J* = 8.6, 2.7 Hz, 1H), 3.68 (s, 2H). **^{13}C NMR** (101 MHz, $CDCl_3$) δ 146.28, 132.54, 125.96, 116.91, 116.54, 101.42.

Di-*tert*-butyl (4-bromo-3-iodophenyl)imidodicarbonate 106

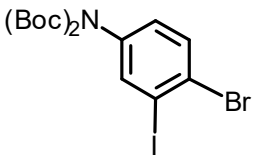

Iodoaniline **105** (5.065 g, 17.0 mmol) was dissolved in tetrahydrofuran (100 mL). Subsequently di-*tert*-butyl dicarbonate (14.841 g, 68.0 mmol, 4.0 equiv.) and 4-(dimethylamino)pyridine (208 mg, 1.70 mmol, 10 mol%) were added. The reaction mixture was stirred under reflux for 2 h. After cooling down to room temperature, the reaction was quenched by the addition of brine (100 mL). The phases were separated and an aqueous layer extracted with ethyl acetate (3 × 150 mL). The combined organic layers were dried over anhydrous $MgSO_4$, the solvent was removed under reduced pressure, and the crude product was purified by flash chromatography on silica gel (hexane-ethyl acetate 4:1) affording aniline derivative **106** (8.048 g, 95%) as a yellow oil. **^{1}H NMR** (400 MHz, $CDCl_3$): δ 7.65 (d, *J* = 2.5 Hz, 1H), 7.59 (d, *J* = 8.5 Hz, 1H), 7.01 (dd, *J* = 8.5, 2.5 Hz, 1H), 1.43 (s, 18H). **^{13}C NMR** (101 MHz, $CDCl_3$): δ 151.29, 139.77, 138.90, 132.46, 129.33, 128.72, 100.28, 83.60, 28.06. **IR** ($CHCl_3$): 2984 m, 2873 w,

1830 w, 1810 m, 1788 s, 1748 vs, 1709 s, 1578, w, 1558 s, 1476 w, 1458 s, 1395 m, 1372 vs, 1362 m, 1307 s, 1279 s, 1252 s, 1149 vs, 1120 vs, 1104 s, 1078 s, 949 w, 875 m, 844 m, 816 w, 657 vw, 638 vw, 464 vw, 436 w cm^{-1}. **ESI MS**: 520 ($[M+Na]^+$, with ^{79}Br). **HR ESI MS**: calcd for $C_{16}H_{21}O_4N^{79}BrINa$ 519.9591, found 519.9592.

Di-*tert*-butyl (4-bromo-3-((trimethylsilyl)ethynyl)phenyl)imidodicarbonate 107

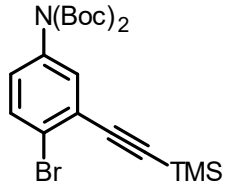

A Schlenk flask was charged with iodo compound **106** (100 mg, 0.2 mmol), $Pd(PPh_3)_2Cl_2$ (3 mg, 0.004 mmol, 2 mol%), CuI (1.5 mg, 0.008 mmol, 4 mol%) and flushed with nitrogen. Then diisopropylamine (2 mL, degassed by 3 freeze pump thaw circles) and trimethylsilylacetylene (34 µL, 0.24 mmol, 1.2 equiv.) were added *via* syringe and the reaction mixture was stirred for 2 h at 0 °C. The solvent was removed in *vacou* and the crude product purified by flash chromatography (hexane-ethyl acetate 10:1) to obtain alkyne **107** (36 mg, 38%) as a white solid.

M.p.: 124 – 126 °C. **^{1}H NMR** (401 MHz, $CDCl_3$) δ 7.54 (d, *J* = 8.5 Hz, 1H), 7.27 (d, *J* = 2.6 Hz, 1H), 6.94 (dd, *J* = 8.5, 2.6 Hz, 1H), 1.42 (s, 18H), 0.27 (s, 6H). **^{13}C NMR** (101 MHz, $CDCl_3$) δ 151.33, 138.46, 133.07, 132.76, 129.57, 125.91, 124.72, 102.39, 100.46, 83.38, 28.05, -0.08. **IR**: 3020 w, 2983 m, 2904 vw, 2871 vw, 2161 w, 1790 s, 1780 m, 1748 s, 1718 m, 1705 m, 1602 w, 1591 w, 1568 vw, 1476 w, 1464 m, 1395 m, 1371 s, 1364 m, 1278 s, 1252 s, 1152 s, 1104 s, 1038 w, 866 m, 849 vs, 701 vw, 613 vw, 618 w, 466 vw, cm^{-1}. **HR ESI MS**: calcd for $BrC_{21}H_{30}NNaO_4Si$ 490.10197, found 490.10225.

Di-*tert*-butyl (4-bromo-3-((trimethylsilyl)ethynyl)phenyl)imidodicarbonate 108

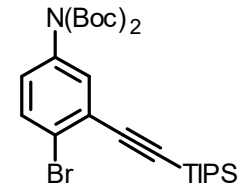

A Schlenk flask was charged with iodo compound **106** (200 mg, 0.4 mmol), $Pd(PPh_3)_2Cl_2$(5.6 mg, 0.004 mmol, 2 mol%), CuI (3 mg, 0.008 mmol, 4 mol%) and flushed with nitrogen. Then diisopropylamine (4 mL,) was added and the mixture was degassed by three freeze pump thaw cycles. Triisopropylsilylacetylene (0.034 ml, 0.24 mmol, 1.2 equiv.) was added *via* syringe and the reaction mixture was stirred for 1 h at room temperature. The solvent was removed *in vacou* and the crude product purified by column chromatography (hexane-ethyl acetate 10:1) to obtain alkyne **108** (85 mg, 38%) as a yellow oil. **^{1}H NMR** (401 MHz, $CDCl_3$) δ 7.54 (d, *J* = 8.5 Hz, 1H),

7.28 (d, *J* = 2.6 Hz, 1H), 6.95 (dd, *J* = 8.5, 2.6 Hz, 1H), 1.43 (s, 18H), 1.14 (m, 21H). **^{13}C NMR** (101 MHz, $CDCl_3$) δ 151.44, 138.34, 133.28, 132.70, 129.35, 126.25, 124.60, 104.17, 97.07, 83.40, 28.03, 18.77, 11.39. **IR** ($CHCl_3$): 3050 w, 2982 s, 2960 vs, 2945 vs, 2866 vs, 1789 vs, 1780 vs, 1748 vs, 1721 s,1705 s, 1601 w, 1592 m, 1567 w, 1479 s, 1465 vs, 1460 s, 1394 s, 1383 s, 1370 vs, 1364 vs, 1277 vs, 1253 vs, 1152 vs, 1120 vs, 1104 vs, 1075 m, 1038 s, 997 m, 883 s, 864 s, 703 w, 679 s, 645 m, 614 m, 464 m cm^{-1}. **HR ESI MS**: calcd for $C_{27}H_{42}O_4N^{79}BrNaSi$ 574.19587, found 574.19593.

4-Bromo-3-((trimethylsilyl)ethynyl)aniline 109

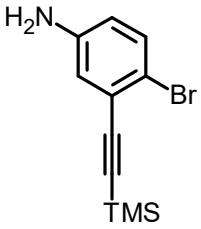

A Schlenk flask was charged with iodoaniline **105** (4.47 g, 15.0 mmol), $Pd(PPh_3)_2Cl_2$ (210 mg, 0.300 mmol, 2 mol%), CuI (115 mg, 0.600 mmol, 4 mol%), and flushed with argon. Then diisopropylamine (120 mL) was added and the mixture was degassed by three freeze pump thaw cycles. The mixture was cooled to 0 °C and (trimethylsilyl)acetylene (2.2 mL, 15.75 mmol, 1.05 equiv.) was added *via* syringe. The cooling bath was removed, the reaction mixture allowed to warm slowly to room temperature and stirred for 16 h. After completion (checked by TLC), the solvent was removed *in vacuo* and the crude product was purified by flash chromatography on silica gel (hexane-ethyl acetate 5:1) to give alkyne **109** (3.962 g, 99%) as a brownish oil. **^{1}H NMR** (400 MHz, $CDCl_3$): δ 7.29 (d, *J* = 8.6 Hz, 1H), 6.82 (d, *J* = 2.9 Hz, 1H), 6.50 (dd, *J* = 8.6, 2.9 Hz, 1H), 3.65 (s, 2H), 0.26 (s, 9H). **^{13}C NMR** (101 MHz, $CDCl_3$): δ 145.39, 132.94, 125.51, 119.74, 117.05, 113.83, 103.40, 98.90, 0.01. **IR** ($CHCl_3$): 3491 w, 3460 vw, 3403 w, 3380 w, 2900 w, 2160 w, 1620 s, 1594 m, 1571 w, 1466 s, 1424 w, 1410 w, 1262 w, 1251 s, 1138 m, 1121 vw, 1032 m, 857 vs, 846 vs, 814 m, 699 w, 465 m cm^{-1}. **EI MS**: 267 ($M^{+\bullet}$, 83), 252 (100), 224 (5), 172 (13), 158 (10), 130 (28), 109 (9), 89 (4), 77 (5). **HR EI MS**: calcd for $C_{11}H_{14}ON^{79}BrSi$ 267.0079, found 267.0073.

tert-Butyl (4-Bromo-3-((trimethylsilyl)ethynyl)carbamate 110

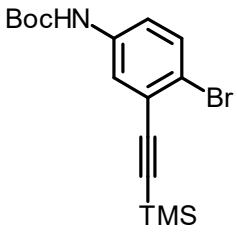

A flask was charged with alkyne **109** (233 g, 0.87 mmol), flushed with argon, and the compound was dissolved in ethanol (1.7 mL). Di-*tert*-butyl dicarbonate (0.3 mL, 1.30 mmol, 1.5 equiv.) was added and the reaction mixture was stirred at room temperature for 16 h. After completion (checked by TLC), all volatiles were removed *in vacuo* and the crude product purified by flash chromatography on silica gel (hexane-ethyl acetate 10:1) to give carbamate **110** (317 mg, 99%) as a beige solid. **M.p.**: 134 – 135 °C (hexane-ethyl acetate). **^{1}H NMR** (401 MHz, $CDCl_3$) δ 7.57 (d, *J* = 2.7 Hz, 1H), 7.44 (d, *J* = 8.7 Hz, 1H), 7.16 (dd, *J* = 8.7, 2.7 Hz, 1H), 6.44 (s, 1H), 1.52 (s, 9H), 0.26 (s, 9H). **^{13}C NMR** (101 MHz, $CDCl_3$) δ 152.47, 137.55, 132.76, 125.74, 123.12, 119.87, 118.90, 99.78, 85.34, 81.24, 28.43, -0.04. **IR** ($CHCl_3$): 3438 m, 3032 w, 2984 m, 2903 w, 2161 w, 1729 s, 1597 m, 1575 m, 1513 s, 1479 m, 1466 m, 1397 s, 1372 s, 1307 vw, 1263 m, 1251 s, 1156 vs, 1143 s, 1121 s, 1038 w, 854 s, 846 s, 813 w, 702 w, 467 w cm^{-1}. **HR EI MS:** calcd for $C_{16}H_{22}NO_2Si^{79}Br$ 367.0603, found 367.0607.

tert-Butyl (4-Bromo-3-ethynylphenyl)carbamate 111

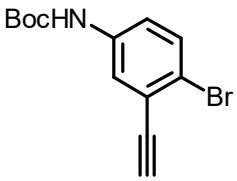

A flask was charged with alkyne **109** (2.792 g, 10.41 mmol), flushed with argon, and the compound was dissolved in ethanol (21 mL). Di-*tert*-butyl dicarbonate (3.59 mL, 15.615 mmol, 1.5 equiv.) was added and the reaction mixture was stirred at room temperature for 16 h. After completion (checked by TLC), all volatiles were removed *in vacuo*. The residue was dissolved in methanol (65 mL), K_2CO_3 (2.16 g, 15.615 mmol, 1.5 equiv.) was added, and the suspension was stirred at room temperature for 3 h. After completion (checked by TLC), the reaction was quenched with a saturated NH_4Cl solution (20 mL) and extracted with dichloromethane (3 × 50 mL). The combined organic layers were dried over anhydrous $MgSO_4$, the solvent was removed *in vacuo*, and the crude product purified by flash chromatography on silica gel (hexane-ethyl acetate 10:1) to give carbamate **111** (2.742 g, 89%, after 2 steps) as an off white solid. **M.p.**: 129 – 131 °C (ethyl acetate). **^{1}H NMR** (400 MHz, $CDCl_3$): δ 7.58 (d, *J* = 2.7 Hz, 1H), 7.46 (d, *J* = 8.8 Hz, 1H), 7.24 (dd, *J* = 8.8, 2.7 Hz, 1H), 6.46 (s, 1H), 3.34 (s, 1H), 1.51 (s, 9H). **^{13}C NMR** (101 MHz, $CDCl_3$): δ 152.44,

137.69, 132.90, 124.74, 123.64, 120.34, 118.65, 81.89, 81.83, 81.35, 28.42. **IR** ($CHCl_3$): 3437 s, 3306 s, 2982 m, 2120 vw, 1728 vs, 1597 s, 1576 s, 1514 vs, 1478 s, 1467 s, 1394 vs, 1377 s, 1370 s, 1270 s, 1241 s, 1156 vs, 1036 m, 867 m, 814 m, 658 m, 630 m, 608 vw, 462 w cm^{-1}. **CI MS**: 296 ($[M+H]^+$ with ^{79}Br). **HR CI MS**: calcd for $C_{13}H_{14}NO_2{}^{79}Br$ 295.0208, found 295.0210.

(+)-*tert*-Butyl (*S*)-(4-bromo-3-((2-(2-(methoxymethoxy)-4-(triisopropylsilyl)but-3-yn-1-yl)naph-thalen-1-yl)ethynyl)phenyl)carbamate 112

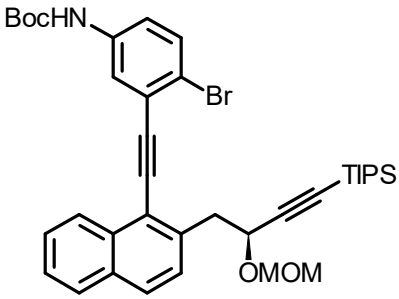

A Schlenk flask was charged with iodide (-)-(*S*)-**83**[31] (1.045 g, 2.00 mmol), $Pd(PPh_3)_2Cl_2$ (28 mg, 0.040 mmol, 2 mol%), CuI (15 mg, 0.080 mmol, 3 mol%), and flushed with argon. Then diisopropylamine (20 mL, prior degassed by three freeze-pump-thaw cycles) was added *via* cannula. Another Schlenk flask was charged with alkyne **111** (0.77 g, 2.60 mmol, 1.3), flushed with argon, and diisopropylamine (25 mL, prior degassed by three freeze-pump-thaw cycles) was added *via* cannula. Then the alkyne solution was added dropwise *via* cannula over 10 min to the iodide solution and the resulting mixture was stirred at room temperature for 16 h. After completion (checked by TLC), the solvent was removed *in vacuo* and the crude product was purified by flash chromatography on silica gel (hexane-ethyl acetate 10:1) to give diyne (*S*)-**112** (1.259 g, 91%) as a yellowish oil. **Optical rotation**: $[\alpha]^{20}_D$ = +21.2° (c 0.288, $CHCl_3$). **^{1}H NMR** (400 MHz, $CDCl_3$): δ 8.55 (d, *J* = 8.4 Hz, 1H), 7.82 (d, *J* = 8.0 Hz, 1H), 7.77 (d, *J* = 8.4 Hz, 1H), 7.59 (ddd, *J* = 8.4, 6.9, 1.3 Hz, 1H), 7.59 – 7.52 (m, 3H), 7.50 (ddd, *J* = 8.0, 6.9, 1.1 Hz, 1H), 7.47 – 7.43 (m, 1H), 6.56 (s, 1H), 4.95 (d, *J* = 6.7 Hz, 1H), 4.87 (t, *J* = 7.2 Hz, 1H), 4.58 (d, *J* = 6.6 Hz, 1H), 3.59 (d, *J* = 7.2 Hz, 2H), 3.08 (s, 3H), 1.54 (s, 9H), 1.04 – 0.99 (m, 21H). **^{13}C NMR** (101 MHz, $CDCl_3$): δ 152.52, 139.03, 137.84, 133.66, 133.03, 132.23, 129.09, 128.51, 128.14, 127.05, 126.54, 126.13, 126.08, 122.88, 119.93, 119.73, 118.50, 106.03, 97.32, 94.21, 90.59, 87.37, 81.21, 66.47, 55.61, 41.80, 28.46, 18.71, 11.28. **IR** ($CHCl_3$): 3438 m, 2866 s, 2826 w, 2208 w, 2169 w, 1728 s, 1596 m, 1574 m, 1515 s, 1478 s, 1463 m, 1383 w, 1370 s, 1245 w, 1155 vs, 1146 s, 1097 w, 1033 s, 1027 s, 998 m, 919 w, 911 w, 884 m, 867 w, 831 w cm^{-1}. **ESI MS**: 712 ($[M+Na]^+$ with ^{79}Br). **HR ESI MS**: calcd for $C_{38}H_{48}O_4N^{79}BrNaSi$ 712.2428, found 712.2430.

(-)-*tert*-Butyl (*S*)-(2-((2-(2-(methoxymethoxy)-4-(triisopropylsilyl)but-3-yn-1-yl)naphthalen-1-yl)ethynyl)-2'-((triisopropylsilyl)ethynyl)-[1,1'-biphenyl]-4-yl)carbamate 114

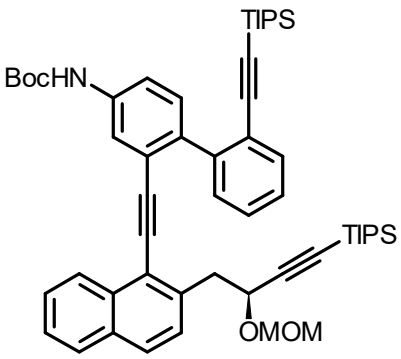

A flask was charged with diyne (*S*)-**112** (1.24 g, 1.795 mmol), $Pd(PPh_3)_2Cl_2$ (126 mg, 0.180 mmol, 10 mol%), K_2CO_3 (260 mg, 1.885 mmol, 1.05 equiv.), boronic acid **113** (705, 2.334 mmol, 1.3 equiv.), and flushed with argon. Then a solvent mixture of toluene (32 mL), n-propanol (32 mL), and water (8 mL) was added and argon was bubbled through the stirred mixture for 10 min. Afterward, the reaction mixture was refluxed for 5 h. After completion (checked by TLC), the solvents were removed in vacuo, the crude product was purified by flash chromatography on silica gel (hexane-ethyl acetate 10:1) to give triyne (S)-**114** (1.526 g, 98%) as a yellowish oil. **Optical rotation**: $[\alpha]^{20}_D$ = -41.7° (c 0.437, $CHCl_3$). **^{1}H NMR** (400 MHz, $CDCl_3$): δ 7.74 – 7.63 (m, 4H), 7.52 (d, J = 6.6 Hz, 1H), 7.53 – 7.48 (m, 1H), 7.46 (d, J = 4.8 Hz, 1H), 7.45 – 7.44 (m, 1H), 7.43 – 7.37 (m, 4H), 7.27 (ddd, J = 8.2, 6.8, 1.2 Hz, 1H), 6.59 (s, 1H), 4.94 (d, J = 6.6 Hz, 1H), 4.78 (t, J = 7.1 Hz, 1H), 4.61 (d, J = 6.6 Hz, 1H), 3.46 – 3.29 (m, 2H), 3.15 (s, 3H), 1.56 (s, 9H), 1.05 – 1.00 (m, 21H), 0.94 – 0.90 (m, 21H). **^{13}C NMR** (101 MHz, $CDCl_3$): δ 152.70, 143.65, 137.97 (2 C), 137.95, 133.55, 133.01, 132.07, 130.91, 130.29, 128.80, 128.22, 127.80, 127.76, 127.33, 126.70, 126.48, 125.78, 123.74, 123.70, 121.78, 120.42, 118.49, 106.12, 105.97, 98.48, 94.38, 94.35, 88.91, 87.23, 80.82, 66.54, 55.67, 41.69, 28.49, 18.71, 18.63, 11.35, 11.28. **IR** ($CHCl_3$): 3440 w, 3306 vw, 3058 w, 2958 s, 2943 s, 2865 s, 2827 w, 2175 vw, 2157 w, 1728 m, 1607 w, 1595 w, 1574 w, 1569 vw, 1563 vw, 1516 m, 1502 m, 1465 m, 1441 w, 1400 w, 1395 w, 1382 w, 1369 m, 1156 s, 1098 m, 1028 m, 997 m, 919 w, 883 m, 867 vw, 816 w, 710 vw, 679 m, 663 m, 502 vw, cm^{-1}. **MALDI MS**: 890 ($[M+Na]^+$). **HR MALDI MS**: calcd for $C_{55}H_{73}NNaO_4Si_2$ 890.4970, found 890.4977.

(-)-*tert*-Butyl (*S*)-(2'-ethynyl-2-((2-(2-(methoxymethoxy)but-3-yn-1-yl)naphthalen-1-yl)ethynyl)-[1,1'-biphenyl]-4-yl)carbamate 115

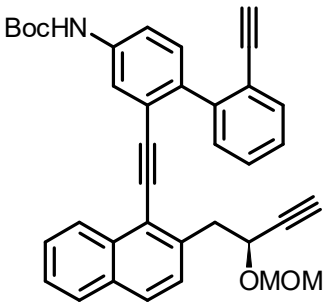

A flask was charged with silylated compound (*S*)-**114** (1.493 g, 1.72 mmol) and dissolved in tetrahydrofuran (22 mL). Then a solution of *n*-tetrabutylammonium fluoride trihydrate (1 M in tetrahydrofuran, 5.16 mL, 5.16 mmol, 3.0 equiv.) was added and the mixture was stirred at room temperature for 6 h. After completion (checked by TLC), the reaction was quenched with methanol (10 mL) and the solvents were removed *in vacuo*. The crude product was purified by flash chromatography on silica gel (hexane-ethyl acetate 5:1) to obtain triyne (*S*)-**115** (890 mg, 93%) as a white solid. **M.p.**: 66 – 67 °C (ethyl acetate). **Optical rotation**: $[\alpha]^{20}_D$ = -24.8° (c 0.262, $CHCl_3$). **^{1}H NMR** (400 MHz, $CDCl_3$): δ 7.74 (d, *J* = 8.1 Hz, 1H), 7.71 – 7.63 (m, 3H), 7.60 – 7.54 (m, 2H), 7.54 – 7.50 (m, 1H), 7.47 – 7.37 (m, 5H), 7.29 (ddd, *J* = 8.3, 6.8, 1.3 Hz, 1H), 6.64 (s, 1H), 4.88 (d, *J* = 6.8 Hz, 1H), 4.72 (ddd, *J* = 7.4, 6.6, 2.1 Hz, 1H), 4.56 (d, *J* = 6.7 Hz, 1H), 3.43 – 3.26 (m, 2H), 3.10 (s, 3H), 3.00 (s, 1H), 2.46 (d, *J* = 2.1 Hz, 1H), 1.56 (s, 9H). **^{13}C NMR** (101 MHz, $CDCl_3$): δ 152.74, 143.59, 138.05, 137.94, 137.48, 133.54, 133.37, 132.09, 130.94, 130.66, 128.72, 128.68, 127.99, 127.91, 127.47, 126.67, 126.50, 125.95, 123.62, 122.10, 121.95, 120.36, 118.40, 98.44, 94.44, 88.95, 82.86, 82.50, 80.98, 80.66, 74.39, 65.93, 55.63, 41.53, 28.50. **IR** ($CHCl_3$): 3437 m, 3307 m, 3059 w, 2982 w, 2932 m, 2826 w, 2208 vw, 2116 vw, 2017 vw, 1727 s, 1607 m, 1595 w, 1575 m, 1563 w, 1516 vs, 1504 s, 1473 m, 1455 w, 1441 m, 1412 m, 1400 m, 1394 m, 1369 m, 1300 w, 1155 vs, 1054 m, 1028 s, 951 w, 940 vw, 922 w, 909 m, 868 w, 821 w, 663 m, 651 m, 640 m, 616 w, 437 w cm^{-1}. **ESI MS**: 578 ($[M+Na]^+$). **HR ESI MS**: calcd for $C_{37}H_{33}NNaO_4$ 578.2302, found 578.2301. **HR APCI MS**: calcd for $C_{37}H_{34}NO_4$ 556.2482, found 556.2482.

(-)-*tert*-Butyl (*S*)-(2-((2-(2-(methoxymethoxy)-4-(triisopropylsilyl)but-3-yn-1-yl)naphthalen-1-yl)ethynyl)-2'-((triisopropylsilyl)ethynyl)-[1,1'-biphenyl]-4-yl)carbamate 116

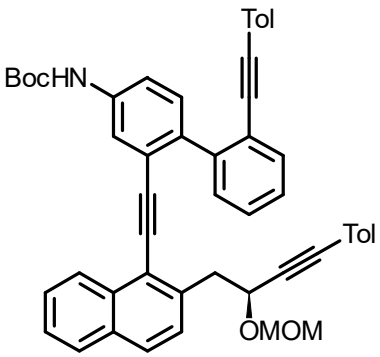

A flask was charged with diyne (*S*)-**115** (1.24 g, 1.795 mmol), $Pd(PPh_3)_2Cl_2$ (126 mg, 0.180 mmol, 10 mol%), K_2CO_3 (260 mg, 1.885 mmol, 1.05 equiv.), boronic acid **10**[26] (705, 2.334 mmol, 1.3 equiv.), and flushed with argon. Then a solvent mixture of toluene (32 mL), *n*-propanol (32 mL), and water (8 mL) was added and argon was bubbled through the stirred mixture for 10 min. Afterward, the reaction mixture was refluxed for 5 h. After completion (checked by TLC), the solvents were removed *in vacuo*, the crude product was purified by flash chromatography on silica gel (hexane-ethyl acetate 10:1) to give triyne (*S*)-**116** (1.526 g, 98%) as a yellowish oil. **Optical rotation**: $[\alpha]^{20}_D$ = -41.7° (c 0.437, $CHCl_3$). **^{1}H NMR** (400 MHz, $CDCl_3$): δ 7.74 – 7.63 (m, 4H), 7.52 (d, *J* = 6.6 Hz, 1H), 7.53 – 7.48 (m, 1H), 7.46 (d, *J* = 4.8 Hz, 1H), 7.45 – 7.44 (m, 1H), 7.43 – 7.37 (m, 4H), 7.27 (ddd, *J* = 8.2, 6.8, 1.2 Hz, 1H), 6.59 (s, 1H), 4.94 (d, *J* = 6.6 Hz, 1H), 4.78 (t, *J* = 7.1 Hz, 1H), 4.61 (d, *J* = 6.6 Hz, 1H), 3.46 – 3.29 (m, 2H), 3.15 (s, 3H), 1.56 (s, 9H), 1.05 – 1.00 (m, 21H), 0.94 – 0.90 (m, 21H). **^{13}C NMR** (101 MHz, $CDCl_3$): δ 152.70, 143.65, 137.97 (2 C), 137.95, 133.55, 133.01, 132.07, 130.91, 130.29, 128.80, 128.22, 127.80, 127.76, 127.33, 126.70, 126.48, 125.78, 123.74, 123.70, 121.78, 120.42, 118.49, 106.12, 105.97, 98.48, 94.38, 94.35, 88.91, 87.23, 80.82, 66.54, 55.67, 41.69, 28.49, 18.71, 18.63, 11.35, 11.28. **IR** ($CHCl_3$): 3440 w, 3306 vw, 3058 w, 2958 s, 2943 s, 2865 s, 2827 w, 2175 vw, 2157 w, 1728 m, 1607 w, 1595 w, 1574 w, 1569 vw, 1563 vw, 1516 m, 1502 m, 1465 m, 1441 w, 1400 w, 1395 w, 1382 w, 1369 m, 1156 s, 1098 m, 1028 m, 997 m, 919 w, 883 m, 867 vw, 816 w, 710 vw, 679 m, 663 m, 502 vw, cm^{-1}. **MALDI MS**: 890 ($[M+Na]^+$). **HR MALDI MS**: calcd for $C_{55}H_{73}NNaO_4Si_2$ 890.4970, found 890.4977.

(-)-(*M*)-*tert*-Butyl (*S*)-(1-(methoxymethoxy)-17,18-di-*p*-tolyl-1,2-dihydrobenzo[g]naphtha-[2,1-c]chrysen-10-yl)carbamate 117

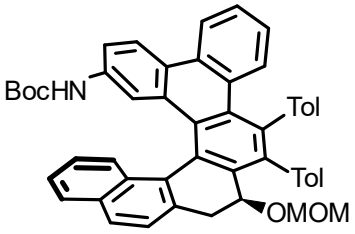

A microwave vial was charged with triyne (*S*)-**116** (206 mg, 0.280 mmol), $Ni(CO)_2(PPh_3)_2$ (54 mg, 0.084 mmol, 30 mol%), closed with a crimp seal, and flushed with argon. Toluene (20 mL) was added and argon was kept to bubble through the stirring mixture for 10 min. Then the mixture was immersed in an oil bath and stirred at 150 °C for 10 min. The mixture was cooled down, the solvent was removed *in vacuo*, and the crude product was purified by flash chromatography on silica gel (hexane-ethyl acetate 5:1) to give dihydrohelicene (-)-(*M*,*S*)-**117** (173 mg, 84%, >99% *de*) as a beige solid. **Chiral HPLC**: Chiralpak IA column (250 × 4.6 mm, 5 µm, Chiral Technologies), mobile phase: heptane-*i*-PrOH (95:5), flow rate: 1 mL/min, retention time: 6.55 min. **M.p.**: 172 – 175 °C. **Optical rotation**: $[\alpha]^{20}_D$ = -320° (c 0.096, $CHCl_3$). **^{1}H NMR** (400 MHz, $CDCl_3$): δ 8.36 (d, *J* = 7.5 Hz, 1H), 8.23 (d, *J* = 9.2 Hz, 1H), 7.83 (d, *J* = 8.2 Hz, 1H), 7.70 (d, *J* = 7.9 Hz, 1H), 7.63 – 7.57 (m, 2H), 7.54 (d, *J* = 8.6 Hz, 1H), 7.49 (dd, *J* = 8.5, 1.1 Hz, 1H), 7.41 (ddd, *J* = 8.1, 7.1, 1.1 Hz, 1H), 7.28 (d, *J* = 8.7 Hz, 1H), 7.19 – 7.12 (m, 2H), 7.10 (dd, *J* = 7.8, 1.8 Hz, 1H), 7.00 (ddd, *J* = 8.4, 7.1, 1.3 Hz, 1H), 6.97 – 6.94 (m, 1H), 6.92 – 6.87 (m, 2H), 6.86 – 6.82 (m, 1H), 6.82 – 6.77 (m, 2H), 6.48 (dd, *J* = 7.8, 1.8 Hz, 1H), 5.68 (s, 1H), 4.51 (t, *J* = 2.7 Hz, 1H), 4.50 – 4.45 (m, 2H), 3.56 (dd, *J* = 15.9, 2.6 Hz, 1H), 3.33 (dd, *J* = 15.8, 2.7 Hz, 1H), 2.97 (s, 3H), 2.32 (s, 3H), 2.29 (s, 3H), 1.43 (s, 9H). **^{13}C NMR** (101 MHz, $CDCl_3$): δ 152.47, 140.60, 139.68, 138.23, 137.18, 136.41, 136.00, 135.87, 135.84, 133.56, 133.32, 132.57, 132.09, 131.88, 131.83, 131.57, 131.53, 131.52, 131.21, 130.64, 130.13, 130.01, 129.57, 128.99, 128.86, 128.82, 128.38, 128.33, 127.90, 127.82, 127.74, 126.45, 126.04, 125.84, 125.77, 124.90, 124.74, 123.93, 122.95, 118.52, 117.56, 97.12, 80.51, 73.67, 55.85, 37.53, 28.40, 21.42, 21.40. **IR** ($CHCl_3$): 3438 w, 3054 w, 2982 m, 2825 w, 1725 s, 1615 m, 1595 vw, 1586 w, 1565 w, 1515 vs, 1472 m, 1441 w, 1413 m, 1393 m, 1369 m, 1309 w, 1155 vs, 1111 w, 1095 m, 1034 s, 959 vw, 910 m, 860 w, 828 m, 809 w, 541 w cm^{-1}. **MALDI MS**: 735 ($[M]^+$). **HR MALDI MS**: calcd for $C_{51}H_{45}NO_4$ 735.3348, found 735.3354. **HR MALDI MS**: calcd for $C_{51}H_{45}NNaO_4$ 758.3241, found 758.3248.

(-)-(*M*)-5,6-Bis(4-methylphenyl)benzo[f]hexahelicen-16-amine 118

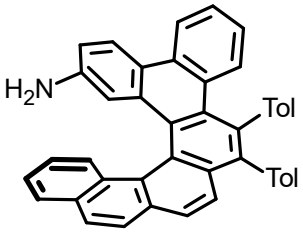

The protected dihydrohelicene (-)-(*M*,*S*)-**117** (30 mg, 0.041 mmol) was placed in a Schlenk flask, flushed with argon, and dissolved in dioxane (1.2 mL). Then an HCl solution (4 M in dioxane, 0.62 mL, 2.46 mmol, 60.0 equiv.) was added and the reaction mixture was stirred at room temperature for 19 h. The orange mixture was poured into a saturated $NaHCO_3$ solution (20 mL) and extracted with dichloromethane. The combined organic layers were dried over anhydrous Na_2SO_4 and the solvent was removed under reduced pressure. The crude product was purified by flash chromatography on reversed phase C-18 silica gel (methanol) to afford the crude aminobenzohelicene (-)-(*M*)-**118** (20 mg, 83%) as a yellow solid. An analytically pure sample was obtained by recrystallization from dichloromethane-heptane upon which an impurity precipitated. **Chiral HPLC**: Chiralpak IA column (250 × 4.6 mm, 5 µm, Chiral Technologies), mobile phase: hexane-chloroform (9:1), flow rate: 1 mL/min, retention time: 6.44 min, optical purity: >99% *ee*. **M.p.**: 215 – 217 °C (heptane). **Optical rotation**: $[\alpha]^{20}_D$ = -931° (c 0.016, $CHCl_3$). **^{1}H NMR** (500 MHz, CD_2Cl_2): δ 8.42 (dd, *J* = 8.3, 1.3 Hz, 1H), 8.20 (d, *J* = 8.6 Hz, 1H), 7.95 – 7.89 (m, 2H), 7.83 (dd, *J* = 8.0, 1.4 Hz, 1H), 7.82 (d, *J* = 8.7 Hz, 1H), 7.71 (d, *J* = 8.6 Hz, 1H), 7.61 (d, *J* = 8.6 Hz, 1H), 7.53 (dd, *J* = 7.7, 2.0 Hz, 1H), 7.50 (d, *J* = 8.4 Hz, 1H), 7.44 (ddd, *J* = 8.2, 7.0, 1.2 Hz, 1H), 7.30 – 7.26 (m, 3H), 7.07–7.04 (m, 1H), 7.00 – 6.92 (m, 3H), 6.82 (ddd, *J* = 8.4, 6.9, 1.4 Hz, 1H), 6.78 (dd, *J* = 7.7, 2.0 Hz, 1H), 6.66 – 6.63 (m, 2H), 6.51 (d, *J* = 2.4 Hz, 1H), 2.37 (s, 3H), 2.32 (s, 3H). **^{13}C NMR** (126 MHz, CD_2Cl_2): δ 145.26, 140.33, 139.25, 137.53, 137.49, 136.53, 136.47, 132.92, 132.83, 132.53, 132.49, 131.95, 131.14, 131.06, 130.74, 130.72, 130.23, 130.14, 129.98, 129.21, 129.09 (2 C), 128.54, 128.43, 128.26, 128.16, 127.98, 127.28, 126.64, 126.57, 126.34, 126.09, 125.70, 124.69, 124.18, 123.50, 122.81, 121.93, 115.91, 112.49, 21.53, 21.51. IR ($CHCl_3$): 3530 vw, 3484 vw, 3442 vw, 3397 w, 3053 m, 1620 vs, 1581 w, 1516 vs, 1404 vw, 1388 m, 1381 m, 1183 m, 1112 m, 1022 m, 827 m, 541 m cm^{-1}. **MALDI MS**: 573 ($[M]^+$). **HR MALDI MS**: calcd for $C_{44}H_{32}N$ 574.2529, found 574.2528. **UV/Vis** (tetrahydrofuran): λ_{max} (log ε) = 211 (4.62), 295 nm (4.46). **Fluorescence** (tetrahydrofuran, λ_{exc} = 430 nm): λ_{max} = 496 nm.

2-Bromo-1-ethynylnaphthalene 128

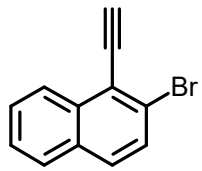

A Schlenk flask was charged with iodonaphthalene **124** (2.997 g, 9.00 mmol), $Pd(PPh_3)_2Cl_2$ (300 mg, 0.450 mmol, 5 mol%), and CuI (171 mg, 0.90 mmol, 10 mol%), then dissolved in diisopropylamine (14 mL) and degassed by three freeze-pump-thaw cycles. (Triisopropylsilyl)acetylene (2.12 mL, 9.45 mmol, 1.05 equiv.) was added and the resulting mixture was allowed to stir at room temperature for 18 h. Afterward, the mixture was filtered through a small pad of silica gel and eluted with dichloromethane (50 mL). The solvents were removed *in vacuo* and a solution of *n*-tetrabutylammonium fluoride trihydrate (4.706 g, 18.0 mmol, 2.0 equiv.) in tetrahydrofuran (12 mL) and methanol (1.0 mL) was added into the flask. After stirring at room temperature for 4 h, the reaction mixture was filtered through a small pad of silica gel (dichloromethane) and solvents were removed under reduced pressure. The crude product was purified by flash chromatography on silica gel (hexane) to afford bromo alkyne **128** (1.528 g, 74%, after 2 steps) as a brownish solid. **M.p.**: 57 – 59 °C (hexane). **^{1}H NMR** (400 MHz, $CDCl_3$): δ 8.36 (d, *J* = 8.4 Hz, 1H), 7.81 (d, *J* = 7.7 Hz, 1H), 7.69 (d, *J* = 8.8 Hz, 1H), 7.63 (d, *J* = 8.9 Hz, 1H), 7.60 (ddd, *J* = 8.3, 6.9, 1.3 Hz, 1H), 7.54 (ddd, *J* = 8.1, 6.9, 1.3 Hz, 1H), 3.82 (s, 1H). **^{13}C NMR** (101 MHz, $CDCl_3$): δ 134.90, 131.72, 130.08, 129.60, 128.39, 128.05, 126.85, 126.33, 125.27, 121.42, 87.22, 80.43. **IR** ($CHCl_3$): 3304 s, 3061 w, 2106 vw, 1619 w, 1579 m, 1568 w, 1560 w, 1501 m, 1478 vw, 1450 w, 1427 w, 1375 w, 1317 w, 1265 m, 1121 m, 1041 m, 654 vs, 624 m, 616 m, 564 m, 435 w cm^{-1}. **ESI MS**: 230 ($[M]^+$, with ^{79}Br). **HR ESI MS**: calcd for $C_{12}H_7{}^{79}Br$ 229.9731, found 229.9737

rac-1-(4-(Dibenzylamino)-2-iodophenyl)-3-(triisopropylsilyl)prop-2-yn-1-ol 125

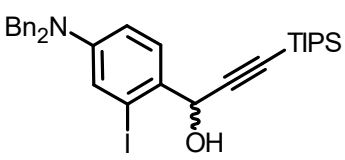

A solution of *n*-butyllithium (2.5 M in hexanes, 2.755 mL, 6.89 mmol, 1.05 equiv.) was added slowly at -78 °C over 2 min to a solution of (triisopropylsilyl)acetylene (1.545 mL, 6.89 mmol, 1.05 equiv.) in tetrahydrofuran (7.870 mL). After stirring at -78 °C for 20 min and at room temperature for 20 min, a solution of benzaldehyde **77** (2.803 mg, 6.56 mmol) in tetrahydrofuran (6.6 mL) was added at -78 °C. The reaction was kept at -78 °C while stirred for 30 min. After completion (checked by TLC), the reaction was quenched

with an HCl solution (1 M, 10 mL). The layers were separated and the aqueous layer extracted with ethyl acetate (3 × 20 mL). The combined organic layers were washed with a saturated $NaHCO_3$ solution (1 × 20 mL), dried over anhydrous $MgSO_4$, and evaporated to dryness. The crude product was purified by column chromatography on silica gel (hexane-methyl *tert*-butyl ether 10:1) to give the secondary alcohol *rac*-**125** (3.810 g, 95%) as a yellow oil. **^{1}H NMR** (300 MHz, $CDCl_3$): δ 7.59 (d, *J* = 8.7 Hz, 1H), 7.39 – 7.27 (m, 6H), 7.25 – 7.19 (m, 5H), 6.74 (dd, *J* = 8.7, 2.7 Hz, 1H), 5.62 (d, *J* = 4.9 Hz, 1H), 4.62 (d, *J* = 2.7 Hz, 4H), 2.23 (d, *J* = 5.4 Hz, 1H), 1.12 – 1.08 (m, 21H). **^{13}C NMR** (75 MHz, $CDCl_3$): δ 150.27, 137.64, 130.59, 129.00, 128.90, 127.30, 126.72, 122.73, 112.50, 106.89, 100.59, 88.15, 68.73, 53.94, 18.77, 11.33. **IR** ($CHCl_3$): 3086 vw, 3062 vw, 3028 w, 2941 m, 2863 m, 1594 s, 1495 s, 1226 m, 1017 s, 729 s, 694 s, 675 s cm^{-1}. **EI MS**: 609 ($M^{+\bullet}$, 11), 566 (2), 217 (2), 91 (100), 65 (7), 43 (7). **HR EI MS**: calcd for $C_{32}H_{40}NISi$ 609.1924, found 609.1945.

rac-*N*,*N*-Dibenzyl-3-iodo-4-(1-(methoxymethoxy)-3-(triisopropylsilyl)prop-2-yn-1-yl)aniline 126

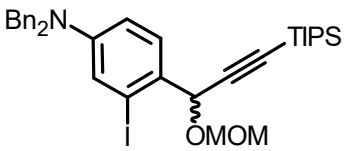

A Schlenk flask was charged with a solution of alkynol *rac*-**125** (610 mg, 1.00 mmol) in dichloromethane (7 mL) and subsequently 4-(dimethylamino)pyridine (12 mg, 0.100 mmol, 10 mol%), *i*-Pr_2NEt (0.244 mL, 1.40 mmol, 1.4 equiv.), and chloromethyl methyl ether (0.114 mL, 1.50 mmol, 1.5 equiv.) were added, the flask was closed with a glass stopper, and the formed solution was stirred at 35 °C for 16 h. Afterward, the reaction was quenched with a saturated $NaHCO_3$ solution (10 mL), the layers were separated, and the aqueous one was extracted with dichloromethane (3 × 15 mL). The combined organic layers were dried over anhydrous $MgSO_4$ and solvent was removed *in vacuo*. The crude product was purified by column chromatography on silica gel (hexane-ethyl acetate 10:1) to give MOM-ether *rac*-**126** (510 mg, 78%) as a colorless oil. **^{1}H NMR** (400 MHz, $CDCl_3$): δ 7.57 (d, *J* = 8.7 Hz, 1H), 7.38 – 7.27 (m, 6H), 7.25–7.18 (m, 5H), 6.76 (dd, *J* = 8.8, 2.7 Hz, 1H), 5.59 (s, 1H), 5.12 (d, *J* = 6.8 Hz, 1H), 4.71 (d, *J* = 6.8 Hz, 1H), 4.62 (d, *J* = 5.7 Hz, 4H), 3.50 (s, 3H), 1.17 – 1.04 (m, 21H). **^{13}C NMR** (101 MHz, $CDCl_3$): δ 150.36, 137.68, 130.10, 128.89, 128.87, 127.28, 126.74, 122.44, 112.70, 104.88, 101.01, 94.41, 89.19, 72.26, 56.81, 53.90, 18.78, 11.34. **IR** ($CHCl_3$): 3088 w, 3065 w, 3032 w, 2958 m, 2945 s, 2866 s, 2826 w, 2170 w, 1597 vs, 1586 m, 1503 s, 1495 s, 1463 m, 1453 m, 1441 w, 1396

m, 1384 w, 1361 m, 1352 m, 1312 vw, 1149 s, 1091 m, 1076 w, 1039 s, 1028 s, 1011 s, 883 m, 810 w, 697 m, 679 m, 659 w, 616 vw cm^{-1}. **ESI MS**: 654 ($[M+H]^+$). **HR ESI MS**: calcd for $C_{34}H_{45}O_2NISi$ 654.2258, found 654.2261.

rac-*N*,*N*-Dibenzyl-3-((2-bromonaphthalen-1-yl)ethynyl)-4-(1-(methoxymethoxy)-3-(triisopro-pylsilyl)prop-2-yn-1-yl)aniline 130

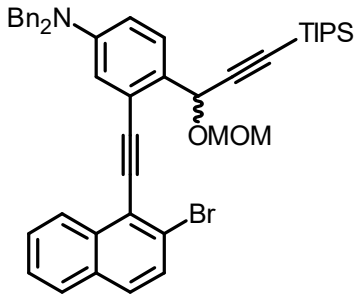

A Schlenk flask was charged with iodide *rac*-**126** (505 mg, 0.772 mmol), $Pd(PPh_3)_2Cl_2$ (11 mg, 0.015 mmol, 2 mol%), CuI (6 mg, 0.031 mmol, 4 mol%), and flushed with argon. Then diisopropylamine (6 mL, prior degassed by three freeze-pump-thaw cycles) was added *via* syringe. Another Schlenk flask was charged with alkyne **128**[27] (214 mg, 0.926 mmol, 1.2 equiv.), flushed with argon, and diisopropylamine (8 mL, prior degassed by three freeze-pump-thaw cycles) was added *via* syringe. Then the alkyne solution was added dropwise *via* syringe to the iodide solution over 3 min and the resulting mixture was stirred at room temperature for 16 h. After completion (checked by TLC), the solvent was removed *in vacuo*, the crude product was purified by flash chromatography on silica gel (hexane-ethyl acetate 10:1) to give diyne *rac*-**130** (468 mg, 80%) as a yellowish oil. **^{1}H NMR** (400 MHz, $CDCl_3$): δ 8.39 – 8.33 (m, 1H), 7.82 – 7.78 (m, 1H), 7.66 – 7.62 (m, 3H), 7.59 – 7.49 (m, 2H), 7.38 – 7.32 (m, 4H), 7.31 – 7.26 (m, 6H), 7.08 (d, *J* = 2.8 Hz, 1H), 6.83 (dd, *J* = 8.8, 2.8 Hz, 1H), 6.10 (s, 1H), 5.12 (d, *J* = 6.7 Hz, 1H), 4.74 (d, *J* = 6.7 Hz, 1H), 4.71 (d, *J* = 6.5 Hz, 4H), 3.31 (s, 3H), 1.07 – 1.05 (m, 21H). **^{13}C NMR** (101 MHz, $CDCl_3$): δ 149.15, 138.16, 134.45, 131.81, 129.72, 129.64, 129.46, 128.89, 128.48, 128.29, 127.81, 127.23, 126.83, 126.75 (2 C), 125.13, 123.19, 122.55, 116.01, 113.92, 105.38, 97.78, 94.37, 89.99, 88.36, 66.26, 56.11, 54.43, 18.78, 11.37. **IR** ($CHCl_3$): 3087 w, 3065 w, 3033 w, 2958 s, 2944 s, 2866 s, 2825 w, 2208 vw, 2170 w, 1601 vs, 1586 m, 1578 m, 1568 m, 1559 m, 1511 s, 1501 s, 1495 s, 1463 m, 1453 s, 1440 m, 1428 w, 1395 m, 1384 m, 1362 m, 1352 m, 1317 m, 1298 m, 1251 m, 1163 m, 1149 s, 1106 m, 1092 m, 1080 m, 1040 s, 1010 vs, 1028 s, 964 s, 921 m, 883 m, 867 vw, 811 s, 697 s, 679 m, 660 m, 651 m, 614 w cm^{-1}. **ESI MS**: 779 ($[M+H+Na]^+$, with ^{79}Br). **HR ESI MS**: calcd for $C_{46}H_{51}O_2N^{79}BrSi$ 756.2867, found 756.2870.

***rac*-*N*,*N*-Dibenzyl-4-(1-(methoxymethoxy)-3-(triisopropylsilyl)prop-2-yn-1-yl)-3-((2-(2-((triiso-propylsilyl)ethynyl)phenyl)naphthalen-1-yl)ethynyl)aniline 131**

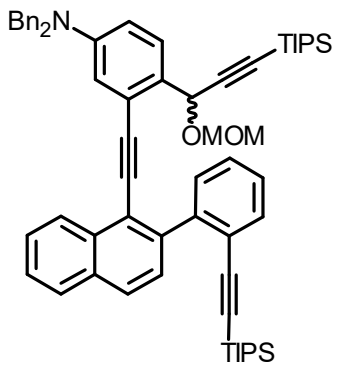

A flask was charged with arene *rac*-**130** (417 mg, 0.551 mmol), $Pd(PPh_3)_2Cl_2$ (39 mg, 0.055 mmol, 10 mol%), K_2CO_3 (80 mg, 0.579 mmol, 1.05 equiv.), boronic acid **10**[17] (216 mg, 0.716 mmol, 1.3 equiv.), and flushed with argon. Then a solvent mixture of toluene (10 mL), *n*-propanol (10 mL), and water (2.5 mL) was added and argon was bubble through the stirred mixture for 10 min. Afterward, the reaction mixture was refluxed for 5 h. The solvents were removed *in vacuo*, the crude was purified by flash chromatography on silica gel (hexane-ethyl acetate 10:1) to give triyne *rac*-**131** (453 mg, 88%) as a yellowish oil. **^{1}H NMR** (400 MHz, $CDCl_3$): δ 8.50 (d, *J* = 8.4 Hz, 1H), 7.85 (d, *J* = 7.9 Hz, 1H), 7.80 (d, *J* = 8.4 Hz, 1H), 7.60 (ddd, *J* = 8.4, 6.9, 1.3 Hz, 1H), 7.58 – 7.54 (m, 2H), 7.54 – 7.48 (m, 2H), 7.40 – 7.34 (m, 5H), 7.33 – 7.28 (m, 2H), 7.26 – 7.22 (m, 4H), 7.11 (td, *J* = 7.6, 1.5 Hz, 1H), 7.03 (td, *J* = 7.6, 1.4 Hz, 1H), 6.71 (dd, *J* = 8.8, 2.8 Hz, 1H), 6.63 (d, *J* = 2.8 Hz, 1H), 5.74 (s, 1H), 5.03 (d, *J* = 6.6 Hz, 1H), 4.63 (d, *J* = 6.7 Hz, 1H), 4.60 (d, *J* = 5.4 Hz, 4H), 3.25 (s, 3H), 1.11 – 1.07 (m, 21H), 0.83 – 0.78 (m, 21H). **^{13}C NMR** (101 MHz, $CDCl_3$): δ 149.33, 144.04, 142.39, 138.16, 133.44, 132.75, 132.62, 130.45, 129.59, 128.87, 128.03, 127.97, 127.94, 127.83, 127.69, 127.41, 127.20, 127.12, 126.92, 126.86, 126.39, 124.04, 123.30, 119.93, 115.29, 113.09, 106.00, 105.57, 96.20, 94.25, 94.20, 90.65, 87.94, 66.12, 56.03, 53.60, 18.81, 18.50, 11.40, 11.23. **IR** ($CHCl_3$): 3087 w, 3063 w, 3033 vw, 2958 vs, 2944 vs, 2866 vs, 2826 w, 2205 vw, 2178 w, 2156 w, 1600 vs, 1585 m, 1562 m, 1511 s, 1495 m, 1469 s, 1463 s, 1453 s, 1443 m, 1397 m, 1383 m, 1361 m, 1354 m, 1175 w, 1149 s, 1091 s, 1076 m, 1046 m, 1028 s, 1010 s, 996 s, 920 m, 883 s, 868 w, 818 s, 700 s, 679 s, 660 m, 613 w, 498 w cm^{-1}. **MALDI MS**: 934 ($[M+H]^+$). **HR MALDI MS**: calcd for $C_{63}H_{76}NO_2Si_2$ 934.5409, found 934.5405.

rac-*N*,*N*-Dibenzyl-3-((2-(2-ethynylphenyl)naphthalen-1-yl)ethynyl)-4-(1-(methoxymethoxy)-prop-2-yn-1-yl)aniline 132

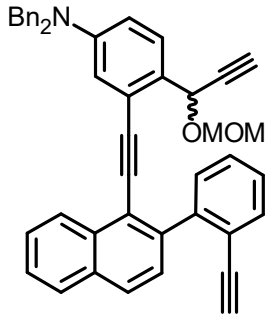

A flask was charged with the silylated compound *rac*-**131** (453 mg, 0.455 mmol) and dissolved in tetrahydrofuran (6.3 mL). Then a solution of tetrabutylammonium fluoride trihydrate (1 M in tetrahydrofuran, 1.5 mL, 1.455 mmol, 3.0 equiv.) was added and the mixture was stirred at room temperature for 2 h. After completion (checked by TLC), the reaction was quenched with methanol (10 mL) and the solvents were removed *in vacuo*. The crude product was purified by flash chromatography on silica gel (hexane-ethyl acetate 5:1) to obtain the deprotected triyne *rac*-**132** (222 mg, 74%) as a yellowish solid. **M.p.**: 59 – 61 °C (hexane-ethyl acetate). **^{1}H NMR** (400 MHz, $CDCl_3$): δ 8.56 (d, *J* = 8.3 Hz, 1H), 7.93 – 7.83 (m, 2H), 7.67 – 7.45 (m, 5H), 7.45 – 7.20 (m, 11H), 7.16 – 7.01 (m, 2H), 6.72 (dd, *J* = 8.5, 2.7 Hz, 1H), 6.61 (d, *J* = 1.9 Hz, 1H), 5.80 (s, 1H), 4.96 (d, *J* = 6.6 Hz, 1H), 4.65 (d, *J* = 6.7 Hz, 1H), 4.61 (s, 4H), 3.31 (s, 3H), 2.86 (s, 1H), 2.57 (d, *J* = 1.8 Hz, 1H). **^{13}C NMR** (101 MHz, $CDCl_3$): δ 149.32, 144.04, 141.98, 138.06, 133.41, 133.10, 132.58, 130.79, 129.09, 128.90, 128.20 (2 C), 127.91, 127.88, 127.54, 127.35, 127.24, 127.16 (2 C), 126.80, 126.64, 123.62, 121.74, 119.85, 115.31, 113.28, 96.03, 94.17, 90.79, 82.85, 82.28, 80.52, 74.71, 65.16, 56.03, 53.75. **IR** ($CHCl_3$): 3307 m, 3087 w, 3064 w, 3032 w, 2955 m, 2826 w, 2205 vw, 2116 w, 2107 w, 1600 vs, 1562 m, 1511 s, 1495 m, 1486 m, 1465 w, 1453 m, 1442 m, 1361 m, 1262 w, 1150 m, 1094 m, 1028 s, 1021 s, 811 w, 697 m, 556 w cm^{-1}. **APCI MS**: 622 ($[M+H]^+$). **HR APCI MS**: calcd for $C_{45}H_{36}O_2N$ 622.2741, found 622.2741.

rac-*N*,*N*-Dibenzyl-4-(1-(methoxymethoxy)-4-(*p*-tolyl)but-2-yn-1-yl)-3-((2-(2-(3-(*p*-tolyl)prop-1-yn-1-yl)phenyl)naphthalen-1-yl)ethynyl)aniline 133

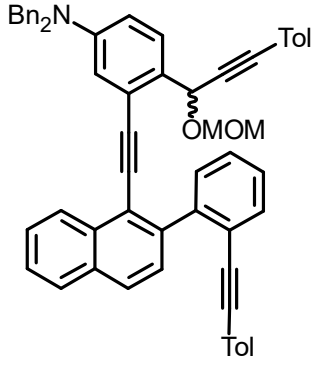

4-Iodotoluene (98 mg, 0.450 mmol, 3.0 equiv.), $Pd(PPh_3)_2Cl_2$ (5 mg, 0.008 mmol, 5 mol%), and CuI (3 mg, 0.015 mmol, 10 mol%) were placed in a Schlenk flask and flushed with argon. Diisopropylamine (1 mL, prior degassed by three freeze-pump-thaw cycles) was added *via* syringe and the mixture was stirred at room temperature for 5 min. Another Schlenk flask was charged with triyne *rac*-**132** (93 mg, 0.150

mmol), flushed with argon, and diisopropylamine (1 mL, prior degassed by three freeze-pump-thaw cycles) was added *via* syringe. Then the triyne solution was added dropwise to the mixture of aryl halide and catalyst *via* syringe over 15 min. The mixture was stirred at room temperature for 16 h. After completion (checked by TLC), the solvent was removed *in vacuo* and the crude product purified by flash chromatography on silica gel (hexane-ethyl acetate 5:1). The desired triyne *rac*-**133** (86 mg, 72%) was obtained as a yellow solid. **M.p.**: 71 – 73 °C (hexane-ethyl acetate). **^{1}H NMR** (400 MHz, $CDCl_3$): δ 8.62 (d, *J* = 8.3 Hz, 1H), 7.90 (d, *J* = 7.7 Hz, 1H), 7.87 (d, *J* = 8.5 Hz, 1H), 7.67 (d, *J* = 8.5 Hz, 1H), 7.63 – 7.52 (m, 4H), 7.45 – 7.41 (m, 1H), 7.39 – 7.29 (m, 8H), 7.25 – 7.21 (m, 4H), 7.10 – 7.04 (m, 4H), 7.02 – 6.93 (m, 4H), 6.71 (dd, *J* = 8.7, 2.8 Hz, 1H), 6.66 (d, *J* = 2.6 Hz, 1H), 6.01 (s, 1H), 5.03 (d, *J* = 6.7 Hz, 1H), 4.66 (d, *J* = 6.7 Hz, 1H), 4.59 (s, 4H), 3.29 (s, 3H), 2.32 (s, 3H), 2.26 (s, 3H). **^{13}C NMR** (101 MHz, $CDCl_3$): δ 149.25, 143.39, 142.34, 138.44, 138.16, 138.14, 133.54, 132.56, 132.10, 131.82, 131.33, 130.89, 129.34, 129.05, 128.98, 128.88, 128.36, 128.13, 128.09, 127.56, 127.54, 127.53, 127.24, 127.21, 127.12, 126.85, 126.53, 123.73, 123.05, 120.43, 119.96, 119.93, 115.35, 113.28, 96.20, 94.17, 92.99, 90.94, 88.61, 87.01, 86.82, 65.97, 56.01, 53.71, 21.60, 21.58. **IR** ($CHCl_3$): 3063 w, 3012 w, 2926 w, 2825 w, 2218 w, 1600 s, 1586 w, 1563 w, 1510 s, 1495 m, 1485 w, 1465 w, 1453 m, 1361 m, 1258 w, 1149 m, 1092 m, 1028 s, 1020 m, 992 w, 819 s, 807 w, 697 m, 556 w cm^{-1}. **APCI MS**: 802 ($[M+H]^+$). **HR APCI MS**: calcd for $C_{59}H_{48}O_2N$ 802.3680, found 802.3682.

N,*N*-Dibenzyl-7-(methoxymethoxy)-5,6-di-*p*-tolyl-7H-fluoreno[4,3-g]chrysen-10-amine 134.

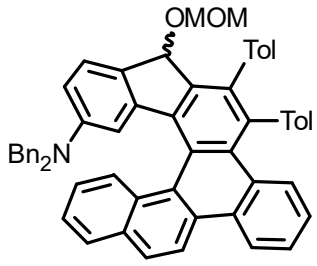

A microwave tube was charged with triyne *rac*-**133** (11 mg, 0.014 mmol) and 1-butyl-2,3-dimethylimidazolium tetrafluoroborate (45 mg), flushed with argon, and dissolved in tetrahydrofuran (4 mL). Then a solution of $CpCo(CO)_2$ (0.5 M in tetrahydrofuran, 28 µL, 0.014 mmol, 1.0 equiv.) was added and the reaction mixture was heated in a microwave reactor at 180 °C for 15 min. The solvent was removed and the residue purified by flash chromatography on silica gel (hexane-ethyl acetate 10:1) to give the crude helical compound **134** (8 mg, 73%) as an off white amorphous solid. As all attempts at separation of diastereoisomers failed, the diastereomeric ratio of 1.7:1.0 was determined by the ^{1}H

NMR analysis (from the comparison of the well resolved signals of the methoxy groups at δ 3.11 and 3.21 ppm). **^{1}H NMR** (400 MHz, $CDCl_3$): The both diastereomers decompose during purification process and all attempts at obtaining clear spectra of the both compounds failed. **ESI MS**: 824 ([M+Na]$^+$). **HR APCI MS**: calcd for $C_{59}H_{48}O_2N$ 802.3680, found 802.3681.

(+)-(*P*,*P*)-1,3-Bis(5,6-di-*p*-tolylhexahelicen-11-yl)-1H-imidazol-3-ium chloride 135

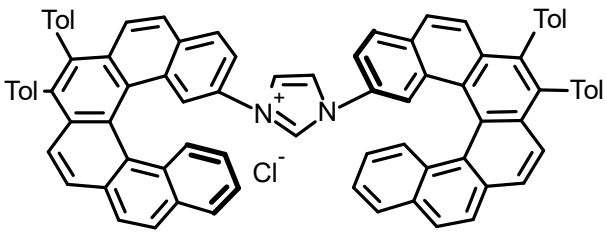

A flask was charged with aminohelicene (+)-(*P*)-**69** (262 mg, 0.5 mmol, 0.5 equiv.) and paraformaldehyde (15 mg, 0.5 mmol, 0.5 equiv.), flushed with argon, toluene (4 mL) was added and the mixture was stirred at room temperature for 1 h. Then another portion of aminohelicene (+)-(*P*)-**69** (262 mg, 0.5 mmol, 0.5 equiv.) as a sol. in toluene (4 mL) was added, the mixture was cooled to 0 °C, aq. sol. of HCl (3.3 N, 0.2 mL, 0.6 mmol, 1.2 equiv.) was added. After allowing the mixture to warm up to room temperature aq. glyoxal sol. (8.8 M, 57 µL, 0.5 mmol) was added, the flask sealed with a glass stopper and stirred at 40 °C for 45 h. The solvent was removed *in vacuo*, the residue dry-loaded on silica gel and purified by column chromatography on silica gel (dichloromethane-methanol 40:1 to 10:1). Imidazolium chloride (+)-(*P*,*P*)-**135** (400 mg, 72%) was obtained as a beige solid. **M.p.**: 297.5 – 303 °C (dichloromethane-methanol). **Optical rotation**: $[\alpha]^{20}_D$ = +1583° (c 0.116 , $CHCl_3$). **^{1}H NMR** (401 MHz, $CDCl_3$) δ 10.15 (s, 1H), 8.22 (dd, *J* = 8.7, 2.3 Hz, 2H), 8.08 (d, *J* = 8.8 Hz, 2H), 7.99 (d, *J* = 8.6 Hz, 2H), 7.94 – 7.74 (m, 12H), 7.71 (d, *J* = 2.2 Hz, 2H), 7.64 (d, *J* = 8.8 Hz, 2H), 7.23 (d, *J* = 7.8 Hz, 2H), 7.20 – 7.08 (m, 16H), 6.77 (ddd, *J* = 8.5, 6.9, 1.4 Hz, 2H), 6.50 (d, *J* = 1.5 Hz, 2H), 2.40 – 2.37 (m, 12H). **^{13}C NMR** (126 MHz, $CDCl_3$) δ 138.90, 138.31, 136.40, 136.37, 135.83, 135.75, 133.77, 133.07, 131.89, 131.78, 131.49, 131.39 (2C), 131.13 (2C), 131.08, 130.77, 130.68, 130.42, 129.57, 129.42, 128.60, 128.47 (2C), 127.95, 127.29 (2C), 127.21 (3C), 127.00, 126.93, 126.79, 126.70, 126.55, 125.61, 123.33, 120.84, 120.68, 119.96, 21.30 (2C). **IR** ($CHCl_3$): 3137 w, 2959 m, 1619 w, 1605 w, 1574 w, 1516 w, 1494 w, 1463w, 1422 m, 1380 w, 1364 w, 1308 w, 1274 w, 1242 w, 1184 w, 1111 w, 1022 w, 815 w cm^{-1}. **HR MALDI MS:** calcd for $C_{83}H_{57}N_2$ 1081.4521, found 1081.4516. **UV/Vis** (tetrahydrofuran): λ_{max}

(log ε) = 270 (5.45), 328 nm (5.22). **Fluorescence** (tetrahydrofuran, λ_{exc} = 380 nm): λ_{max} = 450 nm.

(+)-(*P*,*P*)-1,3-Bis(5,6-di-*p*-tolylbenzo[g]naphtho[2,1-c]chrysen-16-yl)-1H-imidazol-3-ium chloride 136

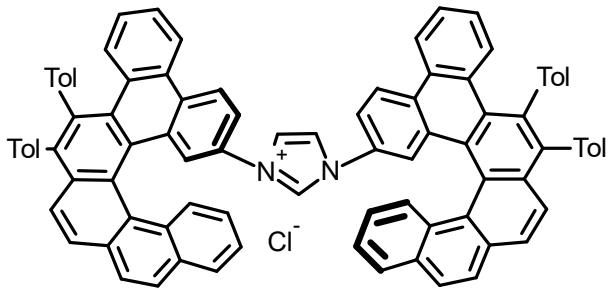

A flask was charged with aminohelicene (-)-(*M*)-**118** (262 mg, 0.5 mmol, 0.5 equiv.) and paraformaldehyde (15 mg, 0.5 mmol), flushed with argon, toluene (4 mL) was added and the mixture was stirred for 1 h at room temperature. Then another portion of aminohelicene (-)-(*M*)-**118** (262 mg, 0.5 mmol, 0.5 equiv.) as a solution in toluene (4 mL) was added, the mixture was cooled to 0 °C, aq. sol. of HCl (3.3 N, 0.2 mL 0.6 mmol, 1.2 equiv.) was added. After allowing the mixture to warm up to room temperature, aq. glyoxal sol. (8.8 M, 57 µL, 0.5 mmol) was added, the flask sealed with a glass stopper and stirred at 40 °C for 17 h. The solvent was removed *in vacuo*, the residue dry-loaded on silica gel and purified by column chromatography on silica gel (dichloromethane-methanol 10:1). Imidazolium chloride (-)-(*M,M*)-**136** (400 mg, 72%) was obtained as a beige solid. **M.p.**: 288 – 291 °C (dichloromethane-methanol). **Optical rotation**: $[\alpha]^{20}_D$ = -860° (c 0.097 , $CHCl_3$). **^{1}H NMR** (600 MHz, $CDCl_3$) δ 10.44 (s, 1H), 8.67 (d, *J* = 8.8 Hz, 2H), 8.56 (d, *J* = 7.5 Hz, 2H), 8.33 (d, *J* = 8.0 Hz, 2H), 7.97 (d, *J* = 8.6 Hz, 2H), 7.91 (d, *J* = 8.4 Hz, 2H), 7.86 (d, *J* = 8.9 Hz, 2H), 7.78 (d, *J* = 8.6 Hz, 2H), 7.76 – 7.73 (m, 4H), 7.67 – 7.61 (m, 4H), 7.58 – 7.54 (m, 2H), 7.52 (dd, *J* = 7.7, 1.9 Hz, 2H), 7.36 (d, *J* = 2.3 Hz, 2H), 7.30 – 7.27 (m, 2H), 7.24 – 7.16 (m, 6H), 7.05 – 7.02 (m, 2H), 6.97 – 6.93 (m, 4H), 6.82 – 6.78 (m, 4H), 6.65 (dd, *J* = 7.7, 1.9 Hz, 2H), 6.34 (s, 2H), 2.39 (s, 6H), 2.32 (s, 6H). **^{13}C NMR** (151 MHz, $CDCl_3$) δ 140.30, 138.93, 137.49, 136.31, 136.15, 136.12, 133.80, 132.54, 132.05, 131.95, 131.52, 131.41, 131.39, 131.25, 131.19, 131.00, 130.46, 130.29, 130.24, 130.09, 129.86, 129.61, 129.01, 128.88, 128.82, 128.56, 128.27, 127.94, 127.44, 127.17, 127.13, 127.04, 126.98, 126.85, 126.74, 126.66, 126.35, 126.18, 126.06, 123.63, 122.73, 120.37, 120.10, 120.00, 21.32, 21.31. **IR** ($CHCl_3$): 3138 w, 3050 w,1605 m, 1571 w, 1546 s, 1515 s, 1405 m, 1296 w, 1274 w, 1184 m, 1142 m, 1111 w, 1022 m, 964 vw, 825 m, 715 w, 583 cm^{-1}. **HR ESI MS:** calcd for $C_{91}H_{61}N_2$ 1181.4829, found 1182.4861. **UV/Vis** (tetrahydrofuran): λ_{max} (log

ε) = 303 (5.29), 258 nm (5.27). **Fluorescence** (tetrahydrofuran, λ_{exc} = 380 nm): λ_{max} = 453 nm.

(-)-(*M*)-3-(5,6-Di-*p*-tolylhexahelicen-11-yl)-1-mesityl-1*H*-imidazol-3-ium perchlorate 140

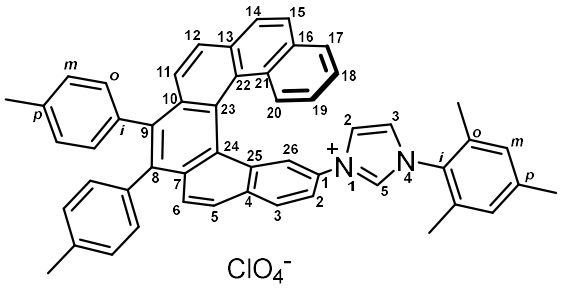

Formamide **137**[73] (349 mg, 1.70 mmol, 1.7 equiv.) was dissolved in acetic anhydride (2.25 mL, 23.80 mmol, 23.8 equiv.) under argon atmosphere. Separately, $HClO_4$ (70 wt-% aq. solution, 0.17 mL, 1.96 mmol, 1.96 equiv.) was mixed with acetic anhydride (1.0 mL) under cooling with an ice bath. This solution was added dropwise to the solution of formamide **137** resulting a brown mixture which was stirred at ambient temperature for 8 h. Ether (8 mL) was then added, resulting in the formation of a brownish precipitate or occasionally in a two phase system. The supernatant liquid was removed by syringe and the residue triturated with ether (3 × 8 mL). The remaining volatiles were removed with a flow of argon to furnish the oxazolium salt **138** as an off-white solid. It was immediately reacted in the next step by suspending crude **138** in toluene (2.0 mL) and adding a solution of (-)-(*M*)-**69** (524 mg, 1.00 mmol) in toluene (7.0 mL). The reaction mixture was stirred at ambient temperature for 21 h, followed by an addition of $HClO_4$ (70 wt-% aq. solution, 150 μL, 1.70 mmol, 1.7 equiv.). The mixture was then stirred at 80 °C for 18 h. After cooling to ambient temperature, all volatiles were removed *in vacuo*, the crude residue was dry-loaded on silica gel and purified by column chromatography on silica gel (dichloromethane-methanol 160 : 1 to 10 : 1) to furnish the imidazolium salt (-)-(*M*)-**140** (409 mg, 52%) as an off-white solid. **M.p.**: 218 – 220 °C (dichloromethane-methanol). **Optical rotation**: $[\alpha]^{20}_D$ = -1171 (c 0.100, $CHCl_3$). **^{1}H NMR** (600 MHz, $CDCl_3$) δ 1.99, 2.04 (2 × s, 2 × 3H, *o*-CH_3, Mes), 2.37, 2.38 (2 × s, 2 × 3H, CH_3, Tol), 2.39 (s, 3H, *p*-CH_3, Mes), 6.84 (ddd, 1H, $J_{19,20}$ = 8.4, $J_{19,18}$ = 6.9, $J_{19,17}$ = 1.3, H-19), 7.04, 7.07 (2 × bs, 2 × 1H, *m*-H, Mes), 7.08 – 7.18 (m, 9H, H-2(Im), *o*- + *m*-H, Tol), 7.32 (ddd, 1H, $J_{18,17}$ = 7.9, $J_{18,19}$ = 6.9, $J_{18,20}$ = 1.0, H-18), 7.35 (t, 1H, $J_{3,2}$ = $J_{3,5}$ = 1.7, H-3(Im)), 7.68 – 7.72 (m, 2H, H-17,20), 7.77 (dd, 1H, $J_{2,3}$ = 8.5, $J_{2,26}$ = 2.3, H-2), 7.77 (d, 1H, $J_{11,12}$ = 8.5, H-11), 7.80 – 7.82 (m, 2H, H-15,26), 7.85 (d, 1H, $J_{6,5}$ = 8.9, H-6), 7.86 – 7.89 (m, 2H, H-5,12), 7.96 (d, 1H, $J_{14,15}$ = 8.6, H-14), 8.10 (d, 1H, $J_{3,2}$ = 8.5, H-3), 8.12 (t, 1H, $J_{5,2}$ =

$J_{5,3}$ = 1.7, H-5(Im)). **^{13}C NMR** (151 MHz, $CDCl_3$) δ 17.42, 17.49 (*o*-CH_3, Mes), 21.20, 21.29, 21.30 (CH_3, Tol and *p*-CH_3, Mes), 119.78 (CH-2), 122.00 (CH-26), 122.63 (CH-2(Im)), 123.29 (C-23), 124.83 (CH-3(Im)), 125.78 (CH-19), 126.67 (CH-11), 126.70 (C-22), 126.74 (CH-18), 126.84 (C-24), 126.95 (CH-12), 127.28 (CH-17), 127.35 (CH-15), 127.37 (CH-14), 127.44 (CH-5), 127.67 (CH-6), 128.15 (CH-20), 128.47, 128.49 (2C), 128.62 (*m*-CH, Tol), 129.53 (C-25), 129.71 (C-21), 129.90, 129.93 (*m*-CH, Mes), 130.22 (*ipso*-C, Mes), 130.39, 130.63 (*o*-CH, Tol), 130.82 (C-1), 130.97 (CH-3), 131.27, 131.31 (C-10,13), 131.33, 131.48 (*o*-CH, Tol), 131.75 (C-16), 132.11 (C-4), 133.18 (C-7), 134.06, 134.09 (*o*-C, Mes), 134.57 (CH-5(Im)), 135.68, 135.76 (*ipso*-C, Tol), 136.41, 136.44 (*p*-C, Tol), 138.35 (C-8), 139.11 (C-9), 141.70 (*p*-C, Mes). **IR** ($CHCl_3$): 3134 w, 3021 w, 2921 w, 1605 w, 1575 w, 1543 m, 1516 m, 1494 w, 1485 w, 1461 w, 1422 w, 1402 w, 1380 w, 1295 w, 1250 w, 1216 m, 1183 w, 1147 w, 1093 s, 1009 w, 930 w, 853 m, 837 m, 819 m, 735 m, 639 w, 632 w cm^{-1}. **HR MALDI MS**: calcd for $C_{52}H_{41}N_2$ 693.3264, found 693.3237. **UV/Vis** (tetrahydrofuran): λ_{max} (log ε) = 327 (4.49), 272 (4.38). **Fluorescence** (tetrahydrofuran, λ_{exc} = 360 nm): λ_{max} = 445 nm.

(-)-(*M*)-3-(5,6-Di-*p*-tolylhexahelicen-11-yl)-1-mesityl-1H-imidazol-3-ium chloride 142

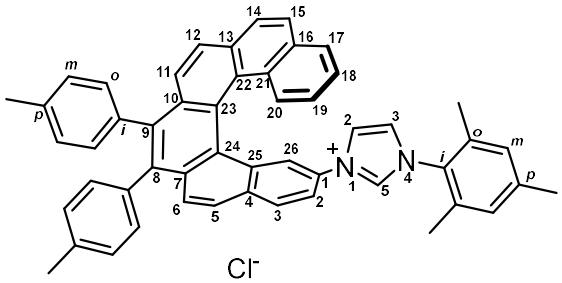

A Pasteur pipette was used as a column and filled with Amberlite IRA-400 (650 mg) and successively flushed with H_2O (10 mL), sat. NaCl sol. (10 mL), H_2O (10 mL), H_2O-methanol (1:1, 10 mL) and methanol (10 mL). Then a solution of Imidazolium perchlorate (-)-(*M*)-**140** (185 mg, 0.254 mmol) in methanol (20 mL) was run through the column using gravity force. The solvent was evaporated *in vacuo* to furnish imidazolium chloride (-)-(*M*)-**142** (165 mg, 97%) as a brownish solid. **M.p.**: 261 – 263 °C (methanol). **Optical rotation**: $[\alpha]^{20}_D$ = -1360 (c 0.132, $CHCl_3$). **^{1}H NMR** (500 MHz, CD_3Cl): 10.27 (bs, 1H, H-5-imid), 8.47 (dd, 1H, $J_{2,3}$ = 8.7, $J_{2,26}$ = 2.4, H-2), 8.10 (d, 1H, $J_{3,2}$ = 8.7, H-3), 7.98 (d, 1H, $J_{14,15}$ = 8.6, H-14), 7.88 (d, 1H, $J_{12,11}$ = 8.5, H-12), 7.85 – 7.87 (m, 2H, H-5,15), 7.83 (bd, 1H, $J_{26,2}$ = 2.4, H-26), 7.81 (d, 1H, $J_{6,5}$ = 8.9, H-6), 7.77 (d, 1H, $J_{11,12}$ = 8.5, H-11), 7.75 (dd, 1H, $J_{17,18}$ = 8.0, $J_{17,19}$ = 1.4, H-17), 7.72 (dd, 1H, $J_{20,19}$ = 8.4, $J_{20,18}$ = 1.2, H-20), 7.32 (ddd, 1H, $J_{18,17}$ = 8.0, $J_{18,19}$ = 6.9,

$J_{18,20}$ = 1.2, H-18), 7.23 (t, 1H, $J_{3,2}$ = $J_{3,5}$ = 1.7, H-3-imid), 7.09 – 7.10, 7.12 – 7.18 (2 × m, 8H, H-*o,m*-Tol), 7.05 (bs, 1H, H-*m*-Mes), 7.02 (t, 1H, $J_{2,3}$ = $J_{2,5}$ = 1.7, H-2-imid), 6.99 (bs, 1H, H-*m*-Mes), 6.85 (ddd, 1H, $J_{19,20}$ = 8.4, $J_{19,18}$ = 6.9, $J_{19,17}$ = 1.4, H-19), 2.37, 2.38 (2 × s, 2 × 3H, CH_3-Tol), 2.35 (s, 3H, CH_3-*p*-Mes), 1.98, 2.17 (2 × s, 2 × 3H, CH_3-*o*-Mes). **^{13}C NMR** (126 MHz, $CDCl_3$): 141.38 (C-*p*-Mes), 138.86 (C-9), 138.39 (C-8), 136.98 (CH-5-imid), 136.40, 136.36 (C-*p*-Tol), 135.83, 135.73 (C-*i*-Tol), 134.31, 133.92 (C-*o*-Mes), 133.12 (C-7), 131.93 (C-4), 131.75 (C-16), 131.50, 131.37 (CH-*o*-Tol), 131.27 (C-1), 131.17 (C-10,13), 130.98 (CH-3), 130.67 (CH-*o*-Tol), 130.48 (C-i-Mes), 130.39 (CH-*o*-Tol), 129.99, 129.76 (CH-*m*-Mes), 129.71 (C-21), 129.41 (C-25), 128.60, 128.46 (CH-*m*-Tol), 128.13 (CH-20), 127.33 (CH-14), 127.26, 127.19, 127.16 (CH-5,6,12,15), 127.10 (CH-17), 126.99 (C-24), 126.81 (C-22), 126.72 (CH-18), 126.65 (CH-11), 125.81 (CH-19), 123.86 (CH-3-imid), 123.32 (C-23), 121.07 (CH-2-imid), 120.63 (CH-26), 120.38 (CH-2), 21.30, 21.29 (CH_3-Tol), 21.15 (CH_3-*p*-Mes), 17.94, 17.63, (CH_3-*o*-Mes). **IR** ($CHCl_3$): 3131 w, 3020 m, 2919 m, 1605 w, 1574 w, 1540 m, 1516 m, 1484, 1461 m, 1401 w, 1380 m, 1309 w, 1296 w, 1216 m, 1183 w, 969 w, 894 w, 852 m, 824 m, 816 m, 670 m, 656 m, 579 w, 534 w cm^{-1}. **HR MALDI MS**: calcd for $C_{52}H_{41}{}^{35}ClN_2$ 728.2953, found 728.2952. **UV/Vis** (tetrahydrofuran): λ_{max} (log ε) = 327 (4.52), 272 (4.83). **Fluorescence** (tetrahydrofuran, λ_{exc} = 360 nm): λ_{max} = 465 nm.

Synthesis of silver-salts

General procedure

Imidazolium salt (+)-(*P*,*P*)-**135** or (-)-(*M*)-**140** (1.0 equiv.) was placed in an oven-dried Schlenk flask, dried under vacuum at 80 °C for 1 h and flushed with argon. Ag_2O (0.8 equiv.) and dichloromethane (20 mL per 1 mmol of imidazolium salt) were added, the flask sealed with a stopcock and the suspension stirred at ambient temperature for 24 h under the exclusion of light. The resulting fine suspension was filtered through a pad of celite and the solvent was removed *in vacuo* to furnish crude silver salt (*P*,*P*,*P*,*P*)-**141** or (*M*,*M*)-**143**.

(*P*,*P*,*P*,*P*)-Bis(1,3-bis(5,6-di-*p*-tolylhexahelicen-11-yl)-1,3-dihydro-2H-imidazol-2-ylidene)silver, chloride **141**

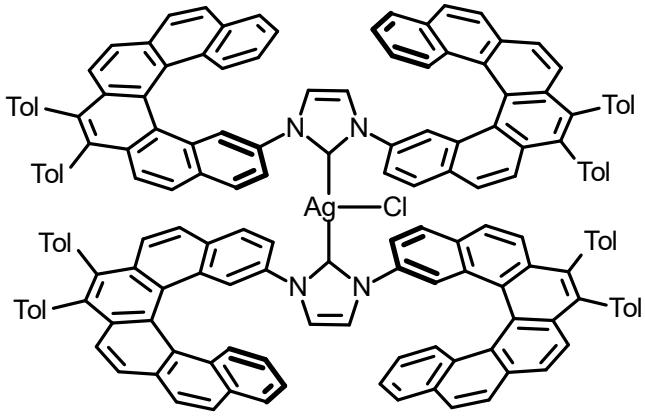

Fine beige solid (128 mg). **ESI MS**: 2268 ($[M\text{-}Cl]^+$).
Prepared according to the general procedure.

(*M*,*M*)-Bis(1-(5,6-di-*p*-tolylhexahelicen-11-yl)-3-mesityl-1,3-dihydro-2H-imidazol-2-ylidene)silver, chloride **143**

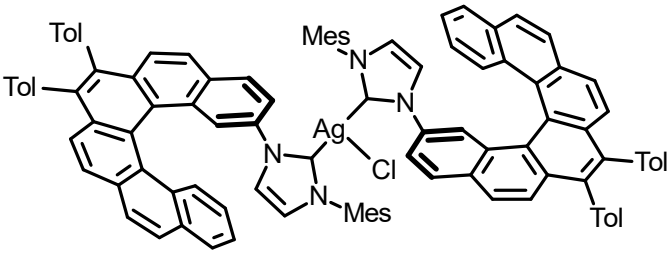

Fine beige solid (180 mg). **ESI MS**: 1492 ($[M\text{-}Cl]^+$).
Prepared according to the general procedure.

(-)-(*M*)-1-(5,6-Di-*p*-tolylhexahelicen-11-yl)-3-mesityl-2,3-dihydro-1*H*-imidazol-2-yl)(2-isopropoxybenz-ylidene)-ruthenium (II) dichloride 147

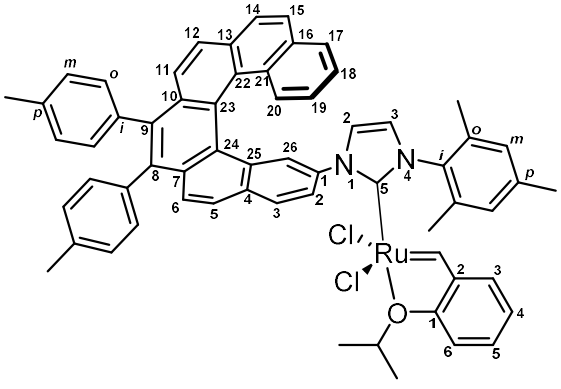

The imidazolium perchlorate (-)-(*M*)-**140** (100 mg, 0.130 mmol) was placed in an oven-dried Schlenk flask and heated at 80 °C under vacuum for 1 h. The flask was then flushed with argon and toluene (0.5 mL) was added. K-amylate (1.5 M solution in toluene, 70 µL, 0.120 mmol, 0.92 equiv.)

was added dropwise to the suspension and the mixture was stirred at ambient temperature for 10 min. The suspension became clear and darkened in color. Ru-complex **144** (69 mg, 0.115 mmol, 0.88 equiv.) was added in one portion and the reaction mixture was stirred at 80 °C for 25 min. It was then cooled to ambient temperature, CuCl (23 mg, 0.230 mmol, 1.77 equiv.) was added, and the mixture was stirred for 15 min. The solvent was removed *in vacuo* and the crude product purified by flash chromatography on silica gel (hexane-ethyl acetate 10 : 1 to 5 : 1) to furnish (-)-(*M*)-**147** (42 mg, 36%) as a dark green solid. **M.p.**: 215 °C (benzene-pentane) (dec.). **Optical rotation**: $[\alpha]^{20}_{D}$ = -1489 (c 0.0293, $CHCl_3$). **^{1}H NMR** (600 MHz, CD_2Cl_2) δ 16.64 (d, 1H, ^{4}J = 0.8, *H*C=Ru), 9.08 (dd, 1H, $J_{2,3}$ = 8.3, $J_{2,26}$ = 2.3, H-2), 8.19 (d, 1H, $J_{3,2}$ = 8.3, H-3), 7.99 (s, 2H, H-14,15), 7.95 – 7.98 (m, 2H, H-5,17), 7.91 (d, 1H, $J_{26,2}$ = 2.3, H-26), 7.91 (d, 1H, $J_{12,11}$ = 8.5, H-12), 7.77 (dd, 1H, $J_{20,19}$ = 8.7, $J_{20,18}$ = 1.2, H-20), 7.73 (d, 1H, $J_{6,5}$ = 8.9, H-6), 7.67 (d, 1H, $J_{11,12}$ = 8.5, H-11), 7.51 (ddd, 1H, $J_{5,6}$ = 8.6, $J_{5,4}$ = 6.8, $J_{5,3}$ = 2.1, H-5(benzylidene)), 7.39 (ddd, 1H, $J_{18,17}$ = 8.0, $J_{18,19}$ = 6.8, $J_{18,20}$ = 1.2, H-18), 7.10 – 7.29 (m, 8H, *o*- + *m*-H, Tol), 7.07, 7.09 (2 × dq, 2H, ^4J = 2.0, 0.7, *m*-H, Mes), 6.85 – 6.94 (m, 3H, H-19, H-3,4(benzylidene)), 6.85 (d, 1H, $J_{6,5}$ = 8.6, H-6(benzylidene)), 6.80 (d, 1H, $J_{3,2}$ = 2.1, H-3(Im)), 6.21 (d, 1H, $J_{2,3}$ = 2.1, H-2(Im)), 4.90 (hept., 1H, J_{vic} = 6.2, C*H*(CH_3)$_2$), 2.46 (s, 3H, *p*-CH_3, Mes), 2.37, 2.40 (2 × s, 2 × 3H, CH_3, Tol), 1.81, 2.10 (2 × s, 2 × 3H, *o*-CH_3, Mes), 1.22, 1.47 (2 × d, 2 × 3H, J_{vic} = 6.2, CH(C*H*$_3$)$_2$). **^{13}C NMR** (151 MHz, CD_2Cl_2) δ 294.86 (CH=Ru), 152.74 (C-1(benzylidene)), 174.53 (C-5(Im)), 145.06 (C-2(benzylidene)), 140.35 (*p*-C, Mes), 139.33 (C-1), 139.04 (C-9), 138.40 (C-8), 138.09 (*o*-C, Mes), 137.70 (*ipso*-C, Mes), 137.45 (*o*-C, Mes), 136.98, 137.03 (*ipso*-C, Tol), 136.89, 136.90 (*p*-C, Tol), 133.48 (C-10), 132.88 (C-16), 132.23 (*o*-CH, Tol), 132.05 (C-13), 131.98 (*o*-CH, Tol), 131.60 (C-7), 131.37 (*o*-CH, Tol), 131.33 (C-4), 131.26 (C-25), 131.10 (*o*-CH, Tol), 131.01 (CH-3), 130.32 (C-21), 129.95 (*m*-CH, Mes), 129.81 (CH-5(benzylidene)), 129.32 (*m*-CH, Mes), 128.86, 128.91, 128.93, 129.01 (*m*-CH, Tol), 128.53 (CH-20), 128.20 (CH-15), 128.17 (CH-17), 127.95 (CH-12), 127.91 (C-24), 127.74 (C-22), 127.69 (CH-14), 127.48 (CH-5), 126.77 (CH-18), 126.46 (CH-11), 126.41 (CH-6), 125.68 (CH-19), 125.20 (CH-3(Im)), 125.20 (CH-26), 124.28 (CH-2(Im)), 124.26 (C-23), 123.08 (CH-4(benzylidene)), 122.79 (CH-2), 122.20 (CH-3(benzylidene)), 113.55 (CH-6(benzylidene)), 75.20 (*C*H(CH_3)$_2$), 22.01, 22.44 (CH(*C*H_3)$_2$), 21.51, 21.55, 21.57 (CH_3, Tol and *p*-CH_3, Mes), 18.13, 18.47 (*o*-CH_3, Mes). **IR** ($CHCl_3$): 3167 w, 3072 w, 3043 w, 3021 m, 2978 m, 2863 w, 1602 w, 1576 w, 1558 w, 1516 m, 1490

w, 1486 m, 1401 m, 1385 m, 1374 m, 1311 m, 1296 m, 1265 m, 1183 w, 1157 w, 1141 w, 1109 m, 936 m, 853 m, 835 m, 751 s, 745 s, 694 m, 587 w, 508 w, 410 w cm^{-1}. **HR MALDI MS**: calcd for $C_{62}H_{52}{}^{35}ClN_2ORu$ 977.2812, found 977.2829. **UV/Vis** (tetrahydrofuran): λ_{max} (log ε) = 325 (4.71), 269 (5.02). **Fluorescence** (tetrahydrofuran, λ_{exc} = 360 nm): λ_{max} = 455 nm.

(+)-(*P*,*P*)-(3-Chloropyridyl)(1,3-bis(5,6-di-*p*-tolylhexahelicen-11-yl)-2,3-dihydro-1H-imidazol-2-yl)palladium(II) chloride 148

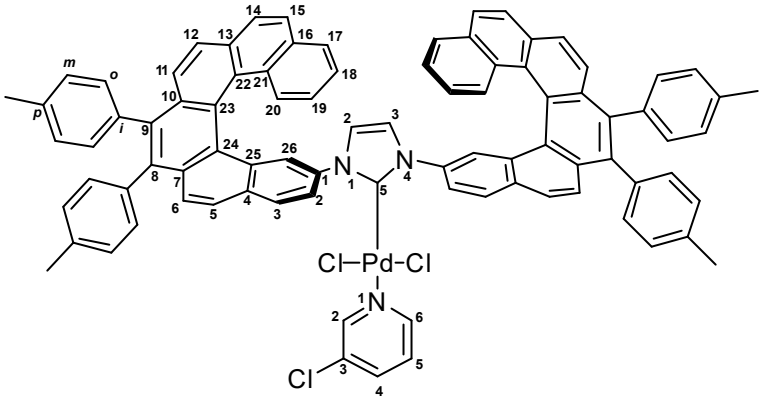

An oven-dried Schlenk flask was charged with crude (*P*,*P*,*P*,*P*)-**141** (60 mg, 0.026 mmol, 0.52 equiv.) and $PdCl_2(MeCN)_2$ (13 mg, 0.05 mmol), flushed with argon and suspended in dichloromethane (0.5 mL). The reaction mixture was stirred for 48 h at ambient temperature under the exclusion of light. Afterward, it was filtered through celite (dichloromethane) and the solvent removed *in vacuo*. The resulting brown solid was placed in an oven-dried Schlenk flask, flushed with argon and dissolved in dichloromethane (0.5 mL). 3-Chloropyridine (14 µL, 0.15 mmol, 3.0 equiv.) was added and the resulting solution stirred for 5 h at ambient temperature. Then, heptane (2 mL) was added, stirred for 5 min, Et_2O (10 mL) was added and the resulting off-white suspension stirred for 16 h at ambient temperature. It was filtered over celite, washed with Et_2O, the residue dissolved with dichloromethane and the solvents removed *in vacuo*. The crude product was recrystallized from methanol/dichloromethane by slow evaporation of the dichloromethane to afford (+)-(*P*,*P*)-**148** (46 mg, 67%) as a beige solid. **M.p.**: 363 °C (dichloromethane-methanol) (dec.). **Optical rotation**: $[\alpha]^{20}_D$ = +1567° (c 0.149, $CHCl_3$). **^{1}H NMR** (600 MHz, $CDCl_3$) δ 8.54 (dd, 2H, $J_{2,3}$ = 8.6, $J_{2,26}$ = 2.2, H-2), 8.45 (dd, 1H, $J_{2,4}$ = 2.4, $J_{2,5}$ = 0.7, H-2-py), 8.36 (dd, 1H, $J_{6,5}$ = 5.6, $J_{6,4}$ = 1.3, H-6-py), 8.11 (d, 2H, $J_{15,14}$ = 8.6, H-15), 8.07 (d, 2H, $J_{14,15}$ = 8.6, H-14), 8.06 (dd, 2H, $J_{17,18}$ = 8.1, $J_{17,19}$ = 1.4, H-17), 7.95 (d, 2H, $J_{3,2}$ = 8.6, H-3), 7.88 (d, 2H, $J_{12,11}$ = 8.8, H-12), 7.83 (d, 2H, $J_{5,6}$ = 8.6, H-5), 7.77 (ddt, 2H, $J_{20,19}$ = 8.7, $J_{20,18}$ = 1.2, $J_{20,15}$ = $J_{20,17}$ = 0.7, H-20), 7.74 (d, 2H, $J_{6,5}$ = 8.6, H-6), 7.73 (d, 2H, $J_{11,12}$ = 8.8, H-11), 7.69 (d, 2H, $J_{26,2}$ =

2.2, H-26), 7.55 (ddd, 1H, $J_{4,5}$ = 8.2, $J_{4,2}$ = 2.4, $J_{4,6}$ = 1.3, H-4-py), 7.42 (ddd, 2H, $J_{18,17}$ = 8.1, $J_{18,19}$ = 6.9, $J_{18,20}$ = 1.2, H-18), 7.08 – 7.21 (m, 16H, H-o,m-Tol), 7.02 (ddd, 1H, $J_{5,4}$ = 8.2, $J_{5,6}$ = 5.6, $J_{5,2}$ = 0.7, H-5-py), 6.83 (ddd, 2H, $J_{19,20}$ = 8.5, $J_{19,18}$ = 6.9, $J_{19,17}$ = 1.4, H-19), 5.64 (s, 2H, H-2,3-imid), 2.37, 2.38 (2 × s, 2 × 6H, CH3-Tol). **^{13}C NMR** (151 MHz, $CDCl_3$): δ 149.94 (CH-2-py), 148.91 (CH-6-py), 146.86 (C-5-imid), 138.35 (C-8), 138.03 (C-9), 137.66 (CH-4-py), 136.34 (C-1), 136.21, 136.27 (C-*i*-Tol), 136.09, 136.10 (C-*p*-Tol), 132.97 (C-10), 132.27 (C-3-py, C-16), 131.40, 131.60 (CH-*o*-Tol), 131.24 (C-13), 130.99 (C-4), 130.91 (C-7), 130.45, 130.85 (CH-*o*-Tol), 130.08 (C-25), 129.90 (C-21), 128.31, 128.38, 128.39, 128.40, 128.43, 128.44 (CH-3,20, CH-*m*-Tol), 127.56 (CH-14), 127.45 (C-24), 127.28 (C-22), 127.23 (CH-15), 127.18 (CH-12), 127.13 (CH-17), 127.00 (CH-5), 126.47 (CH-18), 126.31 (CH-6), 126.17 (CH-11), 125.24 (CH-19), 124.50 (CH-5-py), 123.92 (CH-26), 123.65 (C-23), 123.61 (CH-2,3-imid), 123.42 (CH-2), 21.31 (CH_3-Tol). **IR** ($CHCl_3$): 3181 w, 3066 w, 3048 w, 2920 w, 1602 w, 1572 w, 1557 w, 1516 s, 1486 w, 1444 m, 1405 m, 1285 m, 1265 w, 1146 w, 1118 m, 1108 w, 1058 w, 1022 m, 822 m, 417 w cm^{-1}. **HR ESI MS**: calcd for $C_{83}H_{56}N_2{}^{35}ClPd$ 1221.31614, found 1221.31804. **UV/Vis** (tetrahydrofuran): λ_{max} (log ε) = 326 (4.91), 271 (5.19). **Fluorescence** (tetrahydrofuran, λ_{exc} = 360 nm): λ_{max} = 455 nm.

(-)-(*M*)-(3-Chloropyridyl)(1-(5,6-di-*p*-tolylhexahelicen-11-yl)-3-mesityl-1,3-dihydro-2H-imidazol-2-ylidene)palladium(II) chloride 149

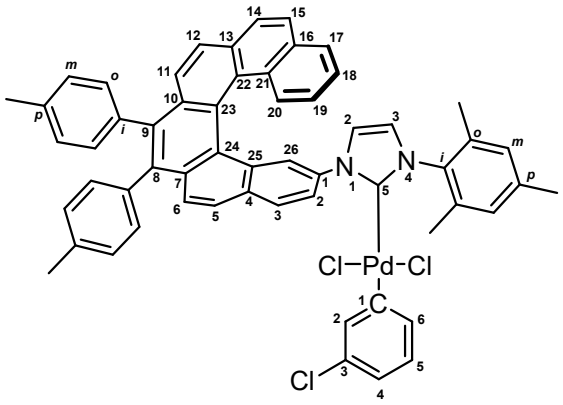

An oven-dried Schlenk flask was charged with crude (*M*,*M*)-**143** (84 mg, 0.055 mmol, 0.55 equiv.) and $PdCl_2(MeCN)_2$ (26 mg, 0.1 mmol), flushed with argon and suspended in dichloromethane (3 mL). The reaction mixture was stirred for 48 h at ambient temperature under the exclusion of light. Afterward, it was filtered through celite (dichloromethane) and the solvent removed *in vacuo*. The resulting brown solid was placed in an oven-dried Schlenk flask, flushed with argon and dissolved in dichloromethane (3 mL). 3-Chloropyridine (19 µL, 0.2 mmol, 2.0 equiv.) was added and the resulting solution stirred for 4 h at ambient temperature. The mixture was filtered through celite (dichloromethane) to remove eventually formed precipitate and

the solvent removed in vacuo. The crude product was recrystallized from methanol/dichloromethane by slow evaporation of the dichloromethane to afford (*M*)-(-)-(*M*)-**149** (78 mg, 80%) as a yellow solid **M.p.**: 360 °C (dichloromethane-methanol) (dec.). **Optical rotation**: $[\alpha]^{20}_D$ = -1401° (c 0.104, $CHCl_3$). **^{1}H NMR** (600 MHz, CD_2Cl_2) δ); 8.84 (dd, 1H, $J_{2,3}$ = 8.5, $J_{2,26}$ = 2.3, H-2), 8.50 (ddd, 1H, $J_{2,4}$ = 2.4, H-2-py, 8.41 (ddd, 1H, $J_{6,5}$ = 5.6, $J_{6,4}$ = 1.5, H-6-py), 8.07 (d, 1H, $J_{3,2}$ = 8.5, H-3), 7.98 (d, 1H, $J_{14,15}$ = 8.7, H-14), 7.94 (d, 1H, $J_{15,14}$ = 8.7, H-15), 7.92 (dd, 1H, $J_{17,18}$ = 8.0, $J_{17,19}$ = 1.4, H-17), 7.89 (d, 1H, $J_{12,11}$ = 8.5, H-12), 7.88 (d, 1H, $J_{5,6}$ = 8.9, H-5), 7.81 (d, 1H, $J_{26,2}$ = 2.3, H-26), 7.78 (dd, 1H, $J_{20,19}$ = 8.4, $J_{20,18}$ = 1.2, H-20), 7.75 (d, 1H, $J_{6,5}$ = 8.9, H-6), 7.72 (d, 1H, $J_{11,12}$ = 8.5, H-11), 7.54 (ddd, 1H, $J_{4,5}$ = 8.2, $J_{4,2}$ = 2.4, $J_{4,6}$ = 1.5, H-4-py), 7.35 (ddd, 1H, $J_{18,17}$ = 8.0, $J_{18,19}$ = 6.8, $J_{18,20}$ = 1.2, H-18), 7.07 – 7.21 (m, 8H, H-*o,m*-Tol), 7.03 (ddd, 1H, $J_{5,4}$ = 8.2, $J_{5,6}$ = 5.6, $J_{5,2}$ = 0.6, H-5-py), 6.97, 7.00 (2 × m, 2 × 1H, H-*m*-Mes), 6.85 (ddd, 1H, $J_{19,20}$ = 8.4, $J_{19,18}$ = 6.8, $J_{19,17}$ = 1.4, H-19), 6.76 (d, 1H, $J_{3,2}$ = 2.0, H-3-imid), 6.01 (d, 1H, $J_{2,3}$ = 2.0, H-2-imid), 2.36, 2.38 (2 × s, 2 × 3H, CH_3-Tol), 2.34 (s, 3H, CH_3-*p*-Mes), 2.15, 2.21 (2 × s, 2 × 3H, CH_3-*o*-Mes). **^{13}C NMR** (151 MHz, $CDCl_3$): 150.15 (CH-2-py), 149.27 (C-5-imid), 149.20 (CH-6-py), 139.26 (C-*p*-Mes), 138.25 (C-9), 137.92 (C-8), 137.56 (CH-4-py), 136.73 (C-1), 136.31 (C-*o*-Mes), 136.25, 136.27 (C-*i*-Tol), 136.14 (C-*o*-Mes), 136.06, 136.07 (C-*p*-Tol), 134.60 (C-*i*-Mes), 132.87 (C-10), 132.12 (C-3-py), 132.11 (C-16), 131.39, 131.60 (CH-*o*-Tol), 131.33 (C-13), 131.06 (C-4), 130.87 (C-7), 130.49, 130.79 (CH-*o*-Tol), 130.25 (C-25), 129.84 (C-21), 129.17, 129.18 (CH-*m*-Mes), 128.41 (CH-*m*-Tol), 128.30 (CH-3,20, CH-*m*-Tol), 127.50 (C-24), 127.46 (CH-14), 128.40 (CH-15), 127.31 (CH-12,17), 127.27 (C-22), 127.06 (CH-5), 126.25 (CH-18), 126.16 (CH-6,11), 125.17 (CH-19), 124.35 (CH-5-py), 123.99 (CH-2), 123.92 (CH-26), 123.83 (CH-3-imid), 123.70 (C-23), 123.53 (CH-2-imid), 21.15, 21.30, 21.31 (CH_3-Tol, CH_3-*p*-Mes), 18.95 (CH_3-*o*-Mes). **IR** ($CHCl_3$): 3164 vw, 3132 w, 2920 w, 1607 w, 1574 w, 1557 w, 1516 m, 1486 m, 1443 m, 1420 m, 1402 w, 1316 w, 1183 w, 1146 w, 1260 w, 1146 w, 1119 m, 1051 m, 852 m, 753 s cm^{-1}. **HR MALDI MS**: calcd for $C_{57}H_{45}Cl_3N_3Pd$ 982.1708, found 982.3163. **HR MALDI MS**: calcd for $C_{52}H_{40}N_2Pd$ 798.2232, found 798.2237. **UV/Vis** (tetrahydrofuran): λ_{max} (log ε) = 325 (4.13), 270 (5.76). **Fluorescence** (tetrahydrofuran, λ_{exc} = 360 nm): λ_{max} = 456 nm.

Enantioselective cyclotrimerization of enantioenriched (+)-(*P*)-benzo[f]naphtho[1,2-j]picene 14

General Procedure

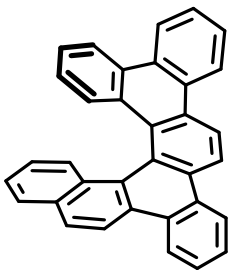

A Schlenk flask was charged with $Ni(acac)_2$ (0.8 mg, 3 µmol, 20 mol%) and imidazolium salt (-)-(*M*,*M*)-**135** or (-)-(*M*,*M*)-**136** (6.6 µmol, 44 mol%). The solids were dried under vacuum at 80 °C for 1 h and flushed with argon. Then tetrahydrofuran (200 µL) and ethylmagnesium chloride (0.148 M sol. in THF, 85 µL, 12.6 µmol, 0.63 equiv.) was added, which resulted in a black solution. After 2 min, triyne **11**[26] (6.4 mg, 20 µmol) was added and the mixture stirred for 4 h at ambient temperature. After completion (checked by TLC), the solvent was evaporated and the crude product purified by flash chromatography (hexane-dichloromethane 7 to 1) to furnish dibenzo helicene (+)-(*P*)-**14** as a white solid.
Analytic data were according to the literature.[26]
Chiral HPLC: Chiralpak IA column (250 × 4.6 mm, 5 µm, Chiral Technologies), mobile phase: heptane-chloroform (7:3), flow rate: 1 mL/min, retention time: 5.28 min (for (+)-isomer) and 8.54 min (for (-)-isomer).

With imidazolium chloride (-)-(*M*,*M*)-**135**

Yield: 7 mg, 70%. Optical purity: 35% *ee*.
Prepared according to the general procedure.

With imidazolium chloride (-)-(*M*,*M*)-**136**

Yield: 5 mg, 50%. Optical purity: 10% *ee*.
Prepared according to the general procedure.

Experimental details for activity tests with achiral substrates

General procedure for activity tests

Solutions of the corresponding metathesis precursor **150**, **152** or **154** (0.117 M in C_7D_8, 0.6 mL, 0.07 mmol) and the appropriate catalyst **156** or (-)-(*M*)-**147** (0.007 M in C_7D_8, 0.1 mL, 0.7 µmol, 1 mol%) were mixed in an NMR tube. The tube was sealed and ^{1}H-NMR spectra were recorded at 40 °C over 1 h at 0.5 min intervals.

RCM of diethyl diallylmalonate **150**

Conversion of starting material was calculated from the integrals of the CH_2-signals of **150** at 2.70 – 2.82 ppm and from the integrals of the CH_2-signals of **151** at 3.05 – 3.12 ppm.

RCM of diethylallylmethylallylmalonate **152**

Conversion of starting material was calculated from the integrals of the CH_2-signals of **152** at 2.80 – 2.90 ppm and from the integrals of the CH_2-signals of **153** at 2.95 – 3.17 ppm.

Enyne RCM of allyl propargyl ether **154**

Conversion of starting material was calculated from the integrals of the OCH_2-signals of **154** at 4.00 – 4.10 ppm and from the integrals of the OCH_2-signals of **155** at 4.40 – 4.55 ppm.

(*E*)-4-Phenylbut-2-en-1-yl acetate 159[148]

General procedure

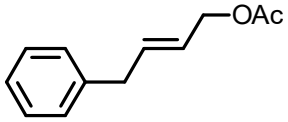

An oven-dried Schlenk was charged with Ru-catalyst (-)-(*M*)-**147** or **156** (4.43 µmol, 1 mol%) and *cis*-1,4-diacetoxy-2-butene (1.273 g, 7.398 mmol, 16.7 equiv.) and flushed with argon. The reactants were dissolved in toluene (2.2 mL), allylbenzene (52 mg, 0.443 mmol) was added rapidly and the resulting mixture was stirred at 40 °C for 20 h. Afterward, the solvent was removed *in vacuo* and the crude product purified by column chromatography on silica gel (hexane-ethyl acetate 10 : 1) to furnish olefin **159** as brownish oil. **^{1}H NMR** (400 MHz, $CDCl_3$) δ 7.35 – 7.28 (m, 2H), 7.25 – 7.17 (m, 3H), 5.99 – 5.90 (m, 1H), 5.69 – 5.60 (m, 1H), 4.58 – 4.54 (m, 2H), 3.42 (d, *J* = 6.8 Hz, 2H), 2.08 (s, 3H). **^{13}C NMR** (101 MHz, $CDCl_3$) δ 171.00, 139.68, 134.69, 128.73, 128.64, 128.63, 128.51, 126.39, 125.36, 65.06, 38.79, 21.16.

The *E*/*Z* ratio was calculated from the integrals (^{1}H NMR) of the CH_2-signals of (*E*)-**159** at 3.42 ppm (d, *J* = 6.8 Hz, 2H) and from the integrals of the CH_2-signals of (*Z*)-**159**[149] at 3.48 ppm (d, *J* = 7.6 Hz, 1H).

With Ru-catalyst (-)-(*M*)-**147**:

Yield: 63 mg, 75%. *E*/*Z* = 9:1.

Prepared according to the general procedure.

With Ru-catalyst **156**:

Yield: 65 mg, 77%. *E*/*Z* = 10:1.

Prepared according to the general procedure.

ARCM of allyl ether 160

Without addition of halides:

An oven-dried Schlenk flask was flushed with argon and solutions of triene **160** (0.1 M, 0.1 mL, 10 µmol) and (-)-(*M*)-**147** (5 µM, 80 µL, 0.4 µmol, 4 mol%) in the respective solvent listed in **Table 1** were added. The mixture was stirred at the temperature and for the time span noted in **Table 1**. After evaporation of all volatiles, $CDCl_3$ (0.4 mL) was added and the conversion was determined by ^{1}H-NMR-spectroscopy. The NMR-sample was filtered through a short pad of neutral alumina and submitted to GC-MS measurement for determination of the enantiomeric excess (*ee*).

With addition of halides:

An oven dried Schlenk-flask was charged with the corresponding halide (0.01 mmol) listed in **Table 1** and flushed with argon. A solution of (-)-(*M*)-**147** (5 µM, 80 µL, 0.4 µmol, 4 mol%) in the respective solvent was added and the mixture was stirred for 1 h at ambient temperature. A solution of triene **160** (0.1 M, 0.1 mL, 10 µmol) in the respective solvent was added and the reaction mixture was stirred at 40 °C for 4 h. After evaporation of all volatiles, the residue was dissolved in $CDCl_3$ (0.4 mL) and the conversion was determined by ^{1}H-NMR-spectroscopy. The NMR-sample was filtered through a short pad of neutral alumina and submitted to GC-MS measurement for determination of the enantiomeric excess (*ee*).

Determination of conversion:

NMR-data of (*R*)-**161** were in accordance with those reported in the literature.[105] Conversion of starting material **160** was calculated from the integral of the –C<u>H</u>=CH$_2$-

signal of **160** at 5.85 – 6.00 ppm and from the integral of the =C<u>H</u>–CH_2O-signal of (*R*)-**161** at 4.70 – 4.82 ppm.

<u>Determination of *ee*-values and assignment of absolute stereochemistry</u>:

A correlation of the sign of optical rotation with absolute configuration has previously been established by Hoveyda, Schrock and coworkers[150] *via* independent synthesis by using a Sharpless epoxidation step, and by Grubbs and coworkers.[105] The latter group reported for (*S*)-**161** with 90% ee: $[\alpha]_D^{25}$ = +116.5 (c = 0.55, $CHCl_3$).[105]

Chiral GC-MS: CP-Chirasil-Dex CB column (25 m, 0.25 mm, 0.25 µm, 7 inch cage), conditions: 60 °C, 1 mL/min flow rate, retention time 30.5 min (for major isomer) and 31.8 min (for minor isomer). **Chiral HPLC**: Chiralpak IA column (250 × 4.6 mm, 5 µm, Chiral Technologies), mobile phase: hexane, flow rate: 1 mL/min, retention time: 8.02 min (for major (-)-isomer) and 8.59 min (for minor (+)-isomer)

The polarimetric traces from HPLC analysis for entry 5, **Table 1** (60% ee) were analyzed and compared with the chiral GC-MS analysis. The major isomer was found to be (-)-**161**, which concludes an absolute configuration of (*R*) for product **161**.

AROCM of bicycloalkene 162

<u>Experimental procedure</u>:

Bicycloalkene **162** (8.0 mg, 50.0 µmol) was dissolved in CH_2Cl_2 (1.0 mL) in an oven-dried Schlenk flask. Styrene **163** (23 mL, 0.20 mmol, 4.0 equiv.) was added, followed by (-)-(*M*)-**147** (0.8 mg, 0.5 µmol, 1 mol %). The reaction vessel was closed and stirred at ambient temperature for 20 h. A small sample of the reaction mixture was submitted to HPLC on chiral stationary phase and to GC-MS. To determine the conversion, the reaction mixture was evaporated, dissolved in $CDCl_3$ and submitted to ^{1}H-NMR spectroscopy.

<u>Determination of conversion</u>:

NMR-spectroscopic data of **164** were in accordance with those reported in the literature.[107] Conversion of starting material **162** was calculated from the integral of the signal of **162** at 1.74 – 1.81 ppm and from the integral of the signal of **164** at 6.50 – 6.56 ppm.

Determination of *ee*:

A correlation of the sign of optical rotation and the absolute configuration has not been established. For these reasons the structure of **164** shown herein has not been specified. **Chiral HPLC**: Chiralpak IA column (250 × 4.6 mm, 5 µm, Chiral Technologies), mobile phase: hexane-isopropanol (4:1), flow rate: 1 mL/min, retention time: 8.57 min (for major (-)-isomer) and 9.62 min (for minor (+)-isomer).

2-Methoxy-1,1'-binaphthalene 168[151]

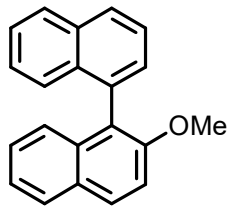

Chiral HPLC: Chiracel OJ-H column (250 × 4.6 mm, 5 µm, Daicel Corporation), mobile phase: hexane-isopropanol (4:1), flow rate: 1 mL/min, retention time: 8.84 min and 15.01 min. **^{1}H NMR** (401 MHz, $CDCl_3$) δ 7.99 (d, *J* = 9.0 Hz, 1H), 7.97 – 7.93 (m, 2H), 7.88 (d, *J* = 8.2 Hz, 1H), 7.62 (dd, *J* = 8.2, 7.0 Hz, 1H), 7.49 – 7.42 (m, 3H), 7.36 – 7.27 (m, 3H), 7.25 – 7.20 (m, 1H), 7.16 (d, *J* = 8.6 Hz, 1H), 3.77 (s, 3H). **^{13}C NMR** (101 MHz, $CDCl_3$) δ 154.75, 134.67, 134.40, 133.83, 133.08, 129.61, 129.15, 128.57, 128.36, 127.93, 127.88, 126.51, 126.31, 125.99, 125.83, 125.71, 125.64, 123.71, 123.36, 113.97, 56.93.

With commercial catalyst **60**

1-bromo-2-methoxynaphthalene **165** (6 mg, 0.025 mmol), boronic acid **167** (6.5 mg, 38 µmol, 1.5 equiv.), catalyst **60** (0.8 mg, 1 µmol, 5 mol%) and KOH (4 mg, 75 µmol, 3 equiv.) were placed in a flask, and it was flushed with argon. Then dioxane (1.8 mL) and H_2O (0.2 mL) were added, and the reaction mixture stirred for 24 h at ambient temperature. Afterward, the solvent was removed and the crude product purified by flash chromatography (hexane-ethyl acetate 5:1) to afford biaryl **168** (24 mg, 86%) as a white solid.

With catalyst (-)-(*M*)-**149**

1-iodo-2-methoxynaphthalene **166** (4.3 mg, 15 µmol), boronic acid **167** (3.9 mg, 23 µmol, 1.5 equiv.), catalyst (-)-(*M*)-**149** (0.7 mg, 0.75 µmol, 5 mol%) and KOH (2.5 mg, 75 µmol, 3.0 equiv.) were placed in a flask, and it was flushed with argon. Then a mixture of dioxane/H_2O (9:1, 300 µL, prior degassed by bubbling with argon) was added, and the reaction mixture stirred for 24 h at ambient temperature. A GC-MS analysis of the crude mixture showed a conversion of 27% to biaryl **168**. Prior

injection into the chiral HPLC the sample was purified by column chromatography (hexane-ethyl 1 : 0 to 5 : 1).

With catalyst (-)-(*P*,*P*)-**148**

1-iodo-2-methoxynaphthalene **166** (4.3 mg, 15 µmol), boronic acid **167** (5.2 mg, 30 µmol, 2.0 equiv.), catalyst (+)-(*P*,*P*)-**148** (1.0 mg, 0.75 µmol, 5 mol%) and KOH (2.5 mg, 75 µmol, 3.0 equiv.) were placed in a flask, and it was flushed with argon. Then a mixture of DMPU/H_2O (10 : 1, 330 µL, prior degassed by bubbling with argon) was added, and the reaction mixture stirred for 18 h at 60 °C. A GC-MS analysis of the crude mixture showed a conversion of 90% to biaryl **168**. Prior injection into the chiral HPLC the sample was purified by column chromatography (hexane-ethyl acetate 1 : 0 to 5 : 1).

Computational methods and full results for DFT-structure optimization

The geometry of complexes (-)-(*M*)-**147**, (+)-(*P*,*P*)-**148** and (-)-(*M*)-**149** were optimized with dispersion corrected RI-DFT and implicit solvent (CH_2Cl_2) model at PBE0[152]/def2-TZVP[153]/GD3[154]/Cosmo[155] level using the Turbomole 7.1. program package.[156]

6. Literature

[1] W. H. Thompson Lord Kelvin, *The Melocular Tactics of a Crystal*, Clarendon Press., **1894**, p. 27.
[2] J. Gal, *Helv. Chim. Acta* **2013**, *96*, 1617-1657.
[3] J. B. Biot, *Bull. Soc. Philomath.* **1815**, 190-192.
[4] L. Pasteur, *C. R. Séances Acad. Sci.* **1848***,* 26, 535-538.
[5] S. Mason, *Trends Pharmacol. Sci.* **1986**, *7*, 20-23.
[6] W. A. Bonner, *Orig. Life Evol. Biosph.* **1991**, *21*, 59-111.
[7] K. Nishikawa, J. Maruani, E. J. Brändas, G. Delgado-Barrio, P. Piecuch, *Quantum Systems in Chemistry and Physics*, Springer, **2012**, pp. 47-76.
[8] B. Kojić-Prodić, Z. Štefanić, *Symmetry* **2010**, *2*, 884-906.
[9] D. B. Cline, *Symmetry* **2010**, *2*, 1450-1460.
[10] C. Meinert, J. Filippi, L. Nahon, S. V. Hoffmann, L. d'Hendecourt, P. de Marcellus, J. H. Bredehöft, W. H.-P. Thiemann, U. J. Meierhenrich, *Symmetry* **2010**, *2*, 1055-1080.
[11] S. Kojo, *Symmetry* **2010**, *2*, 1022-1032.
[12] M. B. Smith, J. March, *March's Advanced Organic Chemistry Sixth Edition*, Wiley & Sons Inc., **2007**, pp. 141-144.
[13] E. L. Eliel, S. H. Wilen, L. N. Mander, *Stereochemistry of Organic Compounds*, Wiley & Sons Inc., **1994**, pp. 1119-1176.
[14] J. Meisenheimer, K. Witte, *Ber. Dtsch. Chem. Ges.* **1903**, *36*, 4153-4164.
[15] M. S. Newman, D. Lednicer, *J. Am. Chem. Soc.* **1956**, *78*, 4765-4770.
[16] M. S. Newman, W. B. Lutz, D. Lednicer, *J. Am. Chem. Soc*. **1955**, *77*, 3420-3421.
[17] R. H. Martin, *Angew. Chem. Int. Ed.* **1974**, *13*, 649-660.
[18] Scifinder (01/2018), using „helicene" as a search term.
[19] For an overwiev of books and reviews about helicene chemistry see: C. Chen, Y. Shen, *Helicene Chemistry From Synthesis to Applications*, Springer, **2017**, pp. 11.
[20] K. Mori, T. Murase, M. Fujita, *Angew. Chem. Int. Ed.* **2015**, *54*, 6847-6851.
[21] J. Nejedlý, M. Šámal, J. Rybáček, M. Tobrmanová, F. Szydlo, C. Coudret, M. Neumeier, J. Vacek, J. Vacek Chocholoušová, M. Buděšínský, D. Šaman, L. Bednárová, L. Sieger, I. G. Stará, I. Starý, *Angew. Chem. Int. Ed.* **2017**, *56*, 5839-5843.
[22] V. Terrasson, M. Roy, S. Moutard, M. Lafontaine, G. Pèpe, G. Félix, M. Gringas, *RSC Adv.* **2014**, *4*, 32412-32414.
[23] K. Nakano, Y. Hidehira, K. Takahashi, T. Hiyama, K. Nozaki, *Angew. Chem. Int. Ed.* **2005**, *44*, 7136-7138.
[24] A. Moradpour, J. F. Nicoud, G. Balavoine, H. Kagan, *J. Am. Chem. Soc.* **1971**, *93*, 2353-2354.
[25] I. G. Stará, I. Starý, *Aromatic Ring Assemblies, Polycyclic Aromatic Hydrocarbons, and Conjuguted Polyenes*, Thieme, **2010**, *Vol. 45b*, pp. 911.
[26] A. Jančařík, J. Rybáček, K. Cocq, J. V. Chocholoušová, J. Vacek, R. Pohl, L. Bednárová, P. Fiedler, I. Císařová, I. G. Stará, I. Starý, *Angew. Chem. Int. Ed.* **2013**, *52*, 9970-9975.
[27] M. Karras, J. Holec, L. Bednárová, R. Pohl, B. Schmidt, I. G. Stará, I. Starý*, J. Org. Chem.* **2018**, *83*, 5523-5538.
[28] I. Gay Sánchez, M. Šámal, J. Nejedlý, M. Karras, J. Klívar, J. Rybáček, M. Buděšínský, L. Bednárová, B. Seidlerová, I. G. Stará, I. Starý, *Chem. Commun.* **2017**, *53*, 4370-4373.
[29] E. González-Fernández, L. D. M. Nicholls, L. D. Schaaf, C. Farès, C. W. Lehmann, M. Alcarazo, *J. Am. Chem. Soc.* **2017**, *139*, 1428-1431.
[30] J. Žádný, A. Jančařík, A. Andronova, M. Šámal, J. Vacek Chocholoušová, J. Vacek, R. Pohl, D. Šaman, I. Císařová, I. G. Stará, I. Starý, *Angew. Chem. Int. Ed.* **2012**, *51*, 5857-5861.
[31] M. Šámal, S. Chercheja, J. Rybáček, J. Vacek Chocholoušová, J. Vacek, L. Bednárová, D. Šaman, I. G. Stará, I Starý, *J. Am. Chem. Soc.* **2015**, *137*, 8469-8474.
[32] M. Gingras, *Chem. Soc. Rev.* **2013**, *42*, 968-1006.
[33] Y. Dai, T. J. Katz, *J. Org. Chem.* **1997**, *62*, 1274-1285.
[34] Y. Dai, T. J. Katz, D. A. Nichols, *Angew. Chem. Int. Ed.* **1996**, *35*, 2109-2111.
[35] T. R. Kelly, *Acc. Chem. Res.* **2001**, *34*, 514-522.
[36] B. J. Coe, D. Rusanova, V. D. Joshi, S. Sánchez, J. Vávra, D. Khobragade, L. Severa, I. Císarocá, D. Saman, R. Pohl, K. Clays, G. Depotter, B. S. Brunschwig, F. Teplý, *J. Org. Chem.* **2016**, *81*, 1912-1920.
[37] K. Yamamoto, T. Ikeda, T. Kitsuki, Y. Okamoto, H. Chikamatsu, M. Nakazaki, *J. Chem. Soc. Perkin Trans. 1* **1990**, 271-276.

[38] S. Honzawa, H. Okubo, S. Anzai, M. Yamaguchi, K. Tsumoto, I. Kumagai, *Bioorg. Med. Chem.* **2002**, *10*, 3213-3218.
[39] P. Feng, T. Miyashita, H. Okubo, M. Yamaguchi*, J. Am. Chem. Soc.* **1998**, *120*, 10166-10170.
[40] C. Nuckolls, T. J. Katz, T. Verbiest, S. Van Elshocht, H. Kuball, S. Kiesewalter, A. J. Lovinger, A. Persoons, *J. Am. Chem. Soc.* **1998**, *120*, 8656-8660.
[41] J. E. Field, G. Muller, J. P. Riehl, D. Venkataraman, *J. Am. Chem. Soc.* **2003**. *125*, 11808-11809.
[42] J. R. Brandt, L. Pospíšil, L. Bednárová, R. Correa da Costa, A. J. P. White, T. Mori, F. Teplý, M. J. Fuchter, *Chem. Commun.* **2017**, *53*, 9059-9062.
[43] A. J. Lovinger, C. Nuckolls, T. J. Katz, *J. Am. Chem. Soc.* **1998**, *120*, 264-268.
[44] M. T. Reetz, E. W. Beuttenmüller, R. Goddard, *Tetrahedron Lett.* **1997**, *38*, 3211-3214.
[45] D. Nakano, M. Yamaguchi, *Tetrahedron Lett.* **2003**, *44*, 4969-4971.
[46] K. Yavari, P. Aillard, Y. Zhang, F. Nuter, P. Retailleau, A. Voituriez, A. Marinetti, *Angew. Chem. Int. Ed.* **2014**, 53, 861-865.
[47] K. Yamamoto, T. Shimizu, K. Igawa, K. Tomooka, G. Hirai, H. Suemune, K. Usui, *Sci. Rep.* **2016**, *6*, 36211-36218.
[48] Y. Chen, S. Yekta, A. K. Yudin, *Chem. Rev.* **2003**, *103*, 3155-3211.
[49] S. D. Dereher, T. J. Katz, K. Lam, A. L. Rheingold, *J. Org. Chem.* **2000**, *65*, 815-822.
[50] N. Hellou, C. Jahier-Diallo, O. Baslé, M. Srebro-Hooper, L. Toupet, T. Roisnel, E. Caytan, C. Roussel, N. Vanthuyne, J. Autschbach, M. Mauduit, J. Crassous, *Chem. Commun.* **2016**, *52*, 9243-9246.
[51] N. Hellou, M. Srebro-Hooper, L. Favereau, F. Zinna, E. Caytan, L. Toupet, V. Dorcet, M. Jean, N. Vanthuyne, J. A. G. Williams, L. Di Bari, J. Autschbach, J. Crassous, *Angew. Chem. Int. Ed.* **2017**, *56*, 8236-8239.
[52] W. A. Herrmann, D. Baskakov, E. Herdtweck, S. D. Hoffmann, T. Bunlaksananusorn, F. Rampf, Lars Rodefeld, *Organometallics* **2006**, *25*, 2449-2456.
[53] H. Seo, D. Hirsch-Weil, K. A. Abboud, S. Hong, *J. Org. Chem.* **2008**, *73*, 1983-1986.
[54] D. Baskakov, W. A. Hermann, E. Herdtweck, S. D. Hoffmann, *Organometallics* **2007**, *26*, 626-632.
[55] K. J. Cavell, M. C. Elliott, D. J. Nielsen, J. S. Paine, *Dalton Trans.* **2006**, *0*, 4922-4925.
[56] A. Igau, H. Grutzmacher, A. Baceiredo, G. Bertrand, *J. Am. Chem. Soc.* **1988**, *110*, 6463-6466.
[57] H.W. Wanzlick, H.-J. Schönherr*, Angew. Chem. Int. Ed.* **1968**, *7*, 141-142.
[58] K. Öfele, *J. Organomet. Chem.* **1968**, *12*, 42-43.
[59] A. J. Arduengo III, R. L. Harlow, M. Kline, *J. Am. Chem. Soc.* **1991**, *113*, 361-363.
[60] M. N. Hopkinson, C. Richter, M. Schedler, F. Glorius, *Nature* **2014**, *510*, 485-496.
[61] H. W. Wanzlick, *Angew. Chem.* **1962**, *1*, 75-80.
[62] J. Clayden, N. Greevs, S. Warren, P. Wothers, *Organic Chemistry*, Oxford University Press, **2001**, 1st edition, pp. 1060.
[63] F. E. Hahn, M. C. Jahnke, *Angew. Chem.* **2008**, *120*, 3166-3216.
[64] J. Schwarz, V. P. W. Böhm, M. G. Gardiner, M. Grosche, W. A. Herrmann, W. Hieringer, G. Raudaschl-Sieber, *Chem. Eur. J.* **2000**, *6*, 1773-1780.
[65] K. Öfele, W. A. Herrmann, D. Mihalios, M. Elison, E. Herdtweck, W. Scherer, J. Mink, *J. Organomet. Chem.* **1993**, *459*, 177-184.
[66] J. C. Green, R. G. Scurr, P. L. Arnold, F. G. N. Cloke, *Chem Commun.* **1997**, *0*, 1963-1964.
[67] X. Hu, I. Castro-Rodriguez, K. Olsen, K. Meyer, *Organometallics* **2004**, *23*, 755-764.
[68] A. J. Arduengo III, H. V. Rasika Dias, R. L. Harlow, M. Kline, *J. Am. Chem. Soc.* **1992**, *114*, 5530-5534.
[69] P. H. Schneider, H. S. Schrekker, C. C. Silveira, L. A. Wessjohann, A. L. Braga, *Eur. J. Org. Chem.* **2004**, *12*, 2715-2722.
[70] V. Lavallo, Y. Canac, Carsten Präsang, B. Donnadieu, G. Bertrand, *Angew. Chem. Int. Ed.* **2005**, *44*, 5705-5709.
[71] L. Benhamou, E. Chardon, G. Lavigne, S. Bellemin-Laponnaz, V. César, *Chem. Rev.* **2011**, *111*, 2705-2733.
[72] L. Hintermann, *Beilstein J. Org. Chem.* **2007**, *3*, No. 22.
[73] A. Fürstner, M. Alcarazo, V. Cesar, C. W. Lehmann, *Chem. Commun.* **2006**, 2176-2178.
[74] W. A. Herrmann, *Angew. Chem. Int. Ed.* **2002**, *41*, 1290-1309.
[75] E. Peris, R. H. Crabtree, *Coord. Chem Rev.* **2004**, *248*, 2239-2246.
[76] C. M. Crudden, D. P. Allen, *Coord. Chem. Rev.* **2004**, *248*, 2247-2273.
[77] S. Díez-Gonzaález, S. P. Nolan, *Coord. Chem. Rev.* **2007**, *251*, 874-883.
[78] H. Jacobsen, A. Correa, A. Poater, C. Costabile, L. Cavallo, *Coord. Chem. Rev.* **2009**, *253*, 687-703.
[79] H. Clavier, S. P. Nolan, *Chem. Commun.* **2010**, *46*, 841-861.
[80] G. C. Vougioukalakis, R. H. Grubbs, *Chem. Rev.* **2010**, *110*, 1746-1787.
[81] C. Adlhart, P. Chen, *Angew. Chem. Int. Ed.* **2002**, *41*, 4484-4487.

[82] C. Adlhart, P. Chen, *J. Am. Chem. Soc.* **2004**, *126*, 3496-3510.
[83] B. F. Straub*, Angew. Chem. Int. Ed.* **2005**, *44*, 5974-5978.
[84] A. C. Tsipis, A. G. Orpen, J. N. Harvey, *Dalton Trans.* **2005**, 0, 2849-2858.
[85] Y. Zhao, D. G. Truhlar, *Org. Lett.* **2007**, *9*, 1967-1970.
[86] C. A. Tolman, *Chem. Rev.* **1977**, *77*, 313-348.
[87] A. C. Hillier, W. J. Sommer, B. S. Yong, J. L. Peterson, L. Cavallo, S. P. Nolan, *Organometallics* **2003**, *22*, 4322-4326.
[88] L. H. Gade, P. Hofmann, *Molecular Catalysts: Structure and Functional Design*, Wiley-VCH, **2014**, pp. XIX-XXIV.
[89] B. Lindström, L. J. Petterson, *CATTECH* **2003**, *7*, 130-138.
[90] https://www.nobelprize.org/nobel_prizes/chemistry/laureates/ (last opened 10.02.2018)
[91] https://www.nature.com/subjects/asymmetric-catalysis (last opened 11.02.2018)
[92] L. M. Pike, M. P. Enns, D. E. Hornung, *Chem. Senses* **1988**, *13*, 307-309.
[93] P. Hofland, "Reversal of Fortune: How a Vilified Drug Became a Life-saving Agent in the "War" Against Cancer", Onco'Zine: https://oncozine.com/reversal-of-fortune-how-a-vilified-drug-became-a-life-saving-agent-in-the-war-against-cancer/ (last opened 12.02.2018)
[94] https://www.fda.gov/Drugs/GuidanceComplianceRegulatoryInformation/Guidances/ucm122883.htm (last opened 12.02.2018)
[95] R. Noyori, *Angew. Chem. Int. Ed.* **2002**, *41*, 2008-2022.
[96] *Chem. Rev.* **2003**, *103*, 2761-3400.
[97] I. Ojima, *Catalytic Asymmetric Synthesis*, Wiley and Sons Inc., **2010**.
[98] R. H. Grubbs, *Handbook of Metathesis*, Wiley-VCH, **2003**.
[99] K. C. Nicolaou, P. G. Bulger, D. Sarlah, *Angew. Chem. Int. Ed.* **2005**, *44*, 4490-4527.
[100] A. H. Hoveyda, A. R. Zhugralin, *Nature* **2007**, *450*, 243-251.
[101] J.-L. Hérisson, Y. Chauvin*, Makromol. Chem.* **1971**, *141*, 161-176.
[102] T. P. Montgomery, A. M. Johns, R. H. Grubbs, *Catalysts* **2017**, *7*, 87.
[103] T. J. Seiders, D. W. Ward, R. H. Grubbs, *Org. Lett.* **2001**, *3*, 3225-3228.
[104] P.-A. Fournier, S. K. Collins, *Organometallics* **2007**, *26*, 2945-2949.
[105] T. W. Funk, J. M. Berlin, R. H. Grubbs, *J. Am. Chem. Soc.* **2006**, *128*, 1840-1846.
[106] A. Kannenberg, D. Rost, S. Eibauer, S. Tiede, S. Blechert, *Angew. Chem. Int. Ed.* **2011**, *50*, 3299-3302.
[107] J. J. Van Veldhuizen, S. B. Garber, J. S. Kingsbury, A. H. Hoveyda, *J. Am. Chem. Soc.* **2002**, *124*, 4954-4955.
[108] J. J. Van Veldhuizen, D. G. Gillingham, S. B. Garber, O. Kataoka, A. H. Hoveyda, *J. Am. Chem. Soc.* **2003**, *125*, 12502-12508.
[109] T. J. Colacot, *New Trends in Cross-Coupling – Theory and Applications*, The Royal Society of Chemistry, **2015**.
[110] N. Miyaura, A. Suzuki, *Chem. Rev.* **1995**, *95*, 2457-2483.
[111] G. Bringmann, A. J. Price Mortimer, P. A. Keller, M. J. Gresser, J. Garner, M. Breuning, *Angew. Chem. Int. Ed.* **2005**, *44*, 5584-5427.
[112] J. E. Smyth, N. M. Butler, P. A. Keller, *Nat. Prod. Rep.* **2015**, *32*, 1562-1583.
[113] N. L. Allinger, E. L. Eliel, S. H. Wilen, *Topics in Stereochemistry*, John Wiley & Sons, **1983**, pp. 1-81.
[114] C. J. O'Brien, E. A. B. Kantchev, C. Valente, N. Hadei, G. A. Chass, A. Lough, A. C. Hopkinson, M. G. Organ, *Chem. Eur. J.* **2006**, *12*, 4743-4748.
[115] L. Yang, P. Guan, P. He, Q. Chen, C. Cao, Y. Peng, Z. Shi, G. Pang, Y. Shi, *Dalton Trans.* **2012**, *41*, 5020-5025.
[116] L. Benhamou, Céline Besnard, E. P. Kündig, *Organometallics* **2014**, *33*, 260-266.
[117] R. Haraguchi, S. Hoshino, T. Yamazaki, S.-I. Fukuzawa, *Chem. Commun.* **2018**, *54*, 2110-2113.
[118] R. Maity, A. Verma, M. van der Meer, S. Hohloch, B. Sarkar, *Eur. J. Inorg. Chem.* **2016**, 111-117.
[119] both compounds available at: https://www.abcr.de/de/startseite/ (last opened 20.02.2018)
[120] M. Yoshida, M. Higuchi, K. Shishido, *Org. Lett.* **2009**, *11*, 4752-4755.
[121] B. Schmidt, M. Riemer, U. Schilde, *Synlett* **2014**, *25*, 2943-2946.
[122] S. Bartoli, A. Cipollone, A. Squarcia. A. Madami, D. Fattori, *Synthesis* **2009**, *8*, 1305-1308.
[123] D. Boyall, D. E. Frantz, E. M. Carreira, *Org. Lett.* **2002**, *4*, 2605-2606.
[124] S. Kotani, K. Kukita, K. Tanaka, T. Ichibakase, M. Nakajima, *J. Org. Chem.* **2014**, *79*, 4817-4825.
[125] W. A. Herrmann, L. J. Goossen, C. Köcher, G. R. J. Artus, *Angew. Chem. Int. Ed.* **1996**, *35*, 2805-2807.
[126] P. Queval, C. Jahier, M. Rouen, I. Artur, J.-C. Legeay, L. Falivene, L. Toupet, C. Crévisy, Luigi Cavallo, O. Baslé, M. Mauduit, *Angew. Chem. Int. Ed.* **2013**, *52*, 14103-14107.
[127] J. C. Garrison, W. J. Youngs, *Chem. Rev.* **2005**, *105*, 3978-4008.
[128] H. M. J. Wang, I. J. B. Lin, *Organometallics* **1998**, *17*, 972-975.
[129] J. M. Hayes, M. Viciano, E. Peris, G. Ujaque, A. Lledós, *Organometallics* **2007**, *26*, 6170-6183.

[130] Y. Zhang, V. César, G. Storch, N. Lugan, G. Lavigne, *Angew. Chem. Int. Ed.* **2014**, *53*, 6482-6486.
[131] Z. J. Wang, W. R. Jackson, A. J. Robinson, *Green Chem.* **2015**, *17*, 3407-3414.
[132] J. J. Van Veldhuizen, John E. Campell, R. E. Giudici, A. H. Hoveyda, *J. Am. Chem. Soc.* **2005**, *127*, 6877-6882.
[133] T. Ritter, A. Hejl, A. G. Wenzel, T. W. Funk, R. H. Grubbs, *Organometallics* **2006**, *25*, 5740-5745.
[134] J. M. Berlin, S. D. Goldberg, R. H. Grubbs, *Angew. Chem. Int. Ed.* **2006**, *45*, 7591-7595.
[135] L. Falivene, R. Credendino, A. Poater, A. Petta, L. Serra, R. Oliva, V. Scarano, L. Cavallo, *Organometallics* **2016**, *35*, 2286-2293.
[136] C. Costabile, L. Cavallo, *J. Am. Chem. Soc.* **2004**, *126*, 9592-9600.
[137] S. Kress, S. Blechert, *Chem. Soc. Rev.* **2012**, *41*, 4389-4408.
[138] P.-A. Fournier, J. Savoie, B. Stenne, M. Bédard, A. Grandbois, S. K. Collins, *Chem. Eur. J.* **2008**, *14*, 8690-8695.
[139] J.-U. Peters, S. Blechert, *Chem. Commun.* **1997**, *0*, 1983-1984.
[140] C. Valente, S. Calimsiz, K. H. Hoi, D. Mallik, M. Sayah, M. G. Organ, *Angew. Chem. Int. Ed.* **2012**, *51*, 3314-3332.
[141] A.-S. Castanet, F. Colobert, P.-E. Broutin, M. Obringer, *Tetrahedron: Asymmetry* **2002**, *13*, 659-65.
[142] T. A. Kirkland, R. H. Grubbs, *J. Org. Chem.* **1997**, *62*, 7310-7318.
[143] J. B. Binder, I. A. Guzei, T. Raines, *Adv. Synth. Catal.* **2007**, *349*, 395-404.
[144] X. Ling, Y. Xiong, R. Huang, X. Zhang, S. Zhang, C. Chen, *J. Org. Chem*. **2013**, *78*, 5218-5226.
[145] D. R. White, J. T. Hutt, J. P. Wolfe, *J. Am. Chem. Soc.* **2015**, *137*, 11246-11249.
[146] S. H. Reich, M. Melnick, M. J. Pino, M. A. M. Fuhry, A. J. Trippe, K. Appelt, J. F. Davies, B.-W. Wu, L. Musick, *J. Med. Chem.* **1996**, *39*, 2781-2794.
[147] X. Yan, X. Cui, B. Li, L. Li, *Nano Lett.* **2010**, *10*, 1869-1873.
[148] T. Wdowik, C. Samojlowicz, M. Jawiczuk, M. Malinska, K. Wozniak, K. Grela, *Chem. Commun.* **2013**, *49*, 674-676.
[149] A. Dumas, R. Tarrieu, T. Vives, T. Roisnel, V. Dorcet, O.Baslé, M. Maudiut, *ACS Catal.* **2018**, *8*, 3257-3262.
[150] D. S. La, J. B. Alexander, D. R. Cefalo, D. D. Graf, A. H. Hoveyda and R. R. Schrock, *J. Am. Chem. Soc.* **1998**, *120*, 9720-9721.
[151] A. Bermejo, A. Ros, R. Fernández, J. M. Lassaletta, *J. Am. Chem. Soc.* **2008**, *130*, 15798-15799.
[152] M. Ernzerhof, K. Burke and J. P. Perdew, *J. Chem. Phys.* **1996**, *105*, 2798-2803.
[153] F. Weigend and R. Ahlrichs, *Phys. Chem. Chem. Phys.* **2005**, *7*, 3297-3305.
[154] S. Grimme, J. Antony, S. Ehrlich and H. Krieg, *J. Chem. Phys.* **2010**, *132*, 154104.
[155] A. Klamt and G. Schüürmann, *J. Chem. Soc., Perkin Trans. 2*, **1993**, 799-805.
[156] TURBOMOLE V6.1 2009, University of Karlsruhe and Forschungszentrum Karlsruhe GmbH, 1989-2007, TURBOMOLE GmbH, available from http://www.turbomole.com (last opened 2018.01.26).